Université de Montréal

Transformations rédox et spéciation du Hg dans la neige et les eaux de surface de l'extrême arctique et de régions tempérées

Alexandre Poulain

Département de sciences biologiques
Faculté des études supérieures

Thèse présentée à la faculté des études supérieures en vue de l'obtention du grade de Philosophiae Doctor (Ph.D.)
en sciences biologiques

Avril 2007

Université de Montréal
Faculté des études supérieures

Cette thèse intitulée
Transformation rédox et spéciation du Hg dans la neige et les eaux de surface de l'extrême arctique et de régions tempérées

Présentée par
Alexandre Poulain

a été évaluée par un jury composé des personnes suivantes

Kevin Wilkinson	Président-rapporteur
Marc Amyot	Directeur de recherche
Peter G.C. Campbell	Codirecteur
Dolors Planas	Membre du jury
Greg Mierle	Examinateur externe
Kevin Wilkinson	Représentant du doyen

Thèse acceptée le: 24 Avril 2007

Résumé

Le Hg est un polluant global qui peut-être bioaccumulé par les organismes et bioamplifié dans les réseaux trophiques. L'inter-conversion entre les formes réduites et oxydées (Hg(0) and Hg(II)) est importante car elle contrôle la production de la forme élémentaire, moins toxique mais volatile, perdue vers l'atmosphère. Cette thèse vise à mieux comprendre le cycle rédox et la distribution des espèces de Hg dans la neige et les eaux de fonte en régions polaires et tempérées.

Nous avons montré que:

- Dans l'extrême Arctique, l'interface entre la banquise et la neige constitue un site d'accumulation du Hg, possiblement menaçant les communautés biologiques associées à la banquise.
- le Hg(0) nouvellement formé dans la neige est partiellement détruit (photooxydation) lors d'une diminution de la quantité et de la qualité de l'énergie lumineuse incidente.
- Dans les mares et ruisseaux de l'Arctique, la production de Hg^0 diminue suivant un gradient croissant de salinité. Cette altération de la réduction est contrebalancée par la présence de particules. Les exsudats biogéniques (algues et microbes) participent à la destruction du Hg^0 même à l'obscurité.
- Les microbes des régions marines et côtières peuvent affecter la mobilité et la toxicité du Hg grâce à l'expression du gène *mer*A, codant pour la réductase du Hg.
- En régions tempérées, les niveaux de Hg la neige au sol sous la canopée sont affectés par le nivolessivage et par la balance entre oxydation et réduction. La neige déposée sous la canopée représente alors un puits

de Hg, i.e., on peut y observer une accumulation nette de Hg au cours de l'hiver, possiblement libéré lors de la fonte printanière, alors que la neige déposée en milieu ouvert est une source de Hg vers l'atmosphère.

- Dans les eaux de surface des régions tempérées, la réduction est la réaction principale; cependant, l'oxydation du Hg(0) devient prépondérante durant la nuit ou les périodes de faibles intensités lumineuses.

D'un point de vue écotoxicologique nous avons caractérisé des environnements propices à accentuer l'exposition des communautés biologiques au Hg (environnements marins et forestiers) et d'un point de vue géochimique nous avons montré la photooxydation du Hg^0 dans la neige et la réduction microbienne du Hg(II) dans les eaux de l'extrême Arctique. Ces deux mécanismes modifient la mobilité et donc le transfert de Hg entre écosystèmes.

Mots clés : mercure, extrême arctique, cycle redox, résistance microbienne au mercure, banquise, neige, couvert forestier, contamination, photochimie.

Summary

Hg is a global pollutant, a potent neurotoxin which bioaccumulates in organisms and is biomagnified in food webs. The inter-conversion between the various redox states of Hg in snow and waters (Hg^0 and Hg(II)) is critical since it controls the production of the volatile, less toxic, elemental form (Hg^0), which is evaded to the atmosphere.

Specifically we found that:

- The sea ice/snow interface constitutes an important site for Hg accumulation. This finding suggests that the biota living in association with sea ice, which form the base of the Arctic food chain, experience an elevated risk of Hg exposure.
- The newly produced Hg^0 is partly destroyed (photooxidation) following an alteration in light energetic regime.
- In melted snow, streams and pond waters, Hg reduction is hampered over a salinity gradient. This alteration of Hg reduction was counterbalanced by the presence of particles. In saline waters, biogenic exudates were able to oxidize Hg(0).
- Microbes from pristine Arctic coastal and marine environments affect the toxicity and environmental mobility of Hg in remote polar regions through the expression of the *merA* genes coding for the mercuric reductase.
- In temperate areas, mercury concentrations in snow on the ground in forested ecosystems are affected by both throughfall and the balance between oxidation and reduction, which affect mercury dynamics after deposition. Snow deposited under canopy is a sink for Hg, i.e. it accumulates over the winter and may be released during snowmelt, but snow in the open is a source of Hg to the atmosphere.

- In temperate surface waters during the day, reduction was the principal reaction controlling Hg redox cycling but Hg(0) oxidation overcame Hg(II) reduction during the night or at periods of weaker light intensity.

Altogether this thesis has shed new light on Hg dynamics in snow and water. From an ecotoxicological point of view, we characterized which environments may contribute to increase Hg exposure (marine areas and forested environments) and from a geochemical point of view we showed new processes to occur such as the destruction of newly formed Hg^0 and the microbially mediated reduction of Hg(II), both processes altering its mobility and thus its transfers between ecosystems.

Keywords: Mercury, high Arctic, redox cycle, microbial mercury resistance, sea ice, snow, tree cover, contamination, photochemistry.

Tables des matières

Liste des tableaux

Liste des figures

à

Annie,

Jacques

&

Clément

pour toujours avoir été là.

Remerciements

Pour son soutien sans faille en ce qui eut trait à ma formation scientifique, pour sa patience, pour la confiance et la grande liberté d'agir qu'il m'a accordé ; que ce fût lors de nos discussions personnelles et professionnelles, au travers des expériences (inter)nationales qu'il m'a encouragé à entreprendre ou de campagnes d'échantillonnage que j'ai pu réaliser, je tiens à remercier Dr. Marc Amyot. Je me dois aussi de souligner sa disponibilité presque sans limite, qu'il prit l'habitude de quantifier par le nombre de mes intrusions, pas toujours sollicitées mais toujours averties, dans son bureau.

Je tiens à remercier Dr. Peter G.C. Campbell pour son soutien et ses conseils qui m'ont permis d'améliorer, entre autres, les modèles de spéciation du Hg, les manuscrits présentés, la qualité scientifique et linguistique - en français et en anglais - de cette thèse et qui m'a permis de garder à l'esprit la nécessité de la précision des termes.

Je tiens aussi à remercier chaleureusement Dr Tamar Barkay pour m'avoir accueilli au sein de son laboratoire, pour m'avoir initié à la biologie moléculaire et pour avoir fait de mon passage à Rutgers une expérience inoubliable.

Merci au Dr Parisa Ariya, pour sa contribution aux aspects cinétiques et modélisation de ce travail, ainsi que pour son intérêt dans ce projet de recherche. Ses conseils ont toujours permis d'enrichir les articles.

Merci à tous les membres du laboratoire Amyot, à Stéphanie et Ariane, pour vos encouragements, et à Dominic et Valérie pour la très grande qualité de leur travail.

Merci à mes amis et collègues de terrain (très) extrême, Édenise, John et Justin, pour de mémorables moments, faciles et moins faciles passés ensemble.

Merci au Dr R. Carignan, Dr B. Pinel-Alloul et Dr A. Cattaneo qui m'ont permis d'enseigner la limnologie, ce fut une expérience très enrichissante et confirma une vocation.

Merci à Deborah Iqaluk, ranger senior des forces armées canadiennes pour son amitié, son aide, et pour m'avoir transmis sa passion et connaissance de l'extrême Arctique.

Merci à Olivier et Saad pour avoir, au quotidien, participé à faire du doctorat une expérience si agréable.

Merci à Claudette pour son efficacité hors pair, sa patience et pour m'avoir rendu la vie si facile et merci à Ginet'che et à ses midis, pour tout et pour son penchant si particulier envers la psychanalyse.

Merci à Jacques et Louise ainsi qu'à François et Karine pour les très bons moments passés ensemble.

Merci à mes colocataires, Jessica, Simon et Virginie, pour avoir partagé « l'envers du décors » et tout ce qui va avec.

Merci à mes amis, en France, Géraldine, Raphaël, Laure, Hugues, Charles, Sébastien, Élodie, Olivier, Carine, Xavier, Réjane, Fabrice, Magaly, Sébastien, Flavie et Marc.

Merci aux membres du jury d'évaluation de cette thèse pour les commentaires proposés. Ces commentaires ont dans tous les cas contribués à améliorer ce document.

Merci aux sources de financement au travers des bourses d'études du département de sciences biologiques, du GRIL, de la FES et de la financière Manuvie et aux subventions de recherche FQRNT, CRSNG et CFCAS.

Merci à ma tendre et chère Bronwyn, pour avoir toujours été présente, pour ton soutien et ta patience qui m'ont permis de garder la tête sur les épaules.

Enfin, merci à mes parents, Annie et Jacques et à mon frère, Clément.

.

A.J. Poulain : Conception du projet; analyses des échantillons; traitement des données; rédaction initiale et finale.

S.M. Ni Chadhain : analyses des échantillons; traitement des données; rédaction initiale et finale

P.A. Ariya : traitement des données et modélisation cinétique; rédaction finale.

M. Amyot : rédaction finale.

E. Garcia : échantillonnage sur le terrain; rédaction finale.

P.G.C. Campbell : rédaction finale

G. Zylstra : rédaction finale

T. Barkay : Conception du projet; rédaction finale.

Article 6. Garcia E., Poulain A. J., Amyot M., and Ariya P. A. (2005) Diel variations in photoinduced oxidation of Hg-0 in freshwater. *Chemosphere* 59(7), 977-981.

E. Garcia : Conception du projet; échantillonnage sur le terrain; analyses des échantillons; traitement des données; rédaction initiale et finale.

A.J. Poulain : Conception du projet; échantillonnage sur le terrain; analyses des échantillons; traitement des données; rédaction finale.

M. Amyot : Conception du projet; rédaction finale.

P.A. Ariya : rédaction finale.

Article 7. Barkay T. and Poulain A. J. Mercury (micro)biogeochemistry in polar environments (a review). *FEMS Microbiology & Ecology* 59(2) 232-241

T. Barkay : Développement initial du projet; rédaction initiale et finale.

A.J. Poulain : Développement initial du projet; rédaction initiale et finale.

Identification de l'étudiant

Alexandre Poulain [redacted]

Département des sciences biologiques, Faculté des arts et des sciences.

Ph.D. Sciences biologiques (3-235-1-0)

Directeur de thèse : Prof. Marc Amyot, Université de Montréal.

Co-Directeur de thèse : Prof. Peter G.C. Campbell, INRS-eau, terre & environnement.

Description de l'article

Titre : Mercury distribution, partitioning and speciation in coastal vs inland snow of the high Arctic during snowmelt

Auteurs : Poulain A. J., Garcia E., Amyot M., Campbell P. G. C., and Ariya, P.A

Revue : Manuscrit soumis à Geochimica et Cosmochimica Acta (Août 2006); Accepté sous réserve de révision en décembre 2006 (n° manuscrit: W4430)

Déclaration des coauteurs

À titre de coauteur de l'article identifié ci-dessus, je suis d'accord pour qu'Alexandre Poulain inclue cet article dans sa thèse de doctorat qui à pour titre « Spéciation et transformation rédox du Hg dans la neige et les eaux de surface des régions tempérées et polaires ».

Date :	Nom :	Signature :
November 24, 2006	Edmisse Garcia	[redacted]
15/12/2006	MARC AMYOT	
28 nov 2006	Peter Campbell	
Dec 15/06	P. A ARIYA	

Identification de l'étudiant

Alexandre Poulain [redacted]

Département des sciences biologiques, Faculté des arts et des sciences.

Ph.D. Sciences biologiques (3-235-1-0)

Directeur de thèse : Prof. Marc Amyot, Université de Montréal.

Co-Directeur de thèse : Prof. Peter G.C. Campbell, INRS-eau, terre & environnement.

Description de l'article

Titre : Redox transformations of mercury in an Arctic snowpack at springtime

Auteurs : Alexandre J. Poulain, Janick D. Lalonde, Marc Amyot, Justin A. Shead, Farhad Raofie, and Parisa A. Ariya

Revue : Atmospheric Environment (2004), vol. 38 : 6763-6774

Déclaration des coauteurs

À titre de coauteur de l'article identifié ci-dessus, je suis d'accord pour qu'Alexandre Poulain inclue cet article dans sa thèse de doctorat qui à pour titre « Spéciation et transformation rédox du Hg dans la neige et les eaux de surface des régions tempérées et polaires ».

Date :	Nom :	Signature :
November 24, 2006	Louise Garcia	[redacted]
15/12/2006	MARC AMYOT	
28 nov 2006	Peter Campbell	
December 17, 2006	Farhad Raofie	
Dec 15/06	P. A ARIYA	

Identification de l'étudiant

Alexandre Poulain [redacted]

Département des sciences biologiques, Faculté des arts et des sciences.

Ph.D. Sciences biologiques (3-235-1-0)

Directeur de thèse : Prof. Marc Amyot, Université de Montréal.

Co-Directeur de thèse : Prof. Peter G.C. Campbell, INRS-eau, terre & environnement.

Description de l'article

Titre : Redox transformations of mercury in an Arctic snowpack at springtime

Auteurs : Alexandre J. Poulain, Edenise Garcia, Marc Amyot, Peter G.C. Campbell, Farhad Raofie and Parisa A. Ariya

Revue : Manuscrit soumis à Environmental Science & Technlogy (Août 2006); Accepté sous réserve de révision en novembre 2006 (n° manuscrit : es061980bms). Resoumis le 12 décembre 2006

Déclaration des coauteurs

À titre de coauteur de l'article identifié ci-dessus, je suis d'accord pour qu'Alexandre Poulain inclue cet article dans sa thèse de doctorat qui à pour titre « Spéciation et transformation rédox du Hg dans la neige et les eaux de surface des régions tempérées et polaires ».

Date :	Nom :	Signature :
November 24, 2006	Edenise Garcia	[redacted]
15/12/2006	MARC AMYOT	
28 nov 2006	Peter Campbell	
Decembre 17, 2006	Farhad Raofie	
Dec 15/06	P. A ARIYA	

Identification de l'étudiant

Alexandre Poulain [redacted]

Département des sciences biologiques, Faculté des arts et des sciences.

Ph.D. Sciences biologiques (3-235-1-0)

Directeur de thèse : Prof. Marc Amyot, Université de Montréal.

Co-Directeur de thèse : Prof. Peter G.C. Campbell, INRS-eau, terre & environnement.

Description de l'article

Titre : A potential for mercury redox transformations by microbes in the high Arctic

Auteurs : Alexandre J. Poulain, Sinéad M. Ní Chadhain, Parisa A. Ariya, Marc Amyot, Edenise Garcia, Peter G.C. Campbell, Gerben J. Zylstra and Tamar Barkay

Revue : Manuscrit soumis à « Applied and Environmental Microbiology » le 20 Novembre 2006 (n° manuscrit : AEM02701-06).

Déclaration des coauteurs

À titre de coauteur de l'article identifié ci-dessus, je suis d'accord pour qu'Alexandre Poulain inclue cet article dans sa thèse de doctorat qui à pour titre « Spéciation et transformation rédox du Hg dans la neige et les eaux de surface des régions tempérées et polaires ».

Date :	Nom :	Signature :
25 Nov, 2006	Sinéad M. Ní Chadhain	[redacted]
Dec 15/06	P. A. ARIYA	
15/12/2006	MARC AMYOT	
November 24, 2006	Edenise Garcia	
28 nov 2006	Peter Campbell	
11/28/06	Gerben Zylstra	
Nov. 23, 2006	TAMAR BARKAY	

Identification de l'étudiant

Alexandre Poulain [redacted]

Département des sciences biologiques, Faculté des arts et des sciences.

Ph.D. Sciences biologiques (3-235-1-0)

Directeur de thèse : Prof. Marc Amyot, Université de Montréal.

Co-Directeur de thèse : Prof. Peter G.C. Campbell, INRS-eau, terre & environnement.

Description de l'article

Titre : Mercury (micro)biogeochemistry in polar environments

Auteurs : Tamar Barkay and Alexandre J. Poulain

Revue : Article sous presse dans FEMS Microbiology and Ecology

(n° manuscript: FEMSEC-06-05-0249)

Déclaration des coauteurs

À titre de coauteur de l'article identifié ci-dessus, je suis d'accord pour qu'Alexandre Poulain inclue cet article dans sa thèse de doctorat qui à pour titre « Spéciation et transformation rédox du Hg dans la neige et les eaux de surface des régions tempérées et polaires ».

Date :	Nom :	Signature :
Nov. 23, 2006	TAMAR BARKAY	[redacted]

Identification de l'étudiant

Alexandre Poulain [redacted]

Département des sciences biologiques, Faculté des arts et des sciences.

Ph.D. Sciences biologiques (3-235-1-0)

Directeur de thèse : Prof. Marc Amyot, Université de Montréal.

Co-Directeur de thèse : Prof. Peter G.C. Campbell, INRS-eau, terre & environnement.

Description de l'article

Titre : Influence of temperate mixed and deciduous tree covers on Hg concentrations and photoredox transformations in snow

Auteurs : Alexandre J. Poulain, Virginie Roy, & Marc Amyot

Revue : Manuscrit soumis à « Geochimica et Cosmochimica Acta » en décembre 2006 (n° manuscrit : W4656).

Déclaration des coauteurs

À titre de coauteur de l'article identifié ci-dessus, je suis d'accord pour qu'Alexandre Poulain inclue cet article dans sa thèse de doctorat qui à pour titre « Spéciation et transformation rédox du Hg dans la neige et les eaux de surface des régions tempérées et polaires ».

Date :	Nom :	Signature :
24/11/06	Roy Virginie	[redacted]
15/12/2006	MARC AMYOT	

Identification de l'étudiant

Alexandre Poulain [redacted]

Département des sciences biologiques, Faculté des arts et des sciences.

Ph.D. Sciences biologiques (3-235-1-0)

Directeur de thèse : Prof. Marc Amyot, Université de Montréal.

Co-Directeur de thèse : Prof. Peter G.C. Campbell, INRS-eau, terre & environnement.

Description de l'article

Titre : Diel variations in photo-induced oxidation of Hg^0 in freshwater

Auteurs : Edenise Garcia, Alexandre J. Poulain, Marc Amyot, and Parisa A. Ariya

Revue : Article publié dans Chemosphere (2005), vol. 59 :977-981

Déclaration des coauteurs

À titre de coauteur de l'article identifié ci-dessus, je suis d'accord pour qu'Alexandre Poulain inclue cet article dans sa thèse de doctorat qui à pour titre « Spéciation et transformations rédox du Hg dans la neige et les eaux de surface des régions tempérées et polaires ».

Date :	Nom :	Signature :
November 24, 2006	Edenise Garcia	[redacted]
15/12/2006	MARC AMYOT	
Dec 15/06	P. A ARIYA	

Avant propos.

Cette thèse comprend sept publications auxquelles ont participé différents auteurs. La contribution de chaque auteur est la suivante:

Article 1. Poulain A. J., Lalonde J. D., Amyot M., Shead J. A., Raofie F., and Ariya P. A. (2004) Redox transformations of mercury in an Arctic snowpack at springtime. *Atmospheric Environment* 38(39), 6763-6774.

A.J. Poulain : Conception du projet; échantillonnage sur le terrain; analyses des échantillons; traitement des données; rédaction initiale et finale.
J.D. Lalonde : rédaction finale.
M. Amyot : Conception du projet; rédaction finale.
J.A. Shead : échantillonnage sur le terrain; analyses des échantillons.
F. Raofie : analyse des composes organiques.
P.A. Ariya : Conception du projet, rédaction finale.

Article 2. Poulain A. J., Garcia E., Amyot M., Campbell P. G. C., and Ariya, P.A. Mercury distribution, partitioning and speciation in coastal vs inland snow of the high Arctic during snowmelt. Accepté à *Geochimica et Cosmochimica Acta* avec modifications mineures (Avril 2007).

A.J. Poulain : Conception du projet; échantillonnage sur le terrain; analyses des échantillons; traitement des données; rédaction initiale et finale.
E. Garcia : échantillonnage sur le terrain; rédaction finale du manuscrit.
P.G.C. Campbell : Conception du projet; rédaction finale.
M. Amyot : Conception du projet; rédaction finale.

Article 3. Poulain A. J., Roy V., Amyot M. 2007. Influence of tree cover on Hg dynamics in snow in a mixed forest. *In press*, *Geochimica et Cosmochimica Acta*.

A.J. Poulain: Conception du projet; échantillonnage sur le terrain; analyses des échantillons; traitement des données; rédaction initiale et finale.

V. Roy: échantillonnage sur le terrain; analyses des échantillons; rédaction finale.

M. Amyot: Conception du projet; rédaction initiale et finale.

Article 4. Poulain A. J., Garcia E., Ariya P. A., Raofie F., Campbell P. G. C., and Amyot M. 2007. Mercury biological and chemical redox transformations in fresh and salt waters of the High Arctic during spring and summer time. *Environmental Science & Technology,* 41 (6), 1883 -1888

A.J. Poulain: Conception du projet; échantillonnage sur le terrain; analyses des échantillons; traitement des données; rédaction initiale et finale.

E. Garcia: échantillonnage sur le terrain; rédaction finale du manuscrit.

P.A. Ariya: rédaction finale.

F. Raofie: analyse des composes organiques.

P.G.C. Campbell: Conception du projet; rédaction finale.

M. Amyot: Conception du projet; rédaction finale.

Article 5. Poulain A. J., Ni Chadhain S. M., Ariya P. A., Amyot M., Garcia E., Campbell P. G. C., Zylstra G., and Barkay T. 2007. Genes specifying mercury detoxification are expressed by microbes in the High Arctic. *Applied and Environmental Microbiology*.73(7):2230-8

1. Introduction

1.1. Les caractéristiques et propriétés du Hg

Le mercure (Hg, pour hydrargyrum, argent liquide) est le seul métal à être liquide à température ambiante. Ces principales caractéristiques physico-chimiques sont présentées dans le tableau 1.I.

Table 1.I.Propriétés physico-chimiques du Hg

Numéro atomique	80
Configuration électronique	[Xe] $4f^{14}$ $5d^{10}$ $6s^2$
Densité	13.5 $g \cdot cm^{-3}$
Constante de Henry (288K)	0.092 $mol \cdot kg^{-1} \cdot bar^{-1}$
Point de fusion	234.3 K (-38.8°C)
Point d'ébullition	629.9 K (356.7°C)
Electronégativité	2.00 (sur l'échelle de Pauling)
Rayon atomique	150 pm
Masse molaire	200.59 ($g \cdot mol^{-1}$)
Isotopes stables (abondance naturelle %)	^{196}Hg (0.15), ^{198}Hg (9.97), ^{199}Hg (16.87), ^{200}Hg (23.1), ^{201}Hg (13.18), ^{202}Hg (29.86), ^{204}Hg (6.87)

Il existe plusieurs formes de Hg dans l'environnement dont les trois formes principales sont le mercure élémentaire Hg^0, la forme inorganique ionisée Hg^{2+}, et le methylmercure CH_3Hg^+. Le mercure élémentaire est volatile et à tendance à quitter les écosystèmes aquatique via évasion. Sous sa forme ionique le Hg peut exister sous les états d'oxydation (+II) ou (+I); le Hg^+ est instable et n'existe que transitoirement sous la forme Hg_2^{2+}; sa dismutation conduit à la formation de Hg^0 et Hg^{2+}. Le Hg^{2+} est relativement très soluble et très réactif et se lie aux particules ainsi qu'aux ligands inorganiques et

organiques présents dans la phase dissoute. Les formes organiques de Hg (*e.g.* methyl-, dimethyl-, ethyl-, et phenyl- mercure) présente une liaison covalente entre le Hg et un atome de carbone. Certaines formes sont volatiles (e.g. dimethyl- et diethyl-mercure) et peuvent constituer une fraction mesurable du réservoir des formes dissoutes volatiles de Hg (DGM, *Dissolved Gaseous Mercury*) présentes dans les eaux naturelles.

Le mercure est un élément toxique, particulièrement sous sa forme méthylée. Une des démonstrations les plus dramatiques de l'impact du mercure envers les populations humaines a tristement été rendu célèbre lors de la catastrophe de la baie de Minamata dans les années 50. En effet, suite au rejet de methylmercure (CH_3Hg^+) par une usine chimique, plus d'une centaine de personnes sont décédées et plusieurs milliers ont développé des troubles neurologiques, en raison de la consommation de poissons contaminés (57). Cet exemple, dramatique, illustre les conséquences d'une contamination directe en methylmercure; cependant, en raison de sa capacité à voyager sur des très longues distances, le mercure peut être déposé loin des sources ponctuelles de pollution, être transformé en methylmercure *in situ*, et ainsi contaminer les chaines alimentaires des sites éloignés.

1.2. Origine et transport des différentes espèces de mercure

On peut distinguer deux voies majeures d'émission de Hg, i) anthropiques et ii) naturelles. Durant les 70 dernières années, les voies anthropiques ont été dominantes pouvant contribuer jusqu'à 70 % des émissions totales (77, 91, 92, 107). Les sources naturelles de mercure incluent, par exemple, les feux de forêt, les émissions volcaniques, ainsi que les émissions biogénique des océans. Dans le cas du Canada, pour lequel aucun volcan actif n'existe, Richardson et al. (2003) (85) ont estimé que les sources naturelles de Hg sont principalement représentées par les émissions de Hg(0) en provenance de la végétation (51%) ainsi que l'évasion directe de Hg(0) en

provenance du sol (45%). La contribution des sources naturelles dans le réservoir global de Hg est très difficile à établir en raison de la difficulté à quantifier les réémissions de Hg - initialement d'origine anthropique - en provenance du sol, de la végétation ou des écosystèmes aquatiques (85). Les émissions anthropiques de mercure sont majoritairement liées aux processus de combustion (incinérateurs municipaux, centrales thermiques utilisant des combustibles fossiles, rejets industriels, industries minières de l'or et de l'argent et, plus généralement, des industries chimiques utilisant des processus d'oxydoréduction de synthèse). A l'échelle globale, dans l'atmosphère, plus de 95% du Hg total est sous forme élémentaire, Hg^0, dont la concentration oscille entre 1.5 et 3.0 ng/m^3, laissant une faible part aux formes oxydées dont la majorité est associée aux particules (66). Cette proportion augmente cependant avec la proximité des sources directes d'émission tels les incinérateurs, pouvant atteindre 15% (117).

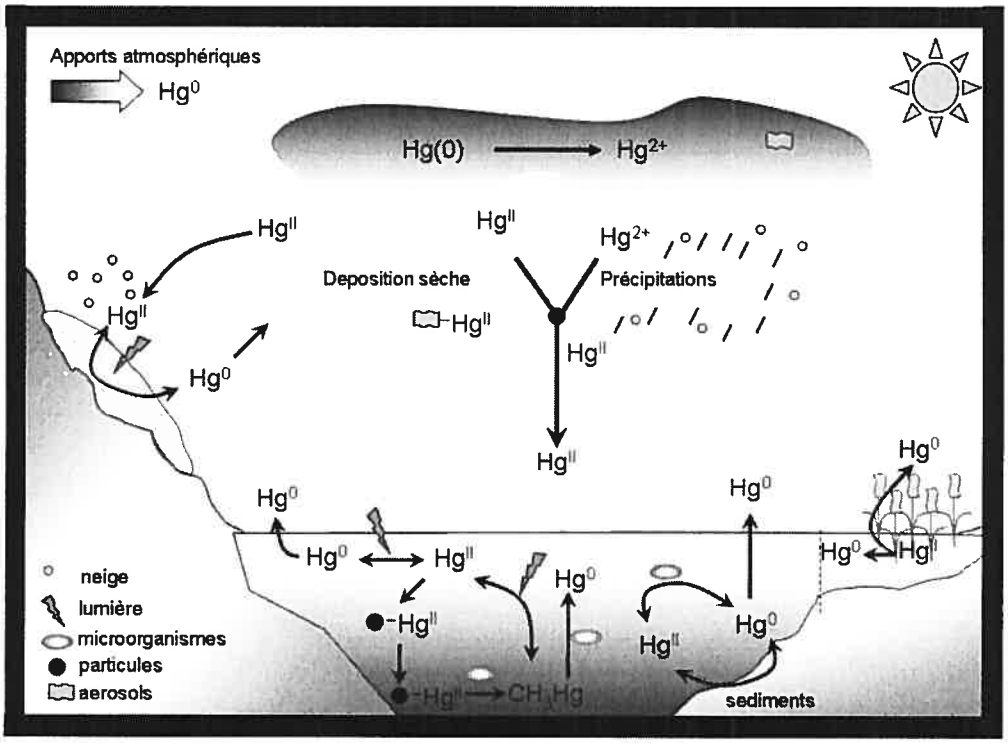

Figure 1.1. Présentation du cycle du Hg.

Le Hg(II) fortement associé aux aérosols, telles les particules de suies, a tendance à se déposer à proximité des zones d'émission. En revanche, le mercure élémentaire, forme volatile, peut voyager pendant 6 à 12 mois dans l'atmosphère (91, 107) en couvrant de très grandes distances. La plus grande part de l'oxydation du Hg(0) atmosphérique se produit soit aux interfaces solide/liquide dans les gouttelettes d'eau constitutives des nuages soit aux interfaces gaz/liquide (64). L'agent principal de ces réactions est l'ozone, mais l'intervention de radicaux tels OH·, ou d'oxydants tels HClO, HSO_3^- ou Cl_2 peut être significative (64). Dans les régions arctiques ou subarctiques les radicaux issus de brome (Br· et BrO·) prennent une place importante dans les processus d'oxydation rapide du Hg (6, 65) conduisant aux pertes de mercure atmosphériques (90).

Une fois oxydé, le Hg(II) posséde une forte affinité pour les surfaces et se retrouve associé aux particules présentes dans l'atmosphère, tels les aérosols. Les deux voies majeures s'offrant alors au mercure pour rejoindre la surface des écosystèmes sont soit les dépositions sèches soit les dépositions humides. On entend par dépositions humides, tous les phénomènes de précipitations telles les averses de pluie ou de neige qui peuvent entraîner le Hg(0) dissous ou le Hg(II) nouvellement oxydé vers la surface de la terre. Les dépositions sèches font référence à la déposition des aérosols.

1.3. Hg dans la neige

Dans la neige des régions tempérées, les concentrations en Hg varient entre < 1 $pmol \cdot L^{-1}$ jusqu'à ca. 60 $pmol \cdot L^{-1}$ (L = litre de neige fondue) à Little Rock Lake (36), dans la région des lacs expérimentaux (58), dans le nord du Wisconsin (62), ou dans la région de la ville de Québec (61)). Les concentrations en Hg dans la pluie sont généralement supérieures à ce qui est observé dans la neige et comprises entre 5 et 300 $pmol \cdot L^{-1}$ (49, 54, 101). Dans les régions polaires, les concentrations en Hg dans la neige sont généralement

basses et comprises en antarctique entre 0.5 et 5 pmol L^{-1} (96) et en arctique < 5 pmol·L^{-1} (65) jusqu'à 25 pmol·L^{-1} (102). Cependant, lors du lever du soleil polaire et ce jusqu'à la fonte des neiges, l'oxydation rapide et massive du Hg atmosphérique (90), phénomène connu sous le nom de « épisode de perte de mercure atmosphérique » (EPMA) ou « mercury depletion events » (MDE), contribue à augmenter les concentrations en Hg à la surface de la neige jusqu'à plus de 1000 fois les niveaux observés durant la nuit arctique (65, 67). De récentes études conduites à Barrow (Alaska, États-Unis) ont permis de mettre en évidence que ces niveaux pouvaient atteindre ca. 100 nmol•L^{-1} dans des cristaux dits « de vapeur » tels que les fleurs de givre et le givre de surface apparaissant lors de la formation de la banquise (26, 27). Un tel enrichissement proviendrait de l'action conjointe de l'oxydation massive du Hg atmosphérique durant les EPMA et de sa condensation sur les cristaux en formation à basse températures. Il est à noter que ces hautes concentrations ont été mises en évidence à proximité de zones d'eau libre telles les polynyes ou les failles dans la banquise.

Peu d'études, par analogie avec celles des systèmes aquatiques, ont permis d'évaluer la distribution ou la dynamique du Hg au sein d'une accumulation de neige. Lalonde et al. (58) ont mis en évidence, dans la région des lacs expérimentaux (ON, Canada), que les concentrations en Hg diminuaient avec la profondeur, atteignant les niveaux les plus bas aux interfaces neige/glace ou neige/sol. Susong et al. (2003) (106) dans l'un de leurs sites d'étude en Idaho ont cependant rapporté des concentrations en Hg à l'interface neige/sol 2-3 fois supérieure à celle enregistrée en surface (de 15 à 45 pmol L^{-1}; Tableau 1) et de manière similaire, à Station Nord au Groenland, Ferrari et al. (2004) (31) ont montré une augmentation des concentrations en Hg avec la profondeur. Cependant, les mécanismes impliqués dans cette distribution verticale du mercure restent inconnus.

basses et comprises en antarctique entre 0.5 et 5 pmol L^{-1} (96) et en arctique < 5 pmol·L^{-1} (65) jusqu'à 25 pmol·L^{-1} (102). Cependant, lors du lever du soleil polaire et ce jusqu'à la fonte des neiges, l'oxydation rapide et massive du Hg atmosphérique (90), phénomène connu sous le nom de « épisode de perte de mercure atmosphérique » (EPMA) ou « mercury depletion events » (MDE), contribue à augmenter les concentrations en Hg à la surface de la neige jusqu'à plus de 1000 fois les niveaux observés durant la nuit arctique (65, 67). De récentes études conduites à Barrow (Alaska, États-Unis) ont permis de mettre en évidence que ces niveaux pouvaient atteindre ca. 100 nmol•L^{-1} dans des cristaux dits « de vapeur » tels que les fleurs de givre et le givre de surface apparaissant lors de la formation de la banquise (26, 27). Un tel enrichissement proviendrait de l'action conjointe de l'oxydation massive du Hg atmosphérique durant les EPMA et de sa condensation sur les cristaux en formation à basse températures. Il est à noter que ces hautes concentrations ont été mises en évidence à proximité de zones d'eau libre telles les polynyes ou les failles dans la banquise.

Peu d'études, par analogie avec celles des systèmes aquatiques, ont permis d'évaluer la distribution ou la dynamique du Hg au sein d'une accumulation de neige. Lalonde et al. (58) ont mis en évidence, dans la région des lacs expérimentaux (ON, Canada), que les concentrations en Hg diminuaient avec la profondeur, atteignant les niveaux les plus bas aux interfaces neige/glace ou neige/sol. Susong et al. (2003) (106) dans l'un de leurs sites d'étude en Idaho ont cependant rapporté des concentrations en Hg à l'interface neige/sol 2-3 fois supérieure à celle enregistrée en surface (de 15 à 45 pmol L^{-1}; Tableau 1) et de manière similaire, à Station Nord au Groenland, Ferrari et al. (2004) (31) ont montré une augmentation des concentrations en Hg avec la profondeur. Cependant, les mécanismes impliqués dans cette distribution verticale du mercure restent inconnus.

Table 1.II. Distribution des concentrations en Hg en surface et en profondeur dans une accumulation de neige.

Sites	[Hg] pmol·L^{-1} en surface*	[Hg] pmol·L^{-1} en profondeur (cm)	Références
Lac 240, ELA, ON.	7	1 (< 50 cm)	(58)
Lac 240, ELA, ON*	4.5	1.7 (< 50 cm)	(58)
Pine Creek Pass. Sud est de l'Idaho.*	20-30	10-18 (100)	(106)
Ahston Hill. Sud est de l'Idaho. *	15	45 (140)	(106)
Station Nord, Groenland. DN.*	< LD	21 (85)	(31)

* litre de neige fondue

1.4. Transformations affectant le Hg dans l'eau et la neige

Une fois le Hg(II) présent à la surface des écosystèmes aquatiques et nivaux (= neigeux), trois grandes réactions peuvent contrôler son destin : i) son association aux particules et leur subséquente sédimentation/mouvement dans la colonne d'eau/de neige ii) sa réduction et iii) sa méthylation. Les réactions de réduction (photochimiques ou biologiques) et/ou son association aux particules permettent respectivement au Hg de quitter le système soit par évasion (i.e. traverser l'interface eau/air et rejoindre le réservoir de Hg atmosphérique) soit par sédimentation, alors que la méthylation conduit à la formation d'une neurotoxine, le methylmercure.

1.4.1. La méthylation et la déméthylation du Hg

L'importance relative entre les réactions de méthylation et de déméthylation contrôle la concentration en MeHg dans les écosystèmes aquatiques et donc le réservoir potentiellement bioaccumulable dans les réseaux trophiques.

La méthylation du Hg

La méthylation du Hg est principalement biologique (53), bien que certains auteurs aient suggéré des processus abiotiques, dépendants de la lumière (98), ou se produisant à l'obscurité (18). Jusqu'à récemment, il était admis que les microorganismes principalement impliqués dans les réactions de méthylation étaient les bactéries sulfato-réductrices (BSR) vivant en anaérobiose et utilisant le sulfate (SO_4^{2-}) comme accepteur terminal d'électron (44). Elles participent ainsi à la formation des espèces réduites de soufre, tels les sulfures (S^{2-}). Il a été suggéré que la méthylation était intimement liée au cycle de l'acetyl-coenzyme A (19). Bien que les BSR soient d'importants

méthylateurs, de récentes études remettent en question les voies métaboliques précédemment suggérées (29) et proposent de nouvelles alternatives impliquant les bactéries ferro-réductrices (37) ou les biofilms périphytiques (20).

La démethylation du Hg

Deux voies biologiques contrôlent la déméthylation du Hg, chacune caractérisée par les produits issus de ce métabolisme. La première voie, la déméthylation oxydative, conduit à la formation de Hg(II) et de CO_2 et serait un sous-produit du métabolisme des BSR et des méthanogènes (70). La seconde voie, la déméthylation réductive, conduit à la formation de CH_4 et de Hg(0) et est le résultat de l'activité des bactéries résistantes au Hg grâce à l'expression de l'opéron *mer*. Cet opéron est un ensemble de gènes codant notamment pour des protéines de transport du Hg, une lyase permettant de briser les liaisons C-Hg, une réductase permettant de réduite le Hg(II) en Hg(0) ainsi que de nombreux facteurs de régulation (9). En complément de ces voies biologiques, il a été démontré que le CH_3Hg pouvait être photodégradé (94) et impliquerait des radicaux hydroxyl ($OH^{\bullet}$) (41) ou l'oxygène singulet (104).

1.4.2. Le cycle redox du Hg

Les transformations biologiques [e.g. réduction par le *mer*-operon ou oxydation intra-cellulaire du Hg(II)] et les réactions abiotiques [e.g. réduction au noir, photoréduction, ou photooxydation], peuvent travailler de concert ou de manière antagoniste en vue d'alternativement réduire ou oxyder le Hg. Ces réactions peuvent se produire dans le but d'en réduire la toxicité [cas de l'opéron] ou lorsque les intermédiaires réactionnels [e.g. cofacteurs, matière organique, etc.], et catalyseurs [e.g. enzymes, énergie lumineuse, etc.] sont rassemblés. Ces réactions qu'elles soient biotiques ou abiotiques sont bien entendu fonction de la spéciation du Hg, i.e. de son état d'oxydation [Hg(II),

Hg(I) ou Hg(0)] et de son association avec les ligands inorganiques ou organiques présent dans le milieu [Hg-L]. Les réactions de réduction et d'oxydation peuvent i) contribuer au recyclage du Hg vers l'atmosphère à l'interface neige-eau/air ii) la limiter en entrant en compétition pour leur substrat commun ou iii) favoriser la methylation en produisant des formes biodisponibles.

Nous présenterons successivement les réactions de réduction puis les réactions d'oxydation pouvant influençant le cycle du Hg. Par souci de clarté et de concision, une synthèse de la littérature de ces réactions est présentée dans les tableaux 1.III et 1.IV. Le tableau 1.IV met l'accent sur le cycle redox du Hg en milieu froid; nous y avons inclus les réactions d'oxydation et de réduction se produisant dans la neige et l'atmosphère. Nous n'en décrirons ci-après que les points majeurs.

La réduction du mercure inorganique

La réduction abiotique du Hg en absence de lumière n'a été observée qu'en milieu anoxique, en absence de chlorure et en présence de substances humiques (1, 2); elle n'a jamais été observée dans la neige. De récentes études ont suggéré qu'elle serait importante dans les sédiments (39, 81). La voie abiotique principale conduisant à la réduction du Hg dans les eaux de surface est la photoréduction (4). La photoréduction du Hg peut être une réaction directe ou indirecte. L'importance relative des voies photochimiques directes [par exemple dans le cas d'un transfert de charge ligand-métal, (40)] ou indirectes [production de radicaux organiques ($RCOO^{\bullet}$) (120) ou inorganiques ($O_2^{-\bullet}$)] dans l'environnement reste cependant à déterminer (119, 120). La réduction photochimique du Hg dans la neige a été mise en évidence par Lalonde et al. (2002 et 2003). L'obtention du spectre d'action polychromatique de la réduction du Hg dans la neige a conduit Lalonde et al. (2003) à conclure que les rayonnements UVB étaient responsables de cette réaction, à l'instar de ce qui avait été observé dans les eaux de surface (4).

Comme présenté dans le Tableau 1.III, il a été démontré que les microorganismes, procaryotes ou eucaryotes, peuvent réduire le Hg directement ou indirectement. Les voies indirectes impliquent à la production de composés biogéniques qui servent d'intermédiaires réactionnels dans les réactions photochimiques (e.g. (63)). La réduction du Hg conduite par les organismes procaryotes peut être induite ou se produire de manière accidentelle. La voie induite est une forme de résistance bactérienne. Lorsque le seuil de tolérance intracellulaire en Hg est atteint, la transcription de l'opéron *mer* débute, conduisant à la synthèse de la réductase du Hg. Bien qu'en laboratoire, il ait été montré que des concentrations inférieures au $pmol \cdot L^{-1}$ puissent induire la réponse d'opérons de fusion (e.g *mer*-lux), les variables contrôlant la réponse de l'opéron *mer* en milieu naturel non contaminé restent encore à déterminer (97). Les algues peuvent aussi réduire le Hg grâce à des processus dépendant ou indépendant de la lumière et ces processus semblent contrôlés par des métabolites extracellulaires plutôt que par des voies enzymatiques spécifiques. Nos propres expériences sur les interactions entre le phytoplancton et le Hg dans un lac méso-oligotrophe du bouclier canadien ont permis de mettre en évidence la réduction du Hg lors de blooms métalimnétiques (83). Les mécanismes précis de cette réduction nous sont encore inconnus mais semblent liés à la photosynthèse ou au mode d'acquisition du carbone. Aucune étude, jusqu'à présent, n'a apporté d'indice quant à l'éventuel rôle des microorganismes sur la réduction du Hg dans la neige ou les eaux de fontes.

Table 1.III. Synthèse de la littérature présentant les différentes voies impliquées dans la réduction du Hg dans les eaux de surface.

Réactions	Gamme de concentrations	Acteurs	Laboratoire (L) milieu naturel (MN)	Références
ABIOTIQUE				
Photochimiques.				
Directe	$\mu mol \cdot L^{-1}$	HgS, HgO, Hg-L	L	(13, 75, 118, 40)
Indirecte	$pmol \cdot L^{-1}$	Hg + Matière Organique Naturelle (MON)	MN	(4, 38, 56, 78, 110)
	$pmol \cdot L^{-1}$	Hg + MON + Fe	MN	(120)
	$pmol \cdot L^{-1}$	MON (composés biogéniques de la diatomée marine *Chaetocerops sp*)	L	(63)
	$pmol \cdot L^{-1}$	Hg dans la neige	MN	(24, 58, 61, 102)
Obscurité.				
	$\mu mol \cdot L^{-1}$	Hg + acides humiques + anoxie	L	(1, 2)
	$pmol \cdot L^{-1}$	Hg + anoxie	MN	(39)
BIOTIQUES				
Bactéries	$\mu mol \cdot L^{-1}$	*mer*-operon	MN	(76, 8)
	$pmol \cdot L^{-1}$	Reductase	MN	(97)
	$\mu mol \cdot L^{-1}$	Cytochrome c Thiobacillus ferooxidans.	L	(52)
		Microbes < 0.3 µm	MN	(71)
	$\mu mol \cdot L^{-1}$	Bactéries réductrices des métaux	L	(115)
	$pmol \cdot L^{-1}$	anoxie, communauté microbienne non identifiée	MN	(81)
Algues	$\mu mol \cdot L^{-1}$	Euglena gracillis	L	(21)
	$\mu mol \cdot L^{-1}$	Chlorella sp.	L	(10)
	$pmol \cdot L^{-1}$	Phytoplancton marin	MN	(7)
	$pmol \cdot L^{-1}$	Phytoplancton mixotrophes	MN	(83)

L'oxydation du mercure élémentaire

Le Hg(0) peut être oxydé dans l'atmosphère lors de son transport (64) ou bien dans des conditions particulières telle que le lever du soleil polaire (28, 90). Lalonde et al. (2001 et 2004) (59, 60) ont mis en évidence la photo-oxydation du Hg(0) dans les eaux de surface, en milieu naturel et en laboratoire, sous l'action du rayonnement UV-A et en présence d'ions chlorure ou de molécule organiques telles que les benzoquinones. Ces mêmes auteurs ont proposé qu'en milieux saumâtres et pendant la période estivale, l'oxydation était, avant l'évasion, responsable de la perte de Hg(0). Grâce à une série d'élégantes expériences, Lalonde et al. (2003) (58) ont suggéré l'importance des ions chlorure dans l'oxydation du Hg(0) dans la neige, puisque suite à l'addition de KCl les auteurs ont observé une diminution de la production nette de Hg^0. Les études de Dommergue et al. (2003) (22) et de Ferrari et al (2004) (31) proposent, sans toutefois le démontrer, que l'oxydation soit une voie permettant de réduire les concentrations en Hg(0) au sein de l'accumulation de neige.
L'importance environnementale de l'oxydation biologique du Hg représente la voie de recherche la moins étudiée du cycle biogéochimique du Hg. Smith et al., (1998) (100) ont mis en évidence, chez *E.coli*, le rôle des hydroxyperoxydases bactériennes comme catalyseurs de l'oxydation du Hg. Siciliano et al. (2002) (97) ont récemment reliés l'activité de l'oxydase des communautés bactériennes et l'évolution des concentrations en Hg^0 dans les eaux de surface d'un lac du bouclier canadien.

Table 1.IV. Synthèse de la littérature présentant les différentes voies impliquées dans le cycle redox du Hg dans la neige et l'atmosphère.

Compartiments	Lieu	Substrat	Intermédiaires réactionnels	Références
RÉDUCTION				
Neige	Alpes françaises	Hg(II)	Lumière	(33)
	Sainte-Foy, QC	Hg(II)	UV-B	(61)
	Alert, NU	Reactive Gaseous Mercury (RGM)	Lumière	(102)
	ELA, ON	Hg(II)	UV-B	(58)
	Kuujjuarapik,QC	$HgCl_n^{2-n}$	Excès de Cl^- +lumière	(24)
OXYDATION				
Atmosphère	Alert, NU	Hg^0	O_3 – lumière	(90)
	Modélisation	Hg^0	Br_2 - BrCl - CH_2O -O_3 - BrO - ClO - lumière	(14-16)
	Alert, AK	Hg^0	O_3 – lumière	(67)
	Neumayer, Antarctica	Hg^0	O_3 – lumière	(28)
	Barrow, AK	Hg^0	Br_2 - BrCl - O_3 - BrO - ClO - $OH^·$ - cristal de neige - UV-B	(65)
	Station Nord, DN	Gaseous Elemental Mercury (GEM)	Cl - ClO - Br - BrO lumière	(99)
	Laboratoire	Hg^0	Halogènes (Br et Cl)	(6)
	Laboratoire	Hg^0	O_3	(80)
	Alert, NU	GEM	Lumière	(102)
Neige	Station Nord, DN	GEM	Lumière	(31)
	Kuujjuarapik, QC	GEM	Lumière	(24)
	ELA, ON	Hg^0	NaCl, lumière	(58)
	Resolute Bay, NU	Volatile Mercury in Snow (VMS)	UV radiations	(84)

1.5. Spéciation du Hg, prise en charge et notion de biodisponibilité.

Comme présenté précédemment, les réactions conduites par les microorganismes et qui influencent le cycle du Hg sont la réduction, l'oxydation la (dé)méthylation, ainsi que les réactions de complexation ou d'adsorption. Les mécanismes identifiés et associés à ces réactions biologiques se produisent dans l'espace intracellulaire (9, 44, 100), bien que d'autres puissent possiblement être extracellulaires, notamment chez les algues (83); une étape de prise en charge est donc, dans la plupart des cas, initialement nécessaire (voir Figure 1.2 pour les détails des réactions conduites par les microorganismes). De manière générale, dans les environnements aquatiques, trois facteurs clés doivent être maîtrisés afin d'appréhender les interactions métaux/organismes (108) : i) la spéciation du métal dans le milieu externe à la cellule, ii) les voies par lesquelles le métal est pris en charge par l'organisme considéré et iii) les effets du métal sur l'organisme. Dans le cadre de ce projet, les deux premiers aspects nous intéressent, i.e., la spéciation du mercure ainsi que le mécanisme de sa prise en charge puisque ceux-ci ont des conséquences majeures sur son cycle biogéochimique.

La spéciation d'un métal dans le milieu extracellulaire réfère, *stricto sensu*, à la nature des espèces chimiques présentes. Comme présenté précédemment, le mercure existe dans l'environnement sous des formes inorganiques (Hg(II), Hg(I), et Hg^0) et organiques (CH_3Hg, $(CH_3)_2Hg$) associées à des inorganiques et organiques. Les formes inorganiques, Hg(II) et Hg^0, nous intéressent particulièrement puisqu'elles sont impliquées, par nature, dans les transformations rédox. Cependant, dans un sens plus large, lorsque l'on parle de la spéciation chimique du Hg dans un environnement aquatique ou lorsque l'on réfère aux espèces de Hg biodisponibles, on associe souvent spéciation à la nature des complexes que le Hg forme avec les ligands inorganiques ou organiques en solution présents dans le milieu. La spéciation physique réfère à

l'évaluation de la distribution d'un métal entre les formes dissoutes, colloïdales ou particulaires.

Le Hg est un cation métallique de type B (tout comme l'Ag ou le Cd) et est décrit comme un cation « mou ». Ses interactions sont en partie de nature covalente et il se lie de préférence aux ligands ayant des atomes d'azote (N) et de soufre (S), ce qui lui confère sa toxicité lors, par exemple, de son association aux protéines entrainant des changements structuraux ou fonctionnels. En solution, un cation métallique n'est jamais réellement « libre », mais hydraté; sous l'effet de l'hydrolyse des molécules d'eau formant sa sphère d'hydratation, il se forme des hydroxocomplexes (e.g. $Hg(OH)_2,(H_2O)_4$). La complexation des ions métalliques avec d'autres ligands est en compétition avec l'hydrolyse (103). Les ligands inorganiques sont HCO_3^-, CO_3^{2-}, Cl^-, SO_4^{2-}, S^{2-}; ces derniers, les ions sulfures, ne sont présents qu'en milieu anoxique (rapidement oxydés en SO_4^{2-}), quoique de récentes études ont permis de mettre en évidence leur présence en milieu oxique par exemple sous forme d'agrégats métalliques (e.g. M_2S_4, M=métal; S=sulfure, (87)), ou plus vraisemblablement, suivant des considérations thermodynamiques, formant des complexes associés aux colloïdes (105). Les ligands organiques sont pour la plupart biogéniques. On peut par exemple citer les acides organiques de petite taille tels les acides aminés, les acides formiques ou acétiques, et les composés de grande taille et complexes tels les acides humiques ou fulviques.

L'importance relative des différents complexes de Hg présents à l'équilibre peut être estimée grâce à différents logiciels, dont MINEQL+(88), en tenant compte des concentrations présentes en solution ainsi que des constantes de complexation avec les ligands présents. Il est important de connaître l'importance relative des différentes espèces présentes puisque la concentration totale en Hg est un mauvais indicateur de sa biodisponibilité (55). Le seul mécanisme caractérisé et impliqué dans le transport actif du Hg(II) au travers de la membrane plasmique est conduit par des protéines codées par

l'opéron *mer* chez les organismes procaryotes. Bien que cet opéron ait été mis en évidence chez de nombreuses bactéries vivant dans les environnements aquatiques (9), la majorité des bactéries actuellement identifiées et impliquées dans le cycle du Hg, telles les sulfato-réductrice, ne possèdent pas cet opéron. Des voies alternatives, chez les BSR, permettant la prise en charge du Hg sont donc à considérer.

Deux écoles de pensée s'opposent encore actuellement en vue de décrire la prise en charge du Hg, particulièrement en anaérobiose, condition pour laquelle la méthylation est favorisée (44). La première est basée sur la diffusion de complexes neutres tels les complexes sulfidiques neutres (HgS^0) (11, 12) ou les chlorocomplexes ($HgCl_2$). Ces derniers complexes ont par exemple été mis en évidence lors du passage au travers de membranes artificielles (48) ou à l'aide d'étude sur les diatomées (72). Le transport actif d'espèces neutres ou positivement chargées, pourrait être facilité en présence d'une variété de composés organiques de faible poids moléculaire, tels des acides aminés (46). Notons que dans le cas proposé d'un transport actif non lié aux mécanismes de résistance, les transporteurs restent encore inconnus mais serait influencés par la présence d'autres métaux (45).

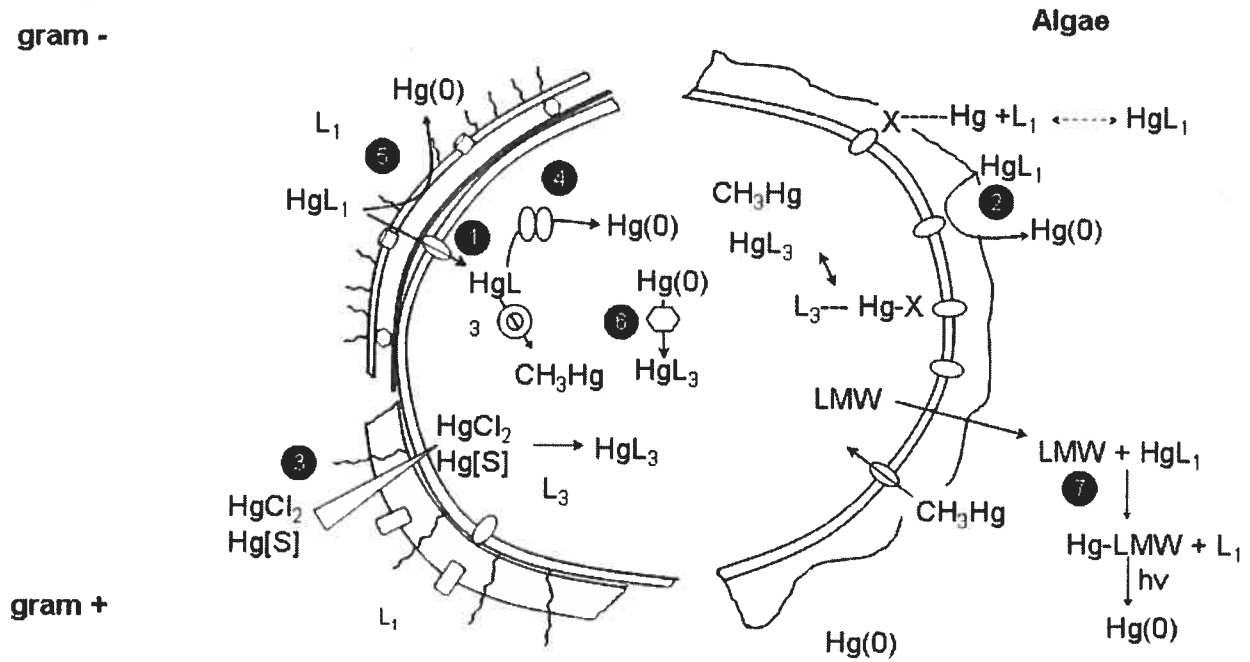

1 : Facilitated transport of Hg(II) (*Barkay et al. 1987*)
2 : Plasmalemma activity of phytoplankton (*Jones et al. 1987*)
3 : Diffusion of Hg (*Benoit et al. 1999*)
4 : merA Hg reduction (*Barkay et al. 1987*)
5 : Cyt c oxidase activity (*Iwahori et al. 2000*)
6 : Intracellular Hg(0) oxidation (*Smith et al. 1998*)
7 : Role of exudates (*Price and Morel 1990; Lanzillotta et al. 2004*)

Poulain A.J. unpublished

Figure 1.2. Transformations biologiques du Hg.

1.6. Problématique et objectifs de recherche.

1.6.1. Problématique

Le mercure est un polluant global posant des risques pour la santé humaine en raison de la toxicité de sa forme méthylée, bioaccumulée par les organismes et bioamplifiée dans les réseaux trophiques. De nombreux pays ont adopté des mesures visant à réglementer la consommation de poisson, principal vecteur de Hg des milieux aquatiques vers les populations humaines, et mettent en place des mesures visant à contrôler son émission dans l'environnement; au Canada, par exemple, la loi canadienne sur la protection de l'environnement [LCPE, 1999] comprend une section consacrée entièrement au contrôle des substances toxiques, incluant le mercure. Bien que les mesures de contrôle des émissions de Hg soient mis en place avec succès dans les pays développés notamment au Canada (diminution des émissions de 77% entre 1990 et 2000) (17), et que ces régulations soient rentables économiquement au niveau global (50), l'utilisation de la combustion du charbon pour la production d'énergie, notamment en Asie, contribue à une augmentation des émissions de Hg dans l'atmosphère (116). Plus de la moitié des dépositions de Hg dans l'hémisphère nord et particulièrement dans l'extrême Arctique est due à son transport en provenance des sources anthropiques notamment originaires d'Asie (109). De plus, il a été démontré que les épisodes de perte de Hg atmosphérique, précédemment décrits, contribuent à une augmentation nette de 44% des dépôts de Hg en Arctique, représentant sur une base annuelle 325 tonnes de Hg (5).

Il est important de mieux comprendre la dynamique et les transformations affectant le Hg dans la neige et les eaux de surface afin d'affiner la modélisation des flux aux interfaces eaux/neige/air. Ce pouvoir de prédiction accru permettra de mieux caractériser sur le plan écotoxicologique l'impact du Hg sur les

écosystèmes aquatiques récepteurs des eaux de fonte en vue de mieux prédire la bioaccumulation du Hg chez les organismes aquatiques; sur le plan géochimique ces données permettront d'affiner la reconstruction historique des dépositions atmosphériques de Hg utilisant les carottes de glace, archives conservées dans les glaciers formés suite à l'accumulation de neige. Ces différents aspects sont discutés ci-dessous.

Le cycle du Hg & l'extrême Arctique.

L'Arctique était considéré autrefois comme un environnement sain. Cependant, durant les 20 dernières années, des travaux y ont mis en évidence des niveaux particulièrement élevés de composés chimiques d'origine industrielle et agricole. Ces contaminants incluent des composés organiques, tels les organochlorés ou les ignifugeants bromés, les métaux et les radionucléides. La contamination de l'écosystème arctique a été mise en évidence dans l'air, les eaux de surface, les sédiments, la neige, les poissons, les mammifères et les oiseaux marins, ainsi que chez les plantes et les animaux terrestres (68). Un nombre croissant d'études associe cette contamination aux changements environnementaux qui affectent tout particulièrement les hautes latitudes (69, 89). Ces changements affectent notamment la pression atmosphérique au niveau de la mer, le mouvement des masses d'air, la dérive des glaces, la date d'initiation et la longueur de la saison de fonte des neiges, et l'intensité et la nature des précipitations (69). La diminution des concentrations en ozone stratosphérique conjuguée à la clarté des écosystèmes aquatiques arctiques rend ces derniers particulièrement sensibles aux radiations ultraviolettes (89). En plus du transport sur de longues distances de polluants originaires des basses latitudes, le développement rapide des activités anthropiques dans le nord (activités minières associées à l'exploration et à l'exploitation de ressources naturelles comme le gaz, le pétrole, les métaux ou les diamants) apporte un stress supplémentaire aux écosystèmes nordiques.

Bien que ces changements affectent de manière dramatique les écosystèmes aquatiques, les écosystèmes terrestres, probablement à plus long terme, seront aussi affectés. Des températures plus élevées vont entraîner la fonte du pergélisol favorisant la croissance de la végétation arbustive ligneuse ainsi que la migration vers le nord de la limite forestière (95). Des variations dans les patterns de dominance des espèces végétales ont déjà été observées. Par exemple, dans le nord-ouest canadien, les populations de feuillus (Quercus, chêne) sont remplacées par des conifères (Abies, sapin), plus résistants et ayant une stratégie de colonisation plus efficace (43). Il ressort clairement, à la vue de ces quelques exemples, que l'ensemble des écosystèmes nordiques et typiquement canadiens est particulièrement vulnérable aux changements environnementaux. Ces derniers affectent notamment les voies par lesquelles les contaminants entrent dans les écosystèmes terrestres et aquatiques et influencent ainsi les transformations biogéochimiques qui affectent leur devenir. Afin de mieux prédire l'influence de ces changements sur le cycle du Hg, il est donc nécessaire de mieux caractériser les variables influençant les transformations qui en affectent le cycle.

Le cycle du Hg & la forêt boréale.

Au cours des 5 dernières années, un grand nombre d'études a déjà été conduit en Arctique et en Antarctique en vue de mieux y comprendre la dynamique du Hg; l'avènement prochain de l'année internationale polaire, canalisant les efforts de chercheurs internationaux en une campagne internationale intense d'observation et d'analyse des composantes chimiques, physiques et biologiques des régions polaires, rend compte de la mobilisation générale de la communauté scientifique envers les écosystèmes nordiques. Cependant, bien que i) le Canada soit recouvert de neige pendant environ 5 mois par année, ii) les forêts du Canada représentent 10% des ressources forestières mondiales et le quart de l'ensemble des forêts boréales et iii) celles-

ci couvrent environ 45% de la superficie terrestre du Canada (418 millions d'hectares), seulement deux études ont été menées, au Québec et en Ontario, afin de comprendre la dynamique du Hg dans la neige (58, 61). Aucune n'a traité de la dynamique du Hg dans la neige sous un couvert forestier. La pêche récréative est une activité très populaire au Canada et peut poser des risques aux consommateurs de poissons en raison de niveaux de Hg trop élevés. Il est donc crucial de mieux comprendre quelles sont les transformations qui contrôlent le devenir du mercure en milieu forestier durant l'hiver ainsi que l'influence du type de végétation sur ces transformations afin de mieux pouvoir prédire l'impact du Hg sur les écosystèmes récepteurs de l'eau de fonte drainant les bassins versants des lacs dédiés à la pêche récréative.

Le cycle du Hg & les carottes de glace.

Les informations historiques conservées dans les carottes des glaces tempérées et polaires permettent de reconstituer l'évolution temporelle des dépositions de métaux comme le mercure ou le plomb (51). En différents endroits du globe, e.g. aux Etats-Unis (92) ou en Antarctique (112), l'utilisation des archives glaciaires indiquent au cours du siècle dernier une augmentation de la fraction anthropique dans le réservoir de Hg atmosphérique, bien qu'une diminution soit observée au cours des 10 dernières années (92). Ces archives, indicatrices de la contamination passée, sont parfois controversées (35), mais importantes lors du développement de réglementations visant le contrôle des émissions industrielles de Hg puisqu'elles permettent de relier la contribution des sources anthropiques de Hg aux patrons de déposition observés sur la planète. Une meilleure connaissance des transformations affectant le cycle du Hg contribuera à l'interprétation des enregistrements historiques stockés dans les glaciers. En effet, ces derniers sont formés lors de l'accumulation d'eau solide résultant de la transformation de la neige en glace. Par conséquent, une

bonne compréhension des processus gouvernant la mobilité et la nature chimique des contaminants dans la neige et les eaux de fonte est primordiale.

1.6.2. Objectifs de recherche

Afin de mieux appréhender la dynamique du Hg dans la neige et les eaux de surface et ainsi apporter des éléments de réponse à la problématique énoncée précédemment, nous avons souhaité i) déterminer la distribution des espèces inorganiques de Hg dans la neige déposée dans les sites côtiers et intérieurs de l'extrême arctique mais aussi dans les zones forestières et dépourvues de végétation des milieux tempérés et ii) déterminer l'importance relative des réactions d'oxydation et de réduction, contrôlant le recyclage du Hg vers l'atmosphère, ainsi que la contribution relative des processus photochimiques et microbiologiques dans ces transformations rédox.

Cette thèse est composée de 7 articles (dont deux en annexes) traitant de la dynamique du Hg en régions polaires et tempérées. Selon une suite logique elle a permis de répondre aux objectifs suivants :

- Déterminer les transformations rédox qui affectent le Hg dans une accumulation de neige en extrême Arctique au printemps.
- Évaluer la distribution des espèces de Hg dans la neige de l'extrême Arctique.
- Déterminer, en milieu tempéré, l'influence du couvert forestier sur la dynamique du Hg dans la neige
- Comprendre l'importance relative des transformations chimiques et biologiques du Hg dans les eaux douces et salées de l'extrême Arctique au printemps et en été.
- Évaluer l'importance des bactéries dans le cycle du Hg dans l'extrême Arctique grâce à l'expression de gènes de résistance au Hg.

En annexe nous proposons deux articles. Le premier traite des variations journalières du cycle photo-rédox du Hg dans les eaux douce de surface en régions tempérées et le second est une synthèse de la littérature « (micro)biogeochemistry of mercury in polar environments » qui résume l'état des connaissances sur le rôle des microbes en région polaire et propose de nouvelles avenues de recherche.

Pour chacun de ces articles, nous présentons ci-dessous une brève mise en contexte ainsi que les objectifs de recherche spécifiques.

Article 1 : Redox transformations of mercury in an Arctic snowpack at springtime

A l'instar de ce qui a été observé dans les eaux de surface (4), le mercure est très dynamique dans la neige (61). En effet, en raison de la photoréduction du Hg(II) en Hg^0, forme volatile, et sa subséquente évasion vers l'atmosphère, on a pu observer d'importantes diminutions des concentrations en Hg dans la neige de surface déposée sur un lac gelé, notamment dans les régions tempérées. Ce processus a été par la suite invoqué pour expliquer la diminution des concentrations en mercure total à la surface de la neige suite aux épisodes de pertes de Hg^0 atmosphérique (23, 24, 30-32, 34, 65, 102). Une fois formé, le Hg^0 peut soit quitter l'accumulation de neige via évasion, soit être ré-oxydé en Hg(II). En régions tempérées, l'oxydation du Hg^0 a été mis en évidence dans les eaux du fleuve Saint-Laurent (59, 60) et associée à la présence d'ions chlorure. Afin de mieux comprendre l'importance des réactions de réduction et d'oxydation dans la neige sur le cycle du Hg nous avons i) établi la dynamique temporelle du mercure total et du Hg^0 à la surface et au sein d'une accumulation de neige et ii) déterminé si la photooxydation du Hg^0 était un processus important dans une accumulation de neige.

Article 2 : Mercury partitioning and speciation in snow of the High Arctic during snowmelt

Les pertes de mercure atmosphérique dans les régions polaires et sub-polaires (24, 28, 67, 82, 90, 102) entraînent lors du printemps arctique une diminution rapide des niveaux de Hg^0 dans l'atmosphère suite à son oxydation massive. Ce phénomène contribue à augmenter les niveaux de Hg dans la neige de surface jusqu'à des niveaux jamais observés aussi loin de sources ponctuelles de pollution (27, 65, 67). Cette oxydation massive du Hg^0 aurait tendance à se produire en milieu marin (ou dans des environnements sous forte influence marine), sites pour lesquels les plus hauts niveaux de Hg dans la neige ont été rapportés (27), et impliquerait des espèces halogénées réactives provenant des aérosols marins (65). De récentes études ont montré que l'oxydation du Hg^0 par les radicaux issus des espèces bromées (telles $Br^{\bullet}$ ou $BrO^{\bullet}$) permettrait d'expliquer la rapidité de ces réactions (6). Les produits principaux de cette oxydation massive du Hg^0 seraient des espèces réactives gazeuses de Hg (RGM, HgX_2, X = halogène) et des espèces particulaires (part. Hg) (42, 90).

Les transformations atmosphériques du Hg affectent donc potentiellement la spéciation du Hg dans la neige de surface, mais la distribution et la nature des formes dissoutes et particulaires de Hg est inconnue. De plus, en raison de la dynamique unique du Hg en milieu marin et de la physiographie de l'extrême Arctique canadien (i.e., un archipel), il est nécessaire de mieux caractériser la dynamique du Hg dans ces environnements contrastés. Dans le cadre de ce premier chapitre, nos objectifs étaient donc d'établir la distribution et la spéciation du Hg (en solution et associé aux particules) dans la neige de surface déposée à l'intérieur des terres et sur la banquise suivant un transect de 100 km englobant deux zones côtières. Nous avons aussi examiné le rôle des interfaces neige/glace afin de déterminer leur potentiel d'accumulation du Hg.

Article 3. Hg dynamics in snow in a mixed forest watershed

Ce n'est que tout récemment que Lalonde et al. (2002 and 2003) ont mis en évidence que le Hg était dynamique dans la neige, grâce à la photoréduction du Hg nouvellement déposé et sa subséquente évasion vers l'atmosphère, processus qui par la suite à été mis en évidence dans l'extrême Arctique (24, 65, 84). Bien que ces études soulignent une composante importante du cycle biogéochimique du Hg, elles se sont principalement intéressées à la neige déposée dans des sites dégagés et fortement éclairés comme la toundra arctique ou la surface gelée d'un lac, donc maximisant l'impact des réactions photochimiques. Bien que des études aient montré l'importance d'un couvert forestier sur le cycle du Hg (47, 101), aucune n'a permis de mieux appréhender les transformations affectant le Hg dans la neige déposée sous un couvert forestier.

En comparant un milieu dit « ouvert » (la surface d'un lac gelé) et un milieu dit « fermé » (la forêt), les objectifs de cette étude sont de i) examiner l'influence de différents types de canopée sur la distribution des espèces de Hg dans la neige, ii) déterminer la distribution des concentrations en mercure total en profondeur et dans chacune des strates constitutives d'une accumulation de neige, iii) de déterminer l'importance relative des réactions de réduction et d'oxydation à chacun des sites et iv) modéliser les flux de Hg dans une accumulation de neige afin de déterminer si, pour chacun des sites choisis, l'accumulation de neige est une source ou un puits de mercure.

Article 4: Mercury biological and chemical redox transformations in fresh and salt waters of the high Arctic during spring and summer time

Les épisodes de pertes de Hg^0 atmosphérique sont une menace envers les écosystèmes arctiques en raison des hauts niveaux enregistrés dans la neige mais aussi car les produits de cette oxydation massive semblent être particulièrement biodisponibles (93). De plus, un nombre croissant d'études

documente une augmentation de la contamination en Hg des réseaux alimentaires arctiques (74) ainsi qu'une exposition croissante des populations humaines au Hg (111). La plupart des travaux conduits dans l'extrême Arctique a mis l'accent sur les transformations affectant le Hg dans la neige durant l'hiver (23-26, 32, 34, 65, 102) ou dans les lacs durant l'été (3, 110). Peu d'études ont traité du cycle redox du Hg durant la période de fonte des neiges (23, 65), et aucune ne s'est intéressée aux mares de la toundra arctique ou au ruisseaux durant l'été. Bien que la littérature fasse mention du rôle des microorganismes sur le cycle redox du Hg (9, 10, 71, 83, 86), aucune étude n'a permis de mettre en évidence l'implication des microorganismes sur le cycle du Hg en régions polaires.

L'objectif de cette étude était i) de déterminer les variables environnementales influençant les processus photorédox dans les eaux douces et salées de l'extrême Arctique et ii) de déterminer l'importance des algues et des tapis microbiens dans le cycle du Hg.

Article 5. Genes specifying mercury detoxification are expressed by microbes in the high Arctic

A l'instar des réactions photochimiques, la reductase du Hg (merA) affecte la mobilité et la biodisponibilité du Hg en convertissant le mercure inorganique ou le methylmercure en mercure élémentaire. La résistance au Hg, codée génétiquement, est répandue parmi les microorganismes (79) et présente dans des environnements extrêmes tels les sources hydrothermales (114) ou le permafrost ancien datant du Pleistocène (73). Cependant, peu d'études rapportent l'expression des gènes codant pour la réductase du Hg en milieux non contaminé (97) et aucune étude n'a considéré le rôle des microorganismes psychrotrophes ou psychrophiles dans le cycle redox du Hg.

Le but de cette étude était de i) déterminer si les gènes de la réductase du Hg étaient présents et exprimés chez les organismes procaryotes adaptés

aux régions polaires et ii) modéliser l'importance relative de la réduction photochimique et microbienne du Hg dans les eaux de l'extrême Arctique.

Article 6. Diel variations in photoinduced oxidation of Hg^0 in freshwater (annexe)

Les transformations affectant l'importance relative des formes réduites et oxydées de Hg jouent un rôle important en vue de contrôler son devenir dans l'environnement. La réduction du Hg(II) en Hg^0, volatile, a été identifiée comme un mécanisme important de perte de Hg vers l'atmosphère (113). En revanche, l'oxydation du Hg tend à augmenter le temps de séjour du Hg dans les écosystèmes, ultimement affectant son accumulation par les organismes aquatiques. Les radiations solaires dans la gamme des UV et du visible influencent la production de Hg^0 et l'on peut observer un cycle journalier dans les concentrations en Hg^0 avec les concentrations maximales observées à midi. Bien que les variables environnementales responsables de la réduction du Hg (e.g., qualité de la matière organique, pH, [Fe], présence de la réductase du Hg, concentration des exsudats biogéniques) ou de son oxydation (e.g. rôle des semi-quinones ou de [Cl^-]) tendent à être mieux connues, les réactions d'oxydation et leur importance au cours de la journée restent cependant les moins étudiées.

L'objectif de cette étude est d'examiner les variations journalières des taux d'oxydation photo-induite du Hg^0 à des niveaux naturels afin de contribuer à une meilleure compréhension de l'importance relative de l'oxydation et de la réduction dans les systèmes naturels.

Article 7 : Mercury (micro)biogeochemistry in polar environments (annexe)

Bien que la contamination des écosystèmes polaires par le Hg soit avérée, les voies microbiennes par lesquels le Hg est transformé restent mal connues. Dans ce chapitre de revue de littérature, nous proposons une

synthèse des connaissances et nous proposons des avenues de recherche sur les processus régissant les transformations du Hg aux hautes latitudes. Pour ce faire, nous avons mis en relation les connaissances dont nous disposions sur i) le cycle du Hg en milieu polaire, ii) la microbiologie des environnements froids et iii) le rôle des microbes dans les transformations du Hg en régions tempérées.

1.7. Références bibliographiques.

1. **Alberts, J. J., J. E. Schindler, R. W. Miller, and D. E. Nutter.** 1974. Elemental mercury production mediated by humic substances. Science **184:**895-897.
2. **Allard, B., and I. Arsenie.** 1991. Abiotic Reduction of Mercury by Humic Substances in Aquatic System - an Important Process for the Mercury Cycle. Water Air and Soil Pollution **56:**457-464.
3. **Amyot, M., D. Lean, and G. Mierle.** 1997. Photochemical formation of volatile mercury in high Arctic lakes. Environmental Toxicology and Chemistry **16:**2054-2063.
4. **Amyot, M., G. Mierle, D. R. S. Lean, and D. J. McQueen.** 1994. Sunlight-Induced Formation of Dissolved Gaseous Mercury in Lake Waters. Environmental Science & Technology **28:**2366-2371.
5. **Ariya, P. A., A. P. Dastoor, M. Amyot, W. H. Schroeder, L. Barrie, K. Anlauf, F. Raofie, A. Ryzhkov, D. Davignon, J. Lalonde, and A. Steffen**. 2004. The Arctic: a sink for mercury. Tellus Series B-Chemical and Physical Meteorology 56:397-403.
6. **Ariya, P. A., A. Khalizov, and A. Gidas.** 2002. Reactions of gaseous mercury with atomic and molecular halogens: Kinetics, product studies, and atmospheric implications. Journal of Physical Chemistry A **106:**7310-7320.
7. **Baeyens, W., and M. Leermakers.** 1998. Elemental mercury concentrations and formation rates in the Scheldt estuary and the North Sea. Marine Chemistry **60:**257-266.
8. **Barkay, T., C. Liebert, and M. Gillman.** 1989. Environmental Significance of the Potential for Mer(Tn21)-Mediated Reduction of Hg-2+ to Hg-0 in Natural-Waters. Applied and Environmental Microbiology **55:**1196-1202.
9. **Barkay, T., S. M. Miller, and A. O. Summers.** 2003. Bacterial mercury resistance from atoms to ecosystems. Fems Microbiology Reviews **27:**355-384.

10. **Ben-Bassat, D., and A. M. Mayer.** 1978. Light induced Hg volatilization and O2 evolution in Chlorella and the effect of DCMU and methylamine. Physiol. Plant **42:**33-38.
11. **Benoit, J. M., C. C. Gilmour, and R. P. Mason.** 2001. Aspects of bioavailability of mercury for methylation in pure cultures of Desulfobulbus propionicus (1pr3). Applied and Environmental Microbiology **67:**51-58.
12. **Benoit, J. M., C. C. Gilmour, R. P. Mason, and A. Heyes.** 1999. Sulfide controls on mercury speciation and bioavailability to methylating bacteria in sediment pore waters. Environmental Science & Technology **33:**951-957.
13. **Brosset, C.** 1987. The Behavior of Mercury in the Physical-Environment. Water Air and Soil Pollution **34:**145-166.
14. **Calvert, J. G., and S. E. Lindberg.** 2005. Mechanisms of mercury removal by O-3 and OH in the atmosphere. Atmospheric Environment **39:**3355-3367.
15. **Calvert, J. G., and S. E. Lindberg.** 2003. A modeling study of the mechanism of the halogen-ozone-mercury homogeneous reactions in the troposphere during the polar spring. Atmospheric Environment **37:**4467-4481.
16. **Calvert, J. G., and S. E. Lindberg.** 2004. The potential influence of iodine-containing compounds on the chemistry of the troposphere in the polar spring. II. Mercury depletion. Atmospheric Environment **38:**5105-5116.
17. **Canada, E.** 2005-04-11 2005, posting date. Substances toxiques, Inventaire détaillé du mercure: Émissions canadiennes de mercure dans l'atmosphère. Bureau national des indicateurs et des rapports environnementaux. [Online.]
18. **Celo, V., D. R. S. Lean, and S. L. Scott.** 2006. Abiotic methylation of mercury in the aquatic environment. Science of the Total Environment **368:**126-137.
19. **Compeau, G. C., and R. Bartha.** 1985. Sulfate-reducing bacteria: principle methylators of mercury in anoxic estuarine sediment. Applied and Environmental Microbiology **50:**498-502.
20. **Desrosiers, M., D. Planas, and A. Mucci.** 2006. Mercury methylation in the epilithon of boreal shield aquatic ecosystems. Environmental Science & Technology **40:**1540-1546.
21. **Devars, S., C. Aviles, C. Cervantes, and R. Moreno-Sanchez.** 2000. Mercury uptake and removal by Euglena gracilis. Archives of Microbiology **174:**175-180.
22. **Dommergue, A., C. P. Ferrari, and C. F. Boutron.** 2003. First investigation of an original device dedicated to the determination of gaseous mercury in interstitial air in snow. Analytical and Bioanalytical Chemistry **375:**106-111.
23. **Dommergue, A., C. P. Ferrari, P. A. Gauchard, C. F. Boutron, L. Poissant, M. Pilote, P. Jitaru, and F. C. Adams**. 2003. The fate of

mercury species in a sub-arctic snowpack during snowmelt. Geophysical Research Letters 30.

24. **Dommergue, A., C. P. Ferrari, L. Poissant, P. A. Gauchard, and C. F. Boutron.** 2003. Diurnal cycles of gaseous mercury within the snowpack at Kuujjuarapik/Whapmagoostui, Quebec, Canada. Environmental Science & Technology **37:**3289-3297.
25. **Douglas, T. A., and M. Sturm.** 2004. Arctic haze, mercury and the chemical composition of snow across northwestern Alaska. Atmospheric Environment **38:**805-820.
26. **Douglas, T. A., M. Sturm, W. R. Simpson, J. D. Blum, L. Alvarez-Aviles, D. Perovich, G. J. Keeler, A. Lammers, and A. Biswas.** 2006. Mercury deposition to snow and ice in Northern Alaska: Exploring the link between the lower atmosphere and the Cryosphere, Eight international conference on mercury as a global pollutant, Madison, WI, USA.
27. **Douglas, T. A., M. Sturm, W. R. Simpson, S. Brooks, S. E. Lindberg, and D. K. Perovich.** 2005. Elevated mercury measured in snow and frost flowers near Arctic sea ice leads. Geophysical Research Letters **32**.
28. Ebinghaus, R., H. H. Kock, C. Temme, J. W. Einax, A. G. Lowe, A. Richter, J. P. Burrows, and W. H. Schroeder. 2002. Antarctic springtime depletion of atmospheric mercury. Environmental Science & Technology 36:1238-1244.
29. **Ekstrom, E. B., F. M. M. Morel, and J. M. Benoit.** 2003. Mercury methylation independent of the acetyl-coenzyme a pathway in sulfate-reducing bacteria. Applied and Environmental Microbiology **69:**5414-5422.
30. **Fain, X., C. P. Ferrari, P. A. Gauchard, O. Magand, and C. Boutron.** 2006. Fast depletion of gaseous elemental mercury in the Kongsvegen Glacier snowpack in Svalbard. Geophysical Research Letters **33**.
31. **Ferrari, C. P., A. Dommergue, C. Boutron, P. Jitaru, and F. C. Adams.** 2004. Profiles of Mercury in the snow pack at Station Nord, Greenland, shortly after polar sunrise. Geophysical Research Letters **31:**L03401.
32. **Ferrari, C. P., A. Dommergue, C. F. Boutron, H. Skov, M. Goodsite, and B. Jensen.** 2004. Nighttime production of elemental gaseous mercury in interstitial air of snow at Station Nord, Greenland. Atmospheric Environment **38:**2727-2735.
33. **Ferrari, C. P., A. Dommergue, A. Veysseyre, F. Planchon, and C. F. Boutron.** 2002. Mercury speciation in the French seasonal snow cover. Science of the Total Environment **287:**61-69.
34. **Ferrari, C. P., P. A. Gauchard, K. Aspmo, A. Dommergue, O. Magand, E. Bahlmann, S. Nagorski, C. Temme, R. Ebinghaus, A. Steffen, C. Banic, T. Berg, F. Planchon, C. Barbante, P. Cescon, and C. F. Boutron**. 2005. Snow-to-air exchanges of mercury in an Arctic seasonal snow pack in Ny-Alesund, Svalbard. Atmospheric Environment 39:7633-7645.

35. **Fitzgerald, W. F., D. R. Engstrom, R. P. Mason, and E. A. Nater.** 1998. Case for atmospheric mercury contamination in remote areas. Environmental Science & Technology **32:**1-7.
36. **Fitzgerald, W. F., R. P. Mason, and G. M. Vandal.** 1991. Atmospheric Cycling and Air-Water Exchange of Mercury over Midcontinental Lacustrine Regions. Water Air and Soil Pollution **56:**745-767.
37. **Fleming, E. J., E. E. Mack, P. G. Green, and D. C. Nelson.** 2006. Mercury methylation from unexpected sources: Molybdate-inhibited freshwater sediments and an iron-reducing bacterium. Applied and Environmental Microbiology **72:**457-464.
38. **Garcia, E., M. Amyot, and P. A. Ariya.** 2005. Relationship between DOC photochemistry and mercury redox transformations in temperate lakes and wetlands. Geochimica et Cosmochimica Acta **69:**1917-1924.
39. **Garcia, E., J. Laroulandie, X. R. Saint-Simon, and M. Amyot.** 2006. Temporal and spatial distribution and production of dissolved gaseous mercury in the Bay St. Francois wetland, in the St. Lawrence River, Quebec, Canada. Geochimica et Cosmochimica Acta **70:**2665-2678.
40. **Gardfeldt, K., and M. Jonsson.** 2003. Is bimolecular reduction of Hg(II) complexes possible in aqueous systems of environmental importance. Journal of Physical Chemistry A **107:**4478-4482.
41. **Gardfeldt, K., J. Sommar, D. Stromberg, and X. B. Feng.** 2001. Oxidation of atomic mercury by hydroxyl radicals and photoinduced decomposition of methylmercury in the aqueous phase. Atmospheric Environment **35:**3039-3047.
42. **Gauchard, P. A., C. P. Ferrari, A. Dommergue, L. Poissant, M. Pilote, G. Guehenneux, C. F. Boutron, and P. Baussand.** 2005. Atmospheric particle evolution during a nighttime atmospheric mercury depletion event in sub-arctic at kuujjuarapik/Whapmagoostui, Quebec, Canada. Science of the Total Environment **336:**215-224.
43. **Gedalof, Z., M. Pellatt, and D. J. Smith.** 2006. From prairie to forest: Three centuries of environmental change at Rocky Point, Vancouver Island, British Columbia. Northwest Science **80:**34-46.
44. **Gilmour, C. C., E. A. Henry, and R. Mitchell.** 1992. Sulfate stimulation of mercury methylation in freshwater sediments. Environmental Science and Technology **26:**2281-2287.
45. **Golding, G. R., C. A. Kelly, and R. Sparling.** 2006. The effect of various physiological conditions on Hg(II) uptake in *Escherichia coli*, Eight international conference on mercury as a global pollutant, Madison, WI, USA.
46. **Golding, G. R., C. A. Kelly, R. Sparling, P. C. Loewen, J. W. M. Rudd, and T. Barkay.** 2002. Evidence for facilitated uptake of Hg(II) by Vibrio anguillarum and Escherichia coli under anaerobic and aerobic conditions. Limnology and Oceanography **47:**967-975.

47. **Graydon, J. A., V. L. S. Louis, S. E. Lindberg, H. H. Mann, and D. P. Krabbenhoft.** 2006. Investigation of mercury exchange between forest canopy vegetation and the atmosphere using a new dynamic chamber. Environmental Science & Technology **40:**4680-4688.
48. **Gutknecht, J.** 1981. Inorganic mercury (Hg 2+) transport through lipid bilayer membranes. Journal of Membrane Biology **61:**61-66.
49. **Hall, B. D., H. Manolopoulos, J. P. Hurley, J. J. Schauer, V. L. St Louis, D. Kenski, J. Graydon, C. L. Babiarz, L. B. Cleckner, and G. J. Keeler**. 2005. Methyl and total mercury in precipitation in the Great Lakes region. Atmospheric Environment 39:7557-7569.
50. **Hylander, L. D., and M. E. Goodsite.** 2006. Environmental costs of mercury pollution. Science of the Total Environment **368:**352-370.
51. **Isaksson, E., M. Hermanson, S. Hicks, M. Igarashi, K. Kamiyama, J. Moore, H. Motoyama, D. Muir, and V. Pohjola.** 2003. Ice cores from Svalbard—useful archives of past climate and pollution history. Physics and Chemistry of the Earth **28:**1217-1228.
52. **Iwahori, K., F. Takeuchi, K. Kamimura, and T. Sugio.** 2000. Ferrous iron-dependent volatilization of mercury by the plasma membrane of Thiobacillus ferrooxidans. Applied and Environmental Microbiology **66:**3823-3827.
53. **Jensen, S., and A. Jernelov.** 1969. Biological methylation of mercury in aquatic organisms. Nature **223:**753-754.
54. **Keeler, G. J., L. E. Gratz, and K. Al-Wali.** 2005. Long-term atmospheric mercury wet deposition at Underhill, Vermont. Ecotoxicology **14:**71-83.
55. **Kelly, C. A., J. W. M. Rudd, V. L. St Louis, and A. Heyes.** 1995. Is total mercury concentration a good predictor of methyl mercury concentration in aquatic systems? Water, Air, & Soil Pollution **80:**715-724.
56. **Krabbenhoft, D. P., J. P. Hurley, M. L. Olson, and L. B. Cleckner.** 1998. Diel variability of mercury phase and species distributions in the Florida Everglades. Biogeochemistry **40:**311-325.
57. **Kudo, A., Y. Fujikawa, S. Miyahara, J. Zheng, H. Takigami, M. Sugahara, and T. Muramatsu.** 1998. Lessons from Minamata mercury pollution, Japan - After a continuous 22 years of observation. Water Science and Technology **38:**187-193.
58. **Lalonde, J. D., M. Amyot, M. R. Doyon, and J. C. Auclair.** 2003. Photo-induced Hg(II) reduction in snow from the remote and temperate Experimental Lakes Area (Ontario, Canada). Journal of Geophysical Research-Atmospheres **108**.
59. **Lalonde, J. D., M. Amyot, A. M. L. Kraepiel, and F. M. M. Morel.** 2001. Photooxidation of Hg(0) in artificial and natural waters. Environmental Science & Technology **35:**1367-1372.
60. **Lalonde, J. D., M. Amyot, J. Orvoine, F. M. M. Morel, J. C. Auclair, and P. A. Ariya.** 2004. Photoinduced oxidation of Hg-0 (aq) in the waters from

the St. Lawrence estuary. Environmental Science & Technology **38:**508-514.

61. **Lalonde, J. D., A. J. Poulain, and M. Amyot.** 2002. The role of mercury redox reactions in snow on snow-to-air mercury transfer. Environmental Science & Technology **36:**174-178.
62. **Lamborg, C. H., W. F. Fitzgerald, G. M. Vandal, and K. R. Rolfhus.** 1995. Atmospheric Mercury in Northern Wisconsin - Sources and Species. Water Air and Soil Pollution **80:**189-198.
63. **Lanzillotta, E., C. Ceccarini, R. Ferrara, E. Dini, E. Frontini, and R. Banchetti.** 2004. Importance of the biogenic organic matter in photo-formation of dissolved gaseous mercury in a culture of the marine diatom Chaetoceros sp. Science of the Total Environment **318:**211-221.
64. **Lin, C. J., and S. O. Pehkonen.** 1999. The chemistry of atmospheric mercury: a review. Atmospheric Environment **33:**2067-2079.
65. **Lindberg, S. E., S. Brooks, C. J. Lin, K. J. Scott, M. S. Landis, R. K. Stevens, M. Goodsite, and A. Richter.** 2002. Dynamic oxidation of gaseous mercury in the Arctic troposphere at polar sunrise. Environmental Science & Technology **36:**1245-1256.
66. **Lindqvist, O., K. Johansson, M. Aastrup, A. Andersson, L. Bringmark, G. Hovsenius, L. Hakanson, A. Iverfeldt, M. Meili, and B. Timm**. 1991. Mercury in the Swedish Environment - Recent Research on Causes, Consequences and Corrective Methods. Water Air and Soil Pollution 55:R11-&.
67. **Lu, J. Y., W. H. Schroeder, L. A. Barrie, A. Steffen, H. E. Welch, K. Martin, L. Lockhart, R. V. Hunt, G. Boila, and A. Richter**. 2001. Magnification of atmospheric mercury deposition to polar regions in springtime: the link to tropospheric ozone depletion chemistry. Geophysical Research Letters 28:3219-3222.
68. **MacDonald, R. W., L. A. Barrie, T. F. Bidleman, M. L. Diamond, D. J. Gregor, R. G. Semkin, W. M. J. Strachan, Y. F. Li, F. Wania, M. Alaee, L. B. Alexeeva, S. M. Backus, R. Bailey, J. M. Bewers, C. Gobeil, C. J. Halsall, T. Harner, J. T. Hoff, L. M. M. Jantunen, W. L. Lockhart, D. Mackay, D. C. G. Muir, J. Pudykiewicz, K. J. Reimer, J. N. Smith, G. A. Stern, W. H. Schroeder, R. Wagemann, and M. B. Yunker**. 2000. Contaminants in the Canadian Arctic: 5 years of progress in understanding sources, occurrence and pathways. Science of the Total Environment 254:93-234.
69. **Macdonald, R. W., T. Harner, and J. Fyfe.** 2005. Recent climate change in the Arctic and its impact on contaminant pathways and interpretation of temporal trend data. Science of the Total Environment **342:**5-86.
70. **Marvin-Dipasquale, M. C., and R. S. Oremland.** 1998. Bacterial methylmercury degradation in Florida Everglades peat sediment. Environmental Science & Technology **32:**2556-2563.

71. **Mason, R. P., F. M. M. Morel, and H. F. Hemond.** 1995. The Role of Microorganisms in Elemental Mercury Formation in Natural-Waters. Water Air and Soil Pollution **80:**775-787.
72. **Mason, R. P., J. R. Reinfelder, and F. M. M. Morel.** 1996. Uptake, toxicity, and trophic transfer of mercury in a coastal diatom. Environmental Science & Technology **30:**1835-1845.
73. **Mindlin, S., L. Minakhin, M. Petrova, G. Kholodii, S. Minakhina, Z. Gorlenko, and V. Nikiforov.** 2005. Present-day mercury resistance transposons are common in bacteria preserved in permafrost grounds since the Upper Pleistocene. Research in Microbiology **156:**994-1004.
74. **Muir, D., B. Braune, B. DeMarch, R. Norstrom, R. Wagemann, L. Lockhart, B. Hargrave, D. Bright, R. Addison, J. Payne, and K. Reimer**. 1999. Spatial and temporal trends and effects of contaminants in the Canadian Arctic marine ecosystem: a review. Science of the Total Environment 230:83-144.
75. **Munthe, J., Z. F. Xiao, and O. Lindqvist.** 1991. The Aqueous Reduction of Divalent Mercury by Sulfite. Water Air and Soil Pollution **56:**621-630.
76. **Nazaret, S., W. H. Jeffrey, E. Saouter, R. Vonhaven, and T. Barkay.** 1994. Mera Gene-Expression in Aquatic Environments Measured by Messenger-Rna Production and Hg(Ii) Volatilization. Applied and Environmental Microbiology **60:**4059-4065.
77. **Nriagu, J. O.** 1989. A Global Assessment of Natural Sources of Atmospheric Trace-Metals. Nature **338:**47-49.
78. **O'Driscoll, N. J., D. R. S. Lean, L. L. Loseto, R. Carignan, and S. D. Siciliano.** 2004. Effect of dissolved organic carbon on the photoproduction of dissolved gaseous mercury in lakes: Potential impacts of forestry. Environmental Science & Technology **38:**2664-2672.
79. **Osborn, A. M., K. D. Bruce, P. Strike, and D. A. Ritchie.** 1997. Distribution, diversity and evolution of the bacterial mercury resistance (mer) operon. Fems Microbiology Reviews **19:**239-262.
80. **Pal, B., and P. A. Ariya.** 2004. Gas-phase HO center dot-Initiated reactions of elemental mercury: Kinetics, product studies, and atmospheric implications. Environmental Science & Technology **38:**5555-5566.
81. **Peretyazhko, T., L. Charlet, B. Muresan, V. Kazimirov, and D. Cossa.** 2006. Formation of dissolved gaseous mercury in a tropical lake (Petit-Saut reservoir, French Guiana). Science of the Total Environment **364:**260-271.
82. **Poissant, L., and M. Pilote.** 2003. Time series analysis of atmospheric mercury in Kuujjuarapik/Whapmagoostui (Quebec). Journal De Physique Iv **107:**1079-1082.
83. **Poulain, A. J., M. Amyot, D. Findlay, S. Telor, T. Barkay, and H. Hintelmann.** 2004. Biological and photochemical production of dissolved

gaseous mercury in a boreal lake. Limnology and Oceanography **49:**2265-2275.

84. **Poulain, A. J., J. D. Lalonde, M. Amyot, J. A. Shead, F. Raofie, and P. A. Ariya.** 2004. Redox transformations of mercury in an Arctic snowpack at springtime. Atmospheric Environment **38:**6763-6774.
85. **Richardson, G. M., I. A. Mitchell, M. Mah-Paulson, T. Hackbarth, and R. G. Garrett.** 2003. Natural emissions of mercury to the atmosphere in Canada. Environ. Rev **11:**17–36.
86. **Rolfhus, K. R., and W. F. Fitzgerald.** 2004. Mechanisms and temporal variability of dissolved gaseous mercury production in coastal seawater. Marine Chemistry **90:**125-136.
87. **Rozan, T. F., M. E. Lassman, D. P. Ridge, and G. W. Luther.** 2000. Evidence for iron, copper and zinc complexation as multinuclear sulphide clusters in oxic rivers. Nature **406:**879-882.
88. **Schecher, W. D., and D. C. McAvoy.** 1992. Mineql+ - a Software Environment for Chemical-Equilibrium Modeling. Computers Environment and Urban Systems **16:**65-76.
89. **Schindler, D. W., and J. P. Smol.** 2006. Cumulative effects of climate warming and other human activities on freshwaters of Arctic and subarctic North America. Ambio **35:**160-168.
90. **Schroeder, W. H., K. G. Anlauf, L. A. Barrie, J. Y. Lu, A. Steffen, D. R. Schneeberger, and T. Berg**. 1998. Arctic springtime depletion of mercury. Nature 394:331-332.
91. **Schroeder, W. H., and J. Munthe.** 1998. Atmospheric mercury - An overview. Atmospheric Environment **32:**809-822.
92. **Schuster, P. F., D. P. Krabbenhoft, D. L. Naftz, L. D. Cecil, M. L. Olson, J. F. Dewild, D. D. Susong, J. R. Green, and M. L. Abbott**. 2002. Atmospheric Mercury Deposition during the Last 270 Years: A Glacial Ice Core Record of Natural and Anthropogenic Sources. Environmental Science & Technology 36:2303-2310.
93. **Scott, K. J.** 2001. Bioavailable mercury in arctic snow determined by a light-emitting mer-lux bioreporter. Arctic **54:**92-95.
94. **Sellers, P., C. A. Kelly, J. W. M. Rudd, and A. R. MacHutchon.** 1996. Photodegradation of methylmercury in lakes. Nature **380:**694-697.
95. **Serreze, M. C., J. E. Walsh, F. S. Chapin, T. Osterkamp, M. Dyurgerov, V. Romanovsky, W. C. Oechel, J. Morison, T. Zhang, and R. G. Barry**. 2000. Observational evidence of recent change in the northern high-latitude environment. Climatic Change 46:159-207.
96. **Sheppard, D. S., J. E. Patterson, and M. K. McAdam.** 1991. Mercury Content of Antarctic Ice and Snow - Further Results. Atmospheric Environment Part a-General Topics **25:**1657-1660.

97. **Siciliano, S. D., N. J. O'Driscoll, and D. R. Lean.** 2002. Microbial reduction and oxidation of mercury in freshwater lakes. Environmental Science and Technology **36:**3064-3068.
98. **Siciliano, S. D., N. J. O'Driscoll, R. Tordon, J. Hill, S. Beauchamp, and D. R. Lean.** 2005. Abiotic production of methylmercury by solar radiation. Environ Sci Technol **39:**1071-7.
99. **Skov, H., J. H. Christensen, M. E. Goodsite, N. Z. Heidam, B. Jensen, P. Wahlin, and G. Geernaert.** 2004. Fate of elemental mercury in the arctic during atmospheric mercury depletion episodes and the load of atmospheric mercury to the arctic. Environmental Science & Technology **38:**2373-2382.
100. **Smith, T., K. Pitts, J. A. McGarvey, and A. O. Summers.** 1998. Bacterial oxidation of mercury metal vapor, Hg(0). Applied and Environmental Microbiology **64:**1328-1332.
101. **St Louis, V. L., J. W. M. Rudd, C. A. Kelly, B. D. Hall, K. R. Rolfhus, K. J. Scott, S. E. Lindberg, and W. Dong.** 2001. Importance of the forest canopy to fluxes of methyl mercury and total mercury to boreal ecosystems. Environmental Science & Technology **35:**3089-3098.
102. **Steffen, A., W. Schroeder, J. Bottenheim, J. Narayan, and J. D. Fuentes.** 2002. Atmospheric mercury concentrations: measurements and profiles near snow and ice surfaces in the Canadian Arctic during Alert 2000. Atmospheric Environment **36:**2653-2661.
103. **Stumm, W., and J. J. Morgan.** 1996. Metal ions in aqueous solution: aspects of coordination chemistry, p. 1022. *In* J. L. Schnoor and A. Zehnder (ed.), Aquatic Chemistry - Chemical Equilibria and rates in natural waters, third edition., Wiley-Intersciences ed. John Wiley and sons, Inc., New-York.
104. **Suda, I., M. Suda, and K. Hirayama.** 1993. Degradation of Methyl and Ethyl Mercury by Singlet Oxygen Generated from Sea-Water Exposed to Sunlight or Ultraviolet-Light. Archives of Toxicology **67:**365-368.
105. **Sukola, K., F. Y. Wang, and A. Tessier.** 2005. Metal-sulfide species in oxic waters. Analytica Chimica Acta **528:**183-195.
106. **Susong, D. D., M. L. Abbott, and D. P. Krabbenhoft.** 2003. Mercury accumulation in snow on the Idaho National Engineering and Environmental Laboratory and surrounding region, Southeast Idaho, USA. Environmental Geology **43:**357-363.
107. **Swain, E. B., D. R. Engstrom, M. E. Brigham, T. A. Henning, and P. L. Brezonik.** 1992. Increasing Rates of Atmospheric Mercury Deposition in Midcontinental North-America. Science:784-787.
108. **Tessier, A., J. Buffle, and P. G. C. Campbell.** 1994. Uptake of trace metals by aquatic organisms, p. 199-232. *In* J. Buffle and R. de Vitre (ed.), Chemical and biological regulation of aquatic systems. Lewis, Boca Raton, Florida.

109. **Travnikov, O.** 2005. Contribution of the intercontinental atmospheric transport to mercury pollution in the Northern Hemisphere. Atmospheric Environment **39:**7541-7548.
110. **Tseng, C. M., C. Lamborg, W. F. Fitzgerald, and D. R. Engstrom.** 2004. Cycling of dissolved elemental mercury in Arctic Alaskan lakes. Geochimica et Cosmochimica Acta **68:**1173-1184.
111. **Van Oostdam, J., S. G. Donaldson, M. Feeley, D. Arnold, P. Ayotte, G. Bondy, L. Chan, E. Dewaily, C. M. Furgal, H. Kuhnlein, E. Loring, G. Muckle, E. Myles, O. Receveur, B. Tracy, U. Gill, and S. Kalhok**. 2005. Human health implications of environmental contaminants in Arctic Canada: A review. Science of the Total Environment:165-246.
112. **Vandal, G. M., W. F. Fitzgerald, C. F. Boutron, and J. P. Candelone.** 1993. Variations in mercury deposition to Antarctica over the past 34,000 years. Nature **362:**621-623.
113. **Vandal, G. M., R. P. Mason, and W. F. Fitzgerald.** 1991. Cycling of Volatile Mercury in Temperate Lakes. Water Air and Soil Pollution **56:**791-803.
114. **Vetriani, C., Y. S. Chew, S. M. Miller, J. Yagi, J. Coombs, R. A. Lutz, and T. Barkay.** 2005. Mercury adaptation among bacteria from a deep-sea hydrothermal vent. Applied and Environmental Microbiology **71:**220-226.
115. **Wiatrowski, H. A., and T. Barkay.** 2006. Reduction of Hg(II) to Hg(0) by dissimilatory metal-reducing bacteria, Eight international conference on mercury as a global pollutant, Madison, WI.
116. **Wu, Y., S. X. Wang, D. G. Streets, J. M. Hao, M. Chan, and J. K. Jiang.** 2006. Trends in anthropogenic mercury emissions in China from 1995 to 2003. Environmental Science & Technology **40:**5312-5318.
117. **Xiao, Z. F., J. Munthe, and O. Lindqvist.** 1991. Sampling and Determination of Gaseous and Particulate Mercury in the Atmosphere Using Gold-Coated Denuders. Water Air and Soil Pollution **56:**141-151.
118. **Xiao, Z. F., J. Munthe, D. Stromber, and O. Lindqvist.** 1994. Photochemical behaviour of inorganic mercury compounds in aqueous solution, p. 581-592. *In* C. J. Watras and J. W. Huckabee (ed.), Mercury pollution: integration and synthesis.
119. **Zhang, H.** 2006. Photochemical redox reactions of mercury, p. 37-79, Recent Developments in Mercury Science. Springer Verlag, Berlin..
120. **Zhang, H., and S. E. Lindberg.** 2001. Sunlight and iron(III)-induced photochemical production of dissolved gaseous mercury in freshwater. Environmental Science & Technology **35:**928-935.

2. Redox transformations of mercury in an Arctic snowpack at springtime

Alexandre J. Poulain, Janick D. Lalonde, Marc Amyot, Justin A. Shead, Farhad Raofie, and Parisa A. Ariya.

Reprinted from Atmospheric Environment, vol. 38: 6763-6774 Copyright (2004).

2.1. Abstract

We investigated the springtime temporal dynamics of both total Hg and gaseous mercury in snowpacks from the High Arctic. *In situ* incubation experiments of snow samples indicated that the production of volatile mercury in snow (VMS) was photo-mediated and occurred in the first 3 cm of snow. The newly produced VMS (consisting mainly of elemental Hg) was partly oxidized back to Hg(II) when light intensity declined or in the absence of UV radiation, probably through a chain of reactions involving photo-induced radicals and organic compounds in the surface snow. During a two week monitoring of total Hg in surface snow, we observed a sharp increase in total Hg concentrations, reaching levels 11 times higher than background concentrations, likely as a result of an atmospheric mercury depletion event. Stratigraphic depth profiles indicated that this increase was restricted to the first 2 cm of the snowpack. Total Hg levels subsequently decreased by 92%, reaching background concentrations within two days after this event. The photoproduction rate of VMS calculated on the basis of this episode could account for subsequent daily loss of total Hg from the surface of the snowpack.

2.2. Introduction

Due to its ability to travel over long distances in the atmosphere, Hg is a global pollutant. Over the last decade, a major concern arose from the discovery of atmospheric mercury depletion events (MDE) in polar (6, 22) and subpolar regions (20). These events partly result from the oxidation of atmospheric elemental Hg, Hg(0), through reaction with ozone, and halogens such as bromine or chlorine (2, 17). These MDEs can lead to an important deposition of Hg in snowpack (19), potentially causing the contamination of terrestrial and aquatic systems upon snowmelt. However, the post-deposition Hg dynamics in Arctic snow is not fully understood. Recent evidence (17, 23) suggests that newly deposited Hg is highly bioavailable, increasing the need to better understand its fate, whether it results from mercury depletion events or from wet and dry depositions.

In temperate urban and remote pristine regions, Lalonde et al. (2002 and 2003) (12, 15) have shown that within 24 hours, approximately 50 % of the newly deposited Hg could be efficiently recycled back to the atmosphere probably through photoreduction. In Arctic regions, Steffen et al. (2002) (24) proposed that reactive gaseous mercury (RGM), thought to be the main product of MDEs (17), could be recycled from the surface of the snowpack back to gaseous elemental mercury (GEM), also through photoreduction. Dommergue et al. (2003) (5) and Ferrari et al. (2004) (7) demonstrated diurnal cycles of interstitial gaseous mercury at the surface and at depth in the snowpack of a sub-Arctic region. Another, yet unexplored, mechanism is the photooxidation of Hg(0) in snow. This process is known to be significant in surface waters, and is thought to be enhanced by chloride ions (13, 14). The purpose of this paper is (i) to establish the temporal dynamics of both total Hg and elemental Hg at the surface and within snowpacks in the High Arctic, during and after a MDE; and (ii) to determine whether photooxidation of Hg occurs in surface snow.

2.3. Experimental section

2.3.1. Sampling sites

Our sampling sites were located on Cornwallis Island, Nunavut, Canada. We monitored cations (Al^{3+}, Ca^{2+}, Fe^{3+}, K^{+}, Mg^{2+}, Mn^{2+}, Na^{+} and Zn^{2+}) as well as anions (Cl^{-}, NO_3^{-}, NO_2^{-}, Br^{-} and SO_4^{2-}) on a regular basis at Mel site, located 74°43'N-95°00'W. We also sampled Small Lake (74°45'N-95°03'W), an inland site (75°05'N-93°43'W) and a coastal (75°02'N-96°20'W) site. Organic compounds were analysed from surface snow sampled at the south shoreline of North Lake (74°50'N-95°05'W) (Figure 2.1).

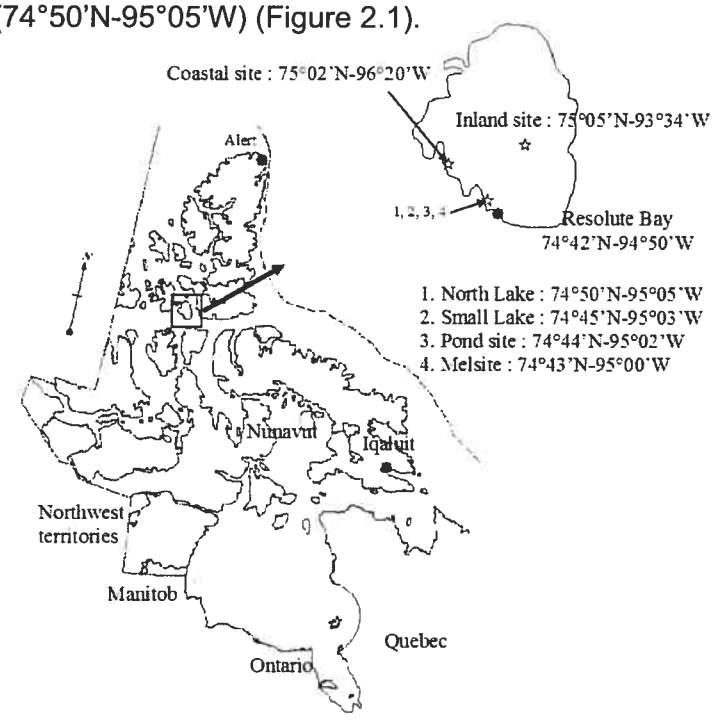

Figure 2.1. Location of Cornwallis Island. Stars represent sampling sites. http://atlas.gc.ca/site/english/maps/reference/outlineprov_terr/index.html. Sampling, monitoring and incubations.

Monitoring was done by collecting triplicate snow samples from the surface of the snowpack. For depth profiles, samples were taken from each snow stratum. Snow strata were determined by the state of metamorphism of the snow grains, as defined the international classification of seasonal snow on the ground (4).

Snow for cation analysis was collected in 30 ml HDPE Nalgene bottles and acidified to 0.1% with HNO_3 (64%). Snow for anion analysis was collected in 20 ml disposable samples vials. All samples were kept at 4°C until analysed. Snow samples for Hg analysis were taken using Teflon bottles previously acid-washed and thoroughly rinsed with milliQ water ($R > 18.2\ M\Omega\ cm^{-1}$).

Experiments consisted of incubating 1L Teflon bottles for various lengths of time under different light treatments. During incubation, bottles were placed horizontally with their cap pointing north. Bottles were regularly and gently rotated every 30 minutes to optimize the distribution of light through the sample. Incubations lasted for 6 to 8 hours and usually started between 8:30 am and 10:00 am. Mylar filters were used to cut most of the UVB radiation (280-320 nm) and UV-Lee filters model 226 were used to prevent UV radiation (280-400 nm) from reaching the samples. PAR (400-700nm) was recorded every one or five minutes using a Smart Sensor HOBO® connected to a data logger.

2.3.2. Chemical analyses

In order to minimize losses of gaseous mercury in snow (VMS) during the analysis, solid snow was sparged directly in the sampling bottle by tightly inserting a porous glass rod into bottle. We used a zero-air generator (Tekran model 1100) to sparge the sample, at a flow rate of 1.5 L min^{-1}. The sample was heated during sparging, by placing it in a hot water bath (approx. 30°C). The bottle was connected to an automated atmospheric mercury analyzer (Tekran™ Model 2537) in order to monitor the decrease of VMS over time (one reading every five minutes). The experimental design was modified from that of Lindberg

et al. (2000)(18) . The sparging step was stopped when snow had melted and when concentrations plateaued at zero. Here we report VMS values in moles per volume of melt water instead of moles per volume of snow, in order to correct for the difference in snow density. The working detection limit of this method was calculated as < 0.01 pmol.L^{-1} or three times the standard deviation of ten system blanks ran on snow with low Hg levels.

Total Hg concentrations in snowmelt were quantified using the method described by Lalonde et al. (2003)(12) and based on Gill and Bruland (1990)(8), using a mercury fluorescence detector (Tekran™ Model 2500). Briefly, Hg in unfiltered snow samples was reduced using 1% $NaBH_4$ (w/v) and 4 M NaOH. Approximately 100 ml of snowmelt was poured into a 250ml glass bubbler and purged for 20 minutes with clean air from a Hg-free air generator (Tekran™ Model 1100) additionally stripped of Hg(0) by passage over a gold filter at a flow rate of ≈ 1 L min^{-1}. The working detection limit of this method was calculated as 0.05 pmol L^{-1} or three times the standard deviation of ten procedural blanks.
Anions were analyzed by ion chromatography using a DIONEX ICS 2000. 25 µL of melted snow were introduced in the injection loop and separation occurred through an AS-17 column topped with a AG-17 precolumn. The elution step involved the passage of a KOH solution with a gradient of concentration from 15 to 30 mmol L^{-1}. Cations were analysed using an inductively coupled plasma atomic emission spectrometer (ICP-AES Vista AX) using an internal standard of Yttrium (5 mg L^{-1}, 371 nm).

Organic compounds in surface snow were analysed using two different methods: (a) electron spray ionization mass spectrometry (ESI-MS); (b) solid phase micro extraction (SPME). For the ESI-MS method, 5 µl of melted snow was injected into the electron spray of mass spectrometer (Thermoquest Finnigan LC QDUO). For the SPME method, manual extraction was performed with several replacement fibre assemblies (Supelco). Four different types of fibers were compared: polyacrylate (85 µm), polydimethyl siloxane (100 µm),

polydimethyl siloxane / divinyl benzene (65 µm) carbowax / divinyl benzene (65 µm). The fibers were conditioned prior to use as recommended by the manufacturer by heating them at different temperatures (250 – 300 °C) for periods between 30 min and 2 h in gas chromatograph injection port. After conditioning the fibers, they were inserted into the solution under magnetic stirring using a Teflon bar and magnetic stirrer. After 5 h adsorption, the fibers were injected directly into the injection port of the gas chromatograph-mass spectrometer (GC-MS) in the splitless mode and held isothermally at 250 °C. Desorption time was 5 min. Chromatographic analyses were performed using Hewlett Packard GC (HP 6890) equipped with a splitless injector and mass spectrometric detection (HP 5973 MSD). The GC was fitted with a 30 × 0.25 mm i.d. column coated with 5 % phenyl methyl siloxane (HP – 5 MS). The column was operated at a constant flow (1.5 mL min^{-1}) of ultra high purity helium. The oven temperature was increased by 5 °C min^{-1} up to 200 °C. Conditions for the mass selective detector were as follows: transfer line temperature 280 °C, 70 eV electron impact, electron multiplayer voltage 2180 V, mass range for full scan 10 to 550 a.m.u.

2.4. Results

2.4.1. Chemical composition of snow

Concentrations of alkaline (e.g. Na^+) and alkaline-earth (e.g. Ca^{2+}, Mg^{2+}) cations as well as of metals (Al^{3+}, Zn^{2+}, Fe^{3+} and Hg^{2+}) covered one to two orders of magnitude (max:min: 22 to 292; Table 1). Anion concentrations were less variable, except for chloride and sulphate (max:min 69 and 151 fold, respectively). The dominant cations were Ca^{2+} (3.6 mg L^{-1}), followed by Na^+ (1.15 mg L^{-1}) and Mg^{2+} (0.96 mg L^{-1}). The dominant anions were Cl^- (0.84 mg L^{-1}) followed by NO_3^- (0.30 mg L^{-1}) and SO_4^{2-} (0.28 mg L^{-1}). pH ranged from acidic to strongly alkaline values (6.2 to 9.5). Amongst the identified organic molecules

(Table 2), aldehydes, ketones, nitriles, aromatics, alkanes, alkenes, and halocarbons were observed.

2.4.2. Temporal and spatial distribution of total Hg and VMS concentrations at Mel site

Total Hg concentrations remained below 15 pmol L^{-1} from June 4 to June 24 (Figure 2.2.) and were consistent with concentrations observed by another team working at the same site (Lahoutifard et al. 2003). However, an important increase was recorded on June 7, reaching 88 ± 39 pmol L^{-1} (Figure 2.2). This increase in total Hg in snow coincided with a mercury depletion event recorded at the same site (Figure 2.2.; Lahoutifard et al. 2003). Total Hg concentrations decreased by 92 % (down to 7.5 pmol L^{-1}) within 48 hours after the event had ended.

Table 2.I. Chemical composition of surface snow and pond water from June 6 to 21 June 21 2003. All concentrations are expressed in $mg.L^{-1}$ expect for Hg expressed in $pmol\ L^{-1}$.

Sampling site	Mel site				Small Lake	Inland site	Coastal Site		Pond water
Lat.(N)	74°43				74°45	75°05	75°02		74°44
Long. (W)	95°00				95°03	93°34	96°20		95°02
Matrices	snow				snow	snow	snow	All snow samples	water
Sampling dates	From 6-Jun to 21-Jun				09-Jun	10-Jun	11-Jun	max/min	19-Jun
	min	max	average	SD					
Al(+III)	0.004	0.316	0.135	0.133	0.010	0.005	0.006	83.42	0.174
Ca(+II)	0.133	9.211	3.636	3.477	0.365	0.048	0.180	190.4	14.107
Fe(+III)	0.002	0.227	0.088	0.087	0.011	0.006	0.005	108.0	0.133
K(+I)	0.014	0.237	0.087	0.075	0.018	0.009	0.116	25.23	0.757
Mg(+II)	0.031	2.662	0.960	0.898	0.081	0.028	0.176	95.41	4.483
Mn(+II)	<0.0002	0.010	0.004	0.004	0.001	0.001	0.001	49.00	0.012
Na(+I)	0.027	3.456	1.153	1.336	0.322	0.216	3.780	141.0	7.815
Zn(+II)	0.001	0.017	0.006	0.005	0.022	0.030	0.020	37.75	0.002
Hg(+II) (±SD)	2.900	111.0	15.00	32.00	12.70 ±4.46	n/a	11.30±3	38.28	14.8±0.4
pH	6.160	9.520	6.860		6.230	5.230	5.540	19500	8.150
Cl(-I)	0.145	1.361	0.841	0.417	0.647	0.677	2.751	18.98	10.104
Br(-I)	0.013	0.044	0.028	0.022	0.011	0.011	< 0.004	4.10	< 0.004
NO2(-I)	0.008	0.032	0.015	0.010	0.007	0.011	< 0.006	4.41	< 0.006
NO3(-I)	0.049	0.698	0.302	0.238	0.542	0.742	n/a	15.14	0.242
SO4(-II)	0.044	0.706	0.281	0.239	0.400	0.245	0.766	17.36	6.661

Table 2.II. Organic compounds extracted from surface snow sample, June, 2003.

Organic compound structure	Empirical formula	Molecular mass	Molecular structure
1,3,5-Cyclohepatriene	C_7H_8	92	
Choloro bezene	C_6Cl_5	112	
1-ethyl, 3-methyl benzene	C_9H_{12}	120	
3-Allylcyclohexane	C_9H_{14}	122	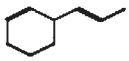
4,6-di(1,1-dimethylethyl)-2-methyl Phenol	$C_{15}H_{24}O$	220	
4-(1-methylethenyl) 1-Cyclohexene, 1-Carboalaldehyde	$C_{10}H_{14}O$	150	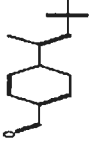
3,4-dihydro-6-m 1(2H)-Naphthalenone	$C_{11}H_{12}O_2$	176	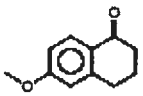
2,2,3-trimethyl 3-cyclopentene-1-acetaldehyde	$C_{10}H_{16}O$	152	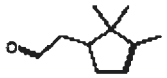
5-methyl hexanenitrile	$C_7H_{13}N$	111	
N-dibutyl formamide,	$C_9H_{19}NO$	157	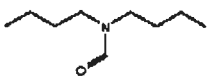
Heptanal	$C_7H_{14}O$	114	
Octanal	$C_8H_{16}O$	128	
Nonanal	$C_9H_{18}O$	142	
Tridecanal	$C_{13}H_{26}O$	198	

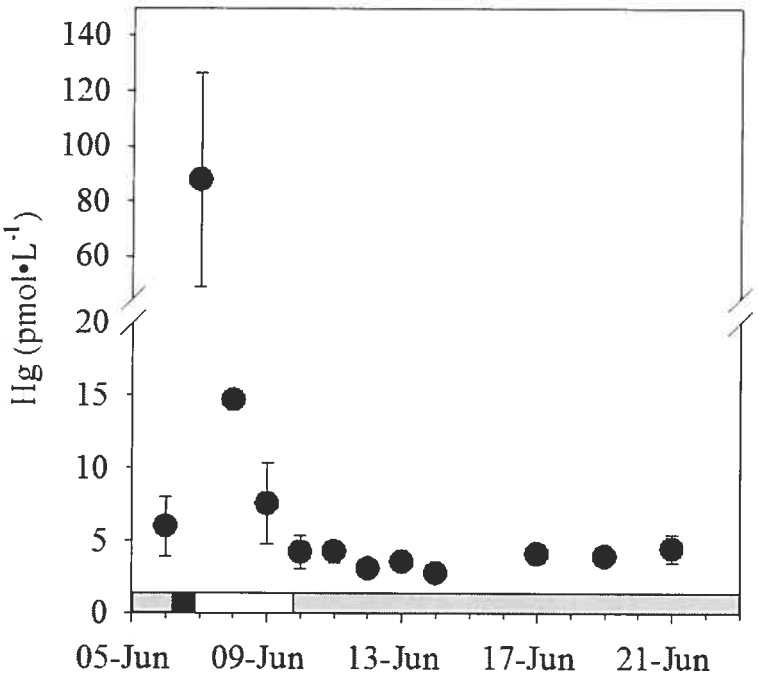

Figure 2.2. Temporal variation of total Hg concentrations at the surface of the snowpack from June 6 to June 21 2003. At the bottom of the graph, black horizontal bar represent sharp depletion of $Hg(0)_{atm}$ concentrations (0 - 1 ng m^{-3}), grey horizontal bars represent Hg_{atm} concentrations (between 1 - 3 ng.m^{-3}), and white bar represent high concentrations of $Hg(0)_{atm}$ (3 - 8 ng.m^{-3}). The length of the bars is representative of the duration of the event. Vertical bars represent the standard deviation of three replicates.

Depth profiles of total Hg in the snowpack were measured on June 7 and 14. On both dates, total Hg concentrations were higher at the surface than at depth (Figure 2.3. A and B). Note that arctic snowpacks usually undergo rapid transformations and that one should not assume that snow strata are totally conserved between sampling dates.

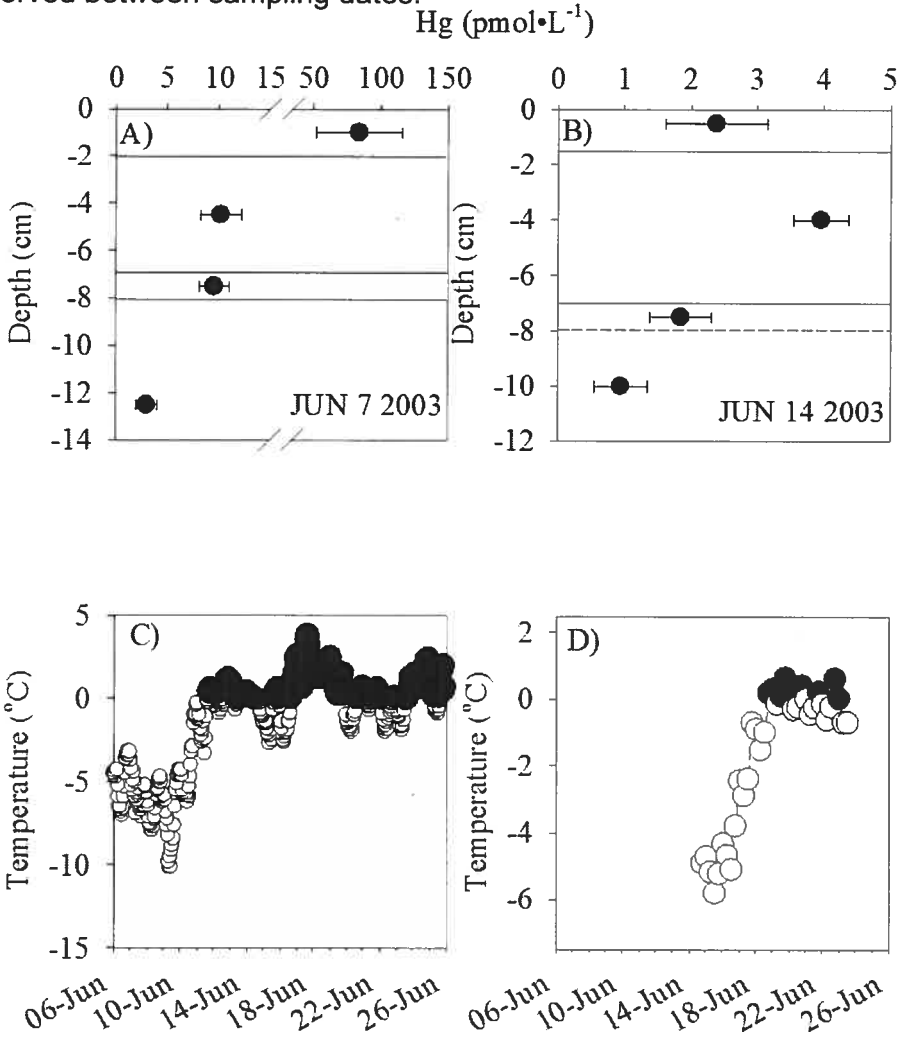

Figure 2.3. Depth profiles carried out on June 7 (A) and June 14 (B). Temporal variation of the temperature at the surface (C) and at the bottom (14 cm) of the snowpack (D). Bars represent the standard deviation of three replicates. Horizontal lines in panels A and B represent limits of adjacent snow strata.

The profile carried out on June 7 (Figure 2.3 A), exhibited Hg concentrations at the surface approximately a hundred times higher than at 12 cm depth. At the surface, snow grains were needle-like and faceted, lightly metamorphosed, characteristic of freshly deposited crystals (Table 3). At depth, crystals were cup-shaped, characteristic of an advanced constructive metamorphism (4).

Table 2.III. State of metamorphism and physical properties of different snow strata on (A) June 7 and (B) June 14 2003.

7-JUNE				
snow stratum	**Temperature (°C)**	**Water content (%)**	**grain type**	**grain size (mm)**
S	-5	20	small faceted and needle-like	0.5
S-1	-4	25	cup shaped	0.5-2
S-2	n/a	90	ice crust	n/a
S-3	-8	28	cup shaped	2-3
14-JUNE				
snow stratum	**Temperature (°C)**	**Water content (%)**	**grain type**	**grain size (mm)**
S	0	36	rounded some faceted	1-2
S-1	-4	50	rounded	2
S-2	n/a	90	ice crust	n/a
S-3	-8	37	cup shaped	3-4

On June 14 (Figure 2.3 B), the two first strata were representative of a single snowfall event. The depth profile on June 14 was determined after the unique important snow fall we encountered (7 cm). Crystals were mainly rounded, typical of warmer temperatures (which induce a quick destructive metamorphism), with few precipitation crystals still visible. This was seen as temperatures at the surface of the snowpack on June 14 were above 0°C (Figure 2.3 C).

From June 12 to June 26, surface temperatures were above the freezing point during the day (Figure 2.3 C). Total Hg concentrations were higher in the pond created by melt water (14 pmol L^{-1}) and in the adjacent slush (10 pmol L^{-1}) than in the solid snow itself (4 pmol L^{-1}) (Figure 2.4 A). The fairly high total mercury concentrations encountered in pond water were likely a consequence of soil leaching, as corroborated by the increase in Mg^{2+} and Ca^{2+} concentrations, compared to surface snow ($[Mg^{2+}]_{snow}$=0.96 mg L^{-1}, $[Mg^{2+}]_{pond}$=4.48 mg L^{-1}, $[Ca^{2+}]_{snow}$=3.63 mg L^{-1}, $[Ca^{2+}]_{pond}$=14.1 mg L^{-1}).

VMS concentrations in surface snow were generally very low and close to the detection limit (0.01 pmol L^{-1}) (Figure 2.4 B). As in the case of dissolved aqueous Hg, VMS in the slush and in the snow (ranging from 0.05 to 0.7 pmol L^{-1}), are lower than dissolved gaseous mercury (DGM) concentrations in pond water (0.92 pmol L^{-1}).

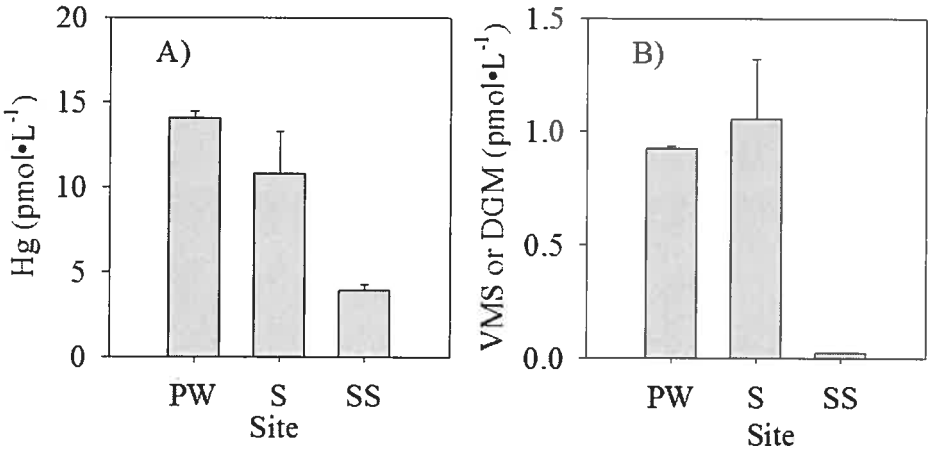

Figure 2.4. VMS and total Hg concentrations in pond of Cornwallis Island (PW: pond water, S: slush, SS: surface snow).

2.4.3. VMS production

During incubation experiments conducted on June 9, VMS concentrations in snow samples kept at the surface did not simply increase with time of exposure to solar radiation. Instead, they co-varied with short-term changes in PAR intensity (Figure 2.5). We averaged PAR data (recorded every minute) over intervals of 5, 15, 30 and 60 minutes preceding the end of the incubation of each sample (referred to below as PAR_t, where t is the period for which data were averaged). PAR averaged over short intervals (PAR_{5min} and PAR_{15min}) better explained the variations observed in VMS concentrations (r^2=0.77 ; p=0.0012 and r^2=0.72 ; p=0.0023, respectively) (Figure 2.6 A and B) than PAR_{30min} and PAR_{60min} (r^2=0.5 ; p=0.018 and r^2=0.38 ; p=0.045, respectively) (Figure 2.6 C and D). No increase in [VMS] was observed in snow incubated at a depth of 3 cm, in contrast to the increase observed in samples exposed to direct sunlight (Figure 2.5). In all experiments, no increase was observed when samples were kept in the dark (Figure 2.5, 2.7 and 2.8).

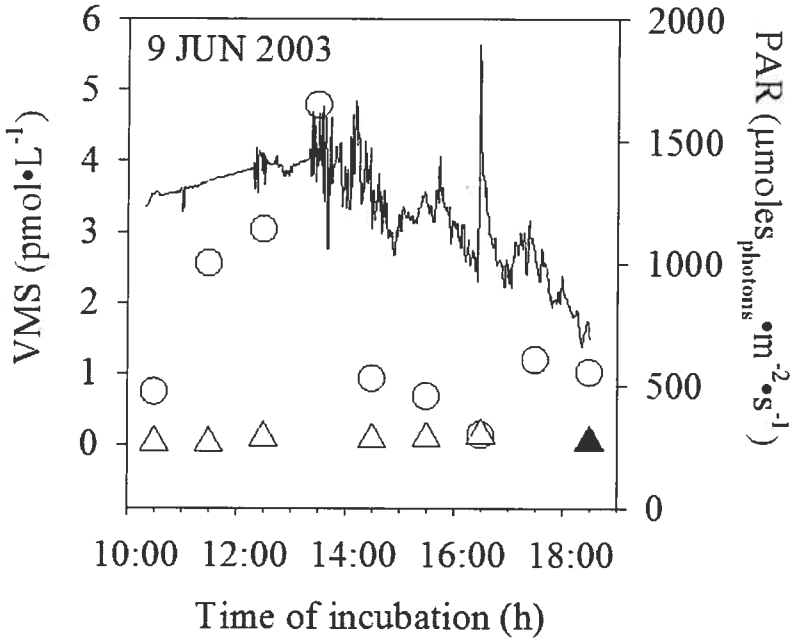

Figure 2.5. Time series of VMS concentrations in snow over time of exposure to the sun on June 9 2003. Open circles represent samples incubated at the surface of the snowpack. Open triangles represent samples incubated under 3 cm of snow. The black triangle represents samples kept in the dark.

An estimated maximum photoproduction rate was calculated based on the June 9 incubation (Figure 2.5). After 3 hours of exposure to the sun, concentrations reached 4.8 pmol L^{-1} corresponding to a photoproduction rate of $[VMS]_{prod}$ = 1.33 pmol L^{-1} h^{-1} ($[VMS]_0$=0.73 pmol L^{-1}). Additional experiments were conducted with pond water. Dissolved gaseous mercury (DGM) concentrations in pond water increased when exposed to the sun leading to a photoproduction rate of 0.9 pmol L^{-1} h^{-1}.

Note that destructive metamorphism was usually observed during incubation, since temperatures hovered around 0°C (Figure 2.3 C). This phenomenon is typical of springtime conditions. Our results are therefore not necessarily representative of what may occur in dry and cold snow. It is likely that, when liquid water is formed, the rate of photoreduction of Hg(II) is altered (21).

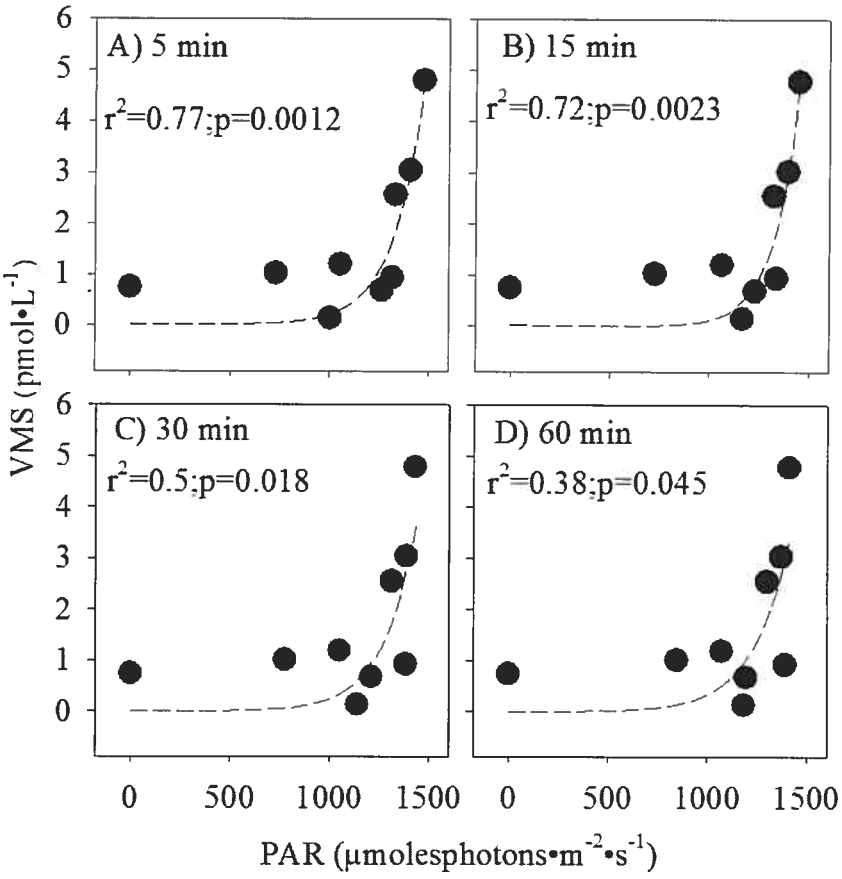

Figure 2.6. Non linear regression between VMS concentrations and PAR averaged 5 (A), 15 (B), 30 (C) and 60 (D) minutes before the end of the incubation for each samples. All regression were significant at the 0.05 level. Regression equation is $[VMS]=a \cdot e^{(b \cdot PAR)}$. In panel A to D a=0.0003 and b=0.006; a=0.0001 and b=0.0081; a=0.0005 and b=0.0064; and a=0.0013 and b=0.0052, respectively.

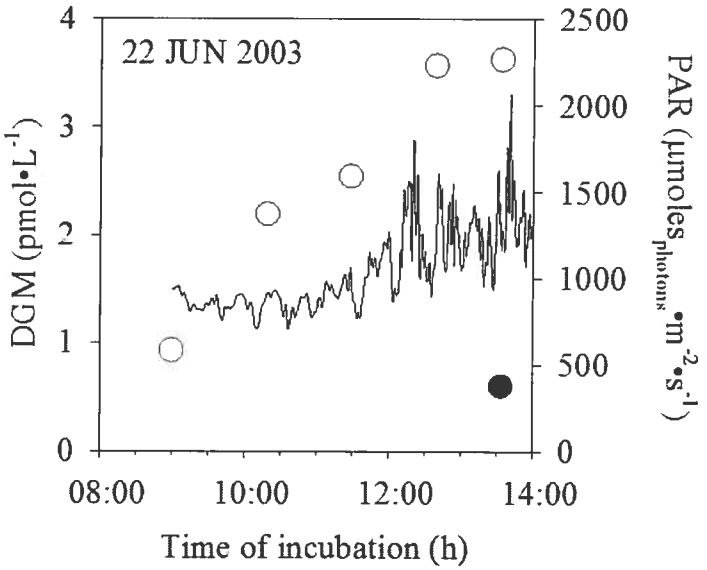

Figure 2.7. Time series of VMS concentrations in pond water over time of exposure to the sun and in the dark on June 22 2003.

2.4.4. Hg^0 oxidation within the snowpack

We observed [VMS] decreases over time in some incubation bottles (Figure 2.5) which may have resulted from Hg(0) oxidation. We therefore conducted a series of experiments to assess the stability of newly formed Hg(0) in snow (Figure 2.8). After 3 h of exposure to the sun, [VMS] increased by a factor 4 to 6 reaching 0.29 and 0.21 pmol L^{-1} on June 13 and 16, respectively (Figure 2.8 A and B). After this initial incubation under the sun, some samples were placed in the dark and their [VMS] were monitored over three additional hours.

On June 13, [VMS] measured in the dark decreased by 63% within 3 hours (black circle, Figure 2.8 A). In samples kept uncovered, concentrations also decreased by 60% (white circle Figure 2.8 A). Note that this last incubation

with uncovered bottles coincided with a strong snowfall and to a decrease of the PAR intensity (from 900 μmol_{photon} m^{-2} s^{-1} down to 500 μmol_{photon} m^{-2} s^{-1}) at 1:00 pm on June 13 (Figure 2.8 A).

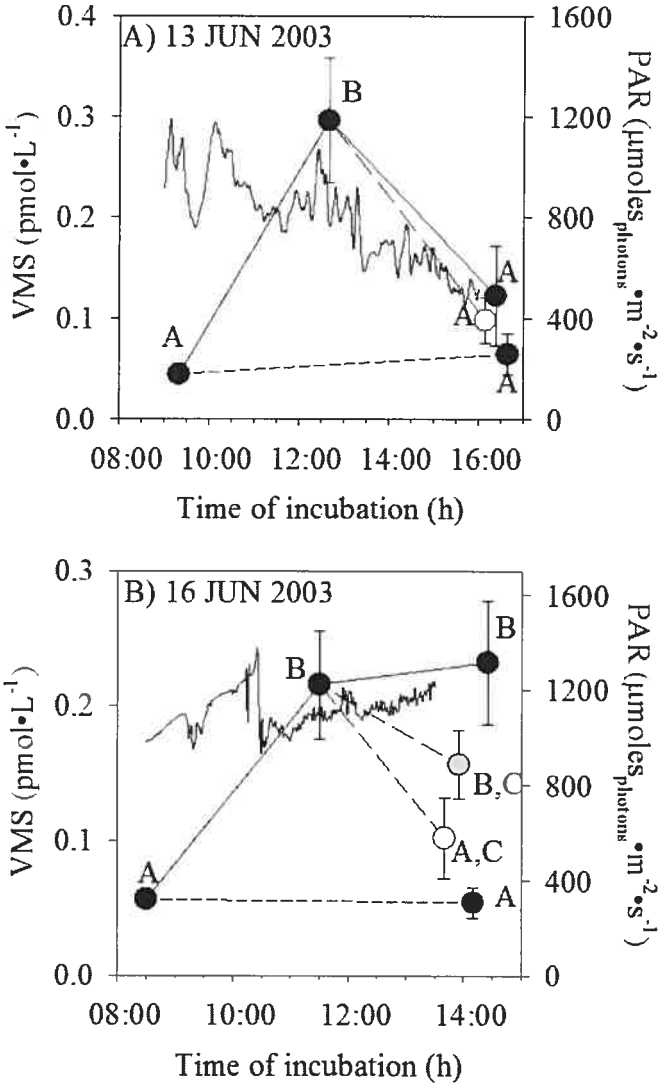

Figure 2.8. Time series of VMS concentrations in snow on (A) June 13 and (B) June 16 2003. In both cases the first step of the incubations led to the production of VMS after a first 3 hours of exposure under the sun. On June 13, after this initial exposure some samples were placed in the dark (closed circle) or kept uncovered (open circle) for another 3 hours. On June 16, after this initial exposure some samples were wrapped in Mylar filters (grey circle) in UV-Lee model 226 filters (open circle) or kept uncovered (closed circle) for another 2 hours. Letters referred to significant differences between treatments after an analysis of variance (ANOVA, systat 8.0). Vertical bars represent the standard deviation of three or four samples.

On June 16, we applied filters to snow samples previously incubated for 3 hours under the sun. When samples were wrapped in Mylar (no UV-B treatment), [VMS] decreased by 30% over a 2 hour period (grey circle, Figure 2.8 B). When samples were wrapped in UV-Lee filters (no UV treatment), [VMS] decreased by 56% (open circles, Figure 2.8 B). When samples were kept exposed to direct sunlight, concentrations did not decrease, but reached a plateau at a value of 0.23 pmol L^{-1} (black circle, Figure 2.8 B). During this experiment no major continuous PAR decrease was recorded and the mean daily PAR was around 1150 μmol_{photon} m^{-2} s^{-1}, with peaks reaching 1500 μmol_{photon} m^{-2} s^{-1} (Figure 2. 8B). No changes in [VMS] were recorded in samples kept in total darkness for 5 hours. Note that these experiments were conducted under springtime conditions, i.e. at near zero temperature; the snow was therefore undergoing destructive metamorphism.

2.5. Discussion

2.5.1. Chemistry of snowpacks from the Resolute Bay area

Distribution of inorganic ions.

The prevalence of anions (chloride, nitrate and sulphate) and cations (calcium, sodium and magnesium) observed at Resolute from June 4 to June 26 agreed well with the results of a previous study on the chemical composition of arctic snowfall (26). The prevalence of chloride, nitrate and sulphate is likely the result of both sea-salt and acid aerosol deposition. The predominance of calcium, sodium and magnesium was probably due to the deposition of both sea-salt and soil or dust aerosols (the bedrock is of calcareous origin). Indeed, mid-June snow packs started to melt (Figure 2.3 C) exposing large areas of bare soil.

Variety of organic molecules.

The probable origins of organics in the arctic snow include: a) long range transport of volatile compounds or of species associated with aerosols originating from southern areas b) transport of aerosols formed over the Arctic ocean (16), c) local deposition of organic aerosols from soil or decaying biota (9) d) the biological and/or photochemical transformations of the previous compounds (3) and e) directly from bioaerosols (1). Several unidentified peaks were observed in mass spectra of snow samples, some of which could correspond to larger molecular weight organic molecules such as peptides and polysaccharides. The smaller organic compounds observed in this study are expected to be formed via oxidation of dissolved organic matter or from biological-chemical or photochemical reactions of organics (3, 25).

A few identified organic compounds exhibit high vapour pressure (e.g. chlorobenzene; 1-ethyl,3-methyl benzene) and one expects a flow of such molecules from snowpack to atmosphere. Some other identified organic compounds, particularly long chain aldehydes, ketones and aromatic compounds, should be retained in the snow. Based on the chemical structure of these groups, one can expect the production of a variety of organic intermediates, including radicals, in presence of large pools of oxidant precursors such as halides, NO_2^- and NO_3^-; these precursors can release active halogen and $OH^\bullet$ radicals in snow, upon photolysis. The production of such radicals will likely lead to changes in the redox chemistry of Hg, as discussed below (see section *4.3.*).

2.5.2. Behaviour of Hg in snow after the atmospheric Hg depletion event

At the exception of a peak recorded on June 7, total Hg concentrations in snow stayed below 15 pmol L^{-1} from June 7 to June 23. The sharp increase on June 7 was likely the result of a depletion event of atmospheric mercury

($Hg(0)_{atm}$), since such an event was observed by another team working at the same site at the same time (11). Total Hg concentrations in surface snow then decreased by 92% within 48 hours.

As initially demonstrated by Lalonde et al. (2002) (15), total Hg loss in surface snow likely resulted from a snow-to-air rather than a snow-to-ground transfer. Indeed, $Hg(0)_{atm}$ concentrations over the snowpack sharply increased after June 7 (11) and no increase in total mercury concentrations was observed deeper in the snowpack after this event (Figure 2.3 A and B). Note that, polar snowpacks are typically exposed to high winds, and therefore undergo continuous changes, making it difficult to follow a specific snow layer over time.

We assessed if daily losses of total Hg following the MDE could be accounted for by VMS photoproduction. From June 9 to June 10 (24 h period), total Hg concentrations at the surface of the snowpack decreased by 3.3 $pmol \cdot L^{-1}$ (Figure 2.2). On June 9, incubation experiments yielded a VMS production of 3.9 pmol L^{-1} over the daily peak of solar radiation (10h00 to 18h00). VMS photoproduction can therefore account for more than the observed loss in total Hg. Note that these are rough estimates, since Hg photooxidation will also affect both losses of total Hg in snow and VMS production in incubation bottles.

No increase in [VMS] was observed in samples incubated under 3 cm of snow or kept in the dark, suggesting that Hg photoreduction occurred at the very surface of the snowpack. According to King and Simpson (2001) (10), we would expect that approximately 75% of incident UV radiation will penetrate to a depth of 3 cm. It is therefore surprising that we observed no photochemically-induced VMS production at 3 cm. King and Simpson's results may not be directly applicable to our study, due to differences in snow type and light penetration patterns. They indeed studied very dry snow at -30°C which would have favoured light penetration. VMS production may also be partly governed by heterogeneous catalysis or by biological catalysis of a biofilm at this interface.

2.5.3. Photooxidation and reduction of mercury

The incubations showed that after an initial increase in [VMS] in samples exposed to the entire solar spectrum, subsequent removal of UV-B radiation led to a decrease in [VMS] of 30% (Figure 2.8). The removal of both UV-B and UV-A radiation and of all radiations led to decreases of 56% and 63%, respectively.

These results indicate that Hg reduction was mainly driven by UV-B radiation. This is in agreement with previous findings in remote temperate locations (12). We further observed an oxidation of newly photo-produced Hg(0). If pre-exposed samples were kept in the dark, exposed to UV-A or visible wavebands, oxidation was favoured over reduction. Our observations illustrate that under low UV-B exposure, one can indeed detect the signature of mercury oxidation.

We identified several organic molecules and halides that could potentially act as oxidants of Hg under these conditions (Table 1 and 2). Evidence for the existence of reactive radicals such as HO, Cl, and Br upon photolysis in snowpack has already been presented (Ariya et al. 1999, Shepson and Sumner 1999). Many such radicals can be produced by irradiation within the UV-A or visible spectra (e.g., Cl can be produced by UV-A photolysis of Cl_2, while Br can be generated by visible photolysis of Br_2). They can also lead to production of other organic radical intermediates. We therefore can speculate that, due to the presence of the reactive radicals, a set of reactions can supply oxidants to transform Hg(0) to Hg(II). Clearly, since mercury redox mechanisms are complex, one also expects reduction of oxidized mercury to occur simultaneously.

2.6. Conclusion

We propose that during arctic springtime, both reduction and oxidation of Hg occurs in snowpacks and are both photo-induced. The reactions occur at the

surface, likely through a chain reaction after the formation of initial radicals. Newly produced VMS that is not quickly exported to the atmosphere is likely to remain within the snowpack because of re-oxidation. Hg travelling throughout the snowpack in its volatile reduced form will alternatively undergo oxidation and reduction when reaching the surface, where pools of photolabile molecules are found. Wind intensity and the extent of its penetration within the snowpack as well as a good knowledge of the physical properties of the snowpack, such as temperature gradients that can control the distribution of volatile species, are therefore critical parameters to better model Hg behaviour in snow especially in the high arctic where snow undergoes a rapid and constant metamorphism.

2.7. Acknowledgements

We gratefully acknowledge funding from CFCAS and COMERN to MA and PAA. We thank Peter G.C. Campbell for his comments on the manuscript. We also would like to thank the Polar Continental Shelf Project for their outstanding logistic help as well as the Nunavut Research Institute that delivered our research license. We thank Melissa Sparling and Debbie Iqaluk for their help in the field.

2.8. Références

1. **Ariya, P. A., and M. Amyot.** 2004. New Directions: The role of bioaerosols in atmospheric chemistry and physics. Atmospheric Environment **38:**1231-1232.
2. **Ariya, P. A., A. Khalizov, and A. Gidas.** 2002. Reactions of gaseous mercury with atomic and molecular halogens: Kinetics, product studies, and atmospheric implications. Journal of Physical Chemistry A **106:**7310-7320.
3. **Ariya, P. A., O. Nepotchatykh, O. Ignatova, and M. Amyot.** 2002. Microbiological degradation of atmospheric organic compounds. Geophysical Research Letters **29**.

4. Colbeck, S. C., E. Akitaya, R. Armstrong, H. Gubler, J. Lafeuille, K. Lied, D. McClung, and E. Morris. 1985. The International Classification for Seasonnal Snow on the Ground.
5. **Dommergue, A., C. P. Ferrari, L. Poissant, P. A. Gauchard, and C. F. Boutron.** 2003. Diurnal cycles of gaseous mercury within the snowpack at Kuujjuarapik/Whapmagoostui, Quebec, Canada. Environmental Science & Technology **37:**3289-3297.
6. Ebinghaus, R., H. H. Kock, C. Temme, J. W. Einax, A. G. Lowe, A. Richter, J. P. Burrows, and W. H. Schroeder. 2002. Antarctic springtime depletion of atmospheric mercury. Environmental Science & Technology 36:1238-1244.
7. **Ferrari, C. P., A. Dommergue, C. F. Boutron, H. Skov, M. Goodsite, and B. Jensen.** 2004. Nighttime production of elemental gaseous mercury in interstitial air of snow at Station Nord, Greenland. Atmospheric Environment **38:**2727-2735.
8. **Gill, G. A., and K. W. Bruland.** 1990. Mercury Speciation in Surface Fresh-Water Systems in California and Other Areas. Environmental Science & Technology **24:**1392-1400.
9. **Kawamura, K., A. Yanase, T. Eguchi, T. Mikami, and L. A. Barrie.** 1996. Enhanced atmospheric transport of soil derived organic matter in spring over the high Arctic. Geophysical Research Letters:3735-3738.
10. **King, M. D., and W. R. Simpson.** 2001. Exctinction of UV radiation in Arctic snow at Alert, Canada (82°N). Journal of Geophysical Research **106:**12499.
11. **Lahoutifard, N., M. C. Sparling, and D. R. S. Lean.** 2003. Interrelationships between atmospheric mercury, mercury speciation in the snow and springtime weather conditions in the high Arctic, 4th general meeting of the Collaborative Mercury Research Network., St Andrew's, NB, Canada.
12. **Lalonde, J. D., M. Amyot, M. R. Doyon, and J. C. Auclair.** 2003. Photo-induced Hg(II) reduction in snow from the remote and temperate Experimental Lakes Area (Ontario, Canada). Journal of Geophysical Research-Atmospheres **108**.
13. **Lalonde, J. D., M. Amyot, A. M. L. Kraepiel, and F. M. M. Morel.** 2001. Photooxidation of Hg(0) in artificial and natural waters. Environmental Science & Technology **35:**1367-1372.
14. **Lalonde, J. D., M. Amyot, J. Orvoine, F. M. M. Morel, J. C. Auclair, and P. A. Ariya.** 2004. Photoinduced oxidation of Hg-0 (aq) in the waters from the St. Lawrence estuary. Environmental Science & Technology **38:**508-514.
15. **Lalonde, J. D., A. J. Poulain, and M. Amyot.** 2002. The role of mercury redox reactions in snow on snow-to-air mercury transfer. Environmental Science & Technology **36:**174-178.

16. **Leck, C., and C. Persson.** 1996. Seasonal and short-term variability in dimethyl sulfide, sulfur dioxide and biogenic sulfur and sea salt aerosol particles in the arctic marine boundary layer during summer and autumn. Tellus Series B-Chemical and Physical Meteorology **48:**272-299.
17. **Lindberg, S. E., S. Brooks, C. J. Lin, K. J. Scott, M. S. Landis, R. K. Stevens, M. Goodsite, and A. Richter.** 2002. Dynamic oxidation of gaseous mercury in the Arctic troposphere at polar sunrise. Environmental Science & Technology **36:**1245-1256.
18. **Lindberg, S. E., A. F. Vette, C. Miles, and F. Schaedlich.** 2000. Mercury speciation in natural waters: Measurement of dissolved gaseous mercury with a field analyzer. Biogeochemistry **48:**237-259.
19. Lu, J. Y., W. H. Schroeder, L. A. Barrie, A. Steffen, H. E. Welch, K. Martin, L. Lockhart, R. V. Hunt, G. Boila, and A. Richter. 2001. Magnification of atmospheric mercury deposition to polar regions in springtime: the link to tropospheric ozone depletion chemistry. Geophysical Research Letters 28:3219-3222.
20. **Poissant, L., and M. Pilote.** 2003. Time series analysis of atmospheric mercury in Kuujjuarapik/Whapmagoostui (Quebec). Journal De Physique Iv **107:**1079-1082.
21. **Schroeder, W., A. Steffen, K. J. Scott, T. Bender, E. Prestbo, R. Ebinghaus, J. Y. Lu, and S. E. Lindberg.** 2003. Summary Report: first international Arctic atmospheric mercury research workshop. Atmospheric Environment **37:**2551-2555.
22. Schroeder, W. H., K. G. Anlauf, L. A. Barrie, J. Y. Lu, A. Steffen, D. R. Schneeberger, and T. Berg. 1998. Arctic springtime depletion of mercury. Nature 394:331-332.
23. **Scott, K. J.** 2001. Bioavailable mercury in arctic snow determined by a light-emitting mer-lux bioreporter. Arctic **54:**92-95.
24. **Steffen, A., W. Schroeder, J. Bottenheim, J. Narayan, and J. D. Fuentes.** 2002. Atmospheric mercury concentrations: measurements and profiles near snow and ice surfaces in the Canadian Arctic during Alert 2000. Atmospheric Environment **36:**2653-2661.
25. **Sumner, A. L., and P. B. Shepson.** 1999. Snowpack production of formaldehyde and its effect on the Arctic troposphere. Nature **398:**230-233.
26. **Toom-Sauntry, D., and L. A. Barrie.** 2002. Chemical composition of snowfall in the high Arctic: 1990-1994. Atmospheric Environment **36:**2683-2693.

3. Mercury distribution and speciation in coastal vs. inland high Arctic snow

Alexandre J. Poulain, Edenise Garcia, Marc Amyot, Peter G.C. Campbell and Parisa A. Ariya.

Manuscrit accepté dans Geochimica et Cosmochimica Acta.

3.1. Abstract

Atmospheric mercury deposition on snow at springtime has been reported in polar regions, potentially posing a threat to coastal and inland ecosystems receiving meltwaters. However, the post-depositional fate of Hg in snow is not well known, and no data are available on Hg partitioning in polar snow. During snowmelt, we conducted a survey of Hg concentrations, partitioning and speciation in surface snow and at depth, over sea ice and over land along a 100 km transect across Cornwallis Island, NU, Canada. Total Hg concentrations [THg] in surface snow were low (less than 20 pmol L^{-1}) and were significantly higher in marine vs. inland environments. Particulate Hg in surface snow represented up to 90% of total Hg over sea ice and up to 59% over land. At depth, [THg] at the snow/sea ice interface (up to 300 pmol•L^{-1}) were two orders of magnitude higher than at the snow/lake ice interface (ca. 2.5 pmol•L^{-1}). Integrated snow columns, sampled over sea-ice and over land, showed that particulate Hg was bound to particles ranging from 0.45 to 2.7 µm in size. Moreover, we present the first evidence that melting snowpacks over sea ice and over lake ice contribute to increase [THg] at the water/ice interfaces. This study indicates that, at the onset of snowmelt, most of the Hg in snow is in particulate form, particularly over sea ice. Low Hg levels in surface snow suggest that part of the Hg deposited through early spring deposition events is lost to the atmosphere from the snowpack before snowmelt but that the sea ice/snow interface may constitute a site for Hg accumulation. Further understanding of the cycling of mercury at the sea ice/snow and sea ice/seawater interfaces - where microorganisms are thriving - is thus warranted to fully understand how mercury entering the arctic food webs.

3.2. Introduction

The discovery of mercury depletion events in the High Arctic (27, 29, 37, 41), Antarctic (13) and in sub-Arctic areas (10, 31), resulting in rapid, near complete depletion of Hg from the atmosphere, provides evidence that atmospheric oxidation of Hg is faster than initially proposed (44). These oxidation processes are thought to occur in marine environments (38), and to involve reactive halogen radicals from sea-salt aerosols (27). Recent studies showed that Br and BrO radicals were the most effective halogens driving gaseous elemental mercury oxidation (4). Together, modeling studies of atmospheric transport of Hg originating from Asia, Europe and to a lesser extent, North America, to higher latitudes combined with the rapid depletion of gaseous elemental mercury suggest that the Arctic is a sink for Hg (3). The main products of Mercury Depletion Events (MDE) are reactive gaseous species and particulate-phase Hg (28, 37, 18) observed an increase in particles larger than 0.3 µm in ambient air during an atmospheric depletion event, as well as a subsequent redistribution of the atmospheric particulate fraction to bigger sizes after the event ended. The same study suggested that particles of a size comprised between 0.5 and 5 µm were more likely to be associated with MDE than the smaller ones. These atmospheric processes may affect the partitioning of Hg in underlying snow, hence the need to better assess Hg association with particles in snow.

The pool of Hg in surface snow, although periodically and dramatically enriched during MDEs (29), decreases at the onset of snowmelt, and can reach low levels that are comparable to what can be found in pristine environments (27, 32, 39, 41). This decrease in total Hg concentrations in the snowpack is likely related to the photoreduction of Hg(II) and its subsequent evasion to the atmosphere (24, 26) or to a loss associated with snowmelt water during early melt episodes (9, 41). Recent work showed that Hg concentrations in direct

proximity to sea ice leads could reach unprecedented levels of *ca.* 4 nmol•L^{-1} (12). These data, together with laboratory studies that underscored that bromine-derived reactive compounds originating from sea-salt aerosols were involved in fast oxidation of atmospheric Hg (4), suggest that Hg cycling in coastal/marine environments is highly dynamic, possibly leading to Hg accumulation in these areas (11). There is therefore a need to better characterize the behaviour of Hg in snow at the interface between marine and inland systems. In particular, there is very limited information available on the partitioning of Hg in marine and inland polar snow.

The purpose of this paper is to establish the distribution, partitioning and speciation of total Hg (THg) in surface snow deposited over land and over sea ice along a 100 km transect encompassing two coastal areas. We also investigated the role of snow/ice interfaces as potential accumulation areas for Hg over sea and lake waters.

3.3. Methods

3.3.1. Sampling protocol and locations

To establish the spatial distribution and speciation of total Hg from marine to inland snow, we sampled surface snow along a transect NW-SE across Cornwallis Island, NU, Canada (Figure 3.1 A) on 17 June 2004. Sampling started over the sea-ice between Little Cornwallis and Cornwallis islands and extended to the sea-ice between Cornwallis and Devon islands for a total of 11 sites (Figure 3.1 B; surface snow physical properties at the 11 transect sampling sites are given in Table 1). Sampling for depth profiles and particulate distribution took place in the south-west part of Cornwallis Island (Figure 3.1 B). Sampling was undertaken while average daily air temperatures started to exceed the freezing point as recorded by Environment Canada at the Resolute Bay station (Figure 3.2 A and B) and when snow was starting to melt. Note that

for each site and snow stratum sampled, temperature was recorded to better assess snow properties.

Transect surface snow sampling

Transect sampling was carried out on 7 June 2004. Snow sampling was done by collecting triplicate snow samples from the first centimetre of the surface of the snowpack by filling 1L fluorinated ethylene propylene copolymer (Teflon FEP) bottles, using a Teflon shovel. All containers used for Hg sampling and analysis were previously acid-washed and thoroughly rinsed with milliQ water (R > 18.2 MΩ.cm). Clean hands / dirty hands techniques were used, and integral Tyvek® body suits and non-powdered gloves were worn at all times in order to avoid contamination.

Snow depth profiles

Snow accumulation over sea ice and over land was sampled on 9 June 2004. For snow depth profiles, triplicate samples were taken from each snow stratum. One replicate corresponded to one litre of snow collected in a Teflon bottle using a Teflon shovel. Snow strata were determined by the state of metamorphism of the snow grains, as defined in the international classification of seasonal snow on the ground (6). Snow grain identification and size determination was carried out in the field, using a binocular over a black, cold (T<0°C), background. Snow density as well as the temperature of the layer at mid depth were also measured. Snow for cation analyses was collected in 30 mL High density polyethylene (HDPE) Nalgene bottles that had previously been thoroughly cleaned, rinsed with ultrapure water and acidified to 0.1% with HCl (64%, Omnitrace grade). Snow for anion analyses was collected in 30 mL HDPE Nalgene bottles, previously thoroughly rinsed with ultrapure water. All samples were kept in the dark and at 4°C until they were analysed. Note that due to the

rapid melt occurring at this time and considering the time required to carry out all the analyses within a few hours of sampling, we could not carry out more than one depth profile at each site.

Lake / seawater depth profiles

Water was pumped from the depth of interest using a neoprene-coated Teflon line and a peristaltic pump (Masterflex™). The neoprene coating protected the water circulating in the tubing from exposure to solar radiation. Prior to deployment in the field, the line was thoroughly washed with HCl 20% (v/v) by continuously circulating the acidic solution through the line for 30 minutes. The line was then carefully rinsed with ultrapure water; achievement of proper rinsing of the line was monitored by measuring the conductivity of the circulating solution and rinsing stopped when the solution reached levels below 3 $\mu S \cdot cm^{-1}$, corresponding to that of ultrapure water. In the field, the line was rinsed with the water at each depth of interest prior to taking samples from that depth. Acid-washed Teflon bottles were rinsed with the water from the depth of interest 4 times prior to the actual sampling; samples were taken in triplicate.

.

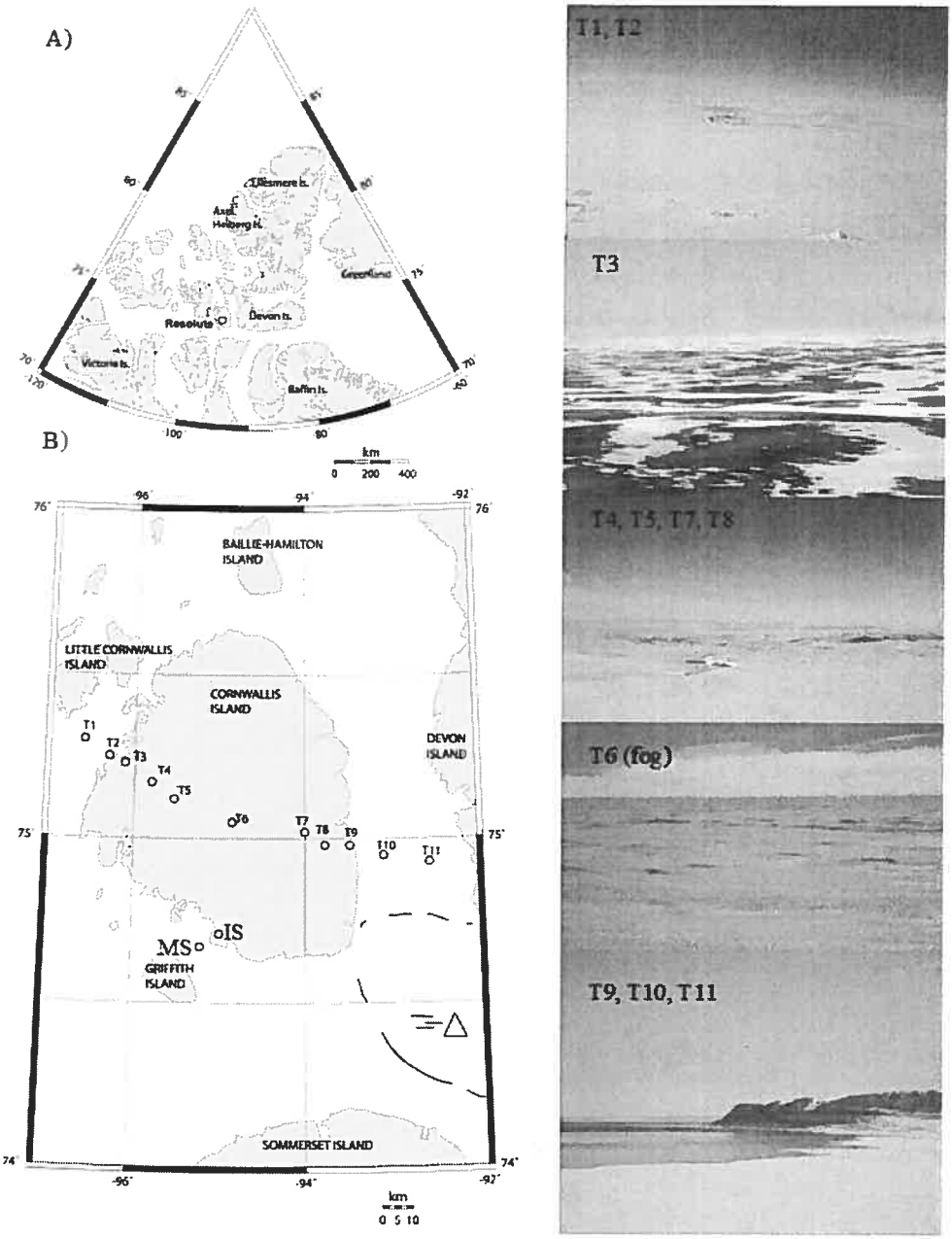

Figure 3.1. A) Location of Cornwallis Island in the Canadian High Arctic. B) Location of sampling sites during the transect survey. Pictures on the right-hand side refer to the transect. Note that the white triangle at the bottom right of the graph refers to open waters area (no ice present), as depicted in picture T9, T10, T11.

Table 3.I. Surface snow physical properties at the 11 sampling sites of the transect. ∩ represents mixed formed crystals (faceted crystals with potentially recent rounding due to decrease in temperature gradient) and ⁂ represent melt cluster.

	Site	Altitude (m; a.s.l.)	Snow density %	Temp surface. (°C)	Temp. bottom. (°C)	Snow depth (cm)	Symbol	Grain size (mm)
T1	Sea ice	0	40	0.5	0	9	∩	2-4
T2	Sea ice	0	48	0.5	0	20	⁂	2-4
T3	Coastal area	10	42	0	-0.5	40	∩	2-4
T4	Inland	178	36	0	-5	46	∩	2
T5	Inland	169	34	-0.5	-9	41	∩	1-5
T6	Inland	236	28	0	-10	36	∩	1-2
T7	Inland	289	42	-0.5	-5	20	⁂	2.4
T8	Inland	220	55	0.5	0	55	⁂	3-4
T9	Coastal area	179	50	0	-4	20	⁂	2-3
T10	Sea ice	0	48	0	0.5	12	∩	2-4
T11	Sea ice	0	42	0	-1	9	∩	2-4

Figure 3.2. Meteorological data. A) From September 2003 to September 2004 and B) from May 2004 to July 2004. Are presented, snow accumulation on the ground, snow precipitation, daily average temperature. Note that upper and lower continuous black lines represent ma×imum and minimum daily temperatures.

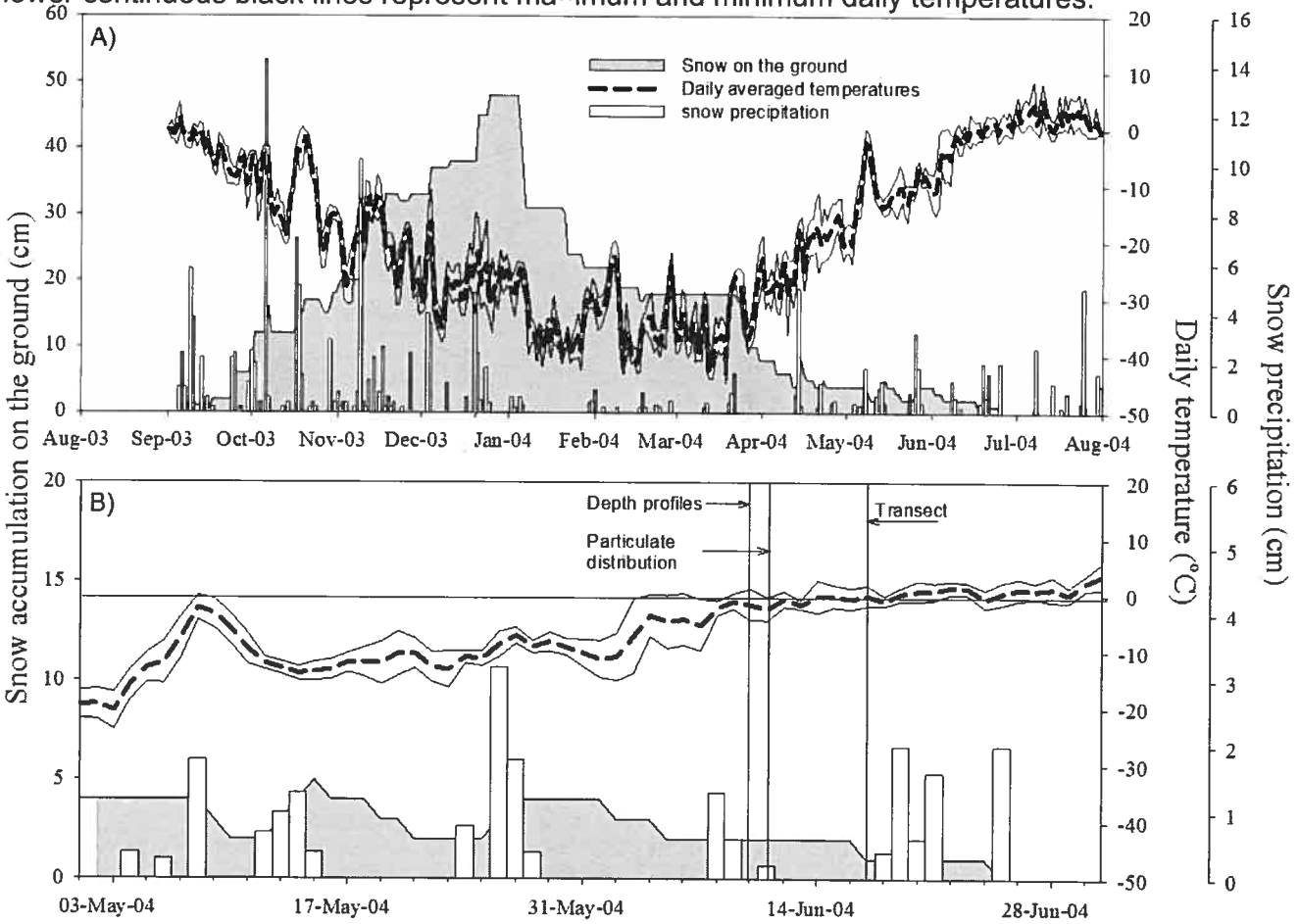

3.3.2. Chemical Analysis and bacterial counts

Total Hg concentrations in snow were quantified with the method described by Lalonde et al. (2003) and based on (20), using a mercury fluorescence detector (Tekran™ Model 2500). Briefly, Hg in water samples was reduced using 1% $NaBH_4$ (w/v) and 4 M NaOH. Approximately 100 mL of water or melted snow was poured into a 250 mL glass bubbler and purged for 15 minutes with clean air from a Hg-free air generator (Tekran™ Model 1100) additionally stripped of Hg(0) by passage over a gold filter at a flow rate of ca. 1 L min^{-1}. The working detection limit of this method, calculated in the field, was 0.45 pmol L^{-1} or three times the standard deviation of ten procedural blanks. Triplicates were systematically taken and typically varied between 0.5 and 10%. Average blank values were below the detection limit.

Anions were analyzed by ion chromatography using a DIONEX ICS 2000. A 25-µL sample of melted snow was introduced into the injection loop and separation occurred through an AS-17 column topped with a AG-17 pre-column. The elution step involved the passage of a KOH solution with a concentration gradient from 15 to 30 mmol L^{-1}. Cations were analysed with an inductively coupled plasma atomic emission spectrometer (ICP-AES Vista AX) using an internal standard of Yttrium (5 mg L^{-1}). With this method, variability is within 5% with very few exceptions where interferences were observed due to high salinity. In these latter cases, samples were diluted and reanalysed to achieve proper replicability.

Bacterial counts were determined using a flow cytometer following the protocol described in (17).

3.3.3. Modeling of the dissolved inorganic speciation of Hg

To assess the inorganic speciation of Hg in melted snow and water, we used a chemical equilibrium program (MINEQL+, version 4.5) (36). Cations and metals entered in the model were calcium, iron, magnesium, mercury, potassium and sodium. Anions used were bromide, chloride, nitrate and sulphate as well as hydroxide derived from the pH of the sample. The solutions were considered to be in equilibrium with the atmosphere and carbonate species were estimated by the model using the pH of the samples. Data were corrected for the ionic strength of the sample; ionic strength was calculated by the model with the Davies equation. Stability constants used in the model are presented in Table 2. We did not model the complexation of Hg with dissolved organic matter (DOM) due to the current lack of consensus regarding binding constants for Hg-DOM complexation reactions. However, we included in our model small organics such as acetate and formate usually found in Arctic snow (46). Hg complexation, whether it is inorganic or organic, is strongly influenced by the pH of the solution. Several studies have shown that the pH of a solution may change upon the dissolution of acidic aerosols (34), likely to be the case during snowmelt. While speciation results presented in this paper were based on the measured pH of melted snow, we also performed a sensitivity test for snow samples in which we ran the model over a pH range of ± 1 pH unit above and below the measured pH value. Moreover, to take into consideration uncertainties inherent in the estimation of the complexation constants, we also ran the model with binding constants ± 1 order of magnitude. Results showed shifts in the relative importance of the species, altogether with differences ranging from 4 to 40% from the initial values, but these variations did not affect the conclusions presented in the paper.

Table 3.II. Reactions and stability constants used in the model Mineql+ ver. 4.5.

Reactions	LogK
$Hg^{2} + 2H_2O \leftrightarrow Hg(OH)_2 + 2H^+$	6.194
$2H^+ + 2Br^- + Hg(OH)_2 \leftrightarrow 2H_2O + HgBr_2$	24.27
$2H^+ + NO_3^- + Hg(OH)_2 \leftrightarrow 2H_2O + HgNO_3^+$	5.761
$2H^+ + 2NO_3^- + Hg(OH)_2 \leftrightarrow 2H_2O + Hg(NO_3)_2$	5.38
$2H^+ + SO_4^{2-} + Hg(OH)_2 \leftrightarrow 2H_2O + HgSO_4$	8.61
$H^+ + Br^- + Hg(OH)_2 \leftrightarrow H_2O + HgBrOH$	12.433
$2H^+ + Br^- + Cl^- + Hg(OH)_2 \leftrightarrow 2H_2O + HgBrCl$	22.181
$H^+ + Cl^- + Hg(OH)_2 \leftrightarrow H_2O + HgClOH$	10.44
$2H^+ + 2Cl^- + Hg(OH)_2 \leftrightarrow 2H_2O + HgCl_2$	20.194
$2H^+ + 3Cl^- + Hg(OH)_2 \leftrightarrow 2H_2O + HgCl_3^-$	21.194
$2H^+ + 4Cl^- + Hg(OH)_2 \leftrightarrow 2H_2O + HgCl_4^{2-}$	21.794
$2H^+ + [HCOOH] + Hg(OH)_2 \leftrightarrow 2H_2O + Hg[HCOOH]$	9.6
$2H^+ + [CH_3COOH] + Hg(OH)_2 \leftrightarrow 2H_2O + Hg[CH_3COOH]$	10.49
$2H^+ + 2[CH_3COOH] + Hg(OH)_2 \leftrightarrow 2H_2O + Hg[CH_3COOH]_2$	13.83

The default logK values in MINEQL+ are taken from "Critical Selected stability Constant of Metal Complexes", National Institute of Standards and Technology (NIST) Standard Reference Database.

Table 3.III. Physico-chemical variables of the transect and depth snow profiles carried out on Cornwallis Island.

Site	pH	bacterial counts ($cell \cdot ml^{-1}$)	Cl^- ($\mu mol \cdot L^{-1}$)	Br^- ($\mu mol \cdot L^{-1}$)	NO_3^- ($\mu mol \cdot L^{-1}$)	SO_4^{2-} ($\mu mol \cdot L^{-1}$)
Fresh snow (26-JUN-04)	6.0	1.20×10^5	6.34	< d.l.	5.213	0.564
Coastal site surface stratum (S1)*	9.0	5.17×10^5	267.6	0.493	2.359	13.98
Coastal middle stratum (S2)*	9.0	1.31×10^5	3620	6.000	5.289	145.0
Coastal bottom stratum (S3)*	8.5	1.58×10^5	1.657×10^5	116.5	< d.l.	2.699×10^4
Inland Site surface	8.4	1.45×10^5	6.157	< d.l.	6.327	0.432
Inland Intermediate stratum 1	8.4	4.46×10^5	42.63	< d.l.	6.098	2.643
Inland Intermediate stratum 2	8.1	2.01×10^5	76.65	< d.l.	8.083	3.254
Inland Site bottom	8.3	2.09×10^5	41.22	< d.l.	5.473	3.196
Transect 1	7.2	1.81×10^5	164.1	0.255	3.230	1.394
Transect 2	7.0	1.40×10^5	17.81	< d.l.	< d.l.	< d.l.
Transect 3	6.7	2.70×10^5	8.709	< d.l.	2.790	< d.l.
Transect 4	6.4	1.42×10^5	14.64	< d.l.	1.743	0.792
Transect 5	5.8	1.03×10^5	10.06	< d.l.	3.384	6.080
Transect 6	5.6	8.71×10^4	14.91	< d.l.	5.706	3.548
Transect 7	5.5	1.56×10^5	10.29	< d.l.	2.657	0.717
Transect 8	5.0	1.44×10^5	12.43	< d.l.	1.641	3.805
Transect 9	7.0	7.24×10^4	18.01	< d.l.	1.268	< d.l.
Transect 10	6.5	1.94×10^5	325.9	0.783	3.138	1.911
Transect 11	6.0	2.65×10^5	307.6	< d.l.	< d.l.	< d.l.

* refers to the snow strata observed over sea ice

3.3.4. Partitioning of Hg onto particles and elemental composition of particles

Partitioning experiments

To identify to which size fraction particulate Hg was bound, one integrated snow column (*ca.* 20L) was collected inland, and one over the sea-ice, on 13 June 2004, in a Tedlar® (polyvinyl fluoride) bag, previously acid washed and rinsed with ultrapure water. After a complete thaw was reached at room temperature, triplicate water samples from each bag were filtered through filters of decreasing porosities: 10 µm (polycarbonate), 2.7 µm (GF/B), 0.7 µm (GF/F), 0.45 µm (Gelman) and 0.2 µm (polycarbonate). The particulate Hg distribution was obtained by subtracting the Hg burden between two filters of consecutive pore sizes. To test for possible adsorption of Hg onto different filters, 125 mL of a standard solution freshly prepared in ultra-pure water (final concentration 10.22±0.35 $pmol \cdot L^{-1}$, n=4) was filtered through polycarbonate (0.2 µm, n=4), Gelman (0.45µm, n=3) and glass fibre (0.7 µm, n=3) filters. The volume of the standard that was filtered corresponded to the volume of the samples filtered, i.e. 125 mL. No significant difference was found between the control and the filtrates from glass fibre filters and Gelman filters. Filtrates from polycarbonate filters yielded values significantly lower than the control by 20% (*t*-test, t=7.08, p=0.002). Results presented in this paper were therefore corrected for this adsorption when polycarbonate filters were used. This method was compared to that of Sarica et al. (2004) which uses a direct mercury analyser and determines Hg content by pyrolysis of the filter; no statistical difference was found using either the subtraction method, presented here, or the pyrolysis method (Wilcoxon, p=0.334). For bacterial counts, Falcon tubes were filled with snow, thawed at 4°C and preserved with glutaraldehyde to a final concentration of 2%.

Elemental composition of particles

In order to assess the elemental composition of the particles present in snow, we used a scanning electron microscope (Hitachi S-3000N Variable Pressure) coupled to an X-ray diffraction (XRD) probe. Melted snow samples, from an integrated snow column, were filtered through glass fibre filters of a nominal porosity of 0.7 µm. Samples included snow collected inland (n=3) and over the sea-ice (n=3). Each filter was freeze-dried and cut to a size of 1 cm^2 in order to be put on an aluminium sample-holder. Prior to microscopic observation and elemental composition determination, filters were coated with an Au-Pd amalgam. Depending on the number of particles in the filters, a minimum of 10 and a maximum of 20 observations were made on each filter. In the microscope field of observation, depending on the magnification used, 5 to 20 particles were present. These particles were targeted for XRD analysis. Note that this technique allowed us to qualitatively determine the elemental inorganic composition; no quantitative analyses were performed on the filters.

3.4. Results

3.4.1. Distribution of total mercury in snow along a transect an with depth, inland and over sea ice.

THg concentrations in surface snow along a transect

Total Hg concentrations ([THg]) were significantly higher in surface snow collected over the sea ice (10.2±3.5 pmol L^{-1}, n=12) than in surface snow collected over land (4.1±3.5 pmol L^{-1}, n=21) (Kruskal-Wallis test, p=0.037) (Figure 3.3 A). However, no significant differences were observed when comparing the dissolved fraction, smaller than 0.2 µm (Kruskal-Wallis test, p=0.72). Snow collected over sea-ice was enriched with chloride ions (0.20±0.14 mmol L^{-1}, n=4) compared to inland snow (0.01±0.003 mmol L^{-1}, n=7) (Figure 3.3

B). The proportion of Hg bound to particles was significantly higher (*t*-test, *t*=-2.92, p=0.016) in snow collected over the sea-ice (79±9%) than in snow collected over land (58±16%). In the middle of Cornwallis Island, at site T6 (Figure 3.3 A), the Hg level (10.6±5.7 pmol L^{-1}, n=3) was higher than at other inland sites (3.0±1.2 pmol L^{-1}, n=18). Note that a heavy fog was present during sampling at this site (Figure 3.1, picture T6). This peak in [THg] corresponded to a maximum in nitrate concentrations (94 µmol L^{-1}) (Figure 3.3 B). Particulate Hg and nitrate concentrations significantly co-varied throughout the island (r=0.67, p=0.024).

THg concentrations at depth within a snow accumulation

In order to compare Hg distribution at various depths within a snow column, two snow packs were sampled, i) over sea ice and ii) inland, over a frozen lake, in the south-western part of Cornwallis Island (see Figure 3.1 B for location, IS for inland site and MS for marine site). We observed clustered rounded crystals over the frozen lake, indicating signs of snowmelt. Over sea ice, rounded crystals were present in the middle stratum and we noted the presence of ice lenses in the center of the accumulation, indicating here again some signs of melt. Similarly to what was observed at the surface, Hg concentrations at depth were higher over sea ice than over land, and associated in a greater proportion with particles (Figure 3.3 A and Figure 3.4 C). These differences between coastal and inland snow were most striking at the snow/ice interface with [THg] two orders of magnitude higher in the coastal snow pack (Figure 3.4 A). In snow collected over sea-ice, [THg] was related to bromide (r^2=0.99, p=0.01) and chloride (r^2=0.99, p=0.028) concentrations. In snow collected inland, however, no relation was observed with chloride, and bromide ions were not detected. It should be noted, however, that the absence of a relationship in the latter case may be related to the smaller range of [Cl^-]

observed within the inland snowpack ($6.1 \cdot 10^{-3}$ to $4.1 \cdot 10^{-2}$ mmol·L^{-1}), compared to the range observed over the sea-ice (0.26 – 163 mmol·L^{-1}).

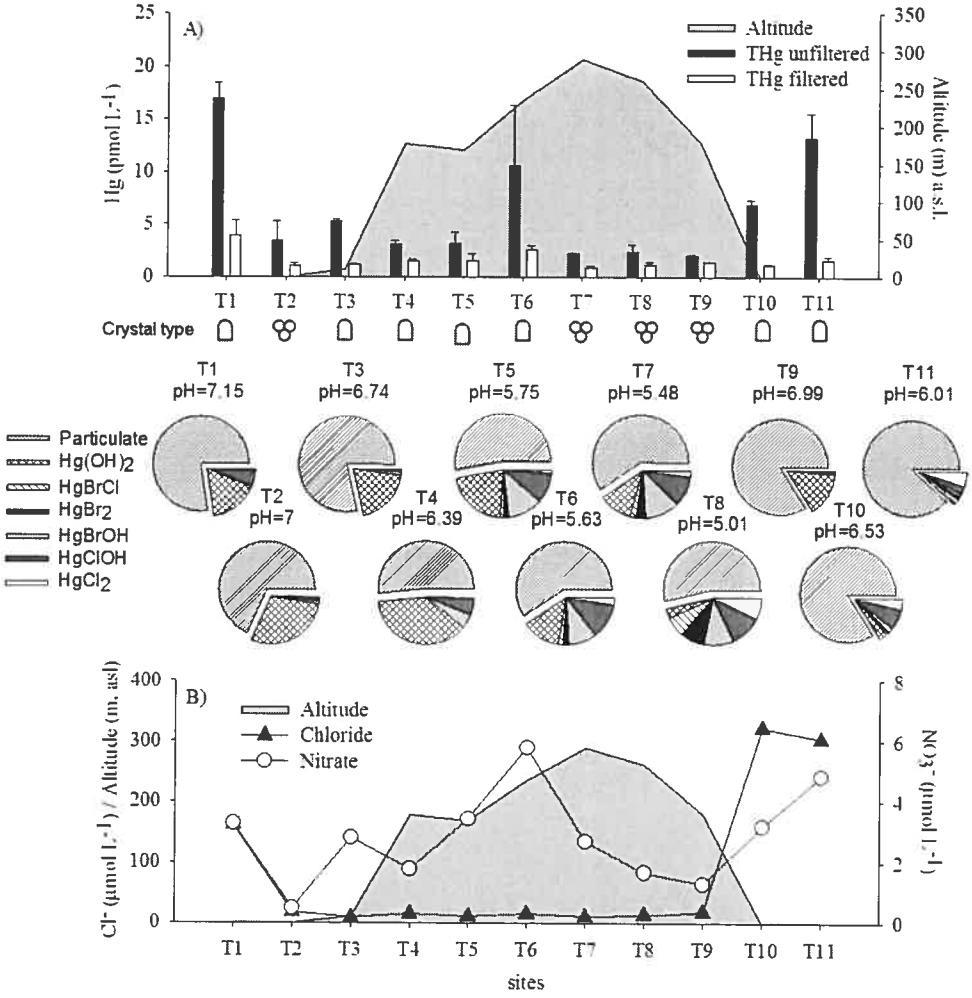

Figure 3.3. A). Total Hg concentrations (black bars) and dissolved Hg concentrations (white bars) over a transect, comprising 11 sites, throughout Cornwallis Island. Pies underneath each set of bars represent the particulate and dissolved inorganic speciation of Hg. B) Chloride and nitrate concentrations for each of the 11 sites. ∩ represents mixed formed crystals (faceted crystals with potentially recent rounding due to decrease in temperature gradient), and ∞ represents melt clusters.

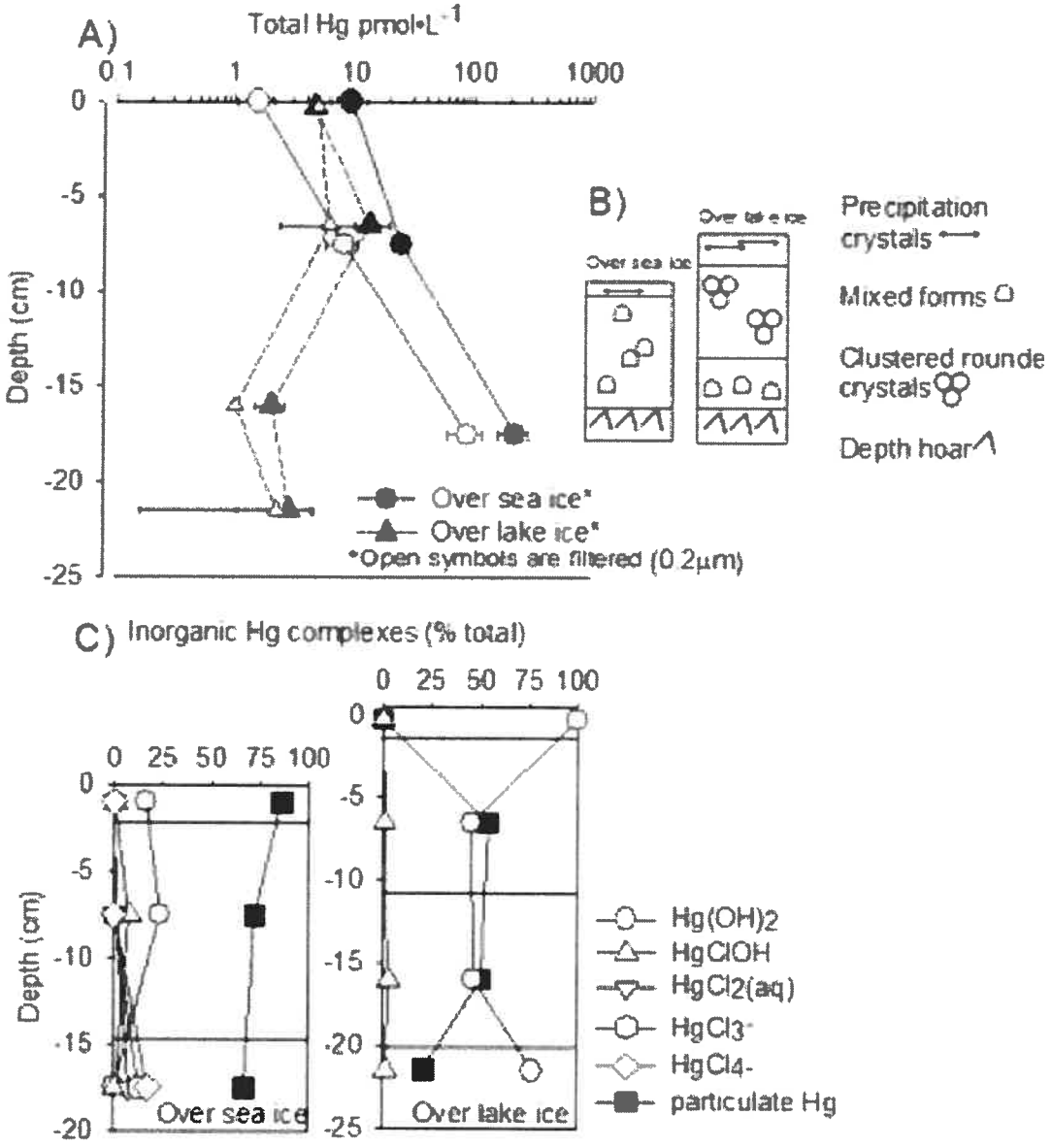

Figure 3.4. A) Depth profile of total mercury over sea ice (circle) and over land (triangles) in unfiltered (closed symbols) and filtered (open symbols) samples. B) Snow stratigraphy at both sites. C) Inorganic speciation of Hg.

3.4.2. Inorganic speciation of Hg in snow and partitioning onto particles.

Inorganic speciation

The inorganic speciation of the dissolved fraction greatly varied as a function of snow pH and halide concentrations. At the marine site, where salinity increased with depth, the dissolved phase was mostly comprised of uncharged complexes at the surface and negatively charged chloro-complexes at depth ($HgCl_3^-$ and $HgCl_4^{2-}$) (Figure 3.4 C). Inland, particulate and dissolved phases were alternately dominant within the profile. The dissolved phase was mainly formed of $Hg(OH)_2$ with some contributions from mixed complexes such as HgClOH (Figure 3.4 C). To test for the effect on Hg speciation of low molecular weight organic molecules present in snow, such as formate and acetate, we used previously published concentrations recorded at Alert (NU, Canada) (46) in our model. Even considering the maximum concentrations recorded for acetate and formate, Hg was still mostly bound to inorganic ligands such as OH^-, Cl^- and Br^-. Similar observations were reported for snow collected at lower latitudes in the French Alps (16). Due to its chemical properties, mercury is expected to have a greater affinity with sulphur-containing ligands than with carboxylic moieties (42). We did not quantify sulphur-containing compounds in snow, however.

Hg partitioning onto particles

No Hg was detected adsorbed to particles of a nominal size greater than 10 µm or smaller than 0.2 µm, both in snow collected over land and in snow collected over sea ice (Figure 3.5 A and B). Most of the particulate Hg was bound to particles ranging from 2.7 µm to 10 µm in snow collected over land (62±23%) and over sea-ice (53±6%) (Figure 3.5 A and 5B). In snow collected inland, the remaining particulate Hg was bound to particles of a size ranging

from 0.7 µm to 2.7 µm (12±11%) and from 0.45 µm to 0.7 µm (20±7%) (Figure 3.5 A). In snow collected over sea ice, the remaining particulate pool was significantly (p=0.004, n=15) more associated with the fraction [0.7 µm-2.7 µm] (32±4%) than with the fraction [0.45 µm-0.7 µm] (17±1%) (Figure 3.5 B). Snow was melted prior to the partitioning experiment. Hence, this experiment only reflects the association of Hg with insoluble or poorly soluble particles. It is therefore likely that the total concentrations of particulate Hg in solid snow, including water-soluble aerosols, were greater than the estimates reported here. To the best of our knowledge this is the first attempt to assess the post-depositional partitioning of Hg between dissolved and solid phases in arctic snow.

Elemental composition of particles

Elements present in the particles in snow included Al, Br, Ca, Fe, K, Na, O and Si. In most cases Si and Al were associated with the same particle, as were O, Mg and Ca, and Fe and O, suggesting the presence of sand grains (aluminosilicates), calcium carbonates and iron oxides. This interpretation was confirmed by visual observations, e.g. in the case of the cubic arrangement of calcium carbonate deposits. Since we used glass fibre filters, the presence of Si might be partly due to contamination from the filter. Note that with this technique we could not assess the composition of organics and soluble aerosols since snow was thawed, and high energy SEM is not adequate for detailed organic analysis.

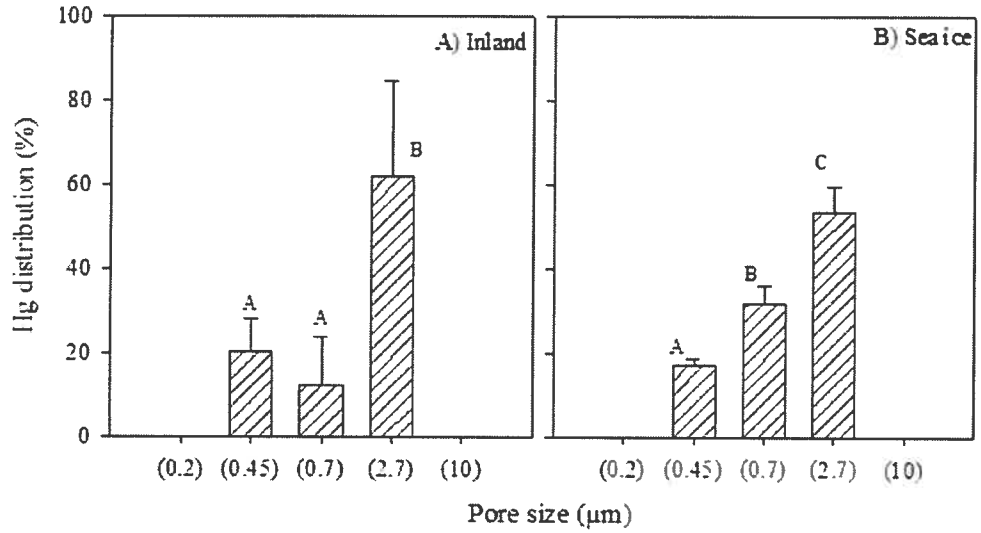

Figure 3.5. Relative distribution of particulate Hg species in snow collected inland and over the sea-ice as a function of particle size. Different letters represent significant differences.

3.4.3. THg concentrations in lake water and seawater underlying a melting snow accumulation

In order to assess the impact of the snowpack on underlying waters, we sampled the whole lake water column, from the surface to a depth of 10 m and the first 11.5 m of the sea water column. At both sites, [THg] concentrations were highest at the surface, between ice edges, and subsequently decreased 3 to 4 fold and stayed fairly stable in the remainder of the sampled zone (Figure 3.6 A and B). For all the other elements analysed, concentrations increased or stayed stable from the surface to a depth of 11.5 m (Table 3.IV, Figure 3.6 B). In seawater, the fraction of Hg bound to particles greater than 0.45 µm in the upper part of the lead was ca. 45% and only 15% and 6% at 5.5 and 11.5 m, respectively, indicating a greater importance of particulate Hg forms at the surface in direct proximity to the snowpack (Figure 3.6 B).

Based on snow thickness and snow density for each stratum, we estimated that the pool of Hg stored in snow over sea ice and over lake ice was ca. 4500 $pmol \cdot m^{-2}$ and 850 $pmol \cdot m^{-2}$, respectively. By comparing THg concentrations in water at depths below the ice (below 2 m), as a reference level for the pre-melt period, and THg concentrations measured at the surface, we calculated that ca. 500 and 100 $pmol \bullet m^{-2}$ of Hg were required, over sea ice and over lake ice, respectively, to increase the concentrations from that of the pre-melt period to the levels observed at the time of sampling. We estimated that melting of only 11% (over sea ice) or 14% (over lake ice) of the snowpack could provide these Hg levels.

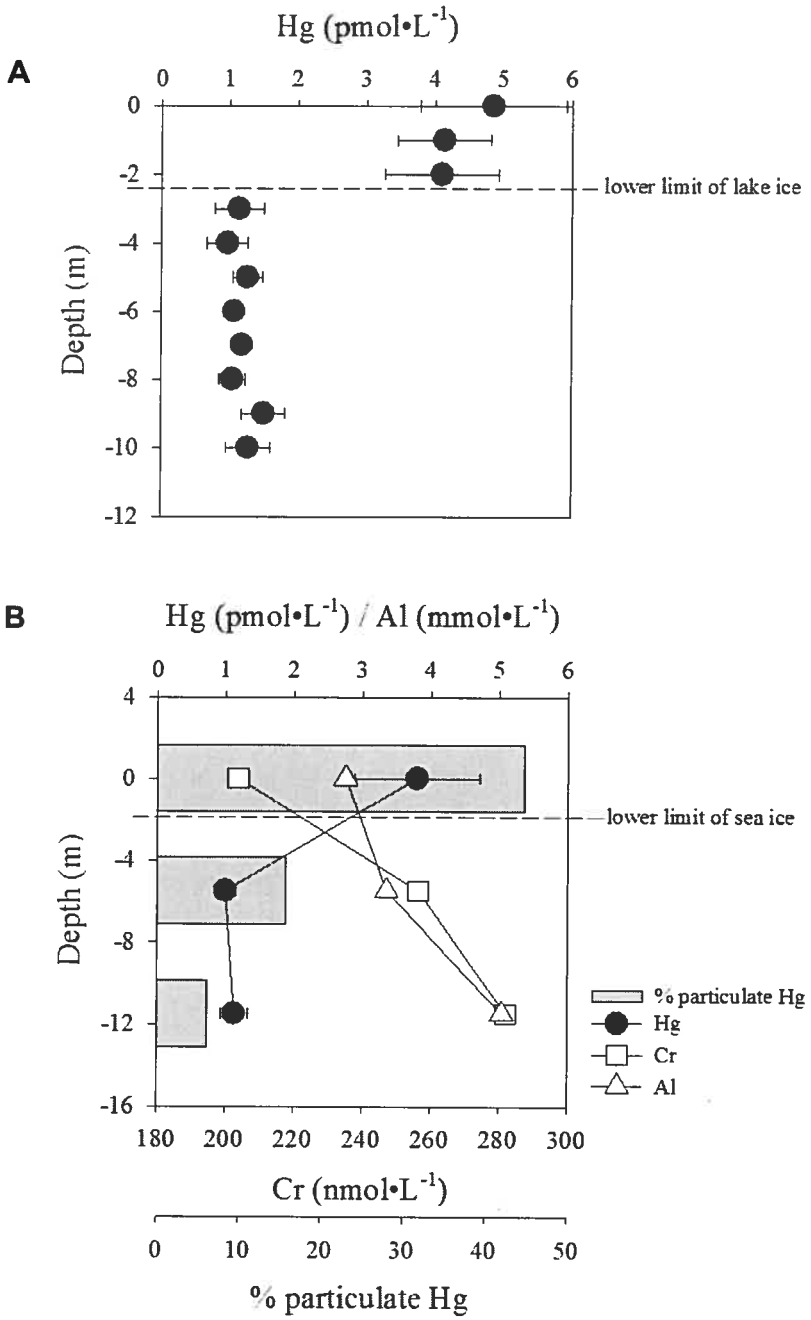

Figure 3.6. Depth profile of total mercury concentrations within the water column of ice-covered North lake (A) and depth profile of total mercury concentrations, down to 11.5 meters, in the Strait of Barrow, between Cornwallis and Griffith Islands. Samples were collected through a 10 to 50 cm crack in sea ice

Table 3.IV. Concentrations of cationic elements within the three snow strata of the accumulation over the sea ice *, as well as at the surface and at depths of 5.5 and 11.5 meter in seawater. Concentrations are expressed in $\mu mol \cdot L^{-1}$. The hatched rectangle represents the sea ice.
*snow strata were defined after the international classification of snow on the ground {Colbeck, 1985 #67} and

	Al	Ca	Cr	Fe	K	Mg	Mn	Na	Ni	Zn	Hg
S1*	4.9×10^{-5}	4.4×10^{-3}	1.8×10^{-5}	6.4×10^{-5}	2.6×10^{-3}	1.2×10^{-2}	5.1×10^{-6}	9.8×10^{-2}	1.8×10^{-5}	2.7×10^{-4}	9.2×10^{-6}
S2*	3.4×10^{-4}	3.9×10^{-2}	3.5×10^{-5}	2.0×10^{-4}	2.7×10^{-2}	1.5×10^{-1}	1.6×10^{-5}	1.2	1.8 x10-5	4.7×10^{-5}	5.9×10^{-5}
S3*	1.5×10^{-3}	3.7	1.8×10^{-5}	4.1×10^{-4}	3.0	16	2.2×10^{-5}	1.3×10^{2}	1.2×10^{-4}	2.6×10^{-5}	2.2×10^{-4}
Sea 0m	2.8×10^{-3}	9.3	2.0×10^{-4}	5.0×10^{-4}	8.1	48	4.6×10^{-5}	4.3×10^{2}	9.3×10^{-4}	9.9×10^{-5}	3.8×10^{-6}
Sea 5.5m	3.4×10^{-3}	9.5	2.6×10^{-4}	5.0×10^{-4}	8.3	50	4.6×10^{-5}	4.4×10^{2}	2.9×10^{-4}	1.1×10^{-4}	1.0×10^{-6}
Sea 11.5m	5.0×10^{-3}	9.7	2.8×10^{-4}	5.0×10^{-4}	8.5	49	4.6×10^{-5}	4.3×10^{2}	7.4×10^{-4}	1.1×10^{-4}	1.1×10^{-6}
[S3] : [Sea 0m]**	0.5	0.4	0.1	0.8	0.4	0.3	0.5	0.3	0.1	0.3	79.0

* refer to Figure 3.4 A. **represents the ratio of the concentrations recorded in the snow stratum directly overlying sea ice over the concentration recorded in surface seawater.

3.5. Discussion

3.5.1. Concentrations and speciation of THg concentrations in surface snow along a transect over land and sea ice

[THg] as well as the proportion of particulate forms of Hg were consistently and significantly higher in snow collected over sea ice (up to 300 pmol L^{-1} and 68 to 88% respectively) than in snow collected over land (up to 15 pmol L^{-1} and 31 to 59% respectively) (Figure 3.3 and Figure 3.4 A and C). High concentrations of Hg were previously reported in Arctic snow samples and were associated with mercury depletion events, more likely to occur in systems under marine influence (12). However, the concentrations reported here are lower than what was observed in other locations in the Arctic (ca. 450 pmol L^{-1}: (29), (27)). Indeed, our results were representative of samples collected during late spring (from 9 to 17 June), a period during which MDE were less likely to occur and associated with a decrease in the pool of THg because of the initiation of snowmelt (15, 27). Note that (25) and (2003) showed that chloride enhanced Hg(0) oxidation in water and decreased Hg(II) reduction when added to snow. Hence, the higher total Hg concentrations in coastal/marine snow may reflect the damping effect of halides on the post-depositional redox cycling of Hg to the atmosphere. In the following section (3.5.2.) we discuss other mechanisms likely to be responsible for a loss of Hg from the snow surface.

The increase in [THg] observed in the middle of Cornwallis Island (Figure 3.3 A) was accompanied by a concomitant increase in [NO_3^-] (Figure 3.3 B). This increase in [THg] was likely the result of deposition of atmospheric Hg associated with fog droplets (note that fog was only present at Site T6). In a recent study in the coastal area around the Bay of Fundy, eastern Canada, (35)) reported very high levels of Hg in fog (two orders of magnitude greater than what we observed in surface snow: up to 425 ng•L^{-1} or ca., 2000 pmol•L^{-1}). The

highest levels reported by these authors were recorded at high altitudes in coastal areas. Hence, it is likely that fog can be a source of Hg to terrestrial ecosystems, as is the case for nutrients (48) and further investigation of its dynamics is warranted.

The particulate fraction of Hg found throughout Cornwallis Island, inland (up to 59%) as well as over sea-ice (up to 88%), was bound to the fraction comprised between 0.45 µm and 10 µm and especially to the fraction between 2.7 µm and 10 µm (Figure 3.5 A and B). These size fractions correspond to the accumulation and coarse modes defined for aerosols and which may be involved in Arctic Haze (40) as well as to the particulate fraction associated with mercury depletion events (18). The accumulation mode includes particles from 0.1 to 1 µm produced mainly through coalescence of smaller particles; the coarse mode is mostly formed of sea-salt and soil particles (>1 µm) (40). The presence of aluminosilicates, calcium carbonates and iron oxides as well as sodium confirms the terrigenous and marine origin of some particles. Since we thawed the snow prior to the partitioning analysis, it is likely that some aerosols disappeared due to the phase change. Hence these observations are more representative of wet snow or snowmelt water rather than dry cold solid snow. Nevertheless, the increased proportion of particles in the range 0.7-2.7 µm over sea ice (ca. 30% Figure 3.5 B) compared to inland (ca. 10% Figure 3.5 A) may reflect the increased importance of sea salt aerosols deposited onto snow in marine environments (47) and which are likely to be involved in fast oxidation of elemental mercury (27).

A growing body of literature supports the presence of microorganisms thriving in the atmosphere associated with aerosols (2, 19), in snow (1, 5) and sea ice (23). It is therefore likely that at the snow/sea ice interface, some particles may be of biological origin. Our own bacterial counts showed that bacterial cells were present at concentrations between 10^4 and 10^5 cells·mL^{-1} in snow over sea ice or over lake ice (Table 3). These concentrations are in good

agreement with previously published numbers for European Arctic snow (Amato et al., 2006). (22) showed that active bacteria are mostly associated with particles in both melted and intact sea ice. This juxtaposition of particulate Hg and bacterial cells suggests that interactions between Hg and polar microorganisms merit further investigation. This biological activity could potentially produce extracellular biogenic sulphur-containing compounds. Such moieties, released into the dissolved phase during snowmelt and exhibiting a very high affinity for mercury, could play a key role in the Hg cycle.

3.5.2. Accumulation of [THg] at the snow/ice interface.

Over sea-ice, [THg] increased with depth and was strongly correlated with concentrations of halides such as chloride or bromide, which are proxies for reactive halogen radicals known to be involved in mercury depletion events (4, 33). The increase of [THg] observed at the bottom of the snowpack at the sea ice/snow interface (Figure 3.4 A) may result from i) infiltration into the snowpack of underlying water with high [THg]; ii) increases of [THg] due to the salt enrichment effect observed during sea ice formation (45); or iii) enrichment from atmospheric origin. We suggest that the very high concentrations recorded at the snow/sea ice interface are due to atmospheric deposition and subsequent redistribution of Hg species, for the following reasons.

First, upward infiltration of underlying water cannot explain high [Hg] at the snow/ice interface, since total Hg concentrations in seawater in this area were the lowest that we observed (1.1 to 3.8 $pmol \cdot L^{-1}$). The salt enrichment effect is also unlikely. Indeed, assuming that dissolved Hg in seawater is mostly present in the form of negatively charged chlorocomplexes ($HgCl_4^{2-}$), based on [Cl^-] and [THg] encountered in the area, and assuming a conservative behaviour for Hg and Cl^- upon freezing, we would expect the Cl/Hg ratio to be conserved. The Cl/Hg ratio in seawater was ca. 10^8, whereas it was much lower (10^3) at the

sea ice/snow interface; therefore, an alternative source of Hg was likely involved.

Douglas et al. (2005) showed that crystals that formed from the vapour phase in direct proximity to open water areas such as leads exhibited Hg concentrations reaching ca. 4 nmol•L^{-1}, which are almost an order of magnitude higher than any reported concentrations in snow in the Arctic (27, 29). The authors proposed that frost flowers and surface hoar crystals developing near the leads may be efficient scavengers of atmospheric oxidized Hg species due to their large specific surface areas, therefore increasing [THg]. Although this process certainly contributes to an increase of [THg] in Arctic marine environments, it is unlikely to explain the observed pattern here since i) we sampled the bottom stratum of the snow accumulation, a layer not directly exposed to air and less subject to deposition of vapour crystals and ii) large open water bodies were not present in proximity to our sampling site. Note that we sampled ca. 100 m from a crack in sea ice which was 10 to 50 cm wide. Open water was present ca. 40 km southwest of the sampling site (Figure 3.1. area with a white triangle, data from Regional Ice Analysis, Eastern Arctic, Canadian Ice service, Environment Canada, 2004).

We propose that Hg was redistributed, possibly associated with particles, after its deposition as a result of alteration of snow physical properties influenced by environmental factors (e.g. wind, temperature gradient and humidity) both during cold conditions (dry snow metamorphism) and during the melting period (wet snow metamorphism). Although the bottom layer where Hg had accumulated showed few signs of destructive metamorphism, we did sample after the surface temperature exceeded 0°C for the first time, and we therefore cannot rule out the possible infiltration of melt waters (note that we did observe some ice lenses within the accumulation). Seasonal snowpacks are heterogeneous, especially on a short spatial scale (ca. 10 m) due to wind, water

percolation and topography (43) and we may have a biased view of the actual physical snow properties prevalent on this date.

That both dry and wet snow metamorphism may influence the redistribution of Hg species is supported by the following reasons. First, it has been shown in previous studies that ionic species behave very differently from one another with respect to their elution sequence from the snowpack. Cragin et al. (1996) concluded that fractionation and preferential elution were strongly influenced by ion exclusion and rearrangement processes occurring during dry snow metamorphism, independent of the melt-freeze cycle. Although this latter study mostly focused on anionic species, it may be a starting point to better understand the behaviour of cationic species such as mercury, especially since it was shown that snow does not exhibit chromatographic properties (8, 14) and should therefore not discriminate among species on the basis of their charge. Rather, the authors argue that the elution sequence is likely controlled by the initial position of the ion in the original snow crystal - i.e. as part of the nuclei or adsorbed at the surface - which is dependent on snow formation and scavenging processes in the atmosphere.

Second, it is likely that processes that drive movement of particulate Hg within the snow accumulation differ from those that affect the migration of dissolved species. The work by (7) suggests that particles smaller than 5 μm (e.g. soot or ash) are more mobile than that of greater size which are virtually immobile until actual massive melt occur. It is common to observe percolation columns of meltwaters, especially during the melting period (21), which bridge the upper and bottom parts of the snow accumulation. These columns may be responsible for the transfer of mercury species deposited at the surface, towards the bottom the accumulation.

3.5.3. Impact of melting inland and marine snowpacks on underlying waters.

Depth profiles carried out in the water column of the lake and the upper part of the seawater column showed that THg concentrations were 3 to 4 times greater at the surface than in the remainder of the water column. This is most likely due to the presence of the melting snowpack which sits on top of the ice. The presence of a greater proportion of Hg bound to particles at the surface of seawater, between sea ice edges, than at depths of 5.5 and 11.5 meters also suggests an influence of the snowpack since most of the Hg present in snow is bound to particles (see above). Note also that when considering all measured cationic elements, only Hg exhibited concentrations higher in snow than in the underlying water (Snow/Sea Hg ratio > 79; see last line of Table 4 and Figure 3.5 B). This represents the first evidence that a melting snowpack contributes to increasing THg concentrations at the sea ice / water interface. Altogether these results tend to suggest that even though an important fraction of the Hg deposited during MDE may be reemitted back to the atmosphere, the interface between sea ice and snow constitutes a build-up site for particulate Hg species that contribute to increased [THg] in surface water.

3.5.4. Conceptual summary.

Conceptual representations of Hg dynamics and distribution in an arctic snowpack from early spring to summer, summarizing the main conclusion of this paper, are presented in Figures 3.7 A and B. Inland sites can experience enhanced mercury deposition due to winds (Figure 3.7 A (1) and (2)), which carry the products of the fast oxidation of GEM occurring in coastal/marine environments (Figure 3.7 B (1)). A growing body of literature shows that mercury depletion events are transitory and when light conditions are optimal, part of the Hg deposited onto snow surface is efficiently recycled back to the atmosphere within days, therefore limiting the impact of deposition to aquatic systems.

However, because of enhanced oxidative processes occurring in the marine environment, the photoreduction of Hg(II) and subsequent evasion of the newly produced Hg(0) are hampered, and hence marine environments tend to accumulate more Hg than inland sites (Figure 3.7 A (3) and Figure 3.7 B (2)). At the onset of snowmelt, Hg was mostly bound to particles, especially over sea-ice. This observation probably reflects both the impact of particle-associated reactions that led to Hg deposition and the subsequent redistribution due to water phase changes. Here, we identify the snow/sea ice interface as a location where Hg accumulates (Figure 3.7 B (3)), reaching concentrations one order of magnitude greater than what is observed at the surface or at inland sites, where no such accumulation was observed (Figure 3.7 A (4)). The mechanisms of Hg transport are still unclear but may involve changes in snow physical properties related to metamorphism. During snowmelt, the presence of percolation columns may also affect downward Hg transport. Another yet totally unknown aspect of Hg cycling in polar areas deals with its dynamics within the heterogeneous matrix of sea ice and namely whether transport and transformation of Hg occur within sea ice (Figure 3.7 A; (4)). As snow melts, we showed that a significant fraction of Hg is exported to aquatic systems, resulting in significant increases in [THg] at the top of the water columns, both at inland (Figure 3.7 A (5)) and coastal sites (Figure 3.7 B (5)). The impact of melting snow packs on underlying seawater (Figures 3.7 A and 3.7 B; (6)), where dense populations of sea ice algae thrive (30), may constitute an important link between arctic Hg cycling and biota contamination.

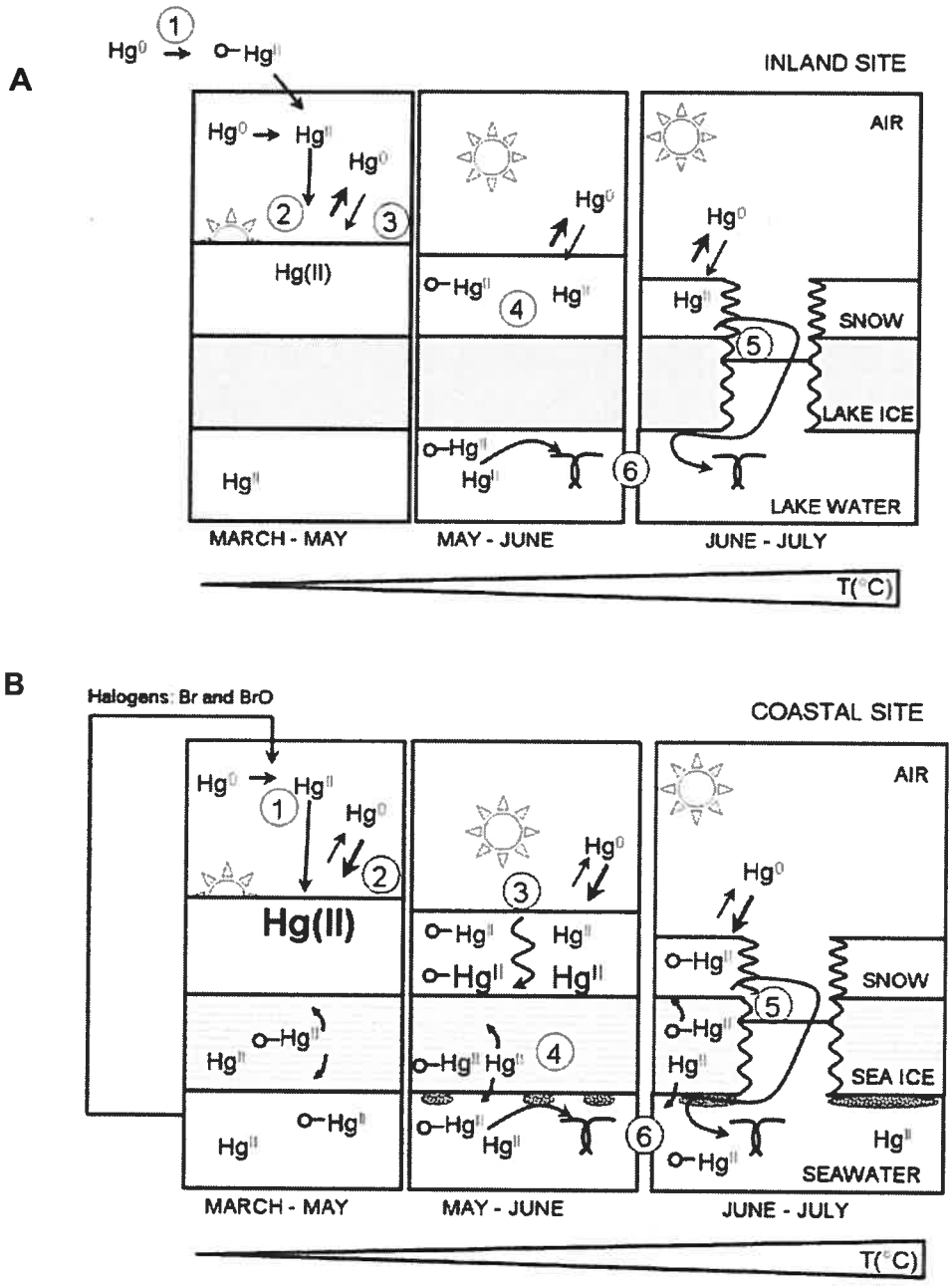

Figure 3.7. Schematic summary of Hg dynamics at the air/snow/sea ice/water interface in a polar environment. Numbers refer to the text.

3.6. Acknowledgements

We gratefully acknowledge funding from the Canadian foundation for climate and atmospheric science (CFCAS), the national sciences and engineering research council of Canada (NSERC) and the collaborative mercury research network (COMERN) to MA and PAA as well as the Science Horizon program to MA. We would like to thank Dr. T. Douglas for his insightful comments as well as two other reviewers who contributed to greatly improve this manuscript. We thank B.E. Keatley for her comments on the manuscript. We also would like to thank the Polar Continental Shelf Project for their logistic support to MA as well as the Nunavut Research Institute that delivered our research license. We express our gratitude to Dr Paul del Giorgio at UQAM for access to the flow cytometer and to Dr. H. Vali for access to the electron microscopy facility at McGill University. We would like to warmly thank Paddy Aqiatusuk as well as Debbie Iqaluk for their outstanding help and support in the field, Louise Pelletier, for her help with the electron microscope at the University de Montréal and Dominic Belanger for his help in the lab.

3.7. Références

1. **Amato, P., R. Hennebelle, O. Magand, M. Sancelme, A.-M. Delort, C. Barbante, C. Boutron, and C. Ferrari.** 2006. Bacterial characterization of the snowcoverat Spitzberg, Svalbard. FEMS Microbiology Ecology **Published article online: 8-Sep-2006; doi: 10.1111/j.1574-6941.2006.00199.x**.
2. **Ariya, P. A., and M. Amyot.** 2004. New Directions: The role of bioaerosols in atmospheric chemistry and physics. Atmospheric Environment **38:**1231-1232.
3. Ariya, P. A., A. P. Dastoor, M. Amyot, W. H. Schroeder, L. Barrie, K. Anlauf, F. Raofie, A. Ryzhkov, D. Davignon, J. Lalonde, and A. Steffen. 2004. The Arctic: a sink for mercury. Tellus Series B-Chemical and Physical Meteorology 56:397-403.

4. **Ariya, P. A., A. Khalizov, and A. Gidas.** 2002. Reactions of gaseous mercury with atomic and molecular halogens: Kinetics, product studies, and atmospheric implications. Journal of Physical Chemistry A **106:**7310-7320.
5. **Carpenter, E. J., S. J. Lin, and D. G. Capone.** 2000. Bacterial activity in South Pole snow. Applied and Environmental Microbiology **66:**4514-4517.
6. **Colbeck, S., E. Akitaya, R. Armstrong, H. Gubler, J. Lafeuille, K. Lied, D. McClung, and E. Morris.** 1985. The International Commission on Snow and Ice of the International Association of Scientific Hydrology and the International Glaciological Society.
7. **Conway, H., A. Gades, and C. F. Raymond.** 1996. Albedo of dirty snow during conditions of melt. Water Resources Research **32:**1713-1718.
8. **Cragin, J. H., A. D. Hewitt, and S. C. Colbeck.** 1996. Grain-scale mechanisms influencing the elution of ions from snow. Atmospheric Environment **30:**119-127.
9. Dommergue, A., C. P. Ferrari, P. A. Gauchard, C. F. Boutron, L. Poissant, M. Pilote, P. Jitaru, and F. C. Adams. 2003. The fate of mercury species in a sub-arctic snowpack during snowmelt. Geophysical Research Letters 30.
10. **Dommergue, A., C. P. Ferrari, L. Poissant, P. A. Gauchard, and C. F. Boutron.** 2003. Diurnal cycles of gaseous mercury within the snowpack at Kuujjuarapik/Whapmagoostui, Quebec, Canada. Environmental Science & Technology **37:**3289-3297.
11. **Douglas, T. A., and M. Sturm.** 2004. Arctic haze, mercury and the chemical composition of snow across northwestern Alaska. Atmospheric Environment **38:**805-820.
12. **Douglas, T. A., M. Sturm, W. R. Simpson, S. Brooks, S. E. Lindberg, and D. K. Perovich.** 2005. Elevated mercury measured in snow and frost flowers near Arctic sea ice leads. Geophysical Research Letters **32**. Art n° L04502
13. Ebinghaus, R., H. H. Kock, C. Temme, J. W. Einax, A. G. Lowe, A. Richter, J. P. Burrows, and W. H. Schroeder. 2002. Antarctic springtime depletion of atmospheric mercury. Environmental Science & Technology 36:1238-1244.
14. **Eichler, A., M. Schwikowski, and H. W. Gaggeler.** 2001. Meltwater-induced relocation of chemical species in Alpine firn. Tellus Series B-Chemical and Physical Meteorology **53:**192-203.
15. **Ferrari, C. P., A. Dommergue, C. Boutron, P. Jitaru, and F. C. Adams.** 2004. Profiles of Mercury in the snow pack at Station Nord, Greenland, shortly after polar sunrise. Geophysical Research Letters **31:**L03401.

16. **Ferrari, C. P., A. Dommergue, A. Veysseyre, F. Planchon, and C. F. Boutron.** 2002. Mercury speciation in the French seasonal snow cover. Science of the Total Environment **287:**61-69.
17. **Gasol, J. M., and P. A. Del Giorgio.** 2000. Using flow cytometry for counting natural planktonic bacteria and understanding the structure of planktonic bacterial communities. Scientia Marina **64:**197-224.
18. **Gauchard, P. A., C. P. Ferrari, A. Dommergue, L. Poissant, M. Pilote, G. Guehenneux, C. F. Boutron, and P. Baussand.** 2005. Atmospheric particle evolution during a nighttime atmospheric mercury depletion event in sub-arctic at kuujjuarapik/Whapmagoostui, Quebec, Canada. Science of the Total Environment **336:**215-224.
19. **Gidlen, T.** 1948. Aerial plankton and its conditions of life. Biological review **23:**109-126.
20. **Gill, G. A., and K. W. Bruland.** 1990. Mercury Speciation in Surface Fresh-Water Systems in California and Other Areas. Environmental Science & Technology **24:**1392-1400.
21. **Jones, G. H., J. W. Pomeroy, D. A. Walker, and R. W. Hoham.** 2001. Snow Ecology: An Interdisciplinary Examination of Snow-Covered Ecosystems. Cambridge University Press, Cambridge, United Kingdom.
22. **Junge, K., H. Eicken, and J. W. Deming.** 2004. Bacterial activity at-2 to-20 degrees C in Arctic wintertime sea ice. Applied and Environmental Microbiology **70:**550-557.
23. **Junge, K., F. Imhoff, T. Staley, and J. W. Deming.** 2002. Phylogenetic diversity of numerically important arctic sea-ice bacteria cultured at subzero temperature. Microbial Ecology **43:**315-328.
24. **Lalonde, J. D., M. Amyot, M. R. Doyon, and J. C. Auclair.** 2003. Photo-induced Hg(II) reduction in snow from the remote and temperate Experimental Lakes Area (Ontario, Canada). Journal of Geophysical Research-Atmospheres **108**.
25. **Lalonde, J. D., M. Amyot, A. M. L. Kraepiel, and F. M. M. Morel.** 2001. Photooxidation of Hg(0) in artificial and natural waters. Environmental Science & Technology **35:**1367-1372.
26. **Lalonde, J. D., A. J. Poulain, and M. Amyot.** 2002. The role of mercury redox reactions in snow on snow-to-air mercury transfer. Environmental Science & Technology **36:**174-178.
27. **Lindberg, S. E., S. Brooks, C. J. Lin, K. J. Scott, M. S. Landis, R. K. Stevens, M. Goodsite, and A. Richter.** 2002. Dynamic oxidation of gaseous mercury in the Arctic troposphere at polar sunrise. Environmental Science & Technology **36:**1245-1256.
28. **Lu, J. Y., and W. H. Schroeder.** 2004. Annual time-series of total filterable atmospheric mercury concentrations in the Arctic. Tellus Series B-Chemical and Physical Meteorology **56:**213-222.

29. Lu, J. Y., W. H. Schroeder, L. A. Barrie, A. Steffen, H. E. Welch, K. Martin, L. Lockhart, R. V. Hunt, G. Boila, and A. Richter. 2001. Magnification of atmospheric mercury deposition to polar regions in springtime: the link to tropospheric ozone depletion chemistry. Geophysical Research Letters 28:3219-3222.

30. **Mundy, C. J., D. G. Barber, and C. Michel.** 2005. Variability of snow and ice thermal, physical and optical properties pertinent to sea ice algae biomass during spring. Journal of Marine Systems **58:**107-120.

31. **Poissant, L., and M. Pilote.** 2003. Time series analysis of atmospheric mercury in Kuujjuarapik/Whapmagoostui (Quebec). Journal De Physique IV **107:**1079-1082.

32. **Poulain, A. J., J. D. Lalonde, M. Amyot, J. A. Shead, F. Raofie, and P. A. Ariya.** 2004. Redox transformations of mercury in an Arctic snowpack at springtime. Atmospheric Environment **38:**6763-6774.

33. **Raofie, F., and P. A. Ariya.** 2004. Product study of the gas-phase BrO-initiated oxidation of Hg-0: evidence for stable Hg1+ compounds. Environmental Science & Technology **38:**4319-4326.

34. **Riordan, E., N. Minogue, D. Healy, P. O'Driscoll, and J. R. Sodeau.** 2005. Spectroscopic and optimization modeling study of nitrous acid in aqueous solution. Journal of Physical Chemistry A **109:**779-786.

35. **Ritchie, C. D., W. Richards, and P. A. Arp.** 2006. Mercury in fog on the Bay of Fundy (Canada). Atmospheric Environment **40:**6321-6328.

36. **Schecher, W. D., and D. C. McAvoy.** 1992. Mineql+ - a Software Environment for Chemical-Equilibrium Modeling. Computers Environment and Urban Systems **16:**65-76.

37. Schroeder, W. H., K. G. Anlauf, L. A. Barrie, J. Y. Lu, A. Steffen, D. R. Schneeberger, and T. Berg. 1998. Arctic springtime depletion of mercury. Nature 394:331-332.

38. **Sprovieri, F., N. Pirrone, M. S. Landis, and R. K. Stevens.** 2005. Oxidation of gaseous elemental mercury to gaseous divalent mercury during 2003 polar sunrise at Ny-Alesund. Environmental Science & Technology **39:**9156-9165.

39. **St Louis, V. L., M. J. Sharp, A. Steffen, A. May, J. Barker, J. L. Kirk, D. J. Kelly, S. E. Arnott, B. Keatley, and J. P. Smol.** 2005. Some sources and sinks of monomethyl and inorganic mercury on Ellesmere Island in the Canadian High Arctic. Environmental Science and technology **39:**2686-2701.

40. **Staebler, R. M., G. Denhartog, B. Georgi, and T. Dusterdiek.** 1994. Aerosol-Size Distributions in Arctic Haze During the Polar Sunrise Experiment 1992. Journal of Geophysical Research-Atmospheres **99:**25429-25437.

41. **Steffen, A., W. Schroeder, J. Bottenheim, J. Narayan, and J. D. Fuentes.** 2002. Atmospheric mercury concentrations: measurements

and profiles near snow and ice surfaces in the Canadian Arctic during Alert 2000. Atmospheric Environment **36:**2653-2661.

42. **Stumm, W., and J. J. Morgan.** 1996. Metal ions in aqueous solution: aspects of coordination chemistry, p. 1022. *In* J. L. Schnoor and A. Zehnder (ed.), Aquatic Chemistry - Chemical Equilibria and rates in natural waters, third edition., Wiley-Intersciences ed. John Wiley and sons, Inc., New-York.
43. **Sturm, M., and C. Benson.** 2004. Scales of spatial heterogeneity for perennial and seasonal snow layers, p. 253-260, Annals of Glaciology, Vol 38, 2004, vol. 38. INT GLACIOLOGICAL SOC, Cambridge.
44. **Swain, E. B., D. R. Engstrom, M. E. Brigham, T. A. Henning, and P. L. Brezonik.** 1992. Increasing Rates of Atmospheric Mercury Deposition in Midcontinental North-America. Science:784-787.
45. **Thomas, D. N., and S. Papadimitriou.** 2003. Biogeochemistry of sea ice., p. 267-302. *In* D. N. Thomas and G. S. Dieckmann (ed.), Sea Ice: An Introduction to its Physics, Chemistry, Biology and Geology. Blackwell Science Ltd., Oxford, England.
46. **Toom-Sauntry, D., and L. A. Barrie.** 2002. Chemical composition of snowfall in the high Arctic: 1990-1994. Atmospheric Environment **36:**2683-2693.
47. **Vogt, R., P. J. Crutzen, and R. Sander.** 1996. A mechanism for halogen release from sea-salt aerosol in the remote marine boundary layer. Nature **383:**327-330.
48. **Weathers, K. C.** 1999. The importance of cloud and fog in the maintenance of ecosystems. Trends Ecol. Evol. **14:**214-215.

4. Influence of temperate mixed and deciduous tree covers on Hg concentrations and photoredox transformations in snow.

Alexandre J. Poulain, Virginie Roy, & Marc Amyot.

Manuscrit sous presse (2007) dans Geochimica et Cosmochimica Acta.

4.1. Abstract.

Mercury dynamics in snow packs under forested canopy are currently unknown, even though these snow packs may represent important Hg pools eventually released towards lakes at snowmelt. We followed Hg distribution and partitioning in snowpacks under different temperate canopy types over space and time, and conducted short-term experiments on Hg redox behaviour in these snow packs. Hg concentrations were ca. 2 times higher in snow deposited under coniferous than deciduous canopies; the lowest concentrations were observed in snow over a frozen lake in the same watershed. In snow on the ground, up to 80% of the Hg was bound to particles between 10 and 70 µm. Incubations of snow *in situ* showed that i) Hg photoreduction and evasion was significant in open areas (lake surface) but was greatly hampered by light attenuation under winter canopies and ii) oxidation of newly produced Hg^0 was a significant process in boreal snow, affecting Hg evasion to the atmosphere. We used a mass balance approach to compare Hg pools in snow packs with wet deposition measured by precipitation collectors. A net gain of Hg was observed in snow under mixed canopies whereas, under a deciduous canopy, the pool of Hg stored at the end of the winter was comparable to that of wet deposition. Snow over lake acted as a winter source of Hg. Whereas most Hg deposited by snow on lakes is lost before snowmelt, Hg deposited on the forested watershed is largely retained in snowpacks, presenting a threat to systems receiving meltwaters.

4.2. Introduction

Snow is highly efficient at scavenging pollutants during crystal growth or during washout from the atmosphere (6, 10). Both organic (4) and inorganic (2) compounds can be incorporated into snow and may contribute to the overall contamination of snowpacks in northern (11) as well as in temperate areas (40, 41). Total Hg concentrations in snow in remote temperate areas usually range from <1 to 60 pmol L^{-1} (9, 35, 21); Lalonde et al., 2003; (38).

Until recently, little of the post-depositional behavior of Hg in snow was understood. Lalonde et al. (2002 and 2003) discovered that more than 50% of newly deposited Hg in snow could be efficiently recycled back to the atmosphere via Hg(II) photoreduction. This mechanism was shown to be of great significance in the Arctic where intensive re-emission of Hg occurred after atmospheric mercury depletion events (MDE) (1, 7, 19, 31, 36). Although these studies underscored important components of the global Hg cycle, they mainly focused on snow deposited onto openly sunlit areas characteristic of the treeless Arctic tundra or the surface of frozen lakes.

Previous studies have shown the importance of the forest canopy in contributing to the flux of total and methyl mercury to forest floors, through throughfall (precipitation which passes through canopy) and litterfall, which together can represent up to 2 to 3 times the annual flux by direct wet deposition (32, 33, 35). These studies were conducted on an annual basis but mostly focused on the growing season. During winter time, the importance of litterfall was considered modest (33) and that of throughfall remains poorly known and overall thought to be of little importance (15). Dry deposition may also affect the pool of Hg in snow. This process is poorly documented and may be significant in the winter, with atmospheric particulate Hg concentrations usually greater than during the remaining of the year (17, 25). It is critical to better understand how the canopy influences Hg dynamics in snow. Indeed Hg redox transformations in

snow may control Hg availability to snow and soils in forested ecosystems, and may subsequently impact sensitive aquatic ecosystems during the spring snowmelt.

In this paper we describe and compare the distribution of total Hg concentrations [THg] as well as Hg dynamics in snowpacks under contrasting canopies of the mixed Canadian forest and over a frozen lake within the same watershed. We examine herein i) the influence of different types of forest canopies on the spatial distribution and partitioning of [THg] in snow, ii) the distribution of [THg] within each stratum of a snowpack, iii) the relative importance of Hg reduction versus oxidation processes in snow under tree cover and over a lake using incubation experiments, and iv) using a mass balance approach, the importance of snow deposited under canopy and over a lake as winter source or sink for Hg.

4.3. Experimental section.

4.3.1. Sampling sites.

This study took place at the Station de Biologie (SBL) of the Université de Montréal, located ca. 75 km north of Montreal, during winters (December – March) 2003 and 2005. Sampling and experiments were undertaken in the forest adjacent to and over the frozen surfaces of Lake Cromwell and Lake Croche. Characteristics of the area are presented in Carignan et al. (3). Briefly, the area is underlain by granitic or anorthosic bedrock covered by 1-5 m of glacial tills. Soils are mostly humic cryorthods (U.S. classification) or orthic ferro-humic podzols (Canadian classification). Annual precipitation averages 1100 mm, with 30% falling as snow. The plant communities on the watersheds of lakes Croche and Cromwell included *Abies* (fir), *Acer* (maple), *Betula* (birch), *Fagus* (beech), *Pinus* (pine), *Picea* (spruce), *Populus* (poplar), and *Thuja* (thuja) (30). The plant communities in the Lake Croche watershed have been classified

into nine community types (Figure 4.1). By area, 3% of the watershed is comprised exclusively of conifers, 40% is exclusively deciduous forest, 56% is mixed coniferous and deciduous forest, and 1% is occupied by a peatland (Figure 4.1). In the text the term «coniferous site» refers to the site with conifers and deciduous trees, and «deciduous sites» to the site with deciduous vegetation only.

Number	Site name	(Co)dominant Genus
1, 2, 20	Pin-Pic	*Pinus* (pine) and *Picea* (spruce)
3, 19, 21	Thu-Bet	*Thuja* (Thuja) and *Betula* (birch)
4	Ac-Fag	*Acer* (maple) and *Fagus* (beech)
5, 6	Ac	*Acer* (maple)
7	Ac-Bet	*Acer* (maple) and *Betula* (birch)
8, 9, 10, 18	Bet-Ac	*Betula* (birch) and *Acer* (maple)
11, 12, 13	Bet-Pop	*Betula* (birch) and *Populus* (poplar)
14, 15	Bet-Abi	*Betula* (birch) and *Abies* (fir)
16, 17	Pin-Bet	*Pinus* (pine) and *Betula* (birch)
22	peat	peatland
23	Lake	Lake

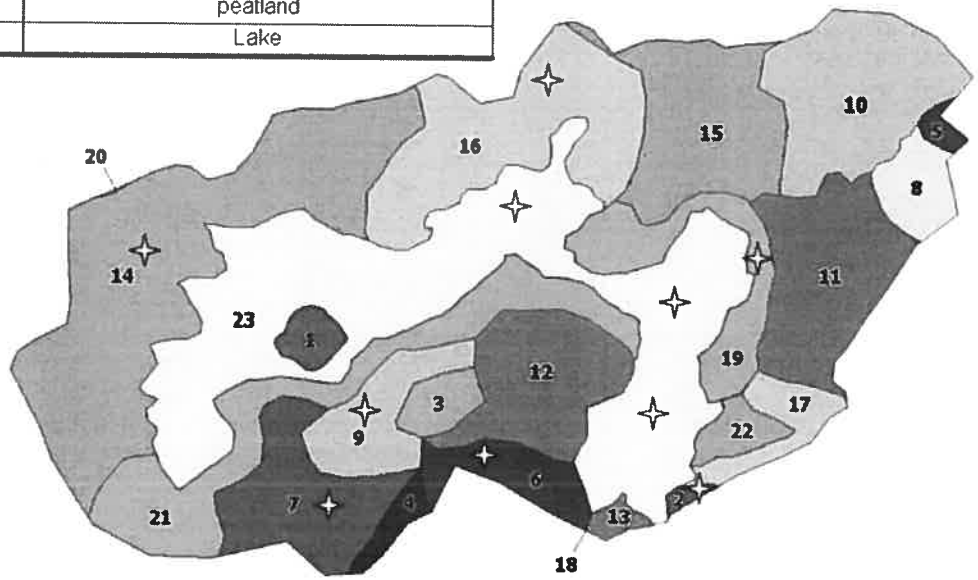

Figure 4.1. Representation of the Lake Croche watershed with the various vegetation types numbered from 1 to 21. Dominant vegetation present is given in the inset table. White stars represent the sampling sites. Map was modified from Savage et al. (2001).

Influence of canopy on Hg dynamics in snow

4.3.2. Temporal series of depth profiles.

Depth profiles for [THg] were carried out from February 26 2003 to March 26 2003 a) in the transition zone between sites dominated by *Pinus* and *Betula*, and b) on the frozen surface of Lake Cromwell (not shown in Figure 4.1). Snow strata within the snow accumulations were determined using the "International classification of snow on the ground" as described in (5). For each snow stratum, snow samples were collected in triplicate using 1L Teflon (FEP) bottles acid washed (20% HNO_3) and thoroughly rinsed with ultrapure water (R = 18.2 MΩ•cm). Bottles were filled using a Teflon shovel or by hand. Non-powdered gloves and Tyvek™ suits were worn at all times during sampling to minimize contamination. Snow samples were kept frozen and in the dark in a cooler until analysis. Major ions were collected in 30 mL Nalgene HDPE bottles, and, in the case of the cation samples, acidified to 0.1 % (HNO_3 64%). For bacterial counts, Falcon tubes were filled with snow, thawed at 4°C and preserved with glutaraldehyde to a final concentration of 2% (12). Some samples were kept frozen and fluorescence of dissolved organic carbon (DOCF) was determined, as a surrogate for DOC reactivity, once samples were melted following the protocol described in Garcia et al. (2005). See Fig. 2A and B for meteorological and snow description of sampling period.

4.3.3. Watershed sampling.

During winter (January-March) 2005, eight sites were selected in the lake Croche watershed, each representative of a major plant community. Each site was cored monthly to assess the distribution of total mercury concentrations in snow on the ground under different types of forest canopy. Seven sites were characterized by distinct vegetation types: Pin-Pic (*Pinus* and *Picea*), Thu-Bet (*Thuja* and *Betula*), Ac (*Acer*), Ac-Bet (*Acer* and *Betula*), Bet-Ac (*Betula* and

Acer), Bet-Abi (*Betula* and *Abies*) and Pin-Bet (*Pinus* and *Betula*), and one site was located on the frozen Lake Croche (white stars, Figure 4.1). Three snow cores were taken at each site using a polycarbonate cylinder (Ø=15.24 cm; L=140cm), serrated at the bottom to better cut through ice lenses. Snow depth, temperature at surface and at depth as well as the nature of snow grains at the bottom was recorded for each site. Sampling took place on January 12, February 4, February 16 and March 13 2005. During the sampling, an effort was made to remove large pieces of litterfall debris and, as soon as samples were thawed, melted snow was filtered through a 250 µm Nitex mesh in order to minimize the litterfall contribution. A meteorological and snow description of the sampling period is provided in Fig. 2B and C.

4.3.4. Total wet Hg deposition.

An automated atmospheric precipitation sampler (TE-78-100 APS; Pacwill environmental®) was used to collect snow and rain and to estimate the total wet deposition load from December 04 to March 05. The collector was made of a plastic bucket (ca. 18 L) lined with a Teflon FEP bag (20 L), with a collection area of ca. 660 cm^2. Because of the presence of a sensor, opening of the collector occurred at the start of a precipitation and ended when it stopped. After each sample retrieval, a new, clean bag was placed in the collector. We did not empty the precipitation collector after each snow and rain event either because we could not get on site or because the amount of precipitation was too low to perform Hg analyses. After collection, samples were thawed in the bag overnight at room temperature, transferred to three 60 mL Teflon vials and immediately preserved with 0.3% BrCl until analysis. The total wet deposition rate was calculated as follows:

$$\text{Total wet Hg deposition } (pmol \cdot m^{-2}) = \Sigma[([THg]*V)/S] \quad (1)$$

where [THg] is the concentration of Hg ($pmol \cdot L^{-1}$), V is the total volume collected (L), and S is the area of the precipitation collector (m^2).

Since snow samples stayed below the freezing point and in the dark in the Teflon bag until analysis, it is unlikely that Hg was lost by adsorption onto the walls of the bag. Because of the occurrence of some rain events, which could have favoured snowmelt and thus Hg adsorption onto the walls, we performed a test where we washed the Teflon bag (10% omnitrace™ HCl in milliQ water) to recover Hg adsorbed onto the walls. The Hg concentrations were very low (0.2 $pmol \cdot L^{-1}$) and represented less than 2% of the [THg] prior to the washing.

4.3.5. Incubations.

Batch Incubation experiments consisted of incubating Teflon or quartz bottles for various lengths of time under different light treatments. During incubation, bottles were placed horizontally with their cap pointing north. Bottles were turned every 30 minutes to optimize the distribution of light through the sample. Incubations usually lasted for 3 to 6 hours and began at 10:00AM. Bottles were incubated either *in situ*, i.e. under the canopy, or over the frozen surface of the lake. Either solid snow or melted snow samples were incubated, depending on the goal of the experiment.

4.3.6. Chemical and biological analyses.

Total Hg analyses were carried out using an automated Tekran 2600 following method 1631 from the USEPA. Briefly, snow samples were melted, filtered through a 150 µm Nitex mesh to prevent debris from clogging the tubing system, poured into 60 mL vials, and spiked with 200 µl BrCl. If processing did not occur within 24 hours, samples spiked with BrCl were kept at 4°C for up to 5 days. In the morning, or after 5 days, the excess of BrCl was neutralized with 30 µl hydroxylamine and samples were reduced in line by stannous chloride (3%). Hg(0) was then quantified by cold vapour atomic fluorescence spectrometry. Reproducibility of the method was within 10%.

For Hg^0 analyses, solid snow was sparged directly in the sampling bottle by tightly inserting a porous glass rod in the bottle. The bottle was connected to an automated atmospheric mercury analyzer (Tekran™ Model 2537) in order to monitor the decrease of [Hg^0] over time (one reading every five minutes). The experimental design is modified from Lindberg et al. (2000). The sparging step was stopped when water in the bottle was under its liquid state and when concentrations reached zero or were below the detection limit. The working detection limit of this method was calculated as < 0.01pmol.L^{-1} or three time the standard deviation of ten system blanks. Reproducibility was within 10%.

Anions were analyzed by ion chromatography using a DIONEX ICS 2000. 25 µL of melted snow were introduced in the injection loop and separation occurred through an AS-17 column topped with an AG-17 precolumn. The elution step involved the passage of a KOH solution with a gradient of concentration from 15 to 30 mmol L^{-1}. Cations were analysed using an ICP-AES (Inductively Coupled Plasma - Atomic Emission Spectrometer, Vista AX) using an internal standard of Yttrium (5 mg L^{-1}, 371 nm). Bacteria were counted by flow cytometry as described in Gasol and Del Giorgio (12).

4.3.7. Particulate Hg distribution.

To identify to which size fraction particulate Hg was bound, an integrated sample of a snow column (*ca.* 20 L) was collected from the *Pinus* site, the *Acer* site, the precipitation collector and over the frozen lake. After a complete thaw was reached at room temperature, water was filtered through filters of decreasing porosities: 70 µm (Teflon mesh), 10 µm (polycarbonate), 2.7 µm (GF/B), 0.7 µm (GF/F). The particulate Hg distribution was obtained by subtracting the Hg burden between two filters of consecutive pore sizes. Because snow was melted prior to the filtration and analysis, this method does not measure soluble aerosols that could be present in solid snow. This method was compared to that of Sarica et al. (2004) which uses a direct mercury

analyser and determines Hg content by pyrolysis of the filter; no statistical difference was found using either the subtraction or the pyrolysis methods (Wilcoxon, p=0.334).

4.3.8. Mass balance.

We assessed the impact of the main fluxes on the Hg budget of snowpack with equation (2):

$$Hg_{snow} = (Hg_{wet} + Hg_{canopy} + Hg_{dry}) - (Hg^0_{evasion} + Hg_{melt.}) \quad (2)$$

Each term is defined as follows:

(a) Hg_{snow} is the total amount of Hg present in snow at the onset of snowmelt (pmol•m^{-2}). It was calculated using equation (3):

$$Hg_{snow} = ([THg]_{core} \bullet V)/S_{core} \quad (3)$$

$[THg]_{core}$ is the concentration of Hg in the integrated snow samples collected using the snow corer (pmol•m^{-3}) in January, February and March; V is the volume of water after snow thawed (m^3); and S_{core} is the surface of the corer (0.018m^2).

(b) Hg_{wet} is the cumulative amount of Hg in wet deposition during the period of study and measured via the precipitation collector and was calculated using Eq. 1.

(c) $Hg_{canopy} + Hg_{dry}$ represents the amount of Hg contributed by canopy and by dry deposition. This was not measured but calculated from equation (2). Note that since we removed plant debris from the snow, litterfall was not considered in this study.

(d) $Hg_{melt.}$ represents Hg potentially lost during warmer winter periods via snowmelt. We assumed that Hg(II) could not be co-transported with water vapour during snow sublimation. Therefore losses via percolation of snowmelt and evasion to the atmosphere were the two only loss mechanisms. We ran two scenarios assuming the presence vs. the absence of basal melt from the snowpacks located under canopy. We estimated ground snowmelt loss under

canopy based on a study carried out in a cool temperate forest using lysimeters (42) at a rate of 0.8 $L \cdot m^{-2} \cdot d^{-1}$, corresponding to a loss of 86.4 $L \cdot m^{-2}$ for the whole period. Indeed, this study showed that even during prolonged sub-freezing temperature, base-flow (i.e. flow of meltwater from the base of the snowpack) was constantly observed. However, temperatures recorded during this study were close to the freezing point and higher than what we observed and hence should be seen as a maximum loss via melt in our case; the amount lost by snowmelt over land was calculated based on equation (4):

Hg_{melt} = Loss of water per unit area x [THg] (4)

[THg] in eq 4 refers to the averaged concentration of Hg in the snow column. The loss via basal melt from the lake was estimated as the difference between the water content at the onset of snowmelt (117 $L \cdot m^{-2}$) compared with the amount of water received via precipitation (260 $L \cdot m^{-2}$). Assuming a sublimation and transport loss equivalent to 24% the snowfall (representing a loss of 62.4 $L \cdot m^{-2}$) (26), 80.6 $L \cdot m^{-2}$ were lost via melt and percolation over the lake.

(e) $Hg^0_{evasion}$ is the amount of Hg lost to the atmosphere via photoreduction and subsequent evasion. The amount evaded was calculated based on reduction rates corrected for the cumulative irradiance received during the time of incubation under direct sunlight (121, 70 and 67 $fmol \cdot L^{-1} \cdot mol_{photon}^{-1} \cdot m^2$ for the *Pinus*, *Acer* and lake site, respectively). Evasion was then calculated assuming that 10% of the snowpack was impacted by photoreduction. and using a cumulative irradiance from December 2004 to March 2005 of 1324.12 $mol_{photon} \cdot m^{-2}$. To take into consideration the canopy effect we corrected for the penetration of light. Three types of snow were assessed: snow collected under coniferous canopy (*Pinus*), snow collected under deciduous canopy (*Acer*) and snow collected at the surface of the lake. Two light sensors simultaneously recorded the incoming irradiance, one under canopy and one in the open. Light attenuation coefficients at the coniferous and the deciduous sites were

calculated as the median ratio between the incoming irradiance under canopy over the incoming irradiance in the open recorded for each site over a period of three days. Under deciduous (*Acer*) canopy, the ratio varied between 0.11 and 1 with a median value of 0.52. Under coniferous (*Pinus*) canopy, the ratio varied between 0.01 and 0.98 with a median value of 0.07.

4.4. Results & discussion.

4.4.1. Spatial distribution of Hg under various types of canopy.

Influence of canopy type

To understand the influence of tree covers on the distribution of [THg], we sampled seven sites of different canopy compositions as well as the surface of the frozen lake throughout the winter. The amount of Hg deposited via wet depositions during the sampling period was known from our precipitation collector.

[THg] in direct wet deposition ranged from 6.5 to 16.2 $pmol \cdot L^{-1}$ (note that we could not calculate the volume-weighted average concentration as we did not collect each event independently, Figure 4.2 C). These values are lower than what are commonly reported during spring, summer, and fall and are in good agreement with previously published data of Hg in precipitation during winter period (18).

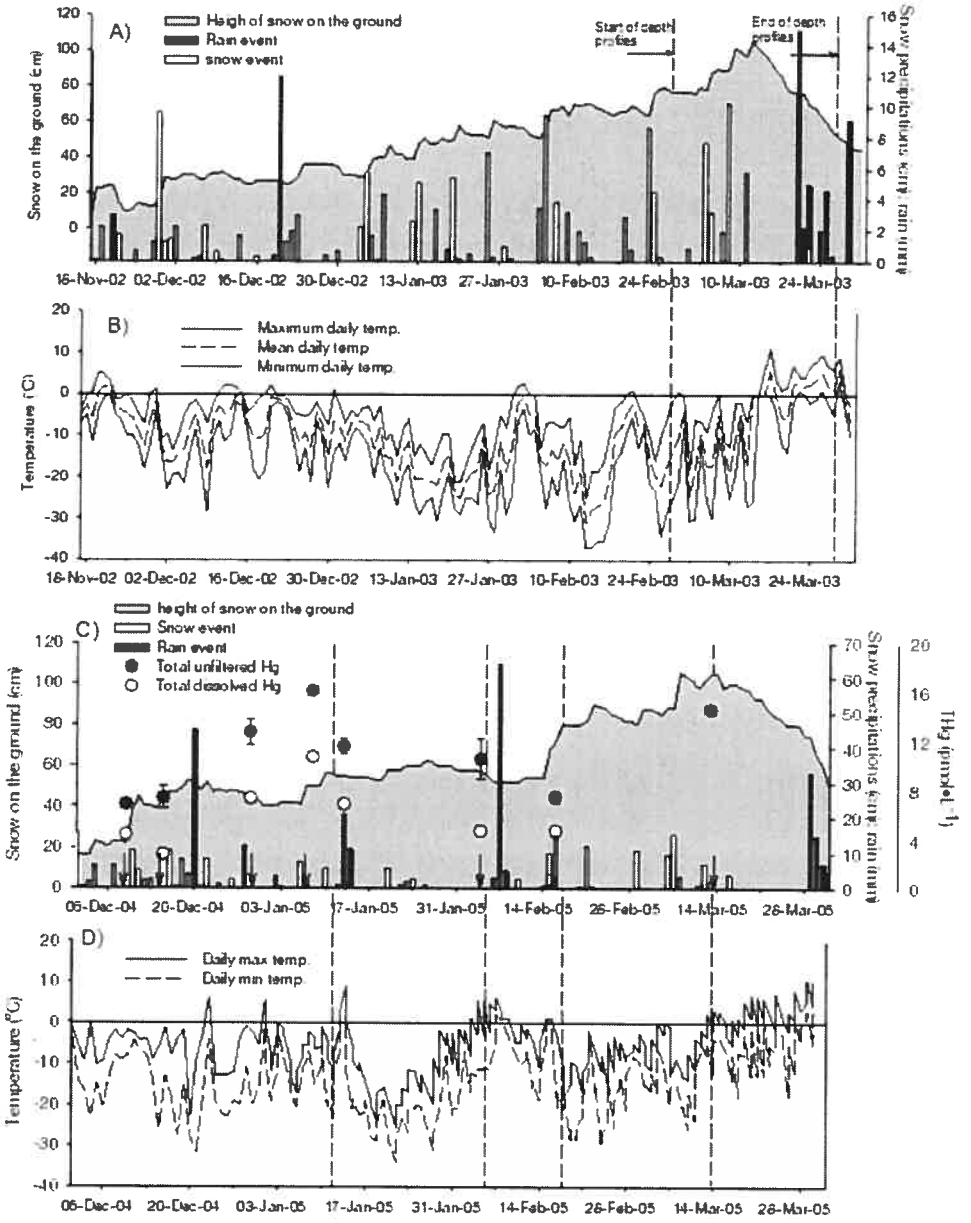

Figure 4.2. Meteorological conditions during our sampling periods. Winter 2002-2003 (panels A and B), winter 2004-2005 (panels C and D). Panel 2C shows total mercury concentrations measured in the precipitation collector during winter 2004-2005. Dashed vertical bars in panels C and D represent watershed sampling dates.

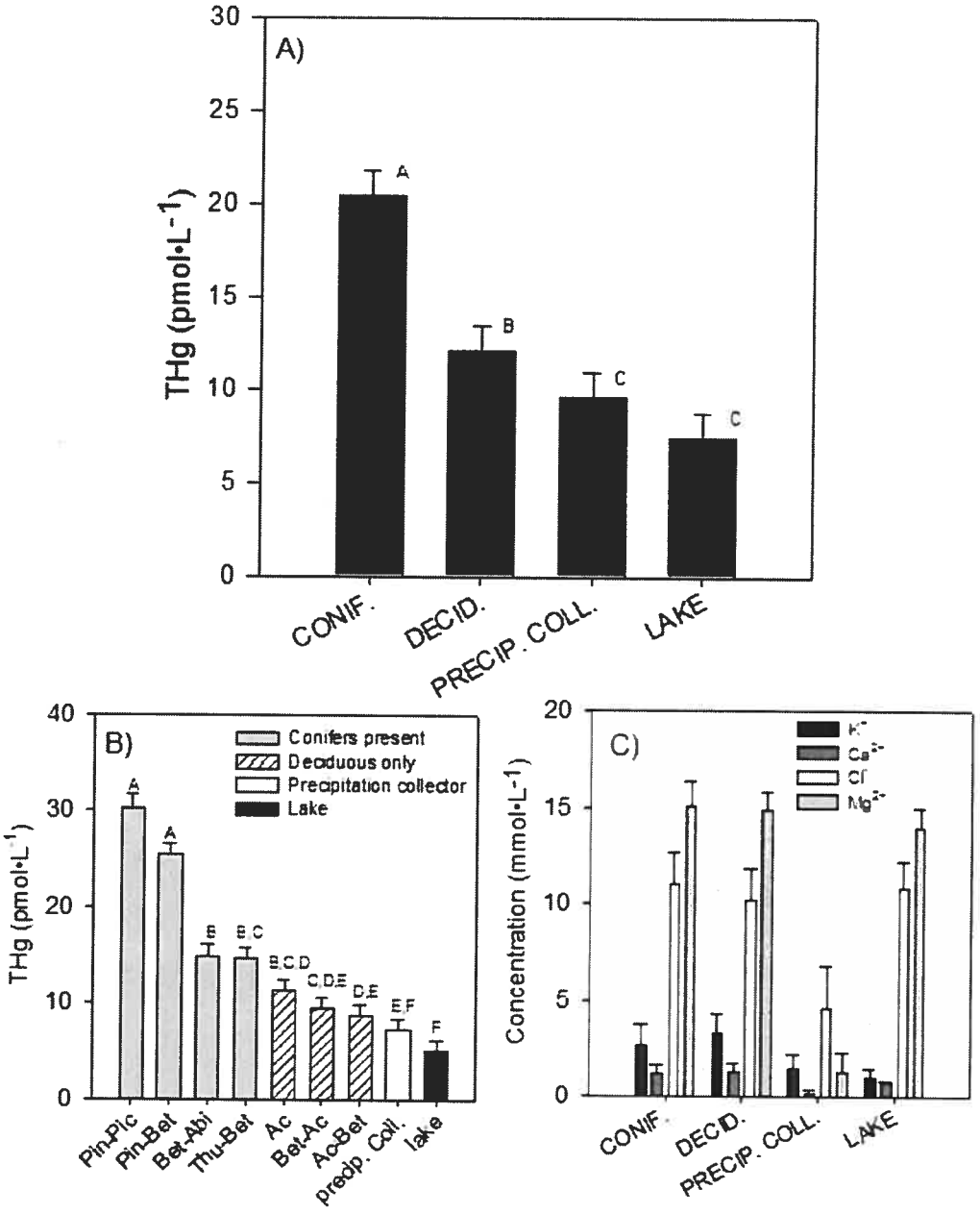

Figure 4.3. [THg] in integrated snow samples over depth. A) Sites pooled together over the winter; using a general linear model, the cross influence of time and sampling site was not significant (p=0.18); B) Details of [THg] for each site at the onset of snowmelt (13 March 2005) and C) distribution of major ions. For A) and B) variance were homogeneous (Bartlett and O'Brien; p>0.05); Data were log transformed to ensure normality (Shapiro-Wilk; p>0.05). Statistical differences were determined using a one-way anova and a Tukey HSD post-hoc test. Same letter indicates no statistical difference (significance at 0.05 level). Values reported are back transformed.

Under all canopy types, [THg] were consistently higher than in the precipitation collector (Figure 4.3 A and 4.3 B). [THg] under coniferous canopies (20.44 ± 1.38 pmol•L^{-1}) were ca. twice as high as those under deciduous-only canopies (12.14 ± 1.29 pmol•L^{-1}) and three times higher than in snow collected over a frozen lake (7.45 ± 1.37 pmol•L^{-1}) (Figure 4.3 A). Over the frozen lake, [THg] were either similar or lower but never higher than in the precipitation collector. Thus, snow samples under canopy are enriched with Hg compared to snow collected in open areas.

Whether it was under canopy or over the frozen lake, major ion concentrations were similar or higher than those collected in the precipitation collector (Figure 4.3 C). Note that the similarity in major ion concentrations in snow over the frozen lake and under canopy is likely related to i) dry deposition and ii) to a redistribution of snow between the forest and the open area. Indeed, because of wind, snow grains are known to be transported over long distances (16).

This pattern of major ion concentrations was different to what was observed for Hg (Figure 4.3 A). Assuming a conservative behaviour of Hg, one would have expected the same pattern for Hg and major ions; because of the lack thereof, it is likely that other processes, affecting only Hg, control its distribution in snow. For instance, because conifers retain their needles throughout the winter, snow deposited in coniferous forest receives less direct sunlight than snow deposited under deciduous trees or in the open. Indeed, photoredox transformations are known to influence Hg concentrations in surface snow and will be detailed below (section 3.3.).

Particulate Hg in snow

Under all canopy types, [THg] were consistently higher than in the precipitation collector (Figure 4.3 A and 4.3 B). [THg] under coniferous canopies (20.44 ± 1.38 pmol•L^{-1}) were ca. twice as high as those under deciduous-only

canopies (12.14 ± 1.29 pmol•L^{-1}) and three times higher than in snow collected over a frozen lake (7.45 ± 1.37 pmol•L^{-1}) (Figure 4.3 A). Over the frozen lake, [THg] were either similar or lower but never higher than in the precipitation collector. Thus, snow samples under canopy are enriched with Hg compared to snow collected in open areas.

Whether it was under canopy or over the frozen lake, major ion concentrations were similar or higher than those collected in the precipitation collector (Figure 4.3 C). Note that the similarity in major ion concentrations in snow over the frozen lake and under canopy is likely related to i) dry deposition and ii) to a redistribution of snow between the forest and the open area. Indeed, because of wind, snow grains are known to be transported over long distances (16).

This pattern of major ion concentrations was different to what was observed for Hg (Figure 4.3 A). Assuming a conservative behaviour of Hg, one would have expected the same pattern for Hg and major ions; because of the lack thereof, it is likely that other processes, affecting only Hg, control its distribution in snow. For instance, because conifers retain their needles throughout the winter, snow deposited in coniferous forest receives less direct sunlight than snow deposited under deciduous trees or in the open. Indeed, photoredox transformations are known to influence Hg concentrations in surface snow and will be detailed below (section 3.3.).

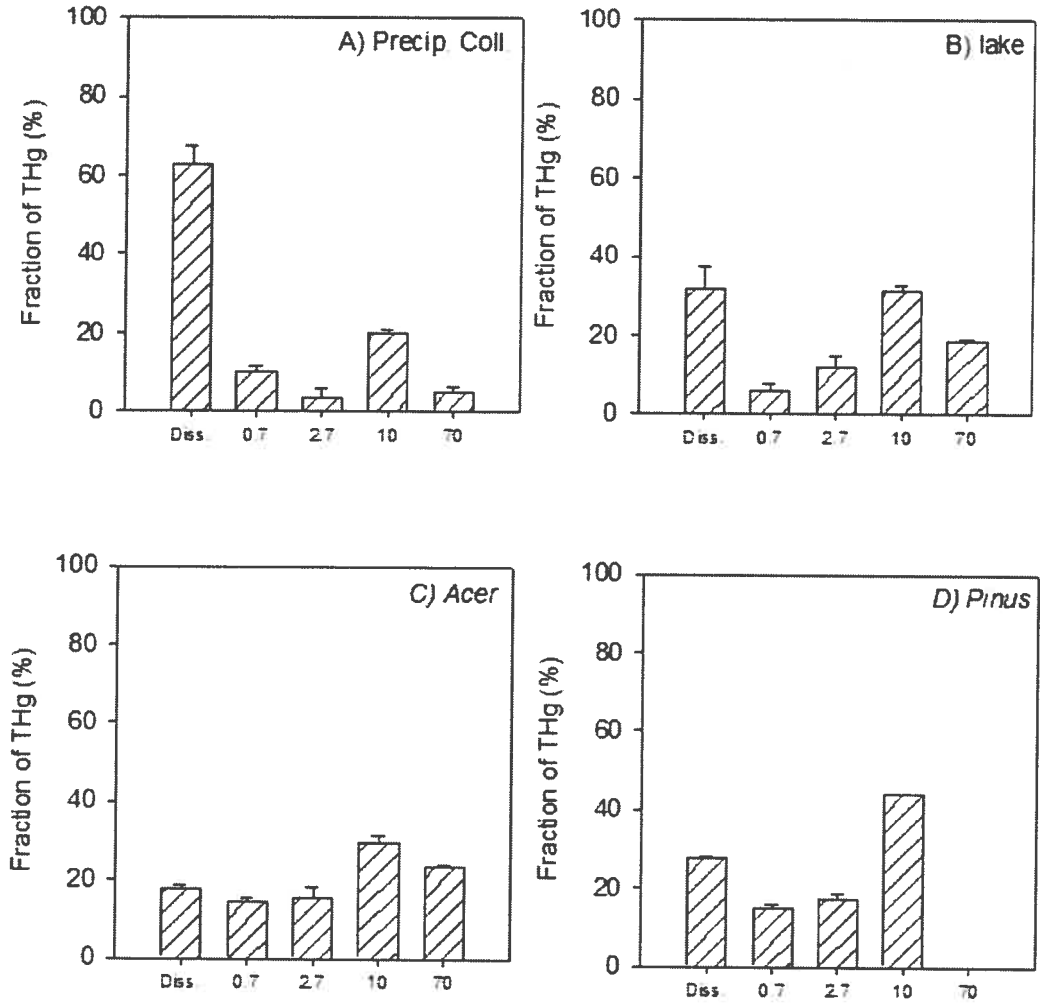

Figure 4.4. Hg partitioning onto particles in A) fresh snow sample in the precipitation collector, and in integrated snow samples (freshly fallen snow + older snow) on the ground collected B) over the frozen lake, C) at the deciduous site (*Acer*) and D) at the site with conifers (*Pinus*). Sample occurred on February 16th 2005. Note that samples were melted prior to the analysis.

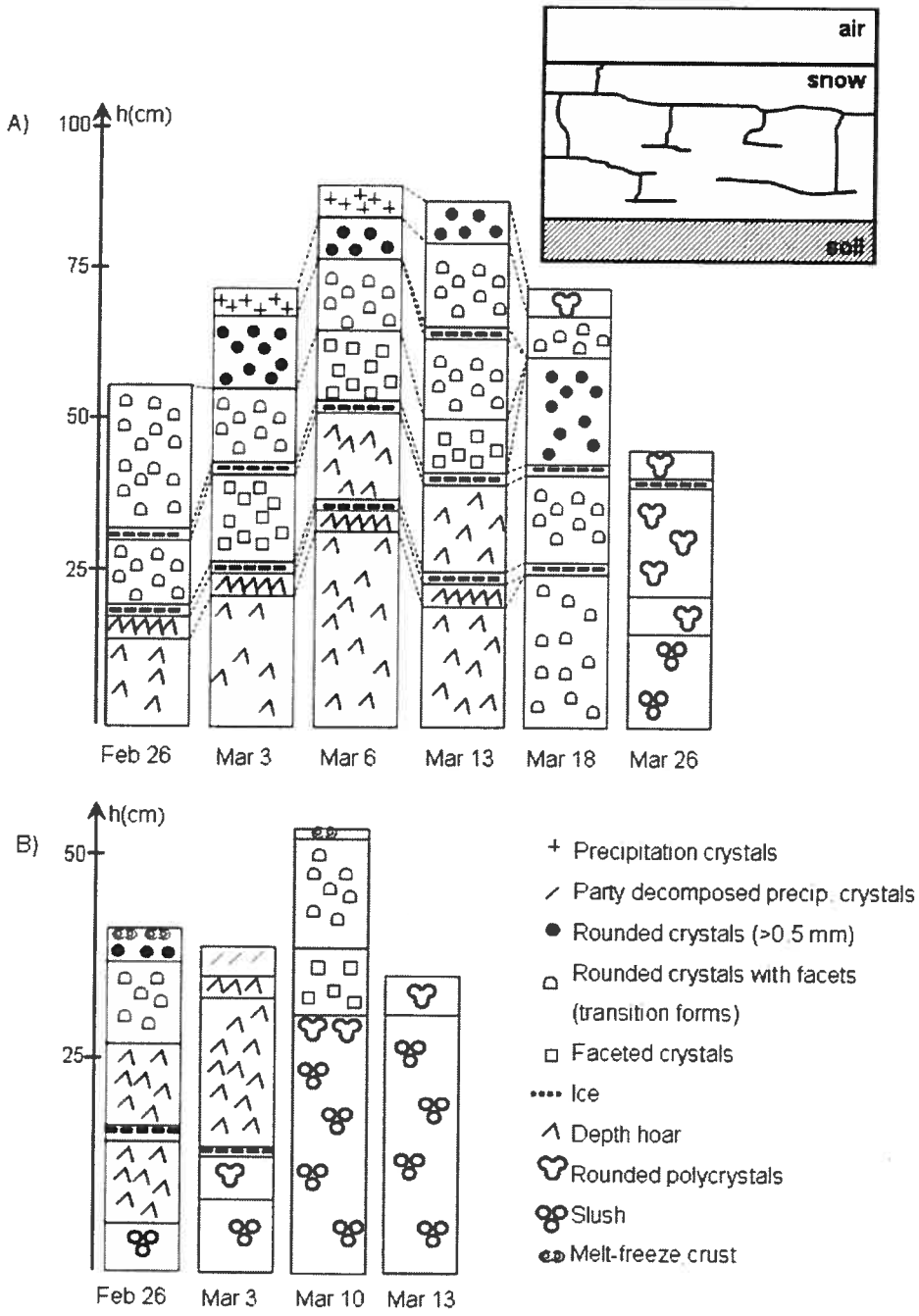

Figure 4.5. Snow stratigraphy over time from February 26 to March 26 A) under a mixed canopy (*Pinus* and *Acer*) and B) over frozen Lake Cromwell. The inset in A) represents the possible distribution of percolation columns within a snow accumulation. The bold arrow represents downward water movement.

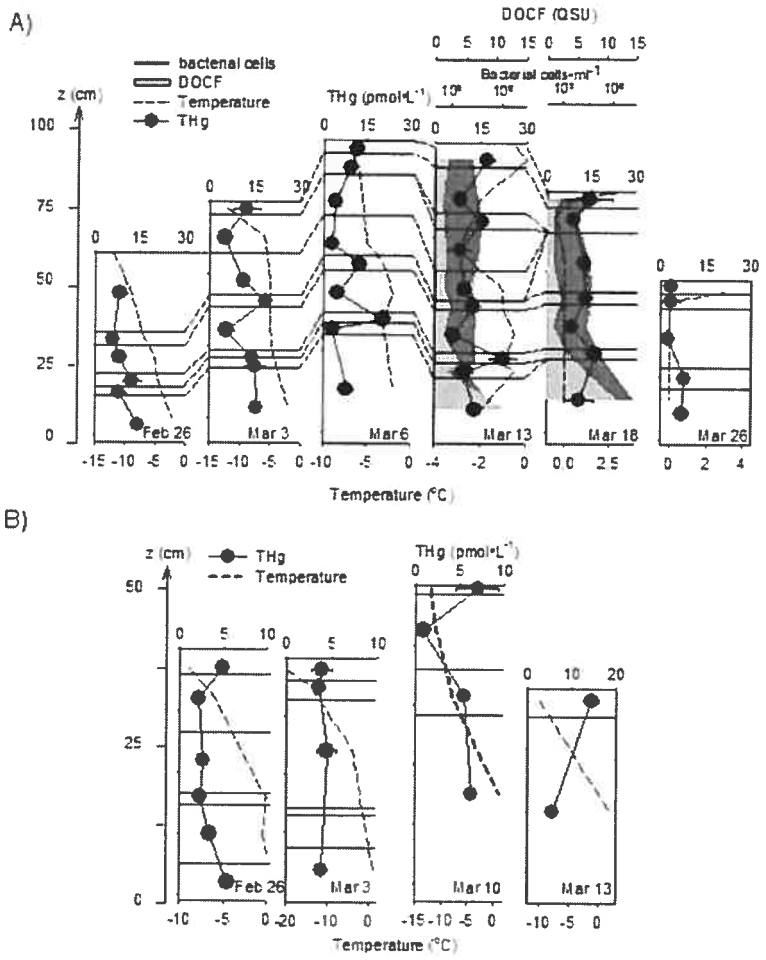

Figure 4.6. Depth profiles of [THg] over time A) in a snow accumulation under a mixed canopy (*Pinus* and *Acer*) and B) over frozen Lake Cromwell. Strata refer to Figure 4.5.

4.4.2. Distribution of Hg with depth

We showed above that in integrated snow samples great variations exist in [THg] under different types of canopy. To further understand Hg distribution within a snow accumulation, we chose to detail the distribution of [THg] within each stratum of a snow accumulation under a mixed canopy and in an open area; we followed this distribution over a period of ca. one month, overlapping with the melting period from February 26 to March 26, 2003.

Snow strata were identified using the state of grain metamorphism. Because of the persistence of two ice layers within the accumulation under canopy, strata identification for various successive samplings was made easier. Thus, the six strata initially sampled on February 26th were retrieved during each of the subsequent samplings until warmer temperatures and rain resulted in the destruction of the stratification. It is on these six strata that we focused our assessment of temporal trends within the accumulation. Over time, strata within the snow accumulation under tree cover were easily identified from one date to another (Figure 4.5 A). Continuity of strata within the snow accumulation over the lake was harder to identify from one date to another (Figure 4.5 B) likely due to greater temperature gradient and wind redistribution of snow after deposition.. The types of snow crystals encountered both over the lake and under canopy were diverse and consistent with both constructive and destructive metamorphism (Figure 4.5 A and 4.5 B) (5).

Under canopy, [THg] exhibited a multimodal profile due to sharp increases at various depths (up to 5 fold compared to adjacent strata; Figure 4.6 A). In contrast, the lake profiles were much smoother (Figure 4.6 B). Overall, the highest [THg] were encountered in ice layers, in precipitation crystals, and in rounded grains characterizing crystals which undergo either no or very slow growth (5). The lowest [THg] concentrations were encountered in kinetic growth forms such as depth hoar, faceted crystals and mixed crystals (Table 1). DOC

fluorescence and bacterial cells increased at the bottom of the accumulation (Figure 4.6 A, on March 13 and 18) which would suggest an influence from the soil; however, no increase was observed in [THg] contrary to what was described by Susong et al. (2003).

Hg did not co-vary over depth with major cations (Ca^{2+}, Mg^{2+}, Na^{+}, and K^{+}) at the lake site or under canopy. Ca^{2+}, Mg^{2+}, Na^{+}, and K^{+} co-varied over the lake (all correlation coefficients > 0.99; $p<0.00001$) and under canopy, although correlations were weaker at this latter site ($0.58<r<0.90$; $p<0.01$).

Over time, [THg] within one stratum did not co-vary with any of the major ionic species assessed. Ca^{2+} and Mg^{2+} ($0.90<r<0.98$; $p<0.05$) as well as Na^{+} and Cl^{-} ($0.88<r<0.99$; $p<0.05$) co-varied together. Although different types of crystals exhibited different [THg] (see above and Table 1), we could not detect any variations of [THg] based on the transition between two types of grains over time within one stratum.

Table 4.I. THg concentrations in snow based on snow grain characteristics.

Crystal type	THg concentration (±SD) ($pmol \cdot L^{-1}$)	n	Statistical difference*
Ice	14.7 (±0.58)	27	A
Precipitation crystals	12.9 (±0.08)	6	A,B
Rounded grains	10.4 (±0.59)	12	A,B,C
Cup shaped crystals	9.0 (±0.58)	30	B,C
Rounded with facets	8.9 (±0.33)	30	B,C
Faceted crystals	5.8 (±0.41)	9	C

* Variances were homogeneous (Bartlett and Levene; $p>0.05$), data were square root transformed to ensure normality (Shapiro-Wilk; $p>0.05$). Statistical differences were determined using a one-way anova and a Tukey HSD post-hoc

test. Same letter indicates no statistical difference (significance at 0.05 level). Values reported are back transformed.

The role of snow metamorphic processes involving vapour transfer between adjacent crystals on Hg distribution in snow is currently poorly understood (8, 16). Our results suggest that constructive snow metamorphism leads to a decrease of Hg concentrations since kinetic growth crystals exhibited lower concentrations (Table 1). However, the temporal resolution with which we sampled the snow accumulation (once to twice a week) is too low to assess transformations occurring at the grain scale and further studies will be required to determine the role of snow metamorphism with respect to variations in [THg]. The appearance of ice layers enriched with Hg may reflect the action of rain on throughfall during the winter. In addition, during warmer periods, percolation columns form within the accumulation which drain water and associated dissolved and particulate chemicals downwards (16); this process is enhanced with rain (37) and also supports the occurrence of ice layers enriched with Hg when temperatures within the snowpack accumulation fell below the freezing point.

When both the depth profiles and the distribution of [THg] under various types of canopy are considered together, our data suggest that Hg in snow behaves differently from major ions. While this has been attributed to photoreduction processes in open areas (21), the importance of redox transformations on Hg dynamics in snow under tree cover is poorly understood. Differences between the roles of redox transformations in open areas and under canopies may explain some of the variations we observed in [THg]. Assessing the relative importance of reduction versus oxidation processes is therefore required to accurately assess Hg distribution in forested areas. In the following section, we describe the role of redox reactions (both reduction and oxidation) in Hg dynamics in snow under contrasting canopies.

4.4.3. Evolution of [THg] over time in surface snow and role of photoredox processes

Evolution of [THg] over time in surface snow.

We monitored [THg] in fresh snow over a 19-hour period both under canopy (mostly coniferous *Thuja*) and over the frozen lake. The first snow samples were collected at 23:00 on January 19 2005, immediately after the end of a snow event (accumulation: 5.6 cm of snow). Subsequent sampling took place every 5 to 6 hours, and no new snowfall occurred. In the open, [THg] in surface snow stayed constant over time (Figure 4.7 A). Under canopy, [THg] increased of ca. 65% over time, in the absence of snowfall.

The difference between [THg] in snow on the ground under canopy and in the open at midnight can be associated to the net contribution of canopy since samples were collected immediately after the precipitation stopped (Figure 4.7 A). Contrasting with what was previously suggested (15), the winter throughfall contribution is substantial and represents, on average, 75% of the wet Hg deposition in the open, which corresponds to previously reported values for the growth season (14, 23, 28, 35).

The increase in [Hg] under canopy over time can be explained i) by direct dry deposition of Hg to the snow; ii) by wind-driven remobilisation of snow intercepted by canopy and enriched with Hg. The impact of dry deposition on snow [THg] is supported by the arrival of an air mass from an industrialized area (City of Montreal), evidenced by changes in wind direction (data not shown). We interpret the lack of increase in [Hg] over the lake as indicative of a balance between dry deposition and a loss mechanism, such as photoreduction of Hg(II).

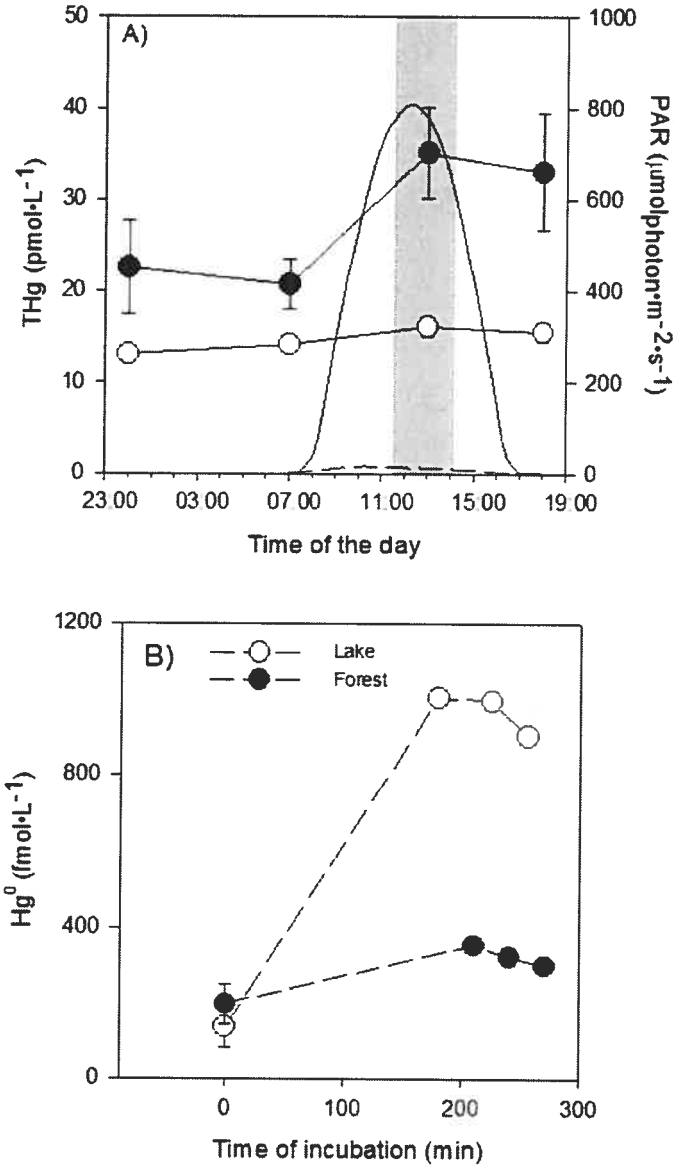

Figure 4.7. A) [THg] over time in surface snow in the open or under a coniferous canopy (*Thuja*) between January 19 and January 20 2005; the straight line represents the PAR in the open and the dashed line the PAR under canopy. The shadowed area represents the period during which the in situ incubation described in B took place; B) Evolution of Hg^0 concentrations over time during in situ incubation of snow under canopy or in the open. Open symbols represent the lake sites and closed symbols the coniferous site (*Thuja*).

Impact of forest canopy on photoreduction of Hg(II)

At both sites, in the open and under canopy, we compared the production of Hg^0 for fresh snow samples incubated *in-situ* for a period of 3 hours (Figure 4.7 B) starting at 11:30 on January 20 2005. [Hg^0] were ca. three times higher at the end of the incubation period in the open area compared to under canopy (Figure 4.7 B) with Hg^0 production rates being 0.04 $pmol \cdot L^{-1} \cdot h^{-1}$ and 0.27 $pmol \cdot L \cdot h^{-1}$ under canopy and in the open, respectively.

Applying these rates to the whole daylight period (10 h), the maximum loss of snow Hg by photoreduction is 0.4 and 2.7 pmoles per litre of melted snow for the canopy and the lake sites, respectively. This represents a loss of THg of 2% (under canopy) to 22% (over the lake). However, no such decrease was observed in our time series (Fig. 7A), indicating that another source of deposited Hg counterbalanced the loss by photoreduction. This source is most likely dry deposition, as discussed in section 3.3.1. Another potential mechanism preventing Hg(0) loss is its oxidation back to Hg(II), discussed in section 3.3.3.

The photoreduction rate recorded in the open is in good agreement with reduction rates in snow reported for remote temperate open areas from the experimental lakes area (ca. 0.25 $pmol \cdot L^{-1} h^{-1}$) (20). Note that reduction rates in snow can reach up to 1.60 $pmol \cdot L^{-1} \cdot h^{-1}$ near urban centres (21).

The lower photoreduction rates we observed under canopy (Fig. 7A) may be due to i) a shadowing effect of the canopy ii) a lower pool of photoreducible Hg present under canopy or/and iii) enhanced oxidation under canopy. To test for these hypotheses, we ran a series of incubation experiments.

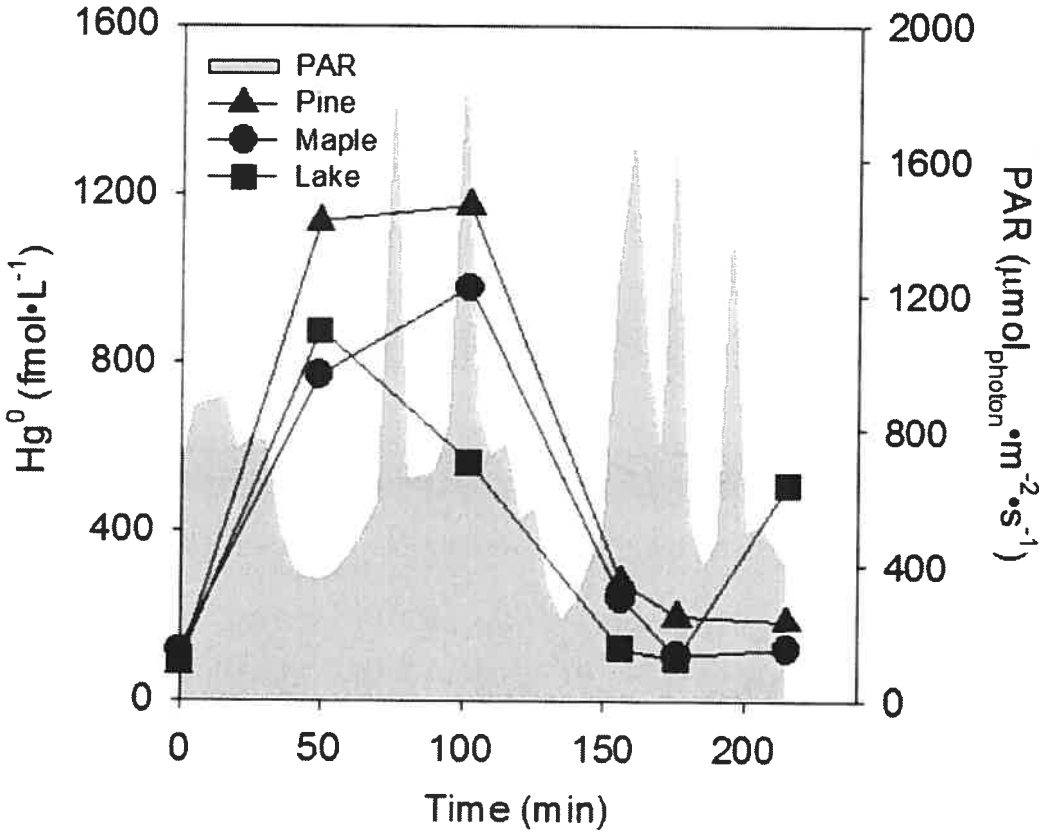

Figure 4.8. Time series of Hg^0 concentrations during incubation of freshly fallen snow on March 13 2005 collected at three sites (coniferous (*Pinus*), deciduous (*Acer*) and the lake) and incubated in the open. Incubation started at 11:00 AM Shadowed area represents the irradiance.

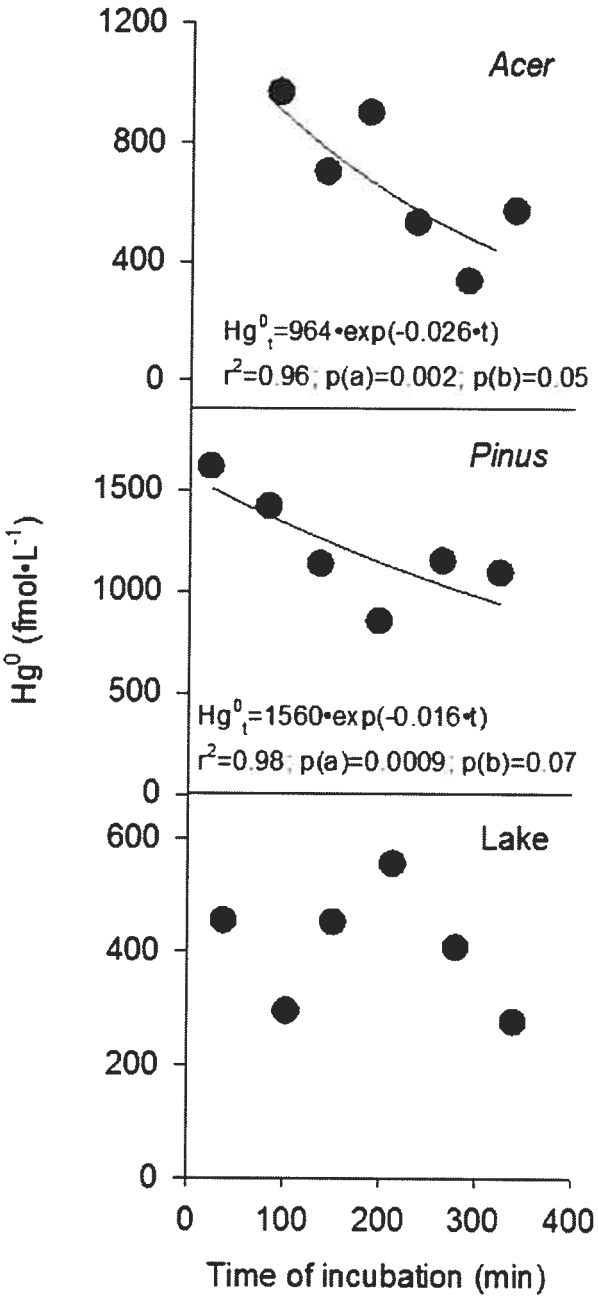

Figure 4.9. [Hg^0] time series in snow samples kept in the dark for ca. 6h after a pre-incubation period of 4 hours (staring at 8:20 AM on February 25 2005) in the open. Samples were collected at the deciduous (*Acer*), coniferous (*Pinus*) and at the lake sites.

Production and loss of Hg(0) in snow

We compared the pool of photoreducible Hg present in freshly deposited snow under coniferous and deciduous canopy to that of an open area by incubating snow samples of both sites in an open area, under direct sunlight (Fig. 8). For the first 50 to 100 min, [Hg^0] increased from 8 to 14 times the initial concentrations, signalling efficient photoreduction in all snow samples (maximum reduction rate were 1.3, 0.8 and 1.0 $pmol \cdot L^{-1} \cdot h^{-1}$, with *Pinus*, *Acer* and lake snows, respectively). However, in all three types of snow, [Hg^0] steadily declined afterwards back to pre-incubation levels (Fig. 8). To further characterize the potential for Hg redox transformations in snow we assessed the fluorescence of DOC (DOCF), as a surrogate for DOC reactivity, in snow deposited under the various types of canopy. DOCF, expressed in quinine sulphate units (QSU) recorded in snow deposited over the lake was approximately two times lower (median = 1.48 QSU; min=0.79, max=1.97) than that of the snow deposited in forested areas (median=3.95 QSU; min=1.18, max=39.6).

Second, to test the oxidative potential of various types of snow, we exposed fresh snow collected from underneath *Pinus*, and *Acer* canopies, as well as from over the frozen lake to natural direct sunlight for four hours during a cloudless day in order to naturally produce Hg^0 at environmental levels under optimum conditions. Snow samples were then placed in total darkness and one sample was analysed every 45 to 50 minutes (Fig. 9). An exponential decline in [Hg^0] was observed for snow samples collected under both types of canopy but no significant decline was observed for snow samples collected over the frozen lake (Fig. 9).

These results indicate that the lower Hg photoreduction rates observed under the canopy compared to the lake (Fig. 7) are not caused by a limitation in the amount of photoreducible Hg (Fig. 8), since i) DOC reactivity was higher in

snow deposited under canopy than in snow deposited over the lake and ii) the highest photo-produced [Hg(0)] were reached in snow sampled under canopy and incubated in an open area. Rather, they are caused by a shadowing effect of the canopy. Also, the presence of Hg^0 oxidation, a process more prevalent under canopy at least under dark conditions (Fig. 9), may also decrease the apparent photoreduction rate. All snow samples showed a pattern of initial reduction followed by oxidation, resulting in no net changes in volatile Hg(0) over time (Fig. 8). This is consistent with the absence of Hg loss by volatilization observed in our 19 h time series (Fig. 7A). Since the time series measurements of Hg(0) production were carried out in closed bottles (Fig. 8), there was no exchange with the atmosphere during incubation. In natural snowpacks, it is likely that part of the initial pool of photo-produced Hg(0) will be lost through evasion, before being re-oxidized. The sequence of reduction-oxidation reactions may result from: 1) the alteration of the ratio between the pools of reductants and oxidants (for instance, the pool of reductants could be depleted after 1h of irradiation, whereas the pool of oxidants remained constant); 2) changes of light regimes favouring one reaction over the other. This reduction-oxidation sequence has already been observed in High Arctic snow (27). Alternatively The absence of a significant decline in Hg(0) levels in the dark for snow collected over the lake may be explained by a pool of Hg(II) somewhat refractory to photoreduction present in snow, as already proposed by Lalonde et al. (2002) which could have yielded to low yet variable levels of Hg(0).

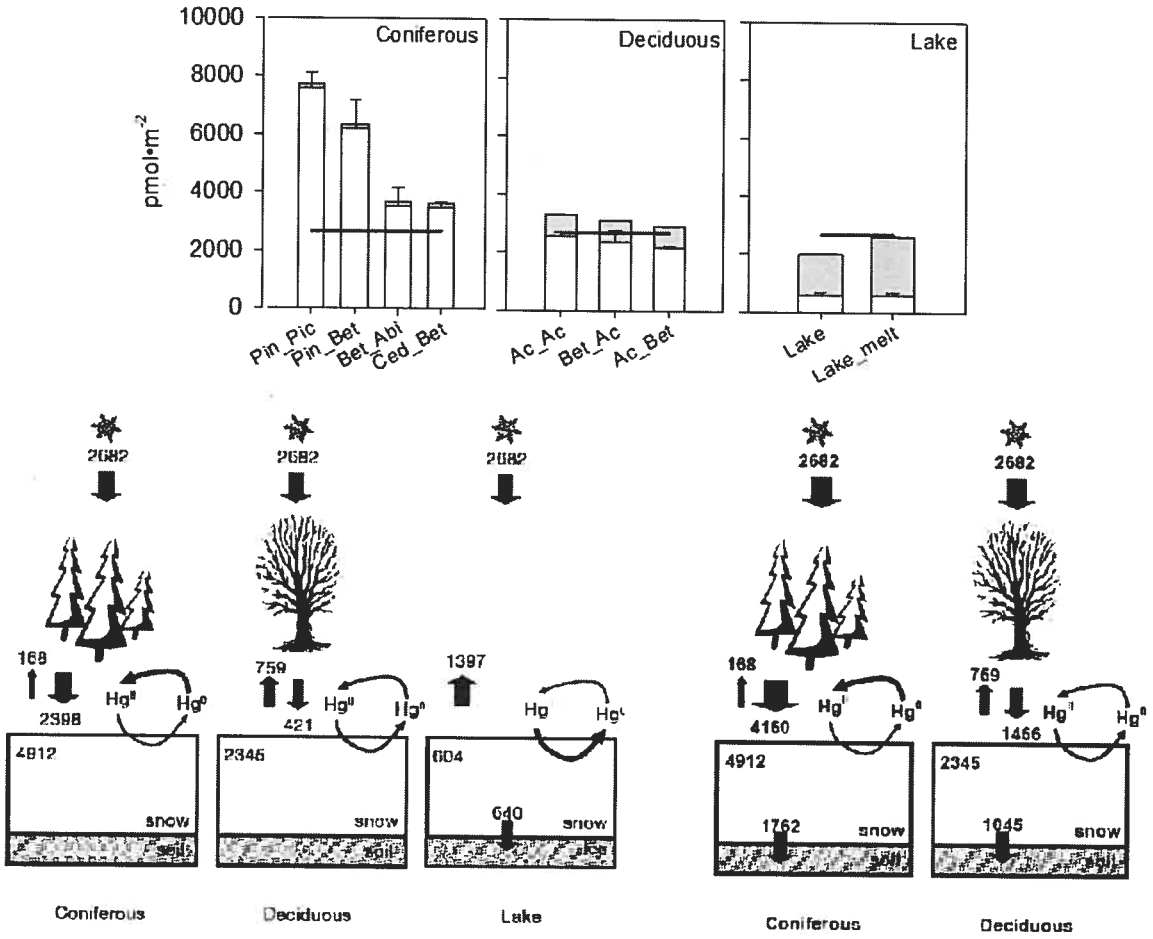

Figure 4.10. A) Mass balance of Hg during the winter (December-March). The horizontal line represent Hg in wet deposition during the period; white bars represent observed Hg pools in snowpacks; stacked grey bars represent calculated losses by evasion; B) conceptual scheme of fluxes of Hg during winter time in a forested ecosystem if basal snow melt at forested sites was not considered in the mass balance and C) when basal snow melt at the forested sites was considered in the mass balance.

4.4.4. Fluxes of Hg in a forested ecosystems during winter time

Shortly before the beginning of snowmelt, we determined the amount of Hg stored within the snow accumulation at the eight study sites, and compared it to the data from the precipitation collector. We evaluated whether canopy and lake snowpacks were winter sources or sinks of Hg, using equation (2). They were considered sources if:

$Hg_{snow} < Hg_{wet.}$; $Hg_{canopy} + Hg_{dry} < Hg^0_{evasion} (+ Hg_{melt})$

They were considered sinks if:.

$Hg_{snow} > Hg_{wet.}$; $Hg_{canopy} + Hg_{dry} > Hg^0_{evasion} (+ Hg_{melt})$

Under coniferous canopy, a net gain of Hg was observed (Fig. 10A). Photoreduction was very limited and we estimated Hg loss via evasion to be on average 2 to 3 % of pool present (wet + canopy contribution). We therefore conclude that, since the canopy greatly contributes to the flux of Hg to the coniferous forest floor during the winter and that redox processes do not efficiently recycle Hg, snowpacks under coniferous canopies are likely sinks for Hg.

The pool of Hg in snow stored under deciduous-only canopies were similar to or lower than the pool deposited during the winter (Figure 4.10 A), suggesting that the amount gained via canopy and dry deposition could partly be lost via evasion (Figure 4.10 A, 4.10 B and 4.10 C). Evasion estimates suggest that between 18 to 24% of the pool present was recycled. The canopy contribution at the deciduous site was significant, suggesting that snow is an efficient scavenger of Hg present on branches, bark and dead leaves remaining in the trees. We conclude that snow under deciduous canopy is neither a winter source or sink for Hg.

Over the lake, ca. 77% of the Hg was lost with respect to wet deposition (Figure 4.10 A). Both percolation and evasion likely contributed to the loss of Hg. Our estimates for evasion and percolation could account for 98% of this loss

(67% and 31% for evasion and percolation, respectively). Clearly, snow in open areas is a winter source of Hg to the atmosphere via evasion or to underlying surface via percolation.

To establish the mass balance, we assessed the possible loss of Hg via percolation of meltwaters during warmer winter periods. The assumption that some of the Hg was lost via percolation of melting snow results in greater estimates of Hg flux for canopy and dry deposition at the forested sites. Canopy and dry deposition contribution were estimated to range between 200 and 1200 $pmol \cdot m^{-2}$ at the deciduous site and to range between ca. 2300 and 4000 $pmol \cdot m^{-2}$ at the coniferous site (no melt or melt scenarios, respectively). These numbers are in good agreement with dry deposition estimated from both published regional particulate Hg and reactive gaseous mercury concentrations and respective deposition velocities (ca. 2100 $pmol \cdot m^{-2}$ for the period) (22, 24, 25, 34).

The contribution of dry deposition to snow at forested sites is difficult to quantify and depends on where, on the canopy, the deposition occurred. Indeed, Hg in intercepted snow exposed to the sun at the top of the canopy would likely behave similarly to Hg in snow over the frozen lake. Therefore a fraction of the dry deposition could be photo-reduced while the other would be trapped in the canopy; their relative importance remains to be determined.

Overall, this study indicates that, whereas most Hg deposited by snow on lakes is lost, mostly to the atmosphere, but also via percolation, before snowmelt, Hg deposited on the forested watershed is largely retained in snowpacks, presenting a threat to systems receiving meltwaters.

4.5. Acknowledgements

This study was funded by NSERC-COMERN and NSERC discovery grant to MA, as well as the Science Horizon program from Environment Canada. We would like to thank Peter G. C. Campbell for comments on the manuscript. We

thank Paul del Giorgio for access to the flow cytometer. We would like to thank D. Belanger for his help in the lab. R. Carignan, J. Mercier, R. Beauséjour, E. Valiquette and the SBL staff are acknowledged for their logistical support. The assistance, in the field, of V. Girard, N. Milot, and M.C. Fontaine was greatly appreciated.

4.6. References.

1. **Aspmo, K., C. Temme, T. Berg, C. P. Ferrari, P. A. Gauchard, X. Fain, and G. Wibetoe** 2006, posting date. Mercury in the atmosphere, snow and melt water ponds in the north atlantic ocean during arctic summer. [Online.]
2. **Barbante, C., C. Boutron, C. Morel, C. Ferrari, J. L. Jaffrezo, G. Cozzi, V. Gaspari, and P. Cescon.** 2003. Seasonal variations of heavy metals in central Greenland snow deposited from 1991 to 1995. Journal of Environmental Monitoring **5:**328-335.
3. **Carignan, R., D. Planas, and C. Vis.** 2000. Planktonic production and respiration in oligotrophic Shield lakes. Limnology and Oceanography **45:**189-199.
4. **Carrera, G., P. Fernandez, R. M. Vilanova, and J. O. Grimalt.** 2001. Persistent organic pollutants in snow from European high mountain areas. Atmospheric Environment **35:**245-254.
5. **Colbeck, S., E. Akitaya, R. Armstrong, H. Gubler, J. Lafeuille, K. Lied, D. McClung, and E. Morris.** 1985. The International Commission on Snow and Ice of the International Association of Scientific Hydrology and the International Glaciological Society.
6. **Collett, J. L., A. S. H. Prevot, J. Staehelin, and A. Waldvogel.** 1991. Physical Factors Influencing Winter Precipitation Chemistry. Environmental Science & Technology **25:**782-788.
7. **Dommergue, A., C. P. Ferrari, L. Poissant, P. A. Gauchard, and C. F. Boutron.** 2003. Diurnal cycles of gaseous mercury within the snowpack at Kuujjuarapik/Whapmagoostui, Quebec, Canada. Environmental Science & Technology **37:**3289-3297.
8. **Eichler, A., M. Schwikowski, and H. W. Gaggeler.** 2001. Meltwater-induced relocation of chemical species in Alpine firn. Tellus Series B-Chemical and Physical Meteorology **53:**192-203.
9. **Fitzgerald, W. F., R. P. Mason, and G. M. Vandal.** 1991. Atmospheric Cycling and Air-Water Exchange of Mercury over Midcontinental Lacustrine Regions. Water Air and Soil Pollution **56:**745-767.

10. **Franz, T. P., and S. J. Eisenreich.** 1998. Snow scavenging of polychlorinated biphenyls and polycyclic aromatic hydrocarbons in Minnesota. Environmental Science & Technology **32:**1771-1778.
11. **Garbarino, J. R., E. Snyder-Conn, T. J. Leiker, and G. L. Hoffman.** 2002. Contaminants in arctic snow collected over northwest Alaskan sea ice. Water Air and Soil Pollution **139:**183-214.
12. **Gasol, J. M., and P. A. Del Giorgio.** 2000. Using flow cytometry for counting natural planktonic bacteria and understanding the structure of planktonic bacterial communities. Scientia Marina **64:**197-224.
13. **Graydon, J. A., V. L. S. Louis, S. E. Lindberg, H. H. Mann, and D. P. Krabbenhoft.** 2006. Investigation of mercury exchange between forest canopy vegetation and the atmosphere using a new dynamic chamber. Environmental Science & Technology **40:**4680-4688.
14. **Grigal, D. F., R. K. Kolka, J. A. Fleck, and E. A. Nater.** 2000. Mercury budget of an upland-peatland watershed. Biogeochemistry **50:**95-109.
15. **Iverfeldt, A.** 1991. Mercury in Forest Canopy Throughfall Water and Its Relation to Atmospheric Deposition. Water Air and Soil Pollution **56:**553-564.
16. **Jones, G. H., J. W. Pomeroy, D. A. Walker, and R. W. Hoham.** 2001. Snow Ecology: An Interdisciplinary Examination of Snow-Covered Ecosystems. Cambridge University Press, Cambridge, United Kingdom.
17. **Keeler, G., G. Glinsorn, and N. Pirrone.** 1995. Particulate Mercury in the Atmosphere - Its Significance, Transport, Transformation and Sources. Water Air and Soil Pollution **80:**159-168.
18. **Keeler, G. J., L. E. Gratz, and K. Al-Wali.** 2005. Long-term atmospheric mercury wet deposition at Underhill, Vermont. Ecotoxicology **14:**71-83.
19. **Lahoutifard, N., M. Sparling, and D. Lean.** 2005. Total and methyl mercury patterns in Arctic snow during springtime at Resolute, Nunavut, Canada. Atmospheric Environment **39:**7597-7606.
20. **Lalonde, J. D., M. Amyot, M. R. Doyon, and J. C. Auclair.** 2003. Photo-induced Hg(II) reduction in snow from the remote and temperate Experimental Lakes Area (Ontario, Canada). Journal of Geophysical Research-Atmospheres **108**.
21. **Lalonde, J. D., A. J. Poulain, and M. Amyot.** 2002. The role of mercury redox reactions in snow on snow-to-air mercury transfer. Environmental Science & Technology **36:**174-178.
22. **Lamborg, C. H., W. F. Fitzgerald, G. M. Vandal, and K. R. Rolfhus.** 1995. Atmospheric Mercury in Northern Wisconsin - Sources and Species. Water Air and Soil Pollution **80:**189-198.
23. **Lee, Y. H., K. H. Bishop, J. Munthe, A. Iverfeldt, M. Verta, H. Parkman, and H. Hultberg.** 1998. An examination of current Hg

deposition and export in Fenno-Scandian catchments. Biogeochemistry **40:**125-135.

24. **Lindberg, S. E., S. Brooks, C. J. Lin, K. J. Scott, M. S. Landis, R. K. Stevens, M. Goodsite, and A. Richter.** 2002. Dynamic oxidation of gaseous mercury in the Arctic troposphere at polar sunrise. Environmental Science & Technology **36:**1245-1256.
25. **Poissant, L., M. Pilote, C. Beauvais, P. Constant, and H. H. Zhang.** 2005. A year of continuous measurements of three atmospheric mercury species (GEM, RGM and Hg-p) in southern Quebec, Canada. Atmospheric Environment **39:**1275-1287.
26. **Pomeroy, J. W., D. M. Gray, K. R. Shook, B. Toth, R. L. H. Essery, A. Pietroniro, and N. Hedstrom.** 1998. An evaluation of snow accumulation and ablation processes for land surface modelling. Hydrological Processes **12:**2339-2367.
27. **Poulain, A. J., J. D. Lalonde, M. Amyot, J. A. Shead, F. Raofie, and P. A. Ariya.** 2004. Redox transformations of mercury in an Arctic snowpack at springtime. Atmospheric Environment **38:**6763-6774.
28. **Rea, A. W., G. J. Keeler, and T. Scherbatskoy.** 1996. The deposition of mercury in throughfall and litterfall in the lake champlain watershed: A short-term study. Atmospheric Environment **30:**3257-3263.
29. **Rea, A. W., S. E. Lindberg, and G. J. Keeler.** 2000. Assessment of dry deposition and foliar leaching of mercury and selected trace elements based on washed foliar and surrogate surfaces. Environmental Science & Technology **34:**2418-2425.
30. **Savage, C.** 2001. Recolonisation forestière dans les basses Laurentides au sud du domaine climacique de l'érablière à bouleau jaune. MSc. Université de Montréal, Montréal.
31. Schroeder, W. H., K. G. Anlauf, L. A. Barrie, J. Y. Lu, A. Steffen, D. R. Schneeberger, and T. Berg. 1998. Arctic springtime depletion of mercury. Nature 394:331-332.
32. **Schwesig, D., and E. Matzner.** 2001. Dynamics of mercury and methylmercury in forest floor and runoff of a forested watershed in Central Europe. Biogeochemistry **53:**181-200.
33. **Sheehan, K. D., I. J. Fernandez, J. S. Kahl, and A. Amirbahman.** 2006. Litterfall mercury in two forested watersheds at Acadia National Park, Maine, USA. Water Air and Soil Pollution **170:**249-265.
34. **Skov, H., J. H. Christensen, M. E. Goodsite, N. Z. Heidam, B. Jensen, P. Wahlin, and G. Geernaert.** 2004. Fate of elemental mercury in the arctic during atmospheric mercury depletion episodes and the load of atmospheric mercury to the arctic. Environmental Science & Technology **38:**2373-2382.
35. **St Louis, V. L., J. W. M. Rudd, C. A. Kelly, B. D. Hall, K. R. Rolfhus, K. J. Scott, S. E. Lindberg, and W. Dong.** 2001. Importance of the

forest canopy to fluxes of methyl mercury and total mercury to boreal ecosystems. Environmental Science & Technology **35:**3089-3098.

36. **Steffen, A., W. Schroeder, J. Bottenheim, J. Narayan, and J. D. Fuentes.** 2002. Atmospheric mercury concentrations: measurements and profiles near snow and ice surfaces in the Canadian Arctic during Alert 2000. Atmospheric Environment **36:**2653-2661.
37. **Sturm, M., and J. Holmgren.** 1993. Rain-Induced Water Percolation in Snow as Detected Using Heat-Flux Transducers. Water Resources Research **29:**2323-2334.
38. **Susong, D. D., M. L. Abbott, and D. P. Krabbenhoft.** 2003. Mercury accumulation in snow on the Idaho National Engineering and Environmental Laboratory and surrounding region, Southeast Idaho, USA. Environmental Geology **43:**357-363.
39. **Tursic, J., B. Podkrajsek, I. Grgic, P. Ctyroky, A. Berner, U. Dusek, and R. Hitzenberger.** 2006. Chemical composition and hygroscopic properties of size-segregated aerosol particles collected at the Adriatic coast of Slovenia. Chemosphere **63:**1193-1202.
40. **Veysseyre, A., K. Moutard, C. Ferrari, K. Van de Velde, C. Barbante, G. Cozzi, G. Capodaglio, and C. Boutron.** 2001. Heavy metals in fresh snow collected at different altitudes in the Chamonix and Maurienne valleys, French Alps: initial results. Atmospheric Environment **35:**415-425.
41. **Veysseyre, A. M., A. F. Bollhofer, K. J. R. Rosman, C. P. Ferrari, and C. F. Boutron.** 2001. Tracing the origin of pollution in French Alpine snow and aerosols using lead isotopic ratios. Environmental Science & Technology **35:**4463-4469.
42. **Whitaker, A. C., and H. Sugiyama.** 2005. Seasonal snowpack dynamics and runoff in a cool temperate forest: lysimeter experiment in Niigata, Japan. HYDROLOGICAL PROCESSES **19:**4179

5. Biological and chemical redox transformations of mercury in fresh and salt waters of the high Arctic during spring and summer

Alexandre J. Poulain, Edenise Garcia, Marc Amyot, Peter G.C. Campbell, Farhad Raofie and Parisa A. Ariya.

Reprinted from Environmental Science & Technology, vol. 41 (6): 1883-1888

5.1. Abstract

It is well-established that atmospheric deposition transports Hg to Arctic regions, but the post-depositional dynamics of Hg that can alter its impact on Arctic food chains are less understood. Through a series of in situ experiments, we investigated the redox transformations of Hg in coastal and inland aquatic systems. During spring and summer, Hg reduction in streams and pond waters decreased over a salinity gradient that increased four-fold. This alteration of Hg reduction due to chloride was counterbalanced by the presence of particles which favoured the conversion of oxidized Hg to its elemental form. In saline waters, biogenic organic materials, produced by algae, were able to promote oxidation of Hg(0) even under dark conditions. Overall these results point to the vulnerability of marine/coastal Arctic systems to Hg, compared to inland systems, with oxidation processes enhancing Hg residence times and thus increasing its potential to enter the food chain.

.

5.2. Introduction

The discovery of mercury depletion events (MDE) in polar areas (9, 11, 26, 38), resulting in rapid, near complete depletion of Hg from the atmosphere, provides evidence that atmospheric oxidation of Hg is faster than initially proposed (44). These oxidation processes are thought to occur in marine-influenced environments (41), and to involve reactive halogen radicals from sea-salt aerosols (26). Recent studies showed that Br and BrO radicals were the most effective halogens driving Hg(0) oxidation (5). Modeling studies of atmospheric transport of Hg originating from Asia, Europe and, to a lesser extent, North America to higher latitudes, combined with the rapid depletion of atmospheric Hg(0), suggest that the Arctic is a sink for Hg (4). These episodes of massive Hg deposition can pose a serious threat to Arctic ecosystems as evidence suggests that newly deposited Hg, whether it results from mercury depletion events or from wet and dry deposition, may be highly bioavailable (26). The enhanced bioavailability of newly deposited Hg species is supported by experiments carried out in temperate areas which linked inorganic Hg in deposition and Hg levels in fish (20, 33). Moreover a growing body of literature documents increases in mercury contamination of the Arctic food chain (29) and increased levels of mercury exposure in indigenous populations (46). In order to better assess the magnitude of the Hg available to the food chain, however, we must first characterize the fate of the newly deposited Hg.

So far most of the work carried out in Subarctic and High Arctic regions on the redox cycling of Hg has focused on Hg dynamics in the atmosphere and in snow (9, 10, 13, 14, 26, 42), and in freshwater lakes (1, 45); to our knowledge, very few studies have dealt with Arctic coastal and marine waters (6). Recent studies suggest that Hg(0) photooxidation is favoured in the presence of chloride (22, 47). Since MDE have been reported to occur under

marine influence, it is critical to better assess the post-depositional dynamics of Hg in these higher salinity environments, and especially in coastal areas.

Only a few studies in Subarctic and Arctic environments have focused on the importance of Hg redox reactions during the snowmelt period (8, 26) or in lakes during summer time (2). No studies have taken place during the short summer in High Arctic areas in ponds and streams, a period during which biological production is high.

Despite the harsh conditions that prevail for most of the year in polar areas, microorganisms such as algae or bacteria can thrive during the very short Arctic summer. Whereas studies in temperate areas have highlighted the role of microorganisms in the Hg redox cycle (7, 24, 28, 39), no study to date has focused on their involvement in Hg cycling in polar areas.

Given the gaps in the current literature, the purpose of this research was (i) to assess the significance of photomediated redox processes in the Arctic Hg cycle in fresh and brackish ponds and streams as well as in saltwaters; (ii) to evaluate the environmental variables affecting this redox cycling (e.g. [Cl^-], particles, [Fe]), and (iii) to determine the importance of algal and microbial mats in this cycle.

5.3. Experimental

5.3.1. Sampling sites

Cornwallis Island provided the opportunity to assess the Hg redox cycle over a wide range of salinities (Figure 5.1). Water types chosen to carry out our incubation experiments were i) snowmelt water ($0.06<[Cl^-]<0.11$ mmol·L^{-1}); ii) freshwater from ponds and streams ($0.11<[Cl^-]<1.61$ mmol·L^{-1}); iii) brackish and salt ponds, usually located in coastal areas or directly on the sea-ice when connected to underlying water ($12<[Cl^-]<26$ mmol·L^{-1}) and finally iv) coastal sea water, with the highest salinity we encountered ($[Cl^-]=517$ mmol·L^{-1}) (Figure

5.1). Detailed water chemistry for the sampling sites is presented in Supplementary Table 1.

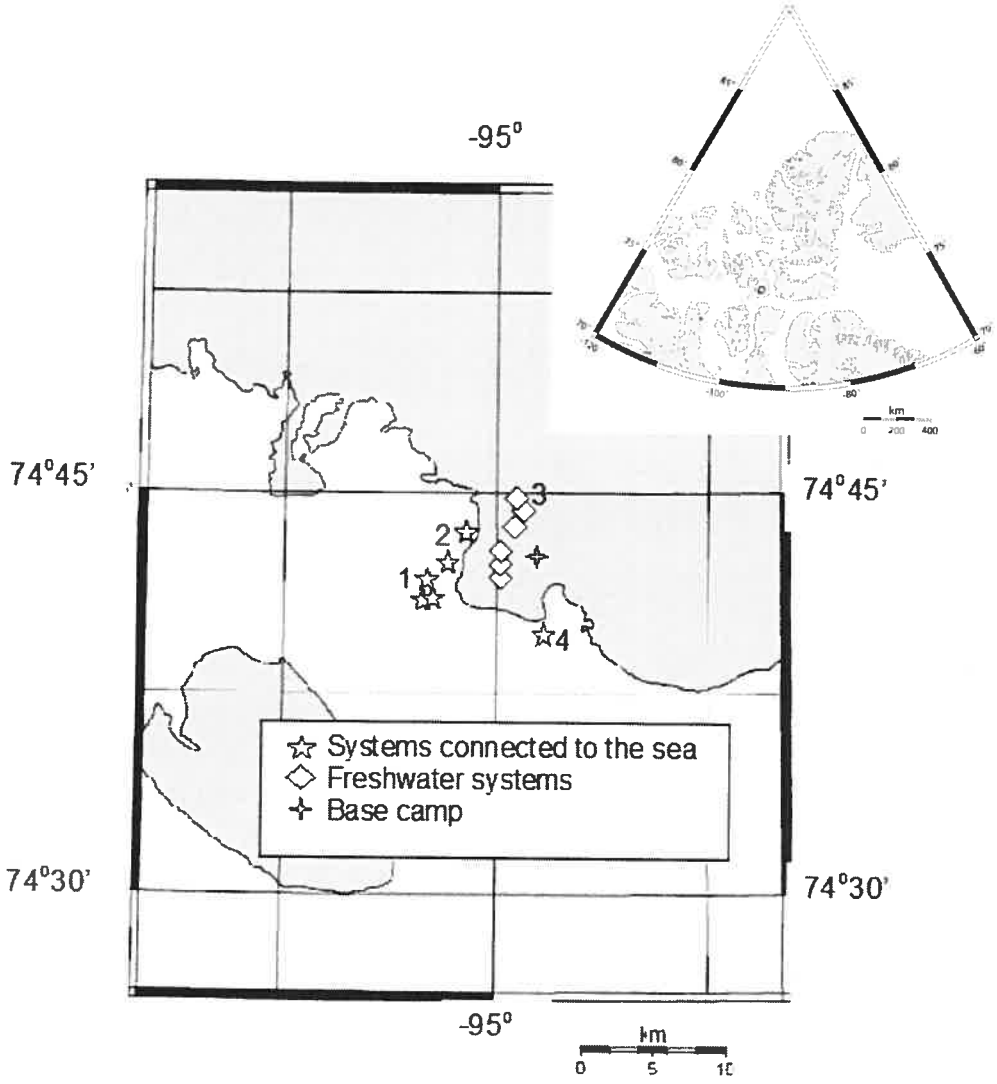

Figure 5.1. Map of the Southwestern shore of Cornwallis Island where we carried out the incubations. Inset is a map of the Canadian High Arctic. Maps were obtained from http://www.aquarius.geomar.de/make_map.html.

5.3.2. Sampling procedure

All containers used for Hg sampling and analysis were acid-washed and thoroughly rinsed with milliQ water (R > 18.2 MΩ·cm). Clean techniques were used and non-powdered gloves were worn at all times to avoid contamination. Surface water for total Hg analysis (THg) was sampled in triplicate using 250 mL Teflon FEP bottles, and rinsed three times with natural water prior to collection. All samples were kept in the dark and at 4°C±2°C until analysis. In order to carry out some incubation experiments, water was collected in the field in quartz bottles and additional water samples were collected using 20 L Teflon (PFA) sampling bags.

5.3.3. Incubations

Incubations were carried out between June 20th and July 25th 2004. During this period, after snowmelt began, air daily temperatures averaged ca. 2°C; the maximum and minimum air temperatures were 8.6°C and -2.2°C, respectively. Incubation experiments were carried out using 500 mL quartz bottles, filled directly in the field or from a Teflon bag shortly after collection. Incubation vessels were exposed outside to environmental conditions and were subjected to various treatments including filtration or the addition of a metabolic inhibitor. Alternative treatments involved either the addition of whole living microorganisms such as algae or microbial mats, or the addition of their exudates, i.e. dissolved biogenic compounds. During incubation, bottles were placed horizontally with their caps pointing north. Incubations lasted between 3 and 8 h and were initiated before noon. Two types of incubation were undertaken: i) time series experiments in which one sample for each treatment was collected and analysed immediately for dissolved gaseous mercury, typically after the first 30 min, and subsequently every hour until a plateau was

reached; and ii) incubation experiments where bottles were exposed for a predefined period of time and triplicate samples were analysed at the beginning and at the end of the incubation period. Note that contrary to other studies (32), we carried out batch incubation experiments. Dark controls were obtained by incubating reactions vessels in the field, either wrapped in aluminium foil or kept in opaque black bags. Filtration was performed by gently pumping out water from the sampling bag, using 0.45 µm in-line polyethersulfone filters (Whatman). Prior to use, filters were acid-washed (HNO_3; 10%), thoroughly rinsed with milliQ water, and then with sampling water.

Exudate additions

Prior to the incubation, water and ca. 300 g wet weight (w.w.) of a consortium of benthic algae and bacteria, from either saline or freshwater ponds, were collected and pre-incubated in a 1L Teflon bottle (final volume 500 mL) exposed outside to natural temperature and sunlight conditions with the cap loosely fastened in order to ensure gas exchange. The bottle was regularly and gently agitated to ensure good gas exchange and prevent the development of anoxic conditions. After a pre-incubation period of 36 hours, water from the bottle was withdrawn and filtered through 0.2 µm syringe glass fibres filters (Whatman) and 25 mL of the filtrate were added to the incubation bottles filled with freshly collected filtered (0.45 µm) water. Note that even if we took great care of gently filtrating the sample, some cells may have been damaged, releasing some of their intracellular content.

Whole benthic cells additions

Prior to the addition of the consortium of algae and bacteria samples into the incubation bottles, detrital material was removed from the biomass by gently washing the mats in pond water. Larger material was removed using Teflon

tweezers. The cleaned biomass was put in clean Petri dishes filled with natural pond water. Some treatments involved the addition of 3-(3',4'-dichlorphenyl)-1,1-dimethylurea (DCMU), an inhibitor of photosynthesis. DCMU solution was added to the Petri dishes prior to the pre-incubation period to a final concentration of 25 µmol L^{-1}. Both treated and untreated biomass was pre-incubated outside overnight. In the morning, biomass treated with DCMU and control biomass were added to the quartz bottles (ca. 25 g) filled with filtered water (0.45 µm) freshly collected from the pond or stream of interest.

Microbial mats were tested for their impact on dissolved gaseous mercury (DGM) production. In the morning, bacterial mats were collected from the bottom of a freshwater pond and 25 g (w.w.) were added to the incubation bottles filled with filtered water (0.45 µm; 500 mL) freshly collected, prior to the incubation.

5.3.4. Elemental composition of particles

In order to assess the elemental composition of the particles present in water, we used a scanning electron microscope (Hitachi S-3000N Variable Pressure) coupled to an X-ray diffraction probe. Stream and pond water was filtered through glass fibre filters of a nominal porosity of 0.7 µm. Each filter was freeze-dried, cut to a size of 1 cm^2, put on an aluminium sample-holder and coated with an Au-Pd amalgam. Ten to twenty random observations were performed per filter and particles targeted in the microscopic field were assessed. This technique allowed us to qualitatively determine the elemental inorganic composition; no quantitative analyses were performed.

5.3.5. Importance of reduction and oxidation reactions.

We used the variations in DGM concentrations between the beginning and end of incubation experiments ($\Delta_{[DGM]}$), normalised for the amount of light received when a plateau was reached and expressed in $fmol \cdot L^{-1} \cdot mol_{photon}^{-1} \cdot m^2$,

as a proxy for the amount of photoreducible Hg. This normalisation allowed a comparison between different days and different treatments.

To assess the dark oxidation of newly produced DGM, we assumed pseudo first-order kinetics, described by the equation:

$$\ln([Hg(0)]_t / [Hg(0)]_0) = -kt \quad (2)$$

where $[Hg(0)]_t$ and $[Hg(0)]_0$ represent DGM concentrations at time t and at the beginning of the incubations, respectively; k is the apparent rate of oxidation of Hg(0) and corresponds, in absolute value, to the slope of the regression of $\ln([Hg(0)]_t / [Hg(0)]_0)$ versus t. We assumed the concentration of oxidizing agent to be in excess and Hg(II) reduction to be insignificant in the dark.

5.3.6. Chemical Analysis.

To minimize losses of dissolved gaseous mercury during the analysis as well as Hg^0 carryover between samples, water was sparged directly in the quartz incubation bottle by tightly inserting a porous glass rod into the bottle. We used a zero-air generator (Tekran model 1100) to sparge the sample at a flow rate of 1.5 $L \cdot min^{-1}$ and at room temperature. The bottle was connected to an automated atmospheric mercury analyzer (Tekran™ Model 2537) to monitor the decrease of DGM over time (one reading every five minutes). The sparging step was stopped when Hg concentrations at decline to non detectable values. The working detection limit of this method is usually < 0.01 $pmol \cdot L^{-1}$ in the lab in Montreal, but in the high Arctic we calculated it as 0.03 $pmol \cdot L^{-1}$ or three times the standard deviation of ten system blanks run on water with low Hg levels (THg < 0.3 $pmol \cdot L^{-1}$; R > 18.2 $M\Omega \cdot cm$). Triplicates were regularly analysed and typically varied between 1 and 9%, although some turbid samples varied by up to 20% (median = 8.8%).

Total Hg concentrations in snow and water were quantified using the method described by Gill and Bruland (1990) (19), using a mercury fluorescence detector (Tekran™ Model 2500) and sodium borohydride as a strong reducing

agent. The working detection limit of this method was previously calculated as 0.45 pmol·L^{-1} or three times the standard deviation of ten procedural blanks. Triplicates were systematically analysed and typically varied between 0.5 to 10% and up to 20% for some very turbid samples (median = 8.4%).

Organic compounds in surface snow were analysed using two different methods fully described in Poulain et al. (2004b): (a) electron spray ionization mass spectrometry (ESI-MS); and (b) solid phase micro-extraction (SPME) followed by gas chromatography-mass spectrometry (GC-MS) analysis (See supplementary information for details).

Anions were analyzed by ion chromatography using a DIONEX ICS 2000. A sample (25 µL) of melted snow was introduced into the injection loop and separation occurred through an AS-17 column topped with a AG-17 pre-column. The elution step involved the passage of a KOH solution with a concentration gradient from 15 to 30 mmol·L^{-1}. Cations and metals (e.g. total Fe) were analysed with an inductively coupled plasma atomic emission spectrometer (ICP-AES Vista AX) using an internal standard of Yttrium (5 mg·L^{-1}).

5.3.7. Modeling dissolved inorganic Hg speciation.

To assess the inorganic speciation of Hg, we used a chemical equilibrium program (MINEQL+, version 4.5) (37). Stability constants used in the model are presented in Supplementary Table 2. These constants were corrected for the ionic strength of the sample, as calculated by the model. We do not present the complexation of Hg with dissolved organic matter (DOM) due to the current lack of consensus regarding binding constants for Hg-DOM complexation reactions. We report here inorganic Hg speciation since inorganic species are presumed by most authors to be more reactive and more easily reduced (36) than organically complexed species, and because inorganic neutrally charged species are likely more bioavailable than those species bound to organic matter.

It is important to note that the characterization of natural organic matter, especially with respect to the moieties with which Hg is most likely to bind (e.g. R-SH), is essential to adequately model Hg speciation. To the best of our knowledge, no true thermodynamic Hg-DOC binding constants have been reported for organic matter originating from polar environments and conditional constants obtained in other systems are not directly applicable, especially since they exhibit great variability (35). Note that the addition of small organic molecules known to be present in arctic snow (acetate and formate) did not change the inorganic speciation of Hg presented here.

5.4. Results and discussion

5.4.1. Influence of abiotic variables on DGM production

We assessed DGM production through incubation experiments at sites representing a salinity gradient on Cornwallis Island. Chloride concentrations at these sites covered four orders of magnitude from $5 \cdot 10^{-5}$ mol·L^{-1} for flowing meltwaters to 0.5 mol·L^{-1} for coastal seawater (see Supplementary Table 1). We observed a strong decline in DGM production corrected for incoming radiation (Δ_{DGM}) with increasing chloride levels (Figure 5.2). This decline was not correlated to changes in total Hg levels or DOC concentrations, but corresponded to an increase in the relative importance of chlorocomplexes and particulate Hg, concomitant with a decrease in the relative abundance of $Hg(OH)_2$ (Figure 5.3). DGM photoproduction and total iron concentration were not related in freshwater systems, but were positively and significantly related in systems connected to sea water ($r=0.96$, $p=0.0017$, $n=5$ inset in Figure 5.2).

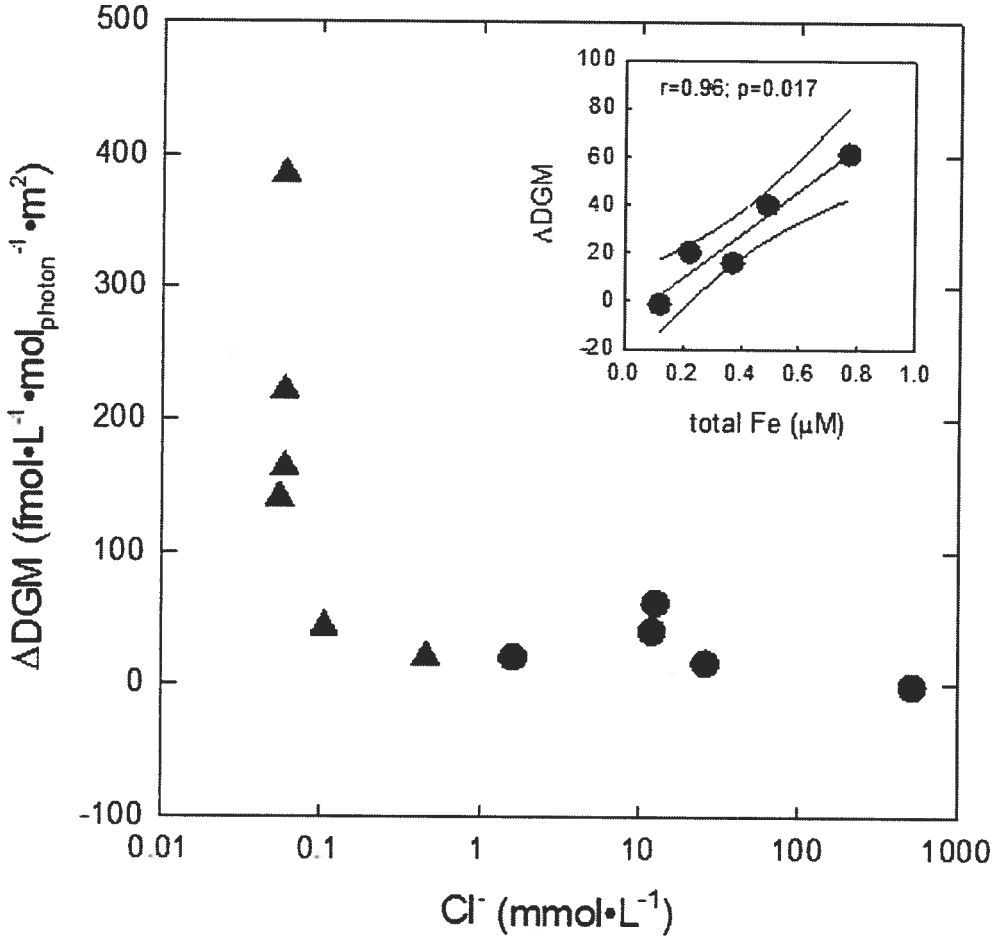

Figure 5.2. Distribution of in-situ DGM production as determined over a gradient of chloride concentrations, normalized for the amount of light received. Triangles represent freshwater sites; circles represent coastal sites connected to seawater. Inset show the relationship between total Fe and DGM production in sites connected to seawater (r=0.96, p=0.017 after 9999 permutations). Note that there is a significant relationship between DGM production and [Cl^-] $Log(\Delta_{DGM})=1.65-0.46\times log[Cl^-]$, n=11, p=0.0012, $r^2=0.70$.

DGM production observed in June, at $[Cl^-]<0.1$ mmol·L^{-1}, was higher (mean = 250 fmol·L^{-1}·mol_{photon}^{-1}·m^2) than any yet reported in unamended waters from temperate areas (3, 15, 31). The Arctic experiences massive depletion of atmospheric mercury during early springtime, increasing the pool of THg in surface snow (27) and possibly that of highly reactive species (26). Although earlier studies showed that massive photo-induced emissions of DGM were observed during the late spring period (8, 26), it is likely that some reactive species are trapped within the snowpack, protected from incoming radiation, and are released upon snowmelt, contributing to the high rates of reduction observed.

Earlier studies showed that Hg^0 oxidation was enhanced in the presence of chloride and organic matter (22, 23), or that chloride may participate in the formation of poorly reducible Hg complexes (18). Lalonde et al. also observed that pre-filtration decreased Hg^0 production in brackish systems (23). To further explore the mechanisms involved in DGM production we carried out a series of experiments in which particles were removed by filtration at both low and high chloride concentrations. Consistently, sites exhibiting the highest chloride concentrations experienced a decrease in DGM photoproduction upon filtration, ranging from 50% in a lagoon system (Figure 5.4 A) to ca. 100% in a salt pond over sea ice (Figure 5.4 B). Filtration caused a decrease for [THg] (from 8.4±0.7 to 5.0±0.1 pmol·L^{-1}) and [TFe] (from 0.11±0.02 to 0.02±0.01 µmol·L^{-1}) (Figure 5.4 C). No DGM production was observed in unfiltered or filtered samples kept in the dark (e.g. Figure 5.4 B). In freshwater systems, the photoproduction of DGM was similar whether or not particles smaller than 0.45 µm were removed (Fig. 4 D). No significant differences were observed between [THg] in unfiltered (4.1±0.9 pmol·L^{-1}) and filtered samples (3.5±0.3 pmol·L^{-1}). Inorganic Hg speciation was largely dominated by uncharged hydroxocomplexes (Figure 5.3).

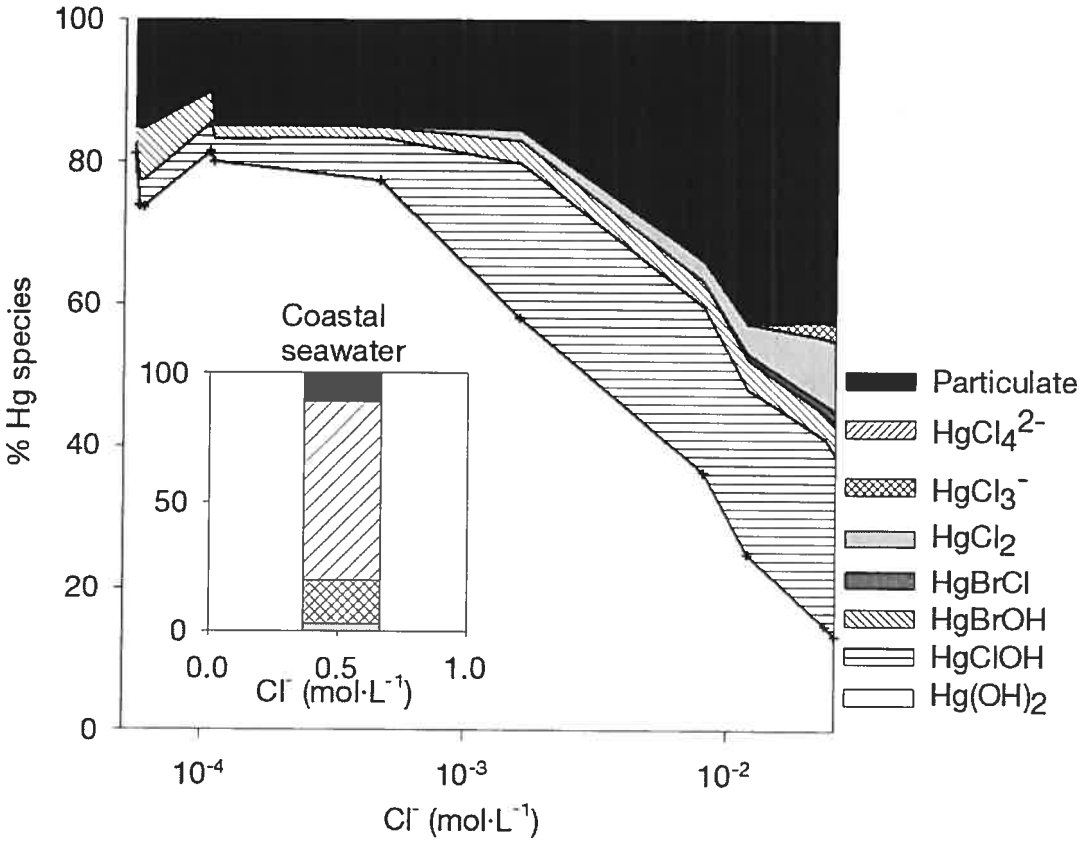

Figure 5.3. Modeling of inorganic Hg speciation over a chloride gradient. Inset represents the calculated speciation of inorganic Hg in coastal seawater. Each cross represents a sampling site (see supplementary Table 1 for detailed water chemistry).

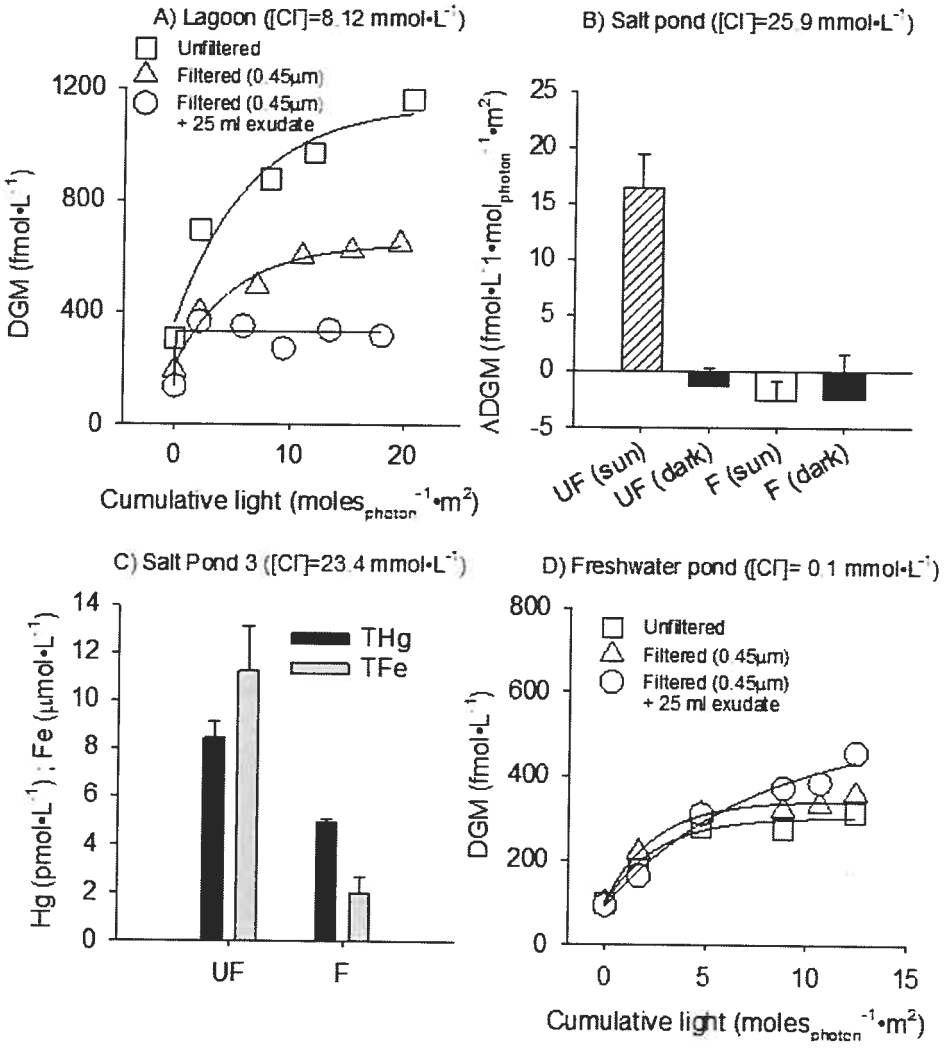

Figure 5.4. A) Times series incubation showing the evolution of [DGM] as a function of the cumulative amount of PAR received during the incubation period in water that was unfiltered, filtered, or filtered but amended with exudates from a microbial and algae consortium collected in the lagoon. B) DGM production in a pond over sea ice in unfiltered (UF) or filtered (F) samples, exposed under natural sunlight or kept in the dark. C) Total Hg and total iron concentrations in unfiltered or filtered saline water from a pond over sea ice. D) Times series incubation showing the evolution of [DGM] as a function of the cumulative amount of PAR received during the incubation period in water that was unfiltered, filtered, or filtered but amended with exudates from microbial and algae consortium collected in a freshwater inland pond.

The decrease of Δ_{DGM} in coastal areas upon filtration suggests that heterogeneous reactions may be involved. Indeed, filtration substantially decreased [THg] and [Fe], especially in brackish and saltwaters. Previous studies indicated that Hg photoreduction can result from heterogeneous processes (17, 23, 30), but the nature of the particles involved has not been described. Analysis of the particles present in both salt and freshwaters incubations revealed the presence of iron oxides amongst sand grains, aluminosilicates, clays and calcium carbonate deposits. It has already been proposed that the iron redox cycle is partly controlled by light (12) and that it is involved in the Hg redox cycle in freshwaters through the formation of highly reducing free radicals, the latter being potentially involved in Hg(0) formation (48). Other studies have shown that Hg photoreduction was enhanced in the presence of both synthetic iron oxides and ambient particles in atmospheric waters (25). In seawater, oxidized and reduced iron species coexist in dissolved and particulate form and the cycling between phases and redox states is affected by the light regime (43). Further experiments are needed to clarify the role of iron in Hg^0 reduction, i.e., to determine whether the pool of photoreducible Hg is partly formed of iron oxide-bound Hg, or if particulate iron species are indirectly involved in Hg reduction (e.g., through reactions associated with the photochemical reductive dissolution of solid Fe species).

Alternatively, the decrease of Δ_{DGM} in coastal areas upon filtration may indicate an implication of microorganisms. However, our dark controls systematically yielded no or low and insignificant DGM production over a 3-5 hour incubation period. Even though we cannot yet offer a definite answer as to the role of microbes in this case, the occurrence of microbial mediated reductive processes is supported by our recent findings that mercury resistance is genetically expressed in coastal Arctic systems (Poulain et al. unpublished). Further research is required to assess and fully understand their role in polar areas. Since our dark controls did not show DGM production over a 3-5 hour

incubation period, we investigated the possible involvement of photobiological processes.

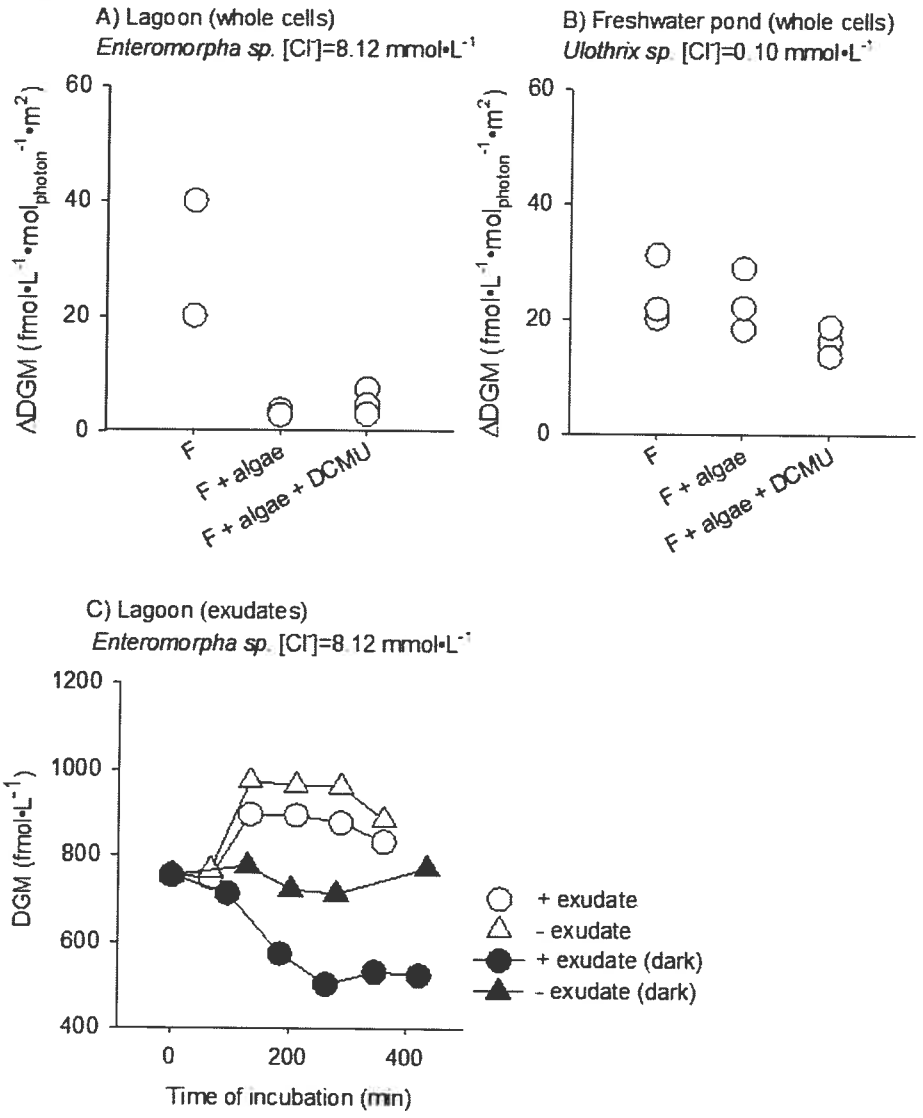

Figure 5.5. DGM production in filtered samples amended or not with whole algal cells. A) Salt water pond amended with microbial consortium comprised of *Enteromorpha sp.* and B) Freshwater pond amended with microbial consortium comprised of *Ulothrix sp.* DCMU refers to treatment were the microbial consortium was treated with an inhibitor of photosynthesis specific to photosystem II. C) Temporal evolution of newly produced DGM in lagoon samples exposed to natural sunlight (open symbols) and kept in the dark (closed symbols) with the addition of microbial and algae consortium exudates (circles) or without the addition of exudates (triangles). F represents filtered (0.45 µm) samples.

5.4.2. Role of photosynthetic organisms in DGM production.

Numerous photosynthetic microorganisms, i.e., algae and cyanobacteria, thrive on Cornwallis Island. To test for the influence of algae and photosynthetic microbial mats on Hg cycling in High Arctic waters, we carried out a series of *in situ* experiments. In order to simulate natural processes as closely as possible, we used species that were abundant at our sites, i.e. benthic organisms. Two filamentous chlorophyte species were chosen for incubations: *Enteromorpha* sp. was used for coastal seawaters and brackish ponds and *Ulothrix* sp. was used for freshwater incubations. It is likely that heterotrophic bacteria were also added along with the algae, representing a consortium of algae and bacteria rather than a mono-specific mat. Microbial mats, which formed a dense black layer on the bottom of ponds and streams, were also composed of both algae and cyanobacteria. The mats were overwhelmingly dominated by the latter, and these included *Nostoc* sp., *Rivularia* sp., *Scytonema* sp., and *Oscillatoria* sp. as identified by light and electron microscopy observations.

We carried out a series of incubations using either whole cells (*Enteromorpha* sp., *Ulothrix* sp., or mats of cyanobacteria) or their exudates, i.e., biogenic compounds (*Enteromorpha* sp. and *Ulothrix* sp.). When whole cells were added to filtered pond saltwater prior to the incubation, Δ_{DGM} decreased to near zero (Figure 5.5 A). We chose to present the replicates instead of an average or a median value since we lost a sample (filtered control in salt water pond) before completion of the analysis. Similarly, when exudates from *Enteromorpha* sp. were added to filtered lagoon water samples prior to incubation, a strong decrease in DGM concentrations was observed compared to the control filtered samples (Figure 5.4 A). DGM photoproduction decreased from 37.0 to 14.4 $fmol \cdot L^{-1} \cdot mol_{photon}^{-1} \cdot m^2$).

Upon the addition of whole cells of *Ulothrix* sp. to filtered fresh pond water (Figure 5.5 B), variations in [DGM] stayed positive and no statistically significant

difference was observed between the treatments. Similarly, no significant difference was noted in the production of DGM with or without the addition of either exudates (Figure 5.4 D) or cyanobacterial mats (data not shown).

Contrary to what was observed in previous studies (28, 34), inhibition of photosynthesis did not significantly affect Hg reduction in both fresh and salt waters (Figure 5.5 A & B).

To better understand why the addition of exudates of the algae and bacteria consortium to brackish water decreased Δ_{DGM}, an experiment was designed to test for the role of exudates in Hg oxidative processes (Figure 5.5 C). After an initial incubation for 3 h in sunlight (data not shown), [DGM] increased up to 757±14 fmol·L^{-1}. Further exposure of the samples to the sun yielded an increase in [DGM] in both samples with or without exudates. However, this increase in [DGM] was less important in the presence of exudates than in the control (Figure 5.5 C). When samples spiked with exudates were kept in the dark, [DGM] decreased by 40% (corresponding to a decrease of -72 fmol·L^{-1}·h^{-1}) and reached a plateau after 3.5 h (Figure 5.5 C), underscoring the occurrence of dark oxidative processes. When no exudates were added, [DGM] stayed stable. The rate of oxidation, calculated from the decrease over time of [DGM] in the dark, was 0.1 h^{-1}, within the range of previously reported values for salt waters, and ca. 5 to 10 times higher than the rates that have previously been encountered in fresh waters (1, 16, 22). Smith et al. (1998) (40) and Siciliano et al. (2002) (39) suggested that Hg(0) oxidation may be carried out by bacteria using an intracellular catalase and are likely coupled to H_2O_2 transformations. This process seems unlikely in our case, since exudates were very gently filtered through 0.2 µm filters and thus most bacteria were removed; note that some cell breakage may have occurred. We identified several organic molecules in exudates collected from incubation of *Enteromorpha* sp. and *Ulothrix* sp. using different mass spectrometry techniques to detect molecules with molecular weight equal to or less than 500 Da (1 Da = 1 g·mol^{-1}). Most of

the identified organic molecules contained aromatic rings rather than aliphatic chains (see supplementary Table 3A and B). There were some similarities in identified molecules in both saline and fresh water samples, but some alcohols and aldehydes were only observed in saline water samples. These differences in composition were systematic for several samples. The formation of alcohols and aldehydes often results from oxidative processes and although they do not constitute a definite proof, these differences in composition suggested a higher oxidative potential for saline water. Note that the SPME technique as it was used in this study does not allow for detection of organic acids, which are expected to be present under a highly oxidized environment.

We could not attribute Hg(0) oxidation observed in salt waters to a single type of biogenic organic material. Rather, the oxidation observed in saline waters was likely the result of either photoinduced processes involving chloride and organic compounds as previously proposed (22) or directly due to the excretion of oxidants. Indeed, it has recently been documented that microorganisms are able to excrete small molecules capable of undergoing multiple redox cycles affecting metal speciation (electron shuttles) (21) and therefore potentially affect the oxidation state of Hg(0).

Our data suggest that biogenic compounds were directly involved in oxidation reactions but that direct incident light was not required. Based on the chemical structure of the organic compounds, the production of a variety of organic intermediates, including radicals, could be expected in the presence of large pools of oxidant precursors (e.g. halides NO_2^- and NO_3^-); these precursors can produce radicals upon photolysis. Clearly, a set of reactions can supply oxidants to transform Hg(0) to Hg(II), the first phase occurring under sunlit conditions, whereas the reactions involving organic compounds can further continue in the dark leading eventually to Hg(0) oxidation. Alternatively, further assessment of the role of electron shuttles in Hg redox reactions should

bring further enlightenment on its overall cycle both in temperate and polar regions.

The results reported here suggest that coastal areas may be more vulnerable to Hg contamination compared to freshwater systems, due to increased Hg residence time because of enhanced oxidative processes. Hg(0) oxidation is promoted both by increased salinity, and the production of oxidative biogenic exudates. This alteration of Hg cycle at higher salinity is however partly counterbalanced with increasing iron concentrations and the presence of particles.

5.5. Acknowledgements

We thank B.E. Keatley for comments on the manuscript as well as those of three anonymous reviewers. We thank the Polar Continental Shelf Project for their outstanding logistic support and the Nunavut Research Institute. We express our gratitude to Dr. H. Vali for access to the electron microscopy facility at McGill University. We thank Paddy Aqiatusuk as well as Debbie Iqaluk for their outstanding help and support in the field. A. Cattaneo, S. Hamelin and L. Pelletier are acknowledged for their help with algae identification and microscope work and D. Bélanger for his help in the lab. This project was funded by the Science Horizon Program of Environment Canada; a CFCAS grant to PAA and MA; a NSERC COMERN and Discovery grant to PAA and MA as well as a FQRNT-Équipe grant to MA and PGCC.

5.6. Supplementary information.

Supplementary table 5.1. Water chemistry of the sampling sites. Data are expressed in $\mu mol \cdot L^{-1}$ but for THg expressed in $pmol \cdot L^{-1}$.

Site	Lat.	Long.	Date	pH	THg	Cl^-	SO_4^{2-}	Br^-	Fe	Ca^{2+}	Mg^{2+}	Na^+	K^+
FMW1	74°43'06	95°01'00	22-Jun	8	6.65 ±0.23	54.9	4.36	< d.l.	0.20	318	120	38.5	3.61
FMW2	74°43'06	95°01'00	22-Jun	7.5	6.69 ±1.5	56.9	6.53	< d.l.	0.24	519	221	43.0	4.78
FMW3	74°43'06	95°01'00	20-Jun	7.5	6.69 ±1.5	59.1	6.99	< d.l.	0.31	322	149	41.0	3.93
Stream	74°43'44	95°01'21	5-Jul	7.76	3.53 ±0.46	106	20.1	< d.l.	0.15	542	163	116	14.7
FWP1	74°43'03	95°01'14	14-Jul	7.87	3.51 ±0.89	110	15.6	< d.l.	0.02	530	252	102	7.53
FWP2	74°42'50	95°01'42	12-Jul	8.2	4.11 ±0.87	471.2	115	< d.l.	0.67	$1.08 \cdot 10^3$	287	566	19.1
Crack	74°44'36	95°03'20	16-Jul	8.05	5.15 ±0.09	$1.61 \cdot 10^3$	89.3	2.41	0.22	506	232	$1.42 \cdot 10^3$	42.2
Lagoon	74°45'00	95°03'13	10-Jul	8.5	6.4 ±0.8	$8.12 \cdot 10^3$	418.	12.5	0.76	442	843	$7.19 \cdot 10^3$	214
SP1	74°43'03	95°05'12	22-Jun	8.5	5.58 ±0.56	$1.20 \cdot 10^4$	641	22.1	0.48	572	$1.14 \cdot 10^3$	$9.61 \cdot 10^3$	210
SP2	74°43'00	95°04'26	27-Jun	8.5	9.39 ±0.26	$2.38 \cdot 10^4$	$1.79 \cdot 10^3$	31.6	0.15	535	$2.21 \cdot 10^3$	$2.09 \cdot 10^4$	433
SP3	74°42'41	95°05'02	24-Jun	8.5	8.43 ±0.71	$2.59 \cdot 10^4$	$2.04 \cdot 10^3$	45.4	0.36	570	$2.53 \cdot 10^3$	$2.45 \cdot 10^4$	502
SW	74°40'30	95°01'21	18-Jul	7.96	1.6 ±0.05	$5.17 \cdot 10^5$	$2.67 \cdot 10^4$	$1.06 \cdot 10^3$	0.12	$9.76 \cdot 10^3$	$4.84 \cdot 10^4$	$4.38 \cdot 10^5$	$8.79 \cdot 10^3$

FMW: Flowing meltwaters; FWP: Freshwater pond; SP: Salt pond; SW: Sea water.

Supplementary table 5.2. Reactions and stability constants used in the model Mineql+ ver. 4.5

Reactions	LogK
$Hg^2 + 2H_2O \leftrightarrow Hg(OH)_2 + 2H^+$	6.194
$2H^+ + 2Br^- + Hg(OH)_2 \leftrightarrow 2H_2O + HgBr_2$	24.27
$H^+ + Br^- + Hg(OH)_2 \leftrightarrow H_2O + HgBrOH$	12.433
$2H^+ + Br^- + Cl^- + Hg(OH)_2 \leftrightarrow 2H_2O +$ HgBrCl	22.181
$H^+ + Cl^- + Hg(OH)_2 \leftrightarrow H_2O + HgClOH$	10.44
$2H^+ + 2Cl^- + Hg(OH)_2 \leftrightarrow 2H_2O + HgCl_2$	20.194
$2H^+ + 3Cl^- + Hg(OH)_2 \leftrightarrow 2H_2O + HgCl_3^-$	21.194
$2H^+ + 4Cl^- + Hg(OH)_2 \leftrightarrow 2H_2O + HgCl_4^{2-}$	21.794

The default log K values in MINEQL+ are taken from "Critical Selected Stability Constants of Metal Complexes", National Institute of Standards and Technology (NIST) Standard Reference Database.

Analyses of organic compounds.

Organic compounds in surface snow were analysed using two different methods: (a) electron spray ionization mass spectrometry (ESI-MS); (b) solid phase micro extraction (SPME). For the ESI-MS method, 5 µl of melted snow was injected into the electron spray of mass spectrometer (Thermoquest Finigan LC QDUO). For the SPME method, manual extraction was performed with several replacement fibre assemblies (Supelco). Four different types of fibers were compared: polyacrylate (85 µm), polydimethyl siloxane (100 µm), polydimethyl siloxane / divinyl benzene (65 µm) carbowax / divinyl benzene (65 µm). The fibers were conditioned prior to use as recommended by the manufacturer by heating them at different temperatures (250 – 300 °C) for

periods between 30 min and 2 h in gas chromatograph injection port. After conditioning the fibers, they were inserted into the solution under magnetic stirring using a Teflon bar and magnetic stirrer. After 5 h adsorption, the fibers were injected directly into the injection port of the gas chromatograph-mass spectrometer (GC-MS) in the splitless mode and held isothermally at 250 °C. Desorption time was 5 min. Chromatographic analyses were performed using Hewlett Packard GC (HP 6890) equipped with a splitless injector and mass spectrometric detection (HP 5973 MSD). The GC was fitted with a 30 × 0.25 mm i.d. column coated with 5 % phenyl methyl siloxane (HP – 5 MS). The column was operated at a constant flow (1.5 mL min^{-1}) of ultra high purity helium. The oven temperature was increased by 5 °C min^{-1} up to 200 °C. Conditions for the mass selective detector were as follows: transfer line temperature 280 °C, 70 eV electron impact, electron multiplayer voltage 2180 V, mass range for full scan 10 to 550 a.m.u.

Supplementary table 5.3. Organic compounds extracted from algae exudates collected in a saltwater pond

Organic Compound	Empirical Formula	Molecular Mass	Molecular Structure
1,2-Benzisothiazole	C_7H_5NS	135	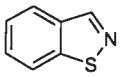
3,5-Dimethyl,3-hexanol	$C_8H_{18}O$	130	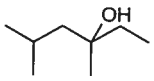
2-Ethyl-hexanal	$C_8H_{16}O$	128	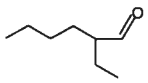
2-Methyl-naphthalene	$C_{11}H_{10}$	142	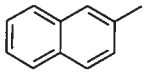
1,2-Dimethyl-benzene	C_8H_{10}	106	
1,2,4-Trimethyl-benzene	C_9H_{12}	120	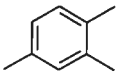
Acetophenone	C_8H_8O	120	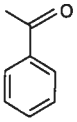
2-Methyl-3-hydroxy-2,4,4-trimethyl- pentyl-propionate	$C_{12}H_{24}O_3$	216	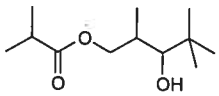

Supplementary table 5.4. Organic compounds extracted from algae exudates collected in a freshwater pond.

Organic Compound	Empirical Formula	Molecular Mass	Molecular Structure
1,2-Benzisothiazole	C_7H_5NS	135	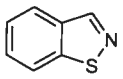
Naphthalene	$C_{10}H_8$	128	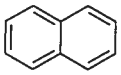
Methyl-benzoate	$C_8H_8O_2$	136	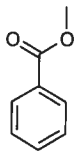
1,2-Dimethyl-benzene	C_8H_{10}	106	
Toluene	C_7H_8	92	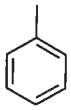
Methoxy-phenyl-oxime	$C_8H_9NO_2$	151	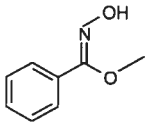
Acetophenone	C_8H_8O	120	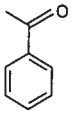
Propanoic acid, 2-methyl-,methyl ester	$C_5H_{10}O_2$	100	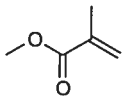

5.7. References.

1. **Amyot, M., G. A. Gill, and F. M. M. Morel.** 1997. Production and loss of dissolved gaseous mercury in coastal seawater. Environmental Science & Technology **31:**3606-3611.
2. **Amyot, M., D. Lean, and G. Mierle.** 1997. Photochemical formation of volatile mercury in high Arctic lakes. Environmental Toxicology and Chemistry **16:**2054-2063.
3. **Amyot, M., G. Mierle, D. R. S. Lean, and D. J. McQueen.** 1994. Sunlight-Induced Formation of Dissolved Gaseous Mercury in Lake Waters. Environmental Science & Technology **28:**2366-2371.
4. Ariya, P. A., A. P. Dastoor, M. Amyot, W. H. Schroeder, L. Barrie, K. Anlauf, F. Raofie, A. Ryzhkov, D. Davignon, J. Lalonde, and A. Steffen. 2004. The Arctic: a sink for mercury. Tellus Series B-Chemical and Physical Meteorology 56:397-403.
5. **Ariya, P. A., A. Khalizov, and A. Gidas.** 2002. Reactions of gaseous mercury with atomic and molecular halogens: Kinetics, product studies, and atmospheric implications. Journal of Physical Chemistry A **106:**7310-7320.
6. **Aspmo, K., C. Temme, T. Berg, C. P. Ferrari, P. A. Gauchard, X. Fain, and G. Wibetoe** 2006, posting date. Mercury in the atmosphere, snow and melt water ponds in the north atlantic ocean during arctic summer. [Online.]
7. **Barkay, T., C. Liebert, and M. Gillman.** 1989. Environmental Significance of the Potential for Mer(Tn21)-Mediated Reduction of Hg-2+ to Hg-0 in Natural-Waters. Applied and Environmental Microbiology **55:**1196-1202.
8. Dommergue, A., C. P. Ferrari, P. A. Gauchard, C. F. Boutron, L. Poissant, M. Pilote, P. Jitaru, and F. C. Adams. 2003. The fate of mercury species in a sub-arctic snowpack during snowmelt. Geophysical Research Letters 30.
9. **Dommergue, A., C. P. Ferrari, L. Poissant, P. A. Gauchard, and C. F. Boutron.** 2003. Diurnal cycles of gaseous mercury within the snowpack at Kuujjuarapik/Whapmagoostui, Quebec, Canada. Environmental Science & Technology **37:**3289-3297.
10. **Douglas, T. A., M. Sturm, W. R. Simpson, S. Brooks, S. E. Lindberg, and D. K. Perovich.** 2005. Elevated mercury measured in snow and frost flowers near Arctic sea ice leads. Geophysical Research Letters **32**.
11. Ebinghaus, R., H. H. Kock, C. Temme, J. W. Einax, A. G. Lowe, A. Richter, J. P. Burrows, and W. H. Schroeder. 2002. Antarctic springtime

depletion of atmospheric mercury. Environmental Science & Technology 36:1238-1244.

12. **Emmenegger, L., R. R. Schonenberger, L. Sigg, and B. Sulzberger.** 2001. Light-induced redox cycling of iron in circumneutral lakes. Limnology and Oceanography **46:**49-61.
13. **Fain, X., C. P. Ferrari, P. A. Gauchard, O. Magand, and C. Boutron.** 2006. Fast depletion of gaseous elemental mercury in the Kongsvegen Glacier snowpack in Svalbard. Geophysical Research Letters **33**.
14. Ferrari, C. P., P. A. Gauchard, K. Aspmo, A. Dommergue, O. Magand, E. Bahlmann, S. Nagorski, C. Temme, R. Ebinghaus, A. Steffen, C. Banic, T. Berg, F. Planchon, C. Barbante, P. Cescon, and C. F. Boutron. 2005. Snow-to-air exchanges of mercury in an Arctic seasonal snow pack in Ny-Alesund, Svalbard. Atmospheric Environment 39:7633-7645.
15. **Garcia, E., M. Amyot, and P. A. Ariya.** 2005. Relationship between DOC photochemistry and mercury redox transformations in temperate lakes and wetlands. Geochimica et Cosmochimica Acta **69:**1917-1924.
16. **Garcia, E., A. J. Poulain, M. Amyot, and P. A. Ariya.** 2005. Diel variations in photoinduced oxidation of Hg-0 in freshwater. Chemosphere **59:**977-981.
17. **Gardfeldt, K., X. B. Feng, J. Sommar, and O. Lindqvist.** 2001. Total gaseous mercury exchange between air and water at river and sea surfaces in Swedish coastal regions. Atmospheric Environment **35:**3027-3038.
18. **Gardfeldt, K., and M. Jonsson.** 2003. Is bimolecular reduction of Hg(II) complexes possible in aqueous systems of environmental importance. Journal of Physical Chemistry A **107:**4478-4482.
19. **Gill, G. A., and K. W. Bruland.** 1990. Mercury Speciation in Surface Fresh-Water Systems in California and Other Areas. Environmental Science & Technology **24:**1392-1400.
20. **Hammerschmidt, C. R., and W. F. Fitzgerald.** 2006. Methylmercury in freshwater fish linked to atmospheric mercury deposition. Environmental Science & Technology **DOI 10.1021/es061480i.**
21. **Hernandez, M. E., and D. K. Newman.** 2001. Extracellular electron transfer. Cellular and Molecular Life Sciences **58:**1562-1571.
22. **Lalonde, J. D., M. Amyot, A. M. L. Kraepiel, and F. M. M. Morel.** 2001. Photooxidation of Hg(0) in artificial and natural waters. Environmental Science & Technology **35:**1367-1372.
23. **Lalonde, J. D., M. Amyot, J. Orvoine, F. M. M. Morel, J. C. Auclair, and P. A. Ariya.** 2004. Photoinduced oxidation of Hg-0 (aq) in the waters from the St. Lawrence estuary. Environmental Science & Technology **38:**508-514.
24. **Lanzillotta, E., C. Ceccarini, R. Ferrara, E. Dini, E. Frontini, and R. Banchetti.** 2004. Importance of the biogenic organic matter in photo-

formation of dissolved gaseous mercury in a culture of the marine diatom Chaetoceros sp. Science of the Total Environment **318:**211-221.

25. **Lin, C. J., and S. O. Pehkonen.** 1997. Aqueous free radical chemistry of mercury in the presence of iron oxides and ambient aerosol. Atmospheric Environment **31:**4125-4137.
26. **Lindberg, S. E., S. Brooks, C. J. Lin, K. J. Scott, M. S. Landis, R. K. Stevens, M. Goodsite, and A. Richter.** 2002. Dynamic oxidation of gaseous mercury in the Arctic troposphere at polar sunrise. Environmental Science & Technology **36:**1245-1256.
27. Lu, J. Y., W. H. Schroeder, L. A. Barrie, A. Steffen, H. E. Welch, K. Martin, L. Lockhart, R. V. Hunt, G. Boila, and A. Richter. 2001. Magnification of atmospheric mercury deposition to polar regions in springtime: the link to tropospheric ozone depletion chemistry. Geophysical Research Letters 28:3219-3222.
28. **Mason, R. P., F. M. M. Morel, and H. F. Hemond.** 1995. The Role of Microorganisms in Elemental Mercury Formation in Natural-Waters. Water Air and Soil Pollution **80:**775-787.
29. Muir, D., B. Braune, B. DeMarch, R. Norstrom, R. Wagemann, L. Lockhart, B. Hargrave, D. Bright, R. Addison, J. Payne, and K. Reimer. 1999. Spatial and temporal trends and effects of contaminants in the Canadian Arctic marine ecosystem: a review. Science of the Total Environment 230:83-144.
30. **Nriagu, J. O.** 1994. Mechanistic Steps in the Photoreduction of Mercury in Natural-Waters. Science of the Total Environment **154:**1-8.
31. **O'Driscoll, N. J., D. R. S. Lean, L. L. Loseto, R. Carignan, and S. D. Siciliano.** 2004. Effect of dissolved organic carbon on the photoproduction of dissolved gaseous mercury in lakes: Potential impacts of forestry. Environmental Science & Technology **38:**2664-2672.
32. **O'Driscoll, N. J., S. D. Siciliano, D. R. S. Lean, and M. Amyot.** 2006. Gross photoreduction kinetics of mercury in temperate freshwater lakes and rivers: Application to a general model of DGM dynamics. Environmental Science & Technology **40:**837-843.
33. Orihel, D. M., M. J. Paterson, C. C. Gilmour, R. A. Bodaly, P. J. Blanchfield, H. Hintelmann, R. C. Harris, and J. W. M. Rudd. 2006. Effect of loading rate on the fate of mercury in littoral mesocosms. Environmental Science & Technology 40:5992-6000.
34. **Poulain, A. J., M. Amyot, D. Findlay, S. Telor, T. Barkay, and H. Hintelmann.** 2004. Biological and photochemical production of dissolved gaseous mercury in a boreal lake. Limnology and Oceanography **49:**2265-2275.
35. **Ravichandran, M.** 2004. Interactions between mercury and dissolved organic matter - a review. Chemosphere **55:**319-331.

36. **Rolfhus, K. R., and W. F. Fitzgerald.** 2001. The evasion and spatial/temporal distribution of mercury species in Long Island Sound, CT-NY. Geochimica et Cosmochimica Acta **65:**407-418.

37. **Schecher, W. D., and D. C. McAvoy.** 1992. Mineql+ - a Software Environment for Chemical-Equilibrium Modeling. Computers Environment and Urban Systems **16:**65-76.

38. Schroeder, W. H., K. G. Anlauf, L. A. Barrie, J. Y. Lu, A. Steffen, D. R. Schneeberger, and T. Berg. 1998. Arctic springtime depletion of mercury. Nature 394:331-332.

39. **Siciliano, S. D., N. J. O'Driscoll, and D. R. Lean.** 2002. Microbial reduction and oxidation of mercury in freshwater lakes. Environmental Science and Technology **36:**3064-3068.

40. **Smith, T., K. Pitts, J. A. McGarvey, and A. O. Summers.** 1998. Bacterial oxidation of mercury metal vapor, Hg(0). Applied and Environmental Microbiology **64:**1328-1332.

41. **Sprovieri, F., N. Pirrone, M. S. Landis, and R. K. Stevens.** 2005. Oxidation of gaseous elemental mercury to gaseous divalent mercury during 2003 polar sunrise at Ny-Alesund. Environmental Science & Technology **39:**9156-9165.

42. **Steffen, A., W. Schroeder, J. Bottenheim, J. Narayan, and J. D. Fuentes.** 2002. Atmospheric mercury concentrations: measurements and profiles near snow and ice surfaces in the Canadian Arctic during Alert 2000. Atmospheric Environment **36:**2653-2661.

43. **Stumm, W., and J. J. Morgan.** 1996. Aquatic Chemistry; Chemical Equilibria and Rates in Natural Waters, Wiley interscience ed. John Wiley & Sons Inc., New-York.

44. **Swain, E. B., D. R. Engstrom, M. E. Brigham, T. A. Henning, and P. L. Brezonik.** 1992. Increasing Rates of Atmospheric Mercury Deposition in Midcontinental North-America. Science:784-787.

45. **Tseng, C. M., C. Lamborg, W. F. Fitzgerald, and D. R. Engstrom.** 2004. Cycling of dissolved elemental mercury in Arctic Alaskan lakes. Geochimica et Cosmochimica Acta **68:**1173-1184.

46. Van Oostdam, J., S. G. Donaldson, M. Feeley, D. Arnold, P. Ayotte, G. Bondy, L. Chan, E. Dewaily, C. M. Furgal, H. Kuhnlein, E. Loring, G. Muckle, E. Myles, O. Receveur, B. Tracy, U. Gill, and S. Kalhok. 2005. Human health implications of environmental contaminants in Arctic Canada: A review. Science of the Total Environment:165-246.

47. **Whalin, L. M., and R. P. Mason.** 2006. A new method for the investigation of mercury redox chemistry in natural waters utilizing deflatable Teflon (R) bags and additions of isotopically labeled mercury. Analytica Chimica Acta **558:**211-221.

48. **Zhang, H., and S. E. Lindberg.** 2001. Sunlight and iron(III)-induced photochemical production of dissolved gaseous mercury in freshwater. Environmental Science & Technology **35**:928-935.

6. A potential for mercury redox transformations by microbes in the high Arctic.

Alexandre J. Poulain, Sinéad M. Ní Chadhain, Parisa A. Ariya, Marc Amyot, Edenise Garcia, Peter G.C. Campbell, Gerben J. Zylstra and Tamar Barkay.

Reprinted from Applied and Environmental Microbiology, vol. 73 (7): 2230-2238

6.1. Abstract

The contamination of polar regions due to the global distribution of anthropogenic pollutants is of great concern because it leads to the bioaccumulation of toxic substances, among them methylmercury, in Arctic food chains. Here we present the first evidence that microbes in the High Arctic possess and express diverse *merA* genes, which specify reduction of ionic mercury (Hg[II]) to the volatile elemental form (Hg[0]). The sampled microbial biomass, collected from microbial mats in a coastal lagoon and from the surface of marine macro-algae, was comprised of bacteria that were most closely related to psychrophiles that had been previously described in polar environments. We used a kinetic redox model, taking into consideration photoredox reactions as well as *mer* mediated reduction, to assess if the potential for Hg(II) reduction by Arctic microbes can affect the toxicity and environmental mobility of mercury in the High Arctic. Results suggested that *mer* mediated Hg(II) reduction could account for most of the Hg(0) that is produced in high Arctic waters. At the surface, with only 5% of metabolically active cells, up to 68% of the mercury pool was resolved by the model as biogenic Hg(0). At depth, because of incident light attenuation, the significance of photoredox transformations declined and *merA* mediated activity could account for up to 90% of Hg(0) production. These findings highlight the importance of microbial redox transformations in the biogeochemical cycling and thus toxicity and mobility of mercury in polar regions.

6.2. Introduction

The contamination of polar regions by pollutants that are formed in lower latitudes and that are subject to global transport is an important issue. In temperate zones, microbial activities impact the toxicity and mobility of these environmental contaminants (8, 37) but their role in the transformations of pollutants at high latitudes remains largely unexplored. Research to date has focused on biodegradation of petroleum products (20, 45), with little attention to the importance of polar microbes in the degradation of other types of organic contaminants (39, 62) or the transformations of metals. This lack of information may become critical since high-latitude ecosystems are currently undergoing major alteration due to environmental changes, which in turn may greatly affect the cycling of contaminants (38).

A growing body of literature documents increases in mercury contamination of the Arctic food chain (42) and increased levels of mercury exposure in indigenous populations (59). The accumulation of mercury in Arctic biota, as in temperate zones, is mostly in the form of the potent neurotoxic substance, methylmercury (16). Because mercury enters the Arctic biosphere in its inorganic form, bioaccumulation depends on *in-situ* synthesis of methylmercury and its subsequent uptake by the microbes and phytoplankton that occupy the base of the Arctic food web. Hence, processes that either directly or indirectly affect methylmercury production modulate the impact of mercury contamination in the Arctic. The source of this mercury is atmospheric deposition. Modeling studies have estimated that 325 tons of mercury are deposited throughout the Arctic over a 1-year cycle (3) with much of it occurring during polar sunrise (24, 36, 55), leading, in some cases, to 1000 fold increases in mercury levels relative to background concentration (23). Mercury deposition is thought to be due to the oxidation of atmospheric elemental mercury, Hg(0), the form in which mercury is globally distributed, by reactive halogen radicals

from sea-salt aerosols (4, 36). Thus, marine and coastal environments in polar regions are more susceptible to mercury deposition than inland areas and there is a need to better understand the post-depositional fate of mercury in these environments.

Along with photochemical processes (2, 56), the bacterial mercuric reductase enzyme (MerA) affects mercury mobility and bioavailability by converting water-soluble inorganic mercury and methylmercury to the volatile elemental form. This is a detoxification process as evidenced by the resumption of microbial growth after the removal of the gaseous Hg(0) (8). Mercury resistance is widespread amongst microorganisms (44) from diverse environments including extreme ones such as hydrothermal vents (60) and permafrost (41). In temperate regions, microbial reduction of mercury affects the production of dissolved gaseous mercury (DGM) in pristine and contaminated aquatic systems (6, 7, 9, 57) as well as the degradation of methylmercury in contaminated aquatic systems (52). To date the role of mercury resistant microbes in redox cycling of mercury in polar regions has not been examined. Here we report that *merA* genes were present and expressed by microbes from remote polar areas. Furthermore, we used a kinetic redox model, to assess the importance of microbial mercury reduction in the production of DGM, and thus its role in mercury biogeochemistry, in Arctic coastal waters.

6.3. Materials and methods

6.3.1. Sampling sites and sample collection.

Samples were taken on the western shoreline of Cornwallis Island, NU, Canada (75°N, 95°W) during the summer 2005. Two different types of samples were collected: i) water and macro-algae, identified as *Fucus* sp. and *Desmarestia* sp., present in seawater in gaps between melting sea-ice, and ii)

thick photosynthetic microbial mats from coastal lagoons on the sea-shore, which are fed daily by tides. In both cases, solid (biomass) and liquid (water) samples were collected and immediately frozen until further processing of the biomass. All containers used for sampling were cleaned and rinsed following trace metal protocols and were sterile. Non powdered gloves were worn at all times during sampling and further handling of the samples.

6.3.2. Mercury analysis.

Total mercury (THg) concentrations in water were quantified using USEPA method 1631 and an automated mercury fluorescence detector (Tekran™ Model 2600). DGM in water was measured following the protocol described in (48). THg in the sampled biomass was measured by thermal decomposition at 750°C using a direct mercury analyzer (DMA 80, Milestone, MLS). Briefly, prior to analyses, samples were freeze-dried. Prior to combustion, 0.05 g samples were further dried in an oxygen stream passing through a quartz tube located inside a controlled heating coil. The combustion gases were further decomposed on a catalytic column at 750 °C. Mercury vapor was collected on a gold amalgamation trap and subsequently desorbed for quantification by atomic absorption spectrometry at 254 nm. The working detection limit of this method was previously calculated as 0.01 ng of mercury or three times the standard deviation of ten procedural blanks.

6.3.3. Modeling of mercury redox transformations in coastal Arctic waters.

The relative importance of Hg(0) production by photochemical or biological reactions as well as its destruction by photochemical reactions were modelled using ACUCHEM modelling software (12) and a custom-designed kinetic code. Model parameters are presented in Table 1. We performed sensitivity studies at initial concentration ranges of THg and DGM as measured

in the field in the Cornwallis Island area. We also performed sensitivity studies on the number of metabolically active bacteria capable of mercury reduction. The model runs were performed over a period of 10 days to ensure that the concentrations of mercury species, i.e., Hg(II), Hg(0) from photoreduction of Hg(II), and Hg(0) from bio-reduction of Hg(II), became independent of initial concentrations used. Additional shorter run models were performed and they did not alter the general conclusions.

Table 6.I. Parameters used in the model simulating mercury redox state in High Arctic sea water.

Model parameters	Values	Reference
Bacterial cells counts (cells ml^{-1}) at depth of:		
surface	$9.49\ 10^5 \pm 1.75\ 10^5$ *	this study
5 m	$5.53\ 10^5 \pm 1.15\ 10^5$ *	
10 m	$4.93\ 10^5 \pm 1.7\ 10^4$ *	
MerA-mediated reduction rates (nmol Hg(II) min^{-1} $mg_{protein}^{-1}$)	10	(45)
Protein content of bacteria ($fg_{protein}$ $cells^{-1}$)	24	(64)
Correction factor for cells containing *mer*A in a given environment	1%	(34)
Correction factor for the effect of cold temperatures on bacterial activity	1%	(48)
Photoreduction rates (h^{-1})	0.43-1.58**	this study (1)
Photooxidation rates (h^{-1})	0.1-1.4**	(33, 62)
UVB attenuation (m^{-1})	0.24 – 4.02***	(10, 25)
UVA attenuation (m^{-1})	0.05 – 2.7***	
Total mercury (ng L^{-1})	0.5	this study (1)
Elemental mercury (ng L^{-1})	0.03***	(19) this study

* Sensitivity studies were performed on 100%, 50%, 10%, 5% and 1% cell viability

** The values of 0.5 and 0.6 h^{-1} were used in the base run. Additional sensitivity studies were performed for lower and upper estimations.

*** Mean values were employed in the base run.

Biological reduction

Biological mercury reduction in arctic sea water was estimated using a *merA* mediated reduction rate of 10 nmol Hg(II) min^{-1} mg $protein^{-1}$ (SD +/- 10%) (46) corrected for the protein content of bacterial cells (65) and calculated at the

surface and at depths of 5 and 10 m. To take into consideration the harsh Arctic conditions, several scenarios were tested. Based on observations indicating that 0.5 to 5% of cells in melted sea-ice were respiring (30), we considered that only 1 and 5% of the cells were active at the surface, and 10% at 5 and 10 m depth. Since the reported Hg(II) reduction rate was obtained at an optimal growth temperature (46), we reduced this rate by 99% to account for the effect of temperature on microbial activities as observed for many reactions in cold environments (49). Finally, not all cells in a given environment carry *mer*-operon genes. Using direct cell counts Liebert and Barkay (35) found that between 1 and 10% of all cells in temperate coastal or marine environments were mercury resistant; to be conservative, we estimated that only 1% of the viable cells expressed mercury resistance in our system.

Photochemical reactions

Photochemical rates of reduction and oxidation were based on previously published data in temperate coastal marine systems and ranged from 0.1 h^{-1} to 1.4 h^{-1} for photooxidation (33, 34, 63) and from 0.4 h^{-1} to 1.58 h^{-1} for photoreduction (1, 63). UV energy attenuation was calculated using an empirical model based on dissolved organic carbon (DOC) concentrations used for Arctic ocean waters (25). DOC concentrations for Arctic water ranged from 43 to 225 µmol L^{-1}, as observed for the central Arctic Ocean (10).

6.3.4. DNA extraction and PCR amplification of *merA* sequences.

Total DNA was extracted from biomass samples and from the concentrated water wash of these biomass samples using the PowerSoil™ DNA Isolation Kit (MoBio, Carlsbad, CA) according to the manufacturer's guidelines. The water used for the wash was collected with the solid samples at the sampling sites. Biomass in the washed suspensions was concentrated by

centrifugation (10,000 rpm, 10 min, 4°C) prior to DNA extraction as above. The presence of *merA* genes in DNA extracts was detected using a nested PCR approach using primers specific for *merA* genes among all gram negative bacteria (43). First, a 1250 bp fragment was amplified using the forward primer (5'-CCA TCG GCG GCW CYT GCG TSA A-3') and the reverse primer (A5-n.R; 5'-ACC ATC GTC AGR TAR GGR AAVA-3') and the following reaction conditions: final volume of 15 to 50 µL containing: 1x buffer, 1.5 mM $MgCl_2$, 0.2 mM dNTPs, 0.4 µM of each forward and reverse primers and 1U Taq polymerase (Fisher). Amplification conditions were as follows: 45 cycles of 10 sec at 94°C, 30 to 60 sec at 54°C and 30 sec at 72°C. The products of these reactions were separated by electrophoresis on a 1% agarose gel. Numerous bands were observed for most Arctic biomass samples. Amplicons of the predicted size (1250 bp) were excised from the gel and purified using a Qiagen DNA gel extraction kit (Qiagen, Valencia, CA) and used as template for a second PCR reaction, which amplified a 291 bp fragment internal to the 1250 bp template. PCR conditions were as described above with the following changes: a concentration of 0.8 µM of the following forward primer A7s-n.F; 5'-CGA TCC GCA AGT GGC IAC BGT-3' and reverse primer A5-n.R; 5'-ACC ATC GTC AGR TAR GGR AAVA-3'. Attempts to directly amplify the 291 bp fragment from Arctic biomass DNA extracts were unsuccessful.

In order to assess the diversity of microbes present, the 16S *r*RNA gene was amplified using the forward primer (27F, 5'-AGAGTTTGATCMTGGCTCAG-3') and the reverse primer (907R, 5'-CCGTCAATTCATTTGAG-3') in 25 µL reactions containing: 1x buffer, 1.5 mM $MgCl_2$, 0.2 mM dNTPs, 0.4 µM of each primers and 1U Taq polymerase (Fisher). Amplification conditions were as follows: 5 minutes at 95 °C, followed by 35 cycles of 10 sec at 94°C, 30 sec at 55°C and 90 sec at 72°C, followed by a final extension of 12 minutes at 72°C.

6.3.5. RNA extraction and cDNA synthesis.

Total RNA was extracted from microbial biomass using the UltraClean™ Microbial RNA Kit (MoBio, Carlsbad, CA), following the manufacturer guidelines. To eliminate contaminating DNA, extracts were treated with RQ1 RNase-free DNase (Promega, Madison, WI), according to the manufacturer's instructions. Reverse transcription was carried out using the SuperScript III Reverse trancriptase (Invitrogen, Carlsbad, CA) according to the manufacturer's instructions and using random hexamers as primers. cDNA was then used as template in PCR to detect *merA* transcripts as described above .

6.3.6. Cloning and sequencing of *merA* and 16S rRNA gene PCR products.

PCR products used for cloning were separated by gel electrophoresis (2% agarose). The 291bp *merA* amplicon was extracted and purified from the gel as above, and cloned into the vector pCR4-TOPO using a TOPO-TA cloning kit (Invitrogen, Carlsbad, CA), according to the manufacturer's instructions. Four libraries were created: i) sea-ice *merA* genes (SI*d*), ii) sea-ice *merA* transcripts (SI*r*), iii) lagoon *merA* genes (LG*d*), and iv) lagoon *merA* transcripts (LG*r*). Plasmid DNA was isolated from 96 clones from each library using the PureLink96 plasmid kit (Invitrogen) and the plasmids screened for inserts of the correct size by restriction digestion with PvuII or by amplification of the cloned region following the PCR protocol described above. Clones containing the 291 bp insert were sequenced using the M13r primer and ABI dye terminator chemistry (BigDye v.3.1, Applied Biosystems, Foster City, CA) on an ABI 3100 Genetic Analyzer. The same protocol was used to clone 16S rRNA gene PCR products from sea-ice and Lagoon DNA.

6.3.7. ARDRA analysis.

For amplified ribosomal DNA restriction analysis (ARDRA) fifty randomly picked colonies per 16S rDNA gene library were each grown overnight at 37°C in LB containing antibiotics. Plasmid DNA extraction was performed using the PureLink 96-well kit (Invitrogen) and the insert amplified using primers 27F-907R. Ten microliters of each amplicon were digested for 3 h at 37°C with 2.5 U of HaeIII and 2.5 U of EcoRI in 20 μl reactions. Restriction patterns were separated on 3% Nusieve agarose gels and stained with SYBR Green I DNA stain. Each different restriction pattern was defined as an operational taxonomic unit (OTU). The distribution of OTUs in each library was determined. Two representatives of each OTU were sequenced using primers M13f and M13r and compared to those in the GenBank database using BLASTN. The efficiency of our sampling effort was assessed using EstimateS (version 7.5; http://purl.oclc.org/estimates). Sample-based rarefaction curves and richness estimations and the percent coverage of clone libraries were computed.

6.3.8. *merA* clone library diversity analysis

A distance matrix of aligned *merA* sequences was generated using the F84 model for nucleotide substitution using the dnadist program in PHYLIP (version 3.6; Department of Genomic Sciences, University of Washington, WA; http://evolution.genetics.washington.edu/phylip.html). This distance matrix was then used to calculate sample coverage and richness estimates in DOTUR (54). Phylotypes were assigned using the furthest neighbor clustering algorithms. *merA* phylotypes were assigned based on a nucleotide sequence identity of 97%. Several tests were then applied to the *merA* clone libraries to estimate sampling efficiency by rarefaction analysis (29) and to calculate nonparametric richness estimates ACE (18) and Chao1 (17) as a function of sampling effort from rarefaction curves following 1000 randomizations.

6.3.9. Phylogenetic Analysis

The *merA* nucleotide sequences were trimmed and assembled using SeqMan (DNAStar, Madison, WI). The DNA sequences were then translated into amino acids and aligned with reference MerA sequences using the ClustalW function in MegAlign (DNAStar). The alignment was exported to MEGA 3.1 and a neighbor joining tree was built with 1000 bootstrap replicates. 16S rRNA nucleotide sequences were trimmed and assembled in a similar manner and the nearest relatives to each OTU determined using BLASTN.

6.3.10. Accession numbers

The nucleotide sequences reported in this study were deposited in the GenBank database with the following accession numbers: DQ408728-DQ408744 and EF379214-EF379240.

6.4. Results

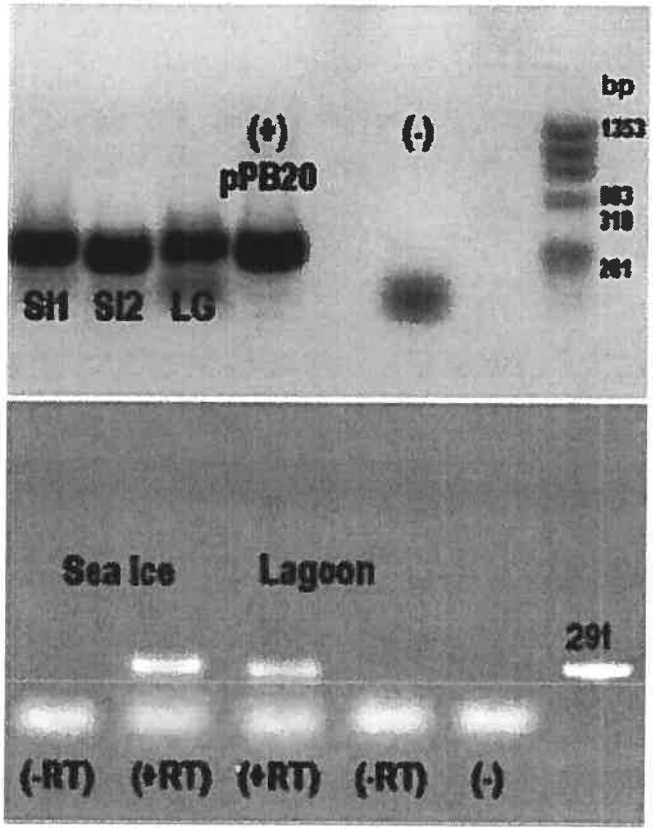

Figure 6.1. *merA* genes and transcripts in microbial biomass. (top) Gel showing 291 bp *mer*A PCR products obtained with sea-ice (SI) and lagoon (LG) DNA extracts as templates; SI1 and LG – DNA obtained by extracting biomass with its associated microbes and SI2 – Extract of a fraction obtained by washing alga with site water; (+) pPB20 – positive control–consisting of *merA* from *Pseudomonas stutzeri* OX (50); PCR blank (-) and a DNA ladder (bp). (bottom) Gel showing *mer*A PCR products following reverse transcriptase reactions (+RT) of RNA extracted from sea-ice and lagoon biomass. (-RT) No RT controls; (-) PCR blank; a 291 bp PCR fragment is shown.

6.4.1. Amplification and cloning of *merA* from Arctic DNA and RNA samples.

Previously described primers to *merA* (43) were used to amplify the *merA* gene from DNA and RNA extracts of microbial biomass samples collected from a benthic biofilm in a coastal lagoon (lagoon) and from a biofilm associated with macroalgae that were retrieved from seawater between blocks of coastal sea-ice (Figure 6.1). Four *merA* clone libraries were constructed using the PCR products of the lagoon and sea-ice communities. Seventeen unique MerA phylotypes were obtained which encompassed the known diversity of MerA among bacteria (Figure 6.2). Over 29% of these phylotypes, all from the lagoon gene library, were related to a putative locus in *Sphingopyxis alaskensis*, a psychrophilic bacterium that had been isolated from Alaskan waters. These MerAs formed a distinct cluster most closely related to the MerAs from Gram positive bacteria (Figure 6.2). A further 18% of the phylotypes observed clustered with a putative MerA from the genome sequence of *Polaromonas* sp. JS666, a genus that was first described in an Antarctic bacterium, *Polaromonas vacuolata*. The remaining *merA* phylotypes, which included the majority of the clones, were closely related to the genetically and biochemically characterized MerAs from Tn*21*, Tn*501* and pDU1358 (Figure 6.2).

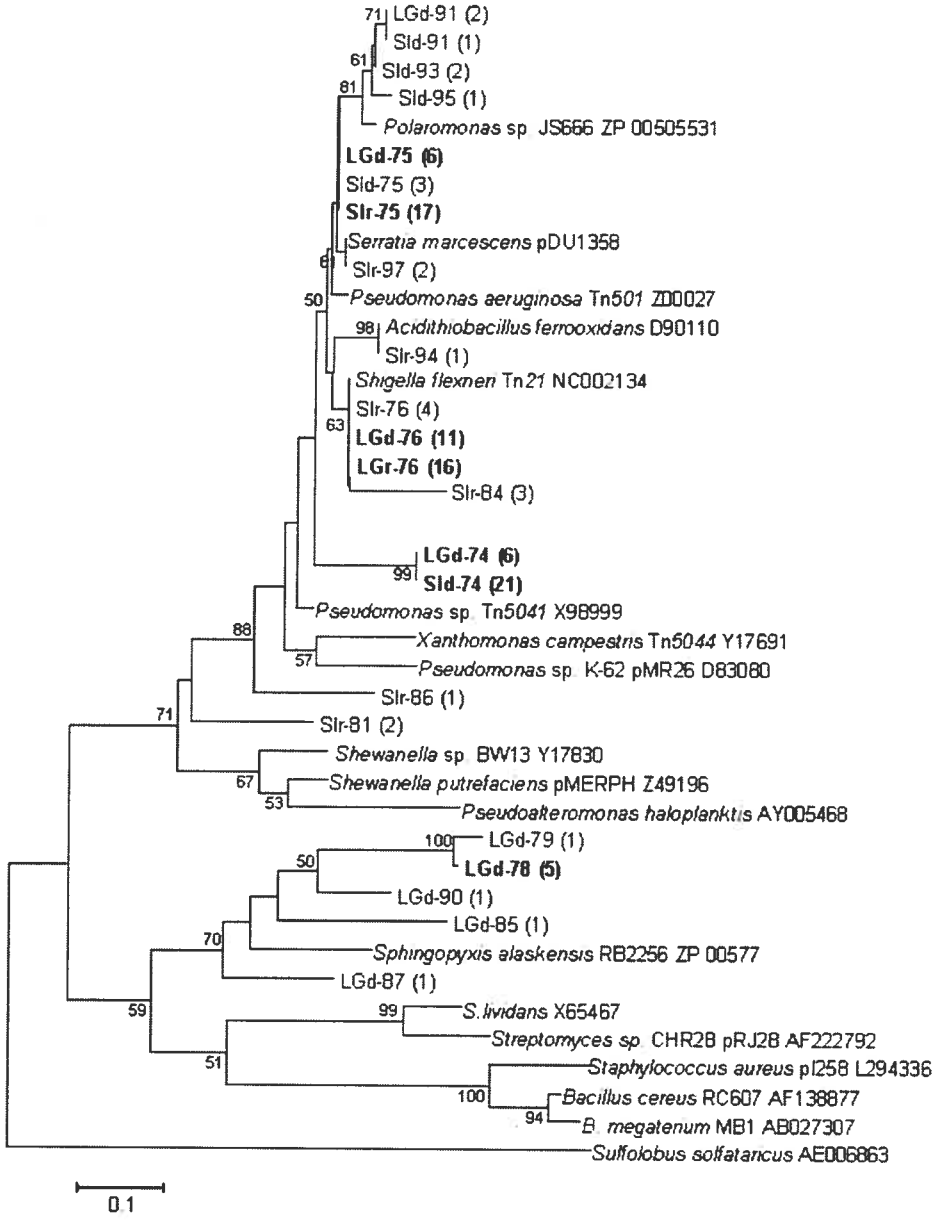

Figure 6.2.Phylogenetic distribution of *merA* phylotypes. The dendrogram was constructed from a ClustalW alignment of the trimmed amino acid sequences by neighbor-joining analysis using Mega 3.1. Bootstrap values greater than 50 are indicated. The number of clones in a particular phylotype is indicated in parentheses. Phylotypes representing > 25% of the clones in a library are highlighted in bold face. Phylotype designations that contain the letters LG originated in the lagoon biomass and those that contain SI in the macro-algae; d and r indicate that the phylotype originated in DNA or RNA clone libraries, respectively. Reference sequences from GenBank include the accession number.

6.4.2. *merA* diversity analysis

Rarefaction curves were constructed for each *merA* library to assess our sampling effort (Figure 6.3). Both sea ice *merA* libraries had been sampled adequately as the rarefaction curves approached a plateau. Furthermore ACE and Chao1 estimates indicate that in both libraries we captured approximately 80% of the predicted phylotypes (Table 2). While the distribution of phylotypes in the sea ice RNA library was more even than in the sea ice DNA library (Figure 6.3) the richness (Chao1 and ACE) and diversity (H') estimates are the same within the sampling error (Table 2). The sea-ice DNA library was dominated by Arct74, which was most closely related to the MerA of Tn*21* (Figure 6.2 and Figure 6.4). Arct74 was not detected in the Sea Ice RNA library. This library was dominated by the second most abundant clone from the DNA library, Arct75 (Figure 6.4). With the exception of Arct75 there was no overlap between the Sea Ice DNA and RNA *merA* libraries.

Table 6.II. Diversity analysis of the *merA* gene fragment libraries[1].

Library	N	n	Chao1	ACE	H'
SI*d*	28	5	5.5 (5.0-13.2)	6.7 (5.2-21.5)	0.88 (0.47-1.28)
SI*r*	30	6	7.3(7.0-13)	8.1 (7.3-11.5)	1.41 (1.03-1.79)
LG*d*	34	9	12 (9.4-32)	13.4 (9.7-35.7)	1.84 (1.56-2.12)
LG*r*	16	1	1 (1-1.1)	Nd	0 (-0.087-0.087)

[1]N, the number of clones sequenced; n, the number of *merA* phylotypes observed; Chao1, the Chao1 non parametric richness estimate, ACE, abundance base coverage estimator; and, H', the Shannon-Weaver diversity index (H'). Numbers in parentheses represent the 95% confidence intervals.

The lagoon DNA library was the most diverse with an H'of 1.84 while the lagoon RNA library was the least diverse with an H'of 0 corresponding to the presence of a single phylotype, Arct76 (Table 2). ACE and Chao1 based coverage estimates indicate that our sequencing effort captured 75% of the predicted phylotypes from the Lagoon DNA library. The single phylotype in the Lagoon RNA library was most closely related to MerA of Tn*21*. Arct76 comprised about one third of the lagoon DNA library (Figure 6.4). A Tn*21*-like MerA locus was previously described in a bacterium from 8000 year-old permafrost (31) and thus, this MerA phylotype may be common in cold environmentss.

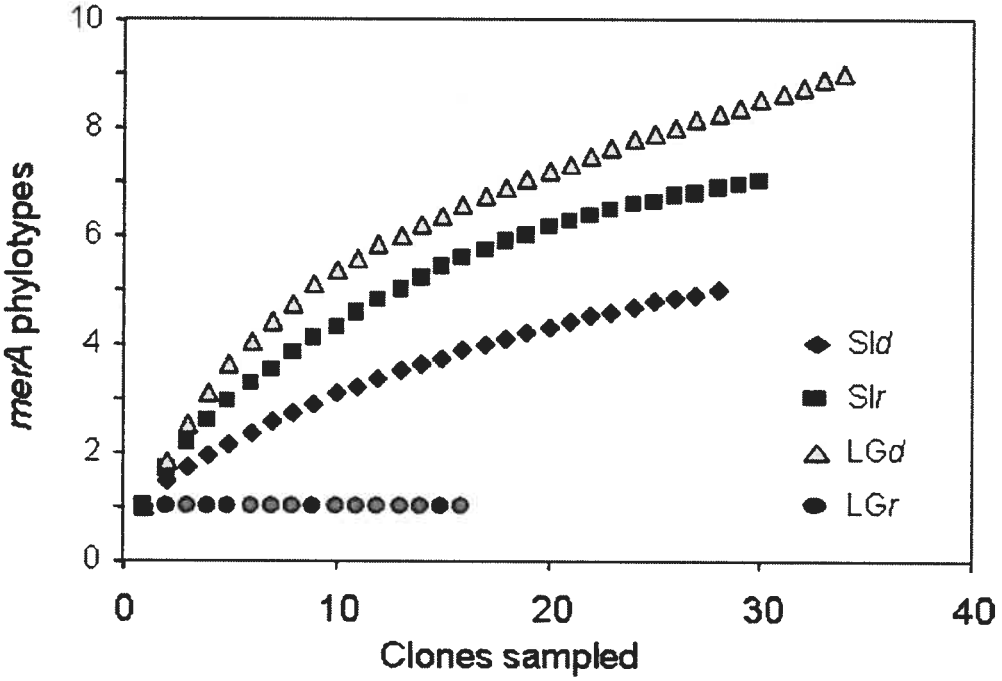

Figure 6.3.*merA* phylotype accumulation curves, the number of clones sampled vs. number of *merA* phylotypes observed.

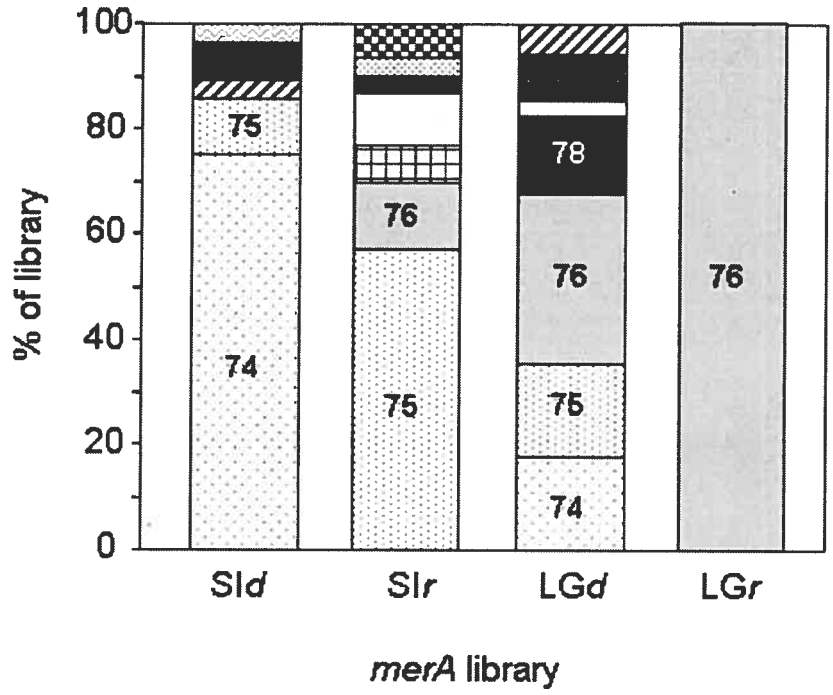

Figure 6.4. Relative abundance of *merA* phylotypes within the four clone libraries. A threshold of 97% nucleotide identity was used to define each *merA* phylotype. SI, sea-ice; LG, lagoon. Different textures indicate different phylotypes and sections with similar texture in each bar denote similar phylotypes that were present in more than one library. Phylotype numbers, provided for those phylotypes that represent at least 10% of a library, correspond to those used as phylotype designation in Fig. 5.2.

6.4.3. Bacterial community analysis

We constructed and analysed 16S rRNA gene clone libraries to examine if microbes that are commonly found in polar regions were present in the sampled lagoon and sea ice biomass. This was confirmed by sequence analysis (Figure 6.5) with the *Alpha-*, *Beta-* and *Gammaproteobacteria*, *Cytophaga-Flavobacterium-Bacteroides* (CFB) group and *Cyanobacteria* dominating the cloned 16S rRNA gene libraries. The Sea Ice community appeared to be dominated by *Proteobacteria* (55% of sequenced clones) while the Lagoon was dominated by *Cyanobacteria* (45% of sequenced clones). The second most abundant phyla were the *proteobacteria* (36%) and the CFB group (30%) for the lagoon and the sea-ice respectively. BLASTN analysis revealed that the closest relatives to these dominant 16S phylotypes were bacteria that are often found in polar coastal, marine and sympagic environments (14) such as *Loktanella vestflodensis* or uncultured Antarctic and Arctic *proteobacteria* (Figure 6.5). The 16S libraries were not sampled to exhaustion (data not shown).

6.4.4. Total mercury levels in water and microbial mats

Total mercury concentrations in coastal water, at both the lagoon and sea ice sites were between 9.4 and 11.5 $pmol \cdot L^{-1}$ corresponding to previously observed concentrations in Arctic seawater (23). Modeling the inorganic speciation of mercury in these samples using MINEQL+ v4.5 (53) showed dominance of negatively charged chlorocomplexes (e.g. $HgCl_4^{2-}$). To further assess the mercury levels to which the sampled microbial communities were exposed we measured THg in *Desmarestia sp.* (Sea ice sample) and in the microbial mats (Lagoon sample). The data showed the former and latter to have 52.5±0.9 $ng \cdot g^{-1}$ (d.w.) and 27.3±2.9 $ng \cdot g^{-1}$ (d.w.), respectively, concentrations

that were 2 to 5 times lower than those reported at lower latitudes for periphyton in boreal lakes (22).

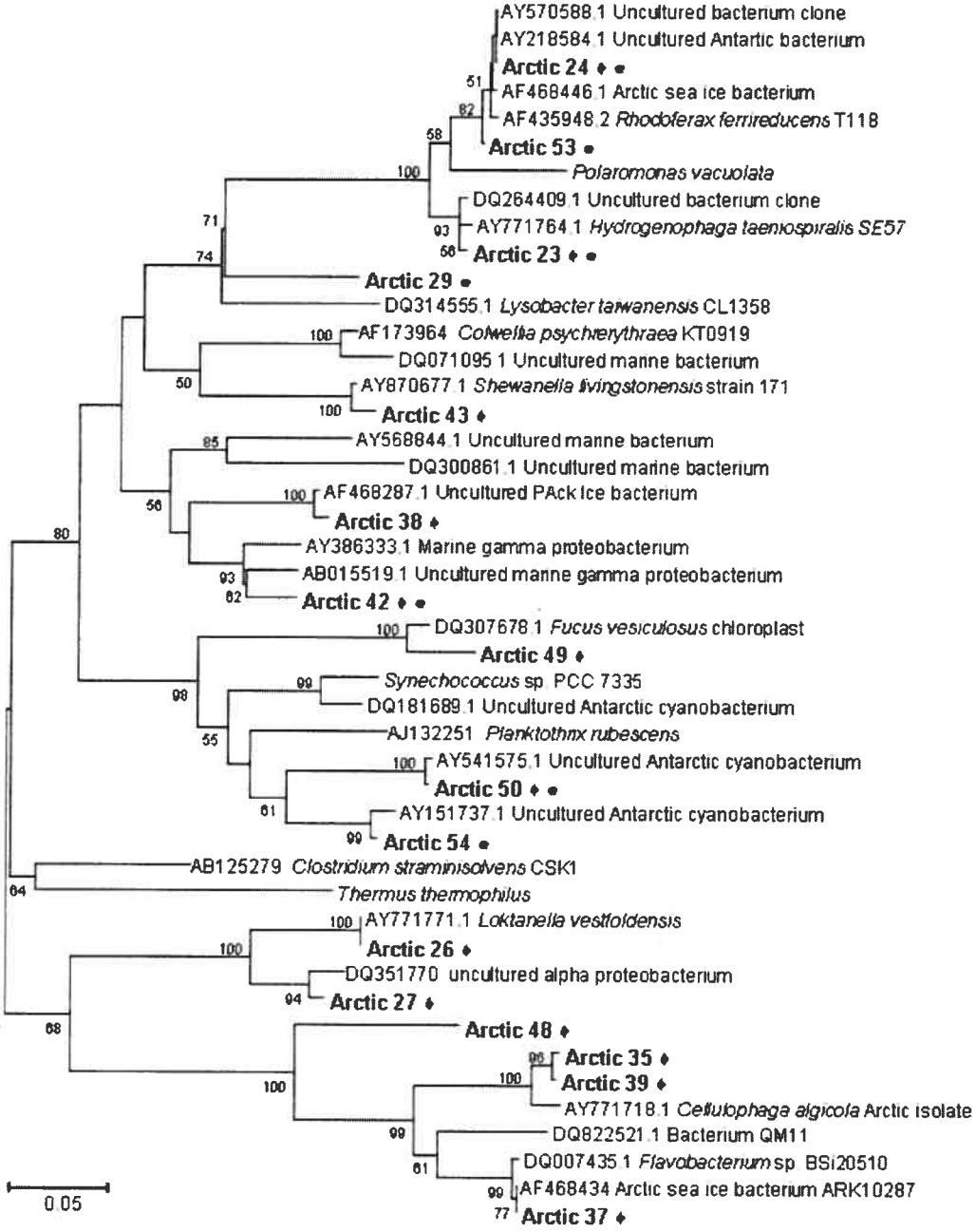

Figure 6.5. 16S rRNA-based phylogeny of Arctic microbial biomass. The dendrogram was constructed from a ClustalW alignment of the trimmed nucleotide sequences by neighbor-joining analysis using Mega 3.1. Bootstrap values greater than 50 are indicated. Key: phylotypes represented in the Sea Ice library, filled diamonds; Lagoon library, filled circles.

6.4.5. Modeling of mercury speciation in seawater

To assess if microbial reduction can constitute a major pathway for mercury cycling in polar regions we used a kinetic redox model (13) in which photooxidation, photo-reduction, and microbial mercury reduction were considered. Mercury speciation was modeled at the surface and at depths of 5 and 10 m (Figure 6.6). Note that microbially-mediated reduction rates were corrected for Arctic conditions that accounted for cell viability and metabolism alteration because of low temperatures (see Materials and Methods). At the sea surface, the steady-state pool of elemental mercury could represent 40 to 80% of the inorganic mercury pool, depending on the assumed proportion of viable bacterial cells. When the model considered 1% of the cells active, >20% of the total pool of inorganic mercury was biogenic Hg(0), and when 5% of the cells were considered active, >55% of the inorganic mercury pool was biogenic Hg(0) (Figure 6.6 A). At a depth of 5 and 10 m, due to UVA and UVB energy attenuation, the relative importance of photochemical processes decreased and microbial reduction could account for up to 94% of the pool of elemental mercury (Figure 6.6 B and 6.6 C).

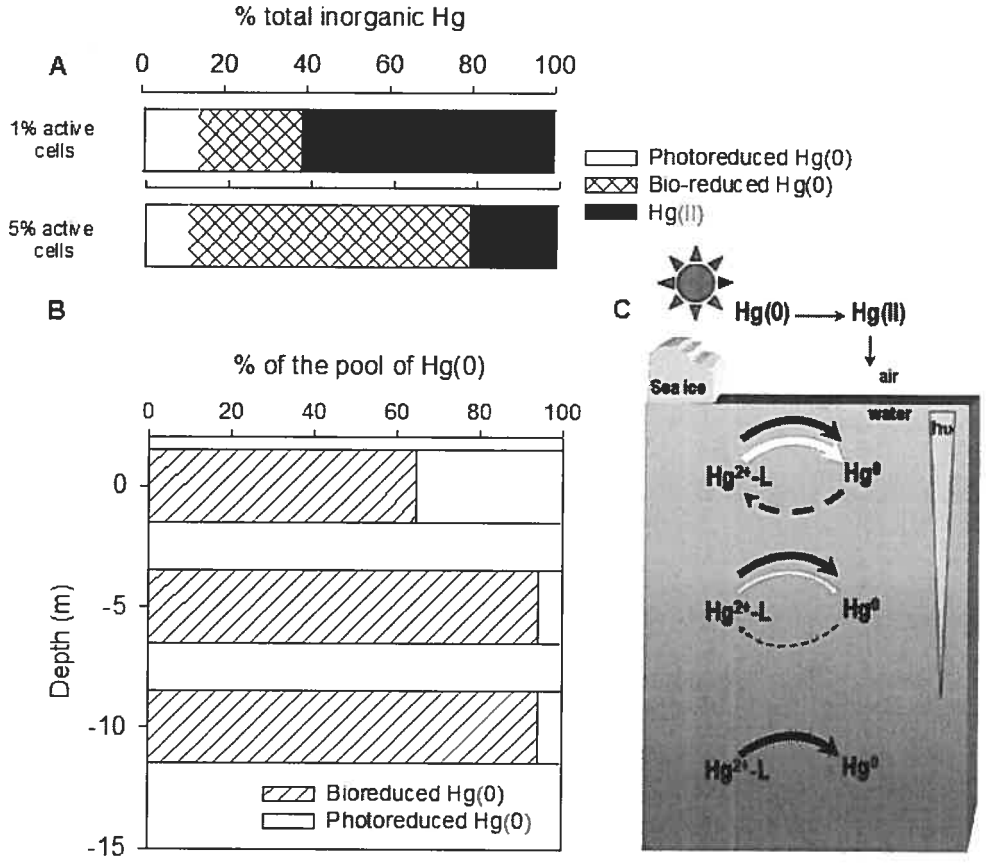

Figure 6.6. Results of modeling of the relative importance of photochemical reactions vs. biologically mediated reduction in mercury redox cycling in sea water in Arctic near coastal environments. **A)** Relative distribution of inorganic mercury species and proportion of Hg(0) that is formed by photochemical and microbial processes, at the sea surface. In this example photoreduction and photooxidation rates were considered to be 0.5 and 0.6 h^{-1}, respectively, and the proportion of active bacterial cells was assumed to be 1 or 5%. **B)** Relative importance of photochemical vs. microbial contributions to the pool of elemental mercury at the surface and at depths of 5 and 10 meters. **C)** A proposed model for redox cycling of mercury in the water column of Arctic near coastal marine environments. Arrow width correlates with the relative quantitative contribution of the depicted process to the total activity at each depth. Black, white and dashed line arrows represent microbially mediated reduction, photoreduction mostly triggered by UVB and photooxidation mostly triggered by UVA, respectively. The grey inverted triangle depicts the gradient in light penetration with depth.

6.5. Discussion

Here we report that *merA* genes and transcripts were detected in High Arctic microbial biomass that contained microbes previously described to inhabit polar environments. These results suggest that mercury resistant organisms are present and active in Arctic coastal environments where critical redox transformations of mercury occur and where methylmercury is accumulated in the marine food chain. Furthermore, modeling efforts are consistent with the possibility the prokaryotic MerA may play an important role in the production of Hg(0) in the high Arctic.

The concentration of Hg(0) in natural waters results from the balance between its production (reduction) and its destruction (oxidation). Because of the attenuation of UV radiation with depth in the water column, both photoreduction and photooxidation decline with increasing depth. Moreover, in coastal and marine systems, because of the presence of chloride, photoreduction is hampered and, in the absence of an alternative pathway for Hg(0) production, oxidation reactions may be prevalent and likely more significant than evasion in controlling the fate of Hg(0) (1, 3, 63). Microbial reduction can account for a significant component of the mercury redox cycling in coastal marine systems from temperate zones (up to 20% of the pool of Hg[0], [51]), although the mechanisms involved remain unknown. Our model (Figure 6.6) suggests that in the high Arctic coastal marine environment the activity of the prokaryotic MerA may potentially be an important source of Hg(0) and, as it is not dependent on light, can occur at any depth or under sea-ice during the winter. These predictions for the role of MerA in Hg(0) production are supported by recent data showing that during winter time the pool of total mercury in surface seawater beneath sea-ice is comprised of up to 50% elemental mercury and can reach a concentration of ca. 0.6 pmol•L^{-1} (V. St-Louis, personal communication) 5 to 10 fold higher than observed in coastal seawater during the ice-free season.

Although very few data exist as to the metabolic activity of microbes under sea ice during polar winter, it is possible that they further increase the pool of reduced mercury at a time of the year when photooxidation processes are greatly reduced. Moreover, because *mer*-operon functions also degrade MeHg, bacteria may decrease the pool of methylmercury available for uptake by Arctic food webs. In this regard, it is important to note that macroalgae such as *Desmarestia sp.* were reported to produce both monomethylmercury and dimethylmercury in polar seawater (47). The importance of mercury resistant microbes that are associated with these macroalgae to mercury cycling is critical to the understanding of contamination pathways in the Arctic.

The discovery of *mer*A transcripts in Arctic microbial biomass was unexpected. The expression of *mer*A is tightly controlled by intracellular concentrations of divalent mercury (15) and its induction requires exposure concentrations in the $nmol \cdot L^{-1}$ range in both pure cultures (64) and in aquatic microbial communities (52). The mercury concentrations we present here and those reported for late spring and summer in meltwaters, lakes, and seawater are in the $pmol \cdot L^{-1}$ range (36, 58), typical of pristine environments. Furthermore, this mercury was mostly present as negatively charged chlorocomplexes, which are poorly bioavailable to microbes (5, 27). Therefore, not only was mercury concentration low in the coastal environments sampled here, but its bioavailability was likely also limited by high concentrations of Cl^-. The induction of *merA* observed in our study may reflect (i) the existence of environmental conditions that enhance mercury bioavailability, or (ii) the presence of micro-niches with high mercury concentrations within the sampled biomass. Our analysis of mercury concentrations involved homogenization steps and would miss such niches.

To understand why *merA* was expressed in the High Arctic an understanding of both the processes that control mercury bioavailability and how these processes are impacted by the uniqueness of the microbial habitats in

high latitudes, is needed. The former are not well-understood beyond the passive diffusion of Hg-sulfide complexes (11) and the facilitated transport of inorganic and organic mercury complexes (26). Niches with high concentrations of mercury can occur in the High Arctic, possibly in association with the complex and heterogeneous nature of sea ice (21). One of the biomass samples described here (SI) was obtained from waters with sea ice and considering the slow degradation of RNA in frozen environments (61), a sea ice origin for the *merA* transcripts detected in this sample may be plausible. This proposition is supported by the dominance of bacteria endemic to sympagic environments in the sampled communities (Figure 6.5). The conditions which control the uptake of mercury are still unclear and may well be as diverse as the environments studied. The occurrence of *merA* expression in Arctic coastal and marine aquatic environments exhibiting low mercury levels, underscores the gap in our current knowledge of Hg-microbe interactions and further investigation of the biogeochemical cycling of mercury in polar environments should elucidate some key aspects of the Arctic mercury cycle.

Many of the MerA phylotypes reported here in Arctic biomass are related to those from microbes that thrive at high latitudes. Forty eight percent were most closely related to putative *mer* loci from the complete genomes of *Sphingopyxis alaskensis* and *Polaromonas vacuolata*, two microbes first isolated from polar environments. This finding attests to the authenticity of the MerA loci that were isolated here as representative of those loci that are present and expressed in microbial communities from polar regions. The remaining MerA phylotypes, which constitute the majority of the clones sequenced, were closely related to MerAs from Tn*21*, Tn*501* and pDU1358. A Tn*21*-related mercury resistance transposon, Tn*5060*, has been previously described in a 8000-10000 year-old Siberian permafrost isolate of *Pseudomonas sp.* (31).

Phylotypes related to Tn*21* and Tn*501* *merA*s dominated in an anaerobic enrichment of mercury contaminated sediment (43) as well as in the microbial

biomass of an acidic and sulfidic mercury rich springs in Yellowstone National Park (Barkay, unpublished). These data suggest that this *merA* locus, which represents the most recently evolved MerA lineage (Figure 6.2), is broadly distributed in many environments. The total number of *merA* phylotypes observed here (Figure 6.2) was low compared to that in the anaerobic enrichment with its 39 *merA* phylotypes. Others have shown that selection for the target genes may increase phylotype diversity (28) while enhanced activities in environmental incubations were associated with a reduced phylotype diversity (40). A more rigorous examination of the relationship of *merA* diversity to mercury resistance and reduction in environmental samples is needed for a clear understanding of how phylotype diversity is related the potential for mercury transformations in various environments.

Two contrasting patterns were observed when the diversity of the DNA and RNA clone libraries that were obtained from the same community were examined; i) high diversity of *merA* genes and low diversity of transcripts in the lagoon and ii) high diversity of both genes and transcripts in the sea ice samples. At this point we can only speculate on why the lagoon and the sea ice communities showed such different patterns. One possibility is that the high diversity of *merA* transcripts in the sea ice reflects the heterogeneous nature of microbial niches within sea ice (see above). Alternatively, it may be related to the in situ temperature at the time of sampling. While Arctic coastal sea water temperatures are usually slightly below 0°C, the temperatures in coastal lagoons may reach a mesophilic range (58) and the temperature at the lagoon at sampling time was 7 °C. Higher temperatures in the lagoon may have accelerated the turnover rate of transcripts while colder conditions in open waters may have slowed mRNA degradation to the point that we detected a greater diversity of expressed *merA* genes in sea ice.

The diversity of expressed genes, not that of the genes that are present in a community, is at the heart of what determines ecosystem function as related to

environmental conditions. While experimental approaches to study expression of biogeochemical functions have been widely used in the last decade, few studies have compared the diversity of functional genes and mRNA transcripts in microbial biomass. Knauth et al. (32) used T-RFLP analysis of both DNA and RNA extracted from microbial biomass of the rice rhizosphere to examine how nitrogen availability and plant host species affected the diversity of the nitrogenase gene, *nifH*. As in our study of *merA*, their results showed significant differences between DNA and mRNA *nifH* profiles underscoring the importance of mRNA based approaches to understanding functional gene diversity. The observation of different *merA* gene and transcript profiles presented here highlights the need to further develop an understanding of how patterns of microbial gene expression are affected by environmental parameters in heterogeneous environments such as the Arctic.

Our discovery of *merA* expression and the results of the model calculations that simulated redox transformations suggest an active role for microbial activities in the cycling of mercury in Arctic coastal and marine environments. Clearly, microbial redox transformations have the potential to drive mercury dynamics in cold environments, and Arctic microbes that possess and express *merA* genes stand to be key players in determining the environmental mobility and toxicity of mercury in high latitude polar regions.

6.6. Acknowledgements

We thank Dr. H. Vandermeulen for his help with algae identification, Drs. J. Brenchley and V. Miteva for stimulating discussions, and B. E. Keatley for comments on the manuscript. We thank Paul del Giorgio for access to flow cytometer. Support by the U.S.A. National Science Foundation (CHE-0221978 and ATM-0322022), the U.S.A. National Institute of Environmental Health and Safety (P42 ES004911), and the Fond Québecois de la Recherche sur la Nature et les Technologies, for funding, is acknowledged.

6.7. References

1. **Amyot, M., G. A. Gill, and F. M. M. Morel.** 1997. Production and loss of dissolved gaseous mercury in coastal seawater. Environ. Sci. Technol. **31:**3606-3611.
2. **Amyot, M., G. Mierle, D. R. S. Lean, and D. J. McQueen.** 1994. Sunlight-induced formation of dissolved gaseous mercury in lake waters. Environ. Sci. Technol. **28:**2366-2371.
3. **Ariya, P. A., A. P. Dastoor, M. Amyot, W. H. Schroeder, L. Barrie, K. Anlauf, F. Raofie, A. Ryzhkov, D. Davignon, J. Lalonde, and A. Steffen**. 2004. The Arctic: a sink for mercury. Tellus Ser. B-Chem. Phys. Meteorol. 56:397-403.
4. **Ariya, P. A., A. Khalizov, and A. Gidas.** 2002. Reactions of gaseous mercury with atomic and molecular halogens: Kinetics, product studies, and atmospheric implications. J. Phys. Chem. A **106:**7310-7320.
5. **Barkay, T., M. Gillman, and R. R. Turner.** 1997. Effects of dissolved organic carbon and salinity on bioavailability of mercury. Appl. Environ. Microbiol. **63:**4267-4271.
6. **Barkay, T., C. Liebert, and M. Gillman.** 1989. Environmental significance of the potential for Mer(Tn*21*)-Mediated Reduction of Hg^{2+} to Hg^0 in natural-waters. Appl. Environ. Microbiol. **55:**1196-1202.
7. **Barkay, T., C. Liebert, and M. Gillman.** 1989. Hybridization of DNA probes with whole-community genome for detection of genes that encode microbial responses to pollutants - *mer* genes and Hg^{2+} resistance. Appl. Environ. Microbiol. **55:**1574-1577.
8. **Barkay, T., S. M. Miller, and A. O. Summers.** 2003. Bacterial mercury resistance from atoms to ecosystems. FEMS Microbiol. Rev. **27:**355-384.
9. **Barkay, T., R. R. Turner, A. Vandenbrook, and C. Liebert.** 1991. The relationships of Hg(II) volatilization from a fresh-water pond to the abundance of *mer*-genes in the gene pool of the indigenous microbial community. Microb. Ecol. **21:**151-161.
10. **Benner, R., P. Louchouarn, and R. M. W. Amon**. 2005. Terrigenous dissolved organic matter in the Arctic Ocean and its transport to surface and deep waters of the North Atlantic. Glob. Biogeochem. Cycle **19:** GB2025.
11. **Benoit, J. M., C. C. Gilmour, R. P. Mason, and A. Heyes.** 1999. Sulfide controls on mercury speciation and bioavailability to methylating bacteria in sediment pore waters. Environ. Sci. Technol. **33:**951-957.
12. **Braun, W., J. T. Herron, and D. K. Kahaner.** 1988. ACUCHEM - a computer-program for modeling complex chemical-reaction systems. Int. J. Chem. Kinet. **20:**51-62.

13. **Braune, B., D. Muir, B. DeMarch, M. Gamberg, K. Poole, R. Currie, M. Dodd, W. Duschenko, J. Eamer, B. Elkin, M. Evans, S. Grundy, C. Hebert, R. Johnstone, K. Kidd, B. Koenig, L. Lockhart, H. Marshall, K. Reimer, J. Sanderson, and L. Shutt.** 1999. Spatial and temporal trends of contaminants in Canadian Arctic freshwater and terrestrial ecosystems: a review. Sci. Total Environ. 230:145-207.

14. **Brinkmeyer, R., K. Knittel, J. Jurgens, H. Weyland, R. Amann, and E. Helmke.** 2003. Diversity and structure of bacterial communities in arctic versus antarctic pack ice. Appl. Environ. Microbiol. **69:**6610-6619.

15. **Brown, N. L., J. V. Stoyanov, S. P. Kidd, and J. L. Hobman.** 2003. The MerR family of transcriptional regulators. FEMS Microbiol. Rev. **27:**145-163.

16. **Campbell, L. M., R. J. Norstrom, K. A. Hobson, D. C. G. Muir, S. Backus, and A. T. Fisk.** 2005. Mercury and other trace elements in a pelagic Arctic marine food web (Northwater Polynya, Baffin Bay). Sci. Total Environ. **351:**247-263.

17. **Chao, A.** 1984. Non-parametric estimation of the number of classes in a population. Scand. J. Stat. **11:**265-270.

18. **Chao, A., and S. M. Lee.** 1992. Estimating the Number of Classes Via Sample Coverage. J. Am. Stat. Assoc. **87**:210-217.

19. **Costa, M., and P. S. Liss.** 1999. Photoreduction of mercury in sea water and its possible implications for Hg(0) air-sea fluxes. Mar. Chem. **68:**87-95.

20. **De Domenico, M., A. Lo Giudice, L. Michaud, M. Saitta, and V. Bruni.** 2004. Diesel oil and PCB-degrading psychrotrophic bacteria isolated from antarctic seawaters (Terra Nova Bay, Ross Sea). Polar Res. **23:**141-146.

21. **Deming, J. W.** 2002. Psychrophiles and polar regions. Curr. Opin. Microbiol. **5:**301-309.

22. **Desrosiers, M., D. Planas, and A. Mucci.** 2006. Mercury methylation in the epilithon of boreal shield aquatic ecosystems. Environ. Sci. Technol. **40:**1540-1546.

23. **Douglas, T. A., M. Sturm, W. R. Simpson, S. Brooks, S. E. Lindberg, and D. K. Perovich.** 2005. Elevated mercury measured in snow and frost flowers near Arctic sea ice leads. Geophys. Res. Lett. **32**: L04502.

24. **Ebinghaus, R., H. H. Kock, C. Temme, J. W. Einax, A. G. Lowe, A. Richter, J. P. Burrows, and W. H. Schroeder**. 2002. Antarctic springtime depletion of atmospheric mercury. Environ. Sci. Technol. 36:1238-1244.

25. **Gibson, J. A. E., W. F. Vincent, B. Nieke, and R. Pienitz.** 2000. Control of biological exposure to UV radiation in the Arctic Ocean: comparison of the roles of ozone and riverine dissolved organic matter. Arctic **53:**372-382.

26. **Golding, G. R., C. A. Kelly, R. Sparling, P. C. Loewen, J. W. M. Rudd, and T. Barkay.** 2002. Evidence for facilitated uptake of Hg(II) by *Vibrio anguillarum* and *Escherichia coli* under anaerobic and aerobic conditions. Limnol. Oceanogr. **47:**967-975.
27. **Gutknecht, J.** 1981. Inorganic mercury (Hg^{2+}) transport through lipid bilayer membranes. J. Membr. Biol. **61:**61-66.
28. **Hobel, C. F. V., V. T. Marteinsson, G. O. Hreggvidsson, and J. K. Kristjansson.** 2005. Investigation of the microbial ecology of intertidal hot springs by using diversity analysis of 16S rRNA and chitinase genes. Appl. Environ. Microbiol. **71:**2771-2776.
29. **Hughes, J. B., J. J. Hellmann, T. H. Ricketts, and B. J. M. Bohannan.** 2001. Counting the uncountable: Statistical approaches to estimating microbial diversity. Appl. Environ. Microbiol. **67:**4399-4406.
30. **Junge, K., H. Eicken, and J. W. Deming.** 2004. Bacterial activity at-2 to-20 degrees C in Arctic wintertime sea ice. Appl. Environ. Microbiol. **70:**550-557.
31. **Kholodii, G., S. Mindlin, M. Petrova, and S. Minakhina.** 2003. Tn*5060* from the Siberian permafrost is most closely related to the ancestor of Tn*21* prior to integron acquisition. FEMS Microbiol. Lett. **226:**251-255.
32. **Knauth, S., T. Hurek, D. Brar, and B. Reinhold-Hurek**. 2005. Influence of different *Oryza* cultivars on expression of *nifH* gene pools in roots of rice. Environ. Microbiol. **7**:1725–1733.
33. **Lalonde, J. D., M. Amyot, A. M. L. Kraepiel, and F. M. M. Morel.** 2001. Photooxidation of Hg(0) in artificial and natural waters. Environ. Sci. Technol. **35:**1367-1372.
34. **Lalonde, J. D., M. Amyot, J. Orvoine, F. M. M. Morel, J. C. Auclair, and P. A. Ariya.** 2004. Photoinduced oxidation of Hg^0(aq) in the waters from the St. Lawrence estuary. Environ. Sci. Technol. **38:**508-514.
35. **Liebert, C., and T. Barkay.** 1988. A direct viable counting method for measuring tolerance of aquatic microbial communities to Hg^{2+}. Can. J. Microbiol. **34:**1090-1095.
36. **Lindberg, S. E., S. Brooks, C. J. Lin, K. J. Scott, M. S. Landis, R. K. Stevens, M. Goodsite, and A. Richter.** 2002. Dynamic oxidation of gaseous mercury in the Arctic troposphere at polar sunrise. Environ. Sci. Technol. **36:**1245-1256.
37. **Lovley, D. R.** 2003. Cleaning up with genomics: Applying molecular biology to bioremediation. Nat. Rev. Microbiol. **1:**35-44.
38. **Macdonald, R. W., T. Harner, and J. Fyfe.** 2005. Recent climate change in the Arctic and its impact on contaminant pathways and interpretation of temporal trend data. Sci. Total Environ. **342:**5-86.
39. **Master, E. R., and W. W. Mohn.** 1998. Psychrotolerant bacteria isolated from Arctic soil that degrade polychlorinated biphenyls at low temperatures. Appl. Environ. Microbiol. **64:**4823-4829.

40. **Metcalfe, A. C., M. Krsek, G. W. Gooday, J. I. Prosser, and E. M. H. Wellington.** 2002. Molecular analysis of a bacterial chitinolytic community in an upland pasture. Appl. Environ. Microbiol. **68:**5042-5050.

41. **Mindlin, S., L. Minakhin, M. Petrova, G. Kholodii, S. Minakhina, Z. Gorlenko, and V. Nikiforov.** 2005. Present-day mercury resistance transposons are common in bacteria preserved in permafrost grounds since the Upper Pleistocene. Res. Microbiol. **156:**994-1004.

42. **Muir, D., B. Braune, B. DeMarch, R. Norstrom, R. Wagemann, L. Lockhart, B. Hargrave, D. Bright, R. Addison, J. Payne, and K. Reimer**. 1999. Spatial and temporal trends and effects of contaminants in the Canadian Arctic marine ecosystem: a review. Sci. Total Environ. 230:83-144.

43. **Ni Chadhain, S. M., J. K. Schaefer, S. Crane, G. J. Zylstra, and T. Barkay.** 2006. Analysis of mercuric reductase (*merA*) gene diversity in an anaerobic mercury-contaminated sediment enrichment. Environ. Microbiol. **8:**1746-1752.

44. **Osborn, A. M., K. D. Bruce, P. Strike, and D. A. Ritchie.** 1997. Distribution, diversity and evolution of the bacterial mercury resistance (*mer*) operon. FEMS Microbiol. Rev. **19:**239-262.

45. **Pepi, M., A. Cesaro, G. Liut, and F. Baldi.** 2005. An antarctic psychrotrophic bacterium *Halomonas* sp. ANT-3b, growing on n-hexadecane, produces a new emulsyfying glycolipid. FEMS Microbiol. Ecol. **53:**157-166.

46. **Philippidis, G. P., L. H. Malmber, W. S. Hu, and J. L. Schottel.** 1991. Effect of gene amplification on mercuric ion reduction activity of *Escherichia coli*. Appl. Environ. Microbiol. **57:**3558-3564.

47. **Pongratz, R., and K. G. Heumann.** 1998. Production of methylated mercury and lead by polar macroalgae - a significant natural source for atmospheric heavy metals in clean room compartments. Chemosphere **36:**1935-1946.

48. **Poulain, A. J., M. Amyot, D. Findlay, S. Telor, T. Barkay, and H. Hintelmann.** 2004. Biological and photochemical production of dissolved gaseous mercury in a boreal lake. Limnol. Oceanogr. **49:**2265-2275.

49. **Price, P. B., and T. Sowers.** 2004. Temperature dependence of metabolic rates for microbial growth, maintenance, and survival. Proc. Natl. Acad. Sci. U.S.A. **101:**4631-4636.

50. **Reniero, D., E. Mozzon, E. Galli, and P. Barbieri.** 1998. Two aberrant mercury resistance transposons in the *Pseudomonas stutzeri* plasmid pPB. Gene **208:**37-42.

51. **Rolfhus, K. R., and W. F. Fitzgerald.** 2004. Mechanisms and temporal variability of dissolved gaseous mercury production in coastal seawater. Mar. Chem. **90:**125-136.
52. **Schaefer, J. K., J. Yagi, J. R. Reinfelder, T. Cardona, K. M. Ellickson, S. Tel-Or, and T. Barkay.** 2004. Role of the bacterial organomercury lyase (MerB) in controlling methylmercury accumulation in mercury-contaminated natural waters. Environ. Sci. Technol. **38:**4304-4311.
53. **Schecher, W. D., and D. C. McAvoy.** 1992. Mineql+ - a software environment for chemical-equilibrium modeling. Comp. Environ. Urb. Sys. **16:**65-76.
54. **Schloss, P. D., and J. Handelsman.** 2005. Introducing DOTUR, a computer program for defining operational taxonomic units and estimating species richness. Appl. Environ. Microbiol. **71:**1501-1506.
55. **Schroeder, W. H., K. G. Anlauf, L. A. Barrie, J. Y. Lu, A. Steffen, D. R. Schneeberger, and T. Berg**. 1998. Arctic springtime depletion of mercury. Nature 394:331-332.
56. **Sellers, P., C. A. Kelly, J. W. M. Rudd, and A. R. MacHutchon.** 1996. Photodegradation of methylmercury in lakes. Nature **380:**694-697.
57. **Siciliano, S. D., N. J. O'Driscoll, and D. R. Lean.** 2002. Microbial reduction and oxidation of mercury in freshwater lakes. Environ. Sci. Technol. **36:**3064-3068.
58. **St Louis, V. L., M. J. Sharp, A. Steffen, A. May, J. Barker, J. L. Kirk, D. J. Kelly, S. E. Arnott, B. Keatley, and J. P. Smol.** 2005. Some sources and sinks of monomethyl and inorganic mercury on Ellesmere Island in the Canadian High Arctic. Environ. Sci. Technol. **39:**2686-2701.
59. **Van Oostdam, J., S. G. Donaldson, M. Feeley, D. Arnold, P. Ayotte, G. Bondy, L. Chan, E. Dewaily, C. M. Furgal, H. Kuhnlein, E. Loring, G. Muckle, E. Myles, O. Receveur, B. Tracy, U. Gill, and S. Kalhok**. 2005. Human health implications of environmental contaminants in Arctic Canada: A review. Sci. Total Environ. 351-352:165-246.
60. **Vetriani, C., Y. S. Chew, S. M. Miller, J. Yagi, J. Coombs, R. A. Lutz, and T. Barkay.** 2005. Mercury adaptation among bacteria from a deep-sea hydrothermal vent. Appl. Environ. Microbiol. **71:**220-226.
61. **Vlassov, A. V., S. A. Kazakov, B. H. Johnston, and L. F. Landweber.** 2005. The RNA world on ice: a new scenario for the emergence of RNA information. J. Mol. Evol. **61:**264-273.
62. **Welander, U.** 2005. Microbial degradation of organic pollutants in soil in a cold climate. Soil. Sediment. Contam. **14:**281-291.
63. **Whalin, L. M., and R. P. Mason.** 2006. A new method for the investigation of mercury redox chemistry in natural waters utilizing deflatable Teflon (R) bags and additions of isotopically labeled mercury. Anal. Chim. Acta **558:**211-221.

64. **Wright, J. G., M. J. Natan, F. M. Macdonnell, D. M. Ralston, and T. V. Ohalloran.** 1990. Mercury(II) thiolate chemistry and the mechanism of the heavy-metal biosensor MerR. Prog. Inorg. Chem. **38:**323-412.

65. **Zubkov, M. V., B. M. Fuchs, H. Eilers, P. H. Burkill, and R. Amann.** 1999. Determination of total protein content of bacterial cells by SYPRO staining and flow cytometry. Appl. Environ. Microbiol. **65:**3251-3257.

7. Conclusions

7.1. Synthèse.

De récentes études ont permis de mettre en évidence une relation entre les dépôts atmosphériques de Hg et la teneur en Hg dans les poissons (17, 27). C'est principalement sous une forme inorganique que le Hg entre dans l'environnement et c'est sous sa forme organique, le methylmercure, qu'il est bioaccumulé par les organismes et bioamplifié dans les réseaux trophiques. La contamination des communautés biologiques, qu'elle soit dans l'extrême Arctique ou en région tempérée, dépend de la synthèse *in-situ* de methylmercure et donc des processus qui directement ou indirectement en affectent la production. Par exemple, Fitzgerald (1993) (14) a proposé que les processus biologiques et chimiques en milieux aquatiques conduisant à la formation de Hg^0 et de MeHg étaient en compétition pour le substrat de la réaction qui serait le Hg(II) labile. Les niveaux de Hg dans les poissons prédateurs seraient donc faibles dans les environnements aquatiques pour lesquels la production de Hg^0 est favorisée.

La neige représente un important réservoir de contaminants atmosphériques en raison de la grande efficacité des cristaux à emprisonner les composés chimiques durant leur formation et leur subséquent dépôt sous forme de précipitation. Le Hg atmosphérique, principalement composé de mercure élémentaire (Hg^0), peut être déposé sous forme de Hg(II) associé aux particules, en solution dans les gouttelettes de pluie ou incorporé dans les flocons de neige vers la surface des écosystèmes terrestres et aquatiques. En raison de la volatilité de sa forme élémentaire, le Hg est globalement distribué et participe à la contamination des écosystèmes terrestres et aquatiques en régions tempérées et polaires (35). En 1998, dans l'extrême Arctique, une équipe canadienne (30) a mis en évidence un nouveau phénomène maintenant connu sous le nom de « mercury depletion events (MDE) » ou « épisodes de

pertes de mercure atmosphérique (EPMA) » débutant à partir du lever du soleil polaire et se terminant lorsque débute la fonte des neiges. Durant cette période, le Hg^0 présent dans l'atmosphère est massivement et rapidement oxydé en Hg(II) sous forme particulaire ou volatile (22, 30) conduisant à une augmentation importante des concentrations en mercure total à la surface de l'accumulation de neige (23). Sur une base annuelle, ces épisodes de déposition massive représentent une augmentation nette de 44% des dépôts totaux de Hg en extrême Arctique (3).

Bien qu'un nombre croissant d'études soit publié sur la dynamique du Hg dans les régions polaires et particulièrement sur les mécanismes impliqués dans les EPMA (4, 9, 22, 32) ou sur leurs impacts sur les niveaux de Hg dans la neige (10, 23, 33), peu d'études se sont intéressées aux transformations rédox affectant ce Hg nouvellement déposé dans la neige (8, 11-13) ou dans les eaux de fonte (7, 22). Il faut noter que ces études mentionnées ci-avant sont basées sur le suivi des concentrations en mercure total ou en Hg^0 dans la neige, l'atmosphère ou les eaux de fonte, notamment grâce au développement de méthodes permettant de concentrer le Hg^0 sur des trappes en or en aspirant l'air interstitiel de l'accumulation de neige (6). Très peu d'études mécanistiques ont été développées en vue de suivre le devenir des espèces de Hg impliquées dans son cycle rédox en milieu polaire (dans la neige et l'eau) et contrôlant son évasion vers l'atmosphère afin de mettre en évidence les variables environnementales responsable de ces transformations. De plus, les données permettant d'estimer la capacité des écosystèmes aquatiques arctiques, durant le printemps et l'été, à recycler le Hg vers l'atmosphère via sa réduction et sa subséquente évasion sont rares (34) et la seule étude expérimentale porte sur un système lacustre (1).

Dans les régions tempérées, bien que le Canada soit recouvert de neige pendant ca. 5 mois par année et que 45% de son territoire soit recouvert de

forêts, aucune étude publiée à ce jour n'a permis d'évaluer dans la neige et les eaux de fonte l'importance des transformations redox affectant son devenir après sa déposition.

Dans ce contexte, cette thèse apporte une contribution significative permettant de mettre en évidence les zones susceptibles d'accumuler le Hg, d'identifier les mécanismes et les variables environnementales qui contrôlent le cycle rédox du Hg, et d'évaluer l'importance relative des réactions de réduction et d'oxydation. L'étude de la distribution des différentes espèces chimiques de Hg dans la neige ainsi que les facteurs environnementaux en affectant les transformations est d'intérêt écotoxicologique puisqu'elle se rapporte à la discipline qui, en combinant les méthodes utilisés en écologie et en toxicologie, étudie les effets d'une substance toxique, particulièrement les contaminants, sur l'environnement; dans ce contexte, ce n'est pas tant l'évaluation de la toxicité du Hg à laquelle nous nous sommes intéressés mais plutôt au suivi des concentrations en Hg dans l'environnement en vue de mieux prédire l'exposition des communautés biologiques à la contamination. Cette étude est aussi d'intérêt biogéochimique puisqu'elle traite de la transformation et du devenir du Hg dans la biosphère grâce à des processus biologiques, chimiques et géologiques; nous sommes intéressés principalement aux processus biologiques et chimiques.

Spécifiquement, dans l'extrême Arctique nous avons mis en évidence que le Hg nouvellement déposé, après son oxydation dans l'atmosphère ((1), Fig. 9A) peut être réduit et donc potentiellement réémis vers l'atmosphère ((2) et (3), Fig. 9A). Cependant, lorsque l'énergie lumineuse incidente diminue en qualité (suppression de certaines longueur d'onde) ou en quantité (diminution de l'éclairement), limitant ainsi la réaction de réduction, une partie du Hg(0) nouvellement formé peut être détruit par oxydation ((4), Fig.9 A). Ceci constitue la première preuve expérimentale de photooxydation d'un métal sous sa forme

élémentaire, le Hg(0), dans la neige. Il est donc important en vue d'affiner les modèles visant à élaborer les bilans en masse de Hg en extrême Arctique de tenir compte du fait, qu'en quelques heures seulement, le Hg(0) nouvellement produit et non exporté vers l'atmosphère peut être de nouveau immobilisé au sein de l'accumulation de neige. Ceci permet d'établir un lien direct entre les changements environnementaux se produisant dans l'extrême Arctique et le cycle du Hg. Un rayonnement énergétique incident plus important lié à une diminution des niveaux d'ozone atmosphérique (24, 26, 31) devrait améliorer l'efficacité avec laquelle le Hg est recyclé vers l'atmosphère en raison de niveaux de radiations UVB plus élevées (1). Cependant, ce mécanisme serait partiellement atténué en raison d'une couverture nuageuse plus grande engendrée par une augmentation globale des température, particulièrement aux pôles (18), entrainant une grande variabilité dans les niveaux de radiations UVB à la surface (24).

Lors de la fonte des neiges et dans les mares et ruisseaux, la réduction du Hg est atténuée avec une augmentation croissante des concentrations en ions chlorures ((5) Fig. 9A). L'influence des ions chlorures dans le cycle rédox du Hg avait déjà été démontrée lors d'ajout de Hg(0) à des solutions d'eau naturelles salées (19, 20). Nous apportons une preuve expérimentale en milieu naturel et sur une gamme de salinité couvrant ca. 4 ordres de grandeur, d'une diminution de la réduction du Hg en raison d'une augmentation de salinité, probablement en raison de la présence croissante d'halogènes. De plus, nous avons mis en évidence l'influence déterminante des particules sur les réactions de réduction ((6) Fig. 9A); en effet une série d'expériences de filtration nous a permis de montrer que la fraction particulaire était nécessaire au recyclage du Hg vers l'atmosphère, faisant potentiellement intervenir des oxydes de fer, particulièrement en milieu salé. Ce résultat ouvre de nouvelles perspectives de recherche quant aux mécanismes impliqués dans la réduction du Hg,

notamment dans le cadre de réactions en phases hétérogènes. Finalement, bien que des études aient montré le rôle des communautés algales dans la réduction du Hg (5, 21, 25, 28), nous apportons la première preuve que les algues en milieu salé ont le potentiel de détruire le Hg^0 nouvellement produit, en présence de lumière et à l'obscurité, participant ainsi à son oxydation ((7) Fig. 9A). Ces données soulignent la vulnérabilité des écosystèmes côtiers et marins à des dépôts accentués de mercure. En effet, l'oxydation du Hg^0 participe à augmenter le temps de séjour du Hg dans le milieu. Les zones situées à l'interface entre les systèmes d'eau douces et marins présentent des concentrations en sulfate optimales pour la méthylation (15). Ensemble ces conditions favoriseraient donc la production de methylmercure.

Nous avons découvert que les microbes proliférant dans les zones côtières marines de l'extrême arctique pouvaient affecter la toxicité et la mobilité des contaminants métalliques dans les régions polaires ((8) Fig. 9A). En effet, nous avons apporté les premières preuves de la présence et de l'expression de divers gènes *mer*A (faisant partie de l'opéron *mer*, responsable de la résistance bactérienne au mercure) codant pour la réductase du mercure, dont certains sont phylogénétiquement associés avec des bactéries psychrophiles. L'utilisation d'un modèle cinétique nous a permis de mettre en évidence que 90% du mercure élémentaire présent dans les eaux de surface de l'océan arctique pouvait être d'origine bactérienne et que le Hg(0) pouvait constituer jusqu'à 70% du réservoir de Hg total. Ceci représente la première preuve que les microbes des régions polaires ont la capacité d'être des acteurs de premier plan dans le cycle biogéochimique du Hg. En effet, bien que les milieux côtiers/marins soient particulièrement propices à la formation de MeHg, l'expression de l'opéron *mer* permettrait de limiter le transfert de Hg vers les organismes situés à la base des chaînes alimentaires en participant à la destruction du MeHg via la déméthylation réductive en plus de contribuer à

recycler le Hg vers l'atmosphère. Cette découverte soulève de nouvelles avenues de recherche impliquant les microorganismes dans les cycles biogéochimiques du Hg aux hautes latitudes que nous avons présentées dans notre chapitre de synthèse sur la (micro)biogéochimie du Hg en régions polaires.

En étudiant la distribution des concentrations en Hg total dans la neige de surface le long d'un transect couvrant ca. 100 km au travers de l'ile de Cornwallis, nous avons montré qu'au moment de la fonte printanière la majorité du Hg est associée aux particules, particulièrement dans la neige déposée sur la banquise (jusqu'à ca. 90%), et majoritairement associé à la fraction particulaire comprise entre 2,7 et 10 µm ((9) Fig. 9A). Les bas niveaux de Hg enregistrés à la surface de la neige démontrent qu'une partie du Hg a été perdu vers l'atmosphère avant la fonte, probablement par photoréduction, mais les concentrations élevées enregistrées en profondeur à l'interface banquise/neige suggèrent que cette interface constitue un site d'accumulation en Hg. Ceci peut représenter un risque important sur les communautés biologiques vivant en association avec la banquise et formant la base des réseaux alimentaires arctique ((10) Fig. 9A).

En régions tempérées, dans un couvert de neige sous un couvert forestier, le cycle du Hg en général, et les transformations rédox affectant son devenir en particulier, restaient inconnus. De plus, bien que l'oxydation du Hg(0) nouvellement produit semble être un processus significatif dans le cycle du Hg, l'importance relative des réactions photo-induites d'oxydation et de réduction au cours de la journée reste mal documentée. Ces travaux ont permis de mettre en évidence que la neige déposée sous un couvert forestier constitue un puits de mercure, i.e. on peut y observer une accumulation nette de Hg au cours de l'hiver ((1) et (2) Fig. 9B); ceci est du à l'action combinée du « nivolessivage », (voir une analogie avec pluviolessivage ou throughfall) de la végétation par la

neige, qui contribue à son enrichissement en Hg, mais aussi à une production nette de Hg(0) beaucoup plus faible sous un couvert végétal. Une plus faible luminosité incidente atteignant la neige déposée sous les arbres limite la photoréduction, et les processus d'oxydation accrus favorisent une accumulation de Hg. En revanche et comme démontré précédemment, le recyclage du Hg vers l'atmosphère semble être une voie majeure de perte de Hg dans la neige déposée en milieu ouvert ((3) Fig. 9B).

Lors de la fonte des neiges les taux de réduction diminuent en fonction du temps ((4) Fig. 9B) soulignant une possible diminution de la réactivité des espèces de Hg photoréductibles lors du ruissellement vers l'eau de lac. Ceci correspond à ce que nous avons observé dans l'extrême Arctique et met en évidence la grande réactivité des espèces atmosphériques de Hg nouvellement déposées. Cette hypothèse est supporté par des travaux réalisés grâce à l'addition d'isotopes stables à des eaux naturelles qui ont montré une évasion importante du Hg nouvellement déposé (2, 29).

A l'instar de ce que nous avons observé dans la neige et afin de savoir si l'oxydation rapide du Hg(0) nouvellement formé était un mécanisme important dans les eaux de surface, nous avons exécuté une série d'expériences permettant de suivre les taux de production et de consommation de Hg(0) au cours d'une période de 24 h. Nous avons montré qu'au maximum d'intensité lumineuse la réduction du Hg était la réaction prépondérante; en revanche durant les périodes de plus faibles intensités lumineuses telles que celles observées le soir ou la nuit, l'oxydation était prépondérante ((5) Fig. 9B). Cependant, les acteurs impliqués dans ces réactions d'oxydoréduction, bien qu'étant probablement de nature organique (16), restent mal connus. De plus, au-delà de la nature exacte des composés réactifs impliqués, les mécanismes réactionnels, bien qu'associé à des cinétiques de pseudo premier ordre, restent non identifiés. Cette absence de données ralentit les efforts de modélisation qui

pourrait permettre d'identifier les écosystèmes « source » ou « puits » de mercure, en quantifiant le réservoir de Hg photoréductible.

Table 7.I. Description de la figure 7.1.

Numéro	Description
1A	Dépositions de Hg à la surface des écosystèmes Arctiques
2A	Photoréduction dans la neige du Hg(II) nouvellement déposé
3A	Évasion du Hg(0) nouvellement produit
4A	Oxydation (photo-induite), dans la neige, du Hg(0) nouvellement produit
5A	Diminution de la réduction du Hg(II), dans l'eau, suivant un gradient croissant de salinité
6A	Les particules (potentiellement des oxydes métalliques) favorisent la réduction du Hg, dans l'eau, particulièrement en milieu salé.
7A	Les exsudats d'algues favorisent l'oxydation du Hg(0) nouvellement formé, dans l'eau, à l'obscurité et à la lumière
8A	Les bactéries, grâce à l'expression des gènes de résistance au Hg, contribuent à la formation de plus de 50% du Hg(0) dans les eaux de surface salées de l'extrême Arctique
9A	Les concentrations en Hg dans la neige sont plus élevées en milieux côtiers et marins qu'à l'intérieur des terres; le Hg est préférentiellement associé aux particules (jusqu'à 90%) dans la neige déposée sur la banquise que dans la neige déposée à l'intérieur des terres. L'interface banquise / neige est un site d'accumulation du Hg
10A	L'accumulation de neige est une source de Hg vers les eaux de surface lors de la fonte, potentiellement menaçant les communautés biologiques associées à la banquise
1B, 2B, 3B	La neige déposée sous un couvert forestier constitue un puits de mercure, i.e. on peut y observer une accumulation nette de Hg au cours de l'hiver. La neige déposée en milieu ouvert est une source de Hg vers l'atmosphère
4B	Les taux de réduction du Hg diminuent avec le temps lors de la fonte
5B	Dans les eaux de surface du bouclier Canadien, la réduction du Hg(II) est la réaction prépondérante durant les périodes de fortes intensités lumineuses; l'oxydation du Hg(0) est prépondérante durant les périodes de faibles intensités lumineuses, le soir ou la nuit

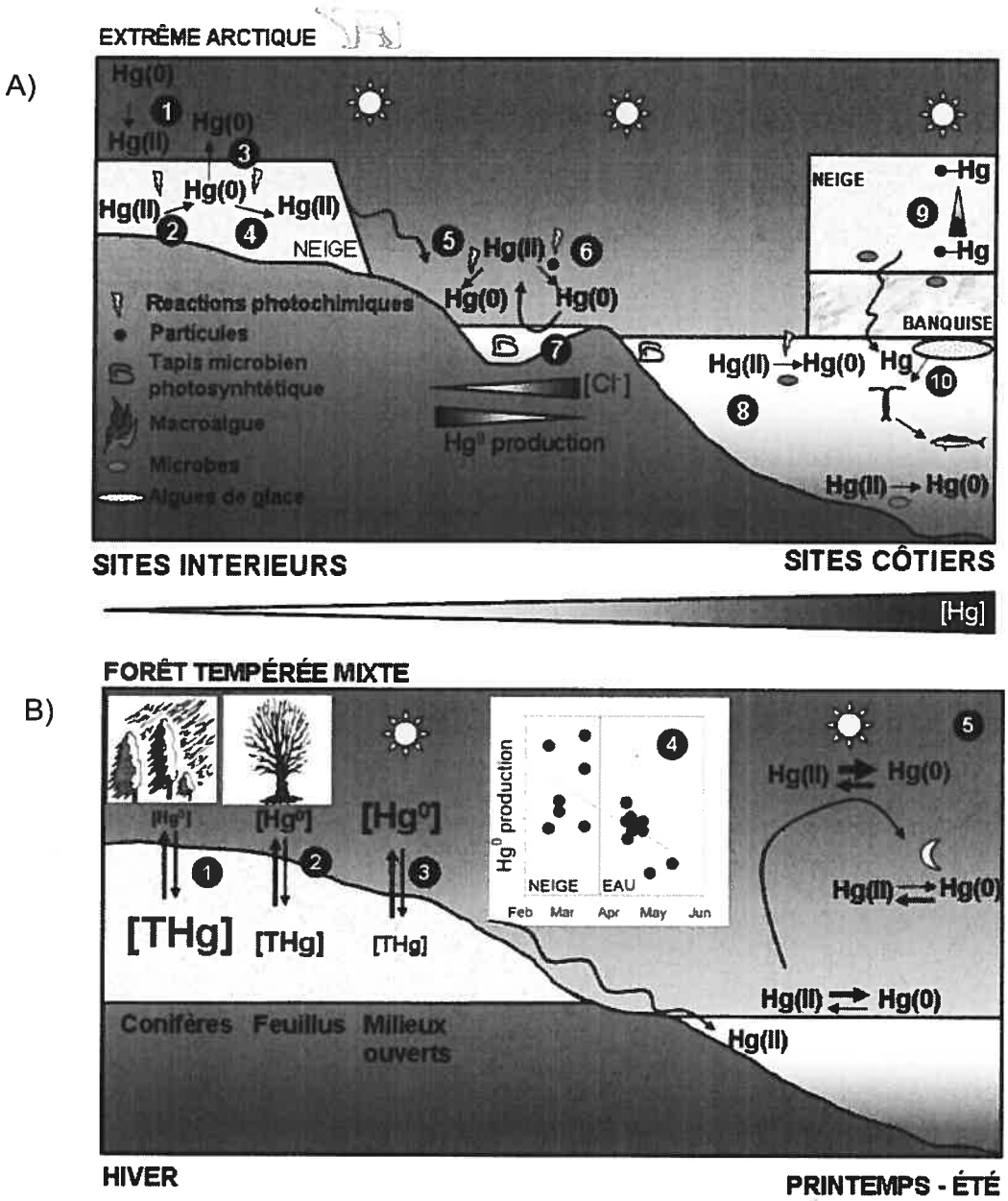

Figure 7.1. Figure synthétisant les principales voies impliquées dans la transformation des espèces inorganiques de Hg dans la neige et les eaux de surface de l'extrême Arctique (panneau du haut) et des régions tempérées (panneau du bas). Les chiffres réfèrent à la description détaillées des ces transformations dans le texte.

7.2. Avenue de recherche

Ces travaux de thèse ont permis de mieux comprendre la dynamique et les transformations affectant le Hg dans la neige et les eaux de surface en régions tempérées et arctiques mais ont aussi révélé certaines limitations à notre approche expérimentale, soulevé de nouvelles questions et ont permis de déterminer de nouvelles avenues de recherche. Pour chacun des objectifs rappelés ci-après, des questions / avenues de recherche sont présentées, de manière non extensive.

Évaluer la distribution des espèces de Hg dans la neige de l'extrême Arctique.

Nous avons contribué à i) déterminer que la majorité du Hg présent dans la neige était associée aux particules d'une taille comprises entre 0.2 µm et 10 µm et ii) identifier l'interface neige/banquise comme un site d'accumulation de Hg. Cependant, une incertitude demeure quant à l'influence d'un changement de phase (passage de l'état solide vers l'état liquide) sur la spéciation du Hg. En raison de la très grande affinité de certains aérosols pour l'eau (caractère hygroscopique) il est probable que l'association du Hg avec les particules soit fortement influencée par l'étape de fonte à laquelle nous avons du soumettre nos échantillons en vue de procéder aux analyses. De plus, en raison de la très haute résolution d'échantillonnage nécessaire à l'étude du mouvement d'espèces chimiques au sein d'une accumulation de neige et que nous n'avons pu atteindre, le mécanisme de transfert du Hg de l'interface air/neige vers l'interface neige/banquise reste spéculatif.

- Il sera important de pouvoir développer des techniques analytiques suffisamment sensibles en vue de déterminer la fraction particulaire de Hg dans la neige solide. Une amélioration de nos techniques analytiques permettrait

aussi de localiser les contaminants métalliques sur les flocons de neige. Ceci est particulièrement important si l'on souhaite déterminer le rôle des microorganismes sur la transformation des contaminants dans la neige solide.

- Quels sont les mécanismes qui affectent la mobilité des contaminants au sein de l'accumulation de neige ? La métamorphose des cristaux de neige (par perte et gain de vapeur d'eau) au sein de l'accumulation de neige est-elle responsable de la migration vers le bas des espèces particulaires ?

Déterminer les transformations rédox qui affectent le Hg dans une accumulation de neige en extrême arctique.

Nous avons montré que la production nette de Hg(0) pouvait rapidement décliner si l'intensité du rayonnement incident diminuait en quantité (diminution de l'éclairement) ou en qualité (suppression des UV). Ceci est un signe de l'oxydation du Hg(0) plus importante à de faibles intensités lumineuses ou en raison de rayonnements moins énergétiques, responsables de l'oxydation. Cependant, nous n'avons pu identifier ni les intermédiaires réactionnels impliqués dans cette oxydation rapide.

- Cette oxydation se produit-elle dans l'espace interstitiel entre les cristaux de neige ou se produit-elle au sein ou à la surface du flocon?

- Quel est le temps de séjour du Hg(0) nouvellement formé au sein d'une accumulation de neige ?

- Sur quelle distance le Hg(0) voyage-t-il au sein de l'accumulation de neige avant d'être réoxydé ?

Ces questions sont importantes en vue de mieux comprendre les échanges air/neige conduisant à une meilleure modélisation du transport du Hg dans un milieu hétérogène tel que la neige.

Comprendre l'importance relative des transformations chimiques et biologiques du Hg dans les eaux douces et salées de l'extrême Arctique au printemps et en été. Évaluer l'importance des bactéries sur le cycle du Hg dans l'extrême Arctique grâce à l'expression de gènes de résistance au Hg.

Nous avons montré que la production de Hg(0) dans l'eau était fortement altérée suivant un gradient croissant de salinité couvrant ca. 4 ordres de grandeur. En milieu salé, les microorganismes, algues et microbes, participent à l'oxydation du Hg(0) nouvellement produit grâce à la production d'exsudats. La filtration (0,45 µm) des eaux salées contribue à diminuer fortement la production de Hg(0). Les microbes extraits de la biomasse collectée en milieux côtiers et marins possèdent et expriment le *mer*-opéron responsable, notamment, de la réduction du Hg(II).

- Quel est le rôle des ions chlorures en particulier, et des halogènes en général, dans les mécanismes d'oxydation du Hg(0) ? Se limitent-ils à stabiliser l'intermédiaire réactionnel, le Hg(I) ? Participent-ils principalement à la formation de radicaux impliqués secondairement dans des réactions d'oxydation ?

- De quelle manière les exsudats participent-ils aux réactions d'oxydation ? Servent-ils de précurseurs aux réactions radicalaires ? Sont-ils des acteurs de premier plan possédant une activité rédox propre ?

- En milieu salé, une diminution de la production de Hg(0) après filtration combinée à une absence de production au noir nous ont conduits à éliminer le rôle des microbes. Cependant notre approche moléculaire nous a permis de mettre en évidence la présence et l'expression des gènes impliqués dans la réduction du Hg. Dans l'état actuel de nos connaissances nous avons expliqué ceci par des temps d'incubation trop courts ne permettant pas de mettre en évidence l'influence de la reductase du Hg. Cependant, notre exercice de

modélisation nous indique que plus de 50% du Hg(0) présent dans les eaux de surface pouvait être d'origine biogénique.

L'évaluation de l'interaction entre les réactions photochimiques et les transformations biologiques devient particulièrement pertinente dans ce cas. Certaines protéines ou enzymes impliquées dans les mécanismes de transformation du Hg pourraient être dépendantes de la lumière. Dans un contexte plus général, il sera intéressant de s'attarder sur le rôle de la lumière comme déclencheur de réactions redox conduites par des microbes, et non liées à la photosynthèse, particulièrement si celles-ci permettent de moduler la mobilité des contaminants.

- La réduction du Hg en phase hétérogène reste mal connue. En raison des propriétés semi-conductrices des oxydes métalliques, il ne serait pas surprenant que ceux-ci puissent être impliqués dans le cycle photorédox du Hg dans les eaux naturelles. Nous faisions ici référence au rôle des oxydes métalliques et particulièrement au rôle des oxydes de fer. Ceux-ci peuvent intervenir de deux manières i) soit par photo-dissolution réductive d'oxyde de fer en présence d'oxalate qui conduisent à la formation de radicaux organiques (e.g. $C_2O_4^{\bullet-}$) qui peuvent réduire le Hg(II) ou ii) en raison des propriétés semi-conductrices des oxydes métalliques et du transfert d'électron de la bande de valence vers la bande de conduction et potentiellement réduire le Hg(II) adsorbé à la surface de l'oxyde. L'énergie associée à la bande interdite (*band gap*) des oxydes de fer (α-Fe_2O_3) est de 2.34 eV (correspondant à λ=516 nm) (41). Un rayonnement lumineux d'énergie supérieure (donc λ<516 nm, correspondant à UVA, UVB ou Visible) pourrait générer ce transfert d'électron et donc réduire le Hg(II) en Hg(0)

- L'oxydation directe du Hg(0) par les microbes représente l'une des réactions du cycle biogéochimique du Hg les plus mal connues. De futures recherches devront permettre d'en évaluer l'importance en milieu naturel.

Déterminer, en milieu tempéré, l'influence du couvert forestier sur la dynamique du Hg dans la neige.

Nous avons montré que la neige déposée sous un couvert forestier tendait à être enrichie en Hg en raison de i) l'influence du nivolessivage de la canopée et ii) d'une atténuation des réactions de réduction combinée à l'oxydation du Hg(0) nouvellement produit.

- Une inconnue subsiste encore quant à la contribution des dépôts secs sur les dépôts de Hg durant l'hiver. Bien que les dépôts secs soient généralement moins importants durant l'hiver car la présence de neige contribue à minimiser les irrégularités du paysage, il est important de quantifier leur importance dans flux de Hg, participant potentiellement à la contamination des écosystèmes durant l'hiver.

- Au-delà d'une mesure de flux qui est nécessaire, il est aussi critique de quantifier la réactivité du mercure apporté par les dépôts secs, notamment en termes de leur capacité à être photoréduits. En effet, il est possible au sein d'une accumulation de neige que le Hg occupe des sites différents (e.g. à la surface des flocons) que ceux occupés par le Hg apporté par les dépôts humides. En raison de leur positionnement en surface du flocon, il est possible que les dépôts secs de Hg soient plus prompts à participer aux réactions photochimiques. De plus, l'émergence de l'étude de la microbiologie atmosphérique et nivale place au premier plan les interactions entre espèces réactives de Hg et les particules, supportant ainsi l'activité possible de microorganismes.

- Dans le chapitre de revue de littérature, nous mentionnons que les bactéries du sol en milieux froids et responsables de la dégradation du MeHg utilisent principalement des composés organiques simples, C1, (*e.g.*, CH_3-Br) comme source de carbone (37). Nous n'établissons pas de lien entre CH_3-Br en

milieu tempéré et l'oxydation du Hg. Cependant un lien très intéressant soulevé par ce commentaire peut être établit.

Les sources naturelles de CH_3-Br en milieux tempérés peuvent être abiotiques ou biotiques (5). La principale source abiotique est l'oxydation de la matière organique couplée au cycle rédox du fer(III), agissant comme accepteur d'électron (38). La lumière ou l'activité des microbes n'est pas requise. La production biogénique d'halocarbures (e.g., CH_3-Br ou CH_3-Cl) est principalement relié à l'activité des champignons dégradant le bois mort en forêt (36). Des travaux récents ont permis de mettre en évidence que la biomasse microbienne d'un sol de toundra atteint son pic annuel d'activité sous un couvert de neige et que la plupart de cette biomasse est composée de champignons (40). Le cycle suivant Figure 7.2. pourrait être proposé pour illustrer le lien entre halocarbures biogéniques et cycle rédox du Hg.

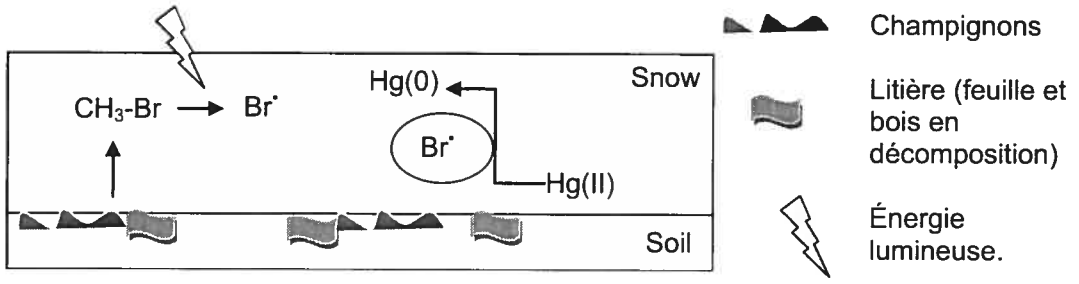

Figure 7.2. Représentation possible du rôle des halocarbures biogéniques sur le cycle rédox du Hg dans la neige.

Mettre en évidence les variations journalières du cycle photo-rédox du Hg dans les eaux douces de surface en régions tempérées.

Cette étude, conduite dans les eaux de surface d'un lac du bouclier canadien, a été initiée à la suite des résultats obtenu dans le chapitre 3 (objectif 2) et démontrant l'instabilité du Hg(0) nouvellement formé par photoréduction. Grâce à ces travaux, nous avons évalué simultanément l'importance relative

des réactions d'oxydation et de réduction dans les eaux de surface au cours d'une journée d'été.

- Les avancées technologiques importantes des dernières années permettent de mesurer en temps « quasi » réel et *in-situ* les concentrations en Hg(0) dans les eaux de surface. Ces concentrations, combinées à des modèles de transfert de Hg(0) à l'interface eau/air (e.g. modèle de la double couche), permettent d'évaluer le flux de Hg(0) perdu vers l'atmosphère. Cependant, ces appareils restent encore coûteux et le développement de modèles prédictifs devient nécéssaire en vue de déterminer la capacité d'un écosystème à perdre du Hg. Ces modèles, afin d'être facilement applicables et de servir de support scientifique dans un contexte législatif, doivent pouvoir être basés des variables simples à mesurer, e.g. [Hg], [DOC], pH, intensité lumineuse et vitesse du vent. L'intégration des données de taux de réduction et d'oxydation obtenus au cours des 10 dernières années, ainsi que l'analyse des variables influençant ces taux, devraient permettre de développer des modèles prédictifs efficaces non seulement à l'échelle locale d'un lac mais aussi à l'échelle régionale voire globale.

7.3. Lien entre sciences de l'environnement et génie génétique / biologie moléculaire

Ces travaux de thèse ont notamment permis de mettre en évidence qu'en extrême Arctique les zones côtières pouvaient être soumises à des concentrations élevées en Hg (rôle des EPMA) associées à une faible perte vers l'atmosphère (réduction altérée, oxydation favorisée). Cependant, c'est aussi dans ces milieux que nous avons mis en évidence l'expression de gènes impliqués dans la résistance au mercure au sein de consortia d'algues et de bactéries. De futures recherches devront permettre d'expliquer les raisons pour lesquelles ces gènes sont exprimés et quelles sont les variables

environnementales qui contrôlent cette expression. Le développement de nouvelles technologies génétiques et moléculaires adaptées aux conditions environnementales permettra de mieux appréhender la dynamique des contaminants en milieu naturel, ainsi que l'action conjointe et synergétique de plusieurs contaminants. En ciblant directement les gènes et les protéines impliqués dans les mécanismes de transport et de transformation des métaux traces, il devient possible de se libérer des artefacts expérimentaux associés à l'ajout de composés chimiques en solution. Cependant pour faire le lien entre un phénotype exprimé par un microbe (e.g. résistance au Hg via sa réduction) et son importance environnementale, il faut aussi caractériser les conditions qui ont conduit à l'expression de ce phénotype. Il devient donc nécessaire de s'intéresser aux interactions que les contaminants, ou un ensemble de contaminants, peuvent avoir avec les gènes ainsi que l'importance des variables environnementales classiques (e.g. pH, force ionique, matière organique) sur l'expression de ces gènes.

Une approche intéressante, associant le génie génétique combiné à la modélisation de la spéciation des métaux dans l'environnement, réside dans l'utilisation de biorapporteurs (Annexe 10.1). Par exemple, dans le cadre de cette thèse nous avons tenté de caractériser les variables biologiques influençant les transformations rédox du Hg. Généralement, afin de cibler des voies métaboliques précises impliquées dans des transformations biogéochimiques, le recours aux inhibiteurs de métabolisme est souvent de mise; dans les travaux de recherche présentés ici nous avons utilisé le DCMU, un inhibiteur du photosystème II (affectant les organismes photosynthétiques eucaryotes ainsi que les cyanobactéries). Cependant, ces inhibiteurs (e.g. inhibiteur de la photosynthèse, des voies de sulfato-réduction, de méthanogénèse, des chaines de transporteur d'électron), bien que très efficaces dans le cadre d'expériences ciblées en solutions contrôlées, peuvent être

entachées d'incertitude lorsqu'utilisés en milieu naturel dont la composition est rarement entièrement définie. Cette incertitude est principalement reliée i) aux interactions possibles que le Hg peut avoir avec ces inhibiteurs et ii) aux interactions que le milieu peut avoir avec ces inhibiteurs. Par exemple, lorsque l'on utilise un inhibiteur afin de contrôler une voie métabolique intracellulaire affectant la spéciation du Hg (rédox ou (dé)méthylation), il est important de savoir si l'inhibiteur affecte, dans un premier temps, la prise en charge du Hg.

Afin d'illustrer l'intérêt des avancées technologiques en génétique et biologie moléculaire adaptées aux sciences de l'environnement nous proposons, en annexe, un bref aperçu de l'utilisation d'un biorapporteur luminescent (*E coli* HMS174 pRB28). L'intérêt d'utiliser un biorapporteur est double, il permet de travailler avec une membrane « vivante » ainsi qu'en temps réel (dans le cas d'un biorapporteur luminescent). Bien que *E. coli* soit généralement associée à une contamination anthropique, elle constitue néanmoins un outil particulièrement efficace car son génome est entièrement séquencé et les voies métaboliques impliquées dans le transport du Hg pourraient être facilement déterminées. Dans un premier temps nous avons testé l'influence de différents inhibiteurs sur la prise en charge du Hg (Annexe 10.2). Bien que l'utilisation du biorapporteur en vue de quantifier le Hg biodisponible reste actuellement controversée et semble limitée aux solutions avec de faibles teneurs en matière organique (Annexe 10.3), son utilisation dans un but qualitatif semble très prometteuse. Par exemple, de nombreuses variables environnementales peuvent être testées en vue de connaître leur influence sur la prise en charge du Hg à des concentrations « trace »; par exemple, le rôle de la matière organique (Annexe 10.4), du pH (Annexe 10.5), du glutathion (Annexe 10.6), ou encore de la spéciation rédox du Hg (Annexe 10.7).

7.4. Références bibliographiques

1. **Amyot, M., D. Lean, and G. Mierle.** 1997. Photochemical formation of volatile mercury in high Arctic lakes. Environmental Toxicology and Chemistry **16:**2054-2063.
2. **Amyot, M., G. Southworth, S. E. Lindberg, H. Hintelmann, J. D. Lalonde, N. Ogrinc, A. J. Poulain, and K. A. Sandilands.** 2004. Formation and evasion of dissolved gaseous mercury in large enclosures amended with (HgCl2)-Hg-200. Atmospheric Environment **38:**4279-4289.
3. **Ariya, P. A., A. P. Dastoor, M. Amyot, W. H. Schroeder, L. Barrie, K. Anlauf, F. Raofie, A. Ryzhkov, D. Davignon, J. Lalonde, and A. Steffen**. 2004. The Arctic: a sink for mercury. Tellus Series B-Chemical and Physical Meteorology 56:397-403.
4. **Ariya, P. A., A. Khalizov, and A. Gidas.** 2002. Reactions of gaseous mercury with atomic and molecular halogens: Kinetics, product studies, and atmospheric implications. Journal of Physical Chemistry A **106:**7310-7320.
5. **Ben-Bassat, D., and A. M. Mayer.** 1978. Light induced Hg volatilization and O2 evolution in Chlorella and the effect of DCMU and methylamine. Physiol. Plant **42:**33-38.
6. **Dommergue, A., C. P. Ferrari, and C. F. Boutron.** 2003. First investigation of an original device dedicated to the determination of gaseous mercury in interstitial air in snow. Analytical and Bioanalytical Chemistry **375:**106-111.
7. **Dommergue, A., C. P. Ferrari, P. A. Gauchard, C. F. Boutron, L. Poissant, M. Pilote, P. Jitaru, and F. C. Adams**. 2003. The fate of mercury species in a sub-arctic snowpack during snowmelt. Geophysical Research Letters 30.
8. **Dommergue, A., C. P. Ferrari, L. Poissant, P. A. Gauchard, and C. F. Boutron.** 2003. Diurnal cycles of gaseous mercury within the snowpack at Kuujjuarapik/Whapmagoostui, Quebec, Canada. Environmental Science & Technology **37:**3289-3297.
9. **Ebinghaus, R., H. H. Kock, C. Temme, J. W. Einax, A. G. Lowe, A. Richter, J. P. Burrows, and W. H. Schroeder**. 2002. Antarctic springtime depletion of atmospheric mercury. Environmental Science & Technology 36:1238-1244.
10. **Ebinghaus, R., C. Temme, S. E. Lindberg, and K. J. Scott.** 2004. Springtime accumulation of atmospheric mercury in polar ecosystems. Journal De Physique Iv **121:**195-208.
11. **Ferrari, C. P., A. Dommergue, C. Boutron, P. Jitaru, and F. C. Adams.** 2004. Profiles of Mercury in the snow pack at Station Nord,

Greenland, shortly after polar sunrise. Geophysical Research Letters **31:**L03401.

12. **Ferrari, C. P., A. Dommergue, C. F. Boutron, H. Skov, M. Goodsite, and B. Jensen.** 2004. Nighttime production of elemental gaseous mercury in interstitial air of snow at Station Nord, Greenland. Atmospheric Environment **38:**2727-2735.
13. **Ferrari, C. P., P. A. Gauchard, K. Aspmo, A. Dommergue, O. Magand, E. Bahlmann, S. Nagorski, C. Temme, R. Ebinghaus, A. Steffen, C. Banic, T. Berg, F. Planchon, C. Barbante, P. Cescon, and C. F. Boutron**. 2005. Snow-to-air exchanges of mercury in an Arctic seasonal snow pack in Ny-Alesund, Svalbard. Atmospheric Environment 39:7633-7645.
14. **Fitzgerald, W. F.** 1993. Presented at the 9th International conference on Heavy Metals in the Environment, Toronto, ON, Canada, 1993.
15. **Fitzgerald, W. F., and C. Lamborg.** 2004. Geochemistry of mercury in the environment, p. 107-148. *In* B. Sherwood Lollar (ed.), Environmental Geochemistry, vol. 9. Elsevier.
16. **Garcia, E., M. Amyot, and P. A. Ariya.** 2005. Relationship between DOC photochemistry and mercury redox transformations in temperate lakes and wetlands. Geochimica et Cosmochimica Acta **69:**1917-1924.
17. **Hammerschmidt, C. R., and W. F. Fitzgerald.** 2006. Methylmercury in freshwater fish linked to atmospheric mercury deposition. Environmental Science & Technology.
18. **Holland, M. M., and C. M. Bitz.** 2003. Polar amplification of climate change in coupled models. Climate Dynamics **21:**221-232.
19. **Lalonde, J. D., M. Amyot, A. M. L. Kraepiel, and F. M. M. Morel.** 2001. Photooxidation of Hg(0) in artificial and natural waters. Environmental Science & Technology **35:**1367-1372.
20. **Lalonde, J. D., M. Amyot, J. Orvoine, F. M. M. Morel, J. C. Auclair, and P. A. Ariya.** 2004. Photoinduced oxidation of Hg-0 (aq) in the waters from the St. Lawrence estuary. Environmental Science & Technology **38:**508-514.
21. **Lanzillotta, E., C. Ceccarini, R. Ferrara, E. Dini, E. Frontini, and R. Banchetti.** 2004. Importance of the biogenic organic matter in photo-formation of dissolved gaseous mercury in a culture of the marine diatom Chaetoceros sp. Science of the Total Environment **318:**211-221.
22. **Lindberg, S. E., S. Brooks, C. J. Lin, K. J. Scott, M. S. Landis, R. K. Stevens, M. Goodsite, and A. Richter.** 2002. Dynamic oxidation of gaseous mercury in the Arctic troposphere at polar sunrise. Environmental Science & Technology **36:**1245-1256.
23. **Lu, J. Y., W. H. Schroeder, L. A. Barrie, A. Steffen, H. E. Welch, K. Martin, L. Lockhart, R. V. Hunt, G. Boila, and A. Richter.** 2001.

Magnification of atmospheric mercury deposition to polar regions in springtime: the link to tropospheric ozone depletion chemistry. Geophysical Research Letters 28:3219-3222.

24. **Madronich, S., R. L. McKenzie, L. O. Björn, and M. M. Caldwell.** 1998. Changes in biologically active ultraviolet radiation reaching the Earth's surface. J. Photochem. Photobiol. B: Biol **46:**5–19.
25. **Mason, R. P., F. M. M. Morel, and H. F. Hemond.** 1995. The Role of Microorganisms in Elemental Mercury Formation in Natural-Waters. Water Air and Soil Pollution **80:**775-787.
26. **McKenzie, R., B. Conner, and G. Bodeker.** 1999. Increased summertime UV radiation in New Zealand in response to ozone loss. Science **285:**1709-1711.
27. **Orihel, D. M., M. J. Paterson, C. C. Gilmour, R. A. Bodaly, P. J. Blanchfield, H. Hintelmann, R. C. Harris, and J. W. M. Rudd**. 2006. Effect of loading rate on the fate of mercury in littoral mesocosms. Environmental Science & Technology 40:5992-6000.
28. **Poulain, A. J., M. Amyot, D. Findlay, S. Telor, T. Barkay, and H. Hintelmann.** 2004. Biological and photochemical production of dissolved gaseous mercury in a boreal lake. Limnology and Oceanography **49:**2265-2275.
29. **Poulain, A. J., D. M. Orihel, M. Amyot, M. J. Paterson, H. Hintelmann, and G. Southworth.** 2006. Relationship between the loading rate of inorganic mercury to aquatic ecosystems and dissolved gaseous mercury production and evasion. Chemosphere.
30. **Schroeder, W. H., K. G. Anlauf, L. A. Barrie, J. Y. Lu, A. Steffen, D. R. Schneeberger, and T. Berg.** 1998. Arctic springtime depletion of mercury. Nature 394:331-332.
31. **Smith, R. C., B. B. Prezelin, K. S. Baker, R. R. Bidigare, N. P. Boucher, T. Coley, D. Karentz, S. Macintyre, H. A. Matlick, D. Menzies, M. Ondrusek, Z. Wan, and K. J. Waters.** 1992. Ozone Depletion - Ultraviolet-Radiation and Phytoplankton Biology in Antarctic Waters. Science 255:952-959.
32. **Sprovieri, F., N. Pirrone, M. S. Landis, and R. K. Stevens.** 2005. Oxidation of gaseous elemental mercury to gaseous divalent mercury during 2003 polar sunrise at Ny-Alesund. Environmental Science & Technology **39:**9156-9165.
33. **Steffen, A., W. Schroeder, J. Bottenheim, J. Narayan, and J. D. Fuentes.** 2002. Atmospheric mercury concentrations: measurements and profiles near snow and ice surfaces in the Canadian Arctic during Alert 2000. Atmospheric Environment **36:**2653-2661.

34. **Tseng, C. M., C. Lamborg, W. F. Fitzgerald, and D. R. Engstrom.** 2004. Cycling of dissolved elemental mercury in Arctic Alaskan lakes. Geochimica et Cosmochimica Acta **68:**1173-1184.
35. **Van Oostdam, J., S. G. Donaldson, M. Feeley, D. Arnold, P. Ayotte, G. Bondy, L. Chan, E. Dewaily, C. M. Furgal, H. Kuhnlein, E. Loring, G. Muckle, E. Myles, O. Receveur, B. Tracy, U. Gill, and S. Kalhok.** 2005. Human health implications of environmental contaminants in Arctic Canada: A review. Science of the Total Environment:165-246.
36. **Harper, D. B.** 1985. Halomethane from halide ion—a highly efficient fungal conversion of environmental significance. Nature **315:**55-57.
37. **Hines, M. E., P. M. Crill, R. K. Varner, R. W. Talbot, J. H. Shorter, C. E. Kolb, and R. C. Harriss.** 1998. Rapid consumption of low concentrations of methyl bromide by soil bacteria. Applied and Environmental Microbiology **64:**1864-1870.
38. **Keppler, F., R. Eiden, V. Niedan, J. Pracht, and H. F. Scholer.** 2000. Halocarbons produced by natural oxidation processes during degradation of organic matter. Nature **403:**298-301.
39. **Schadt, C. W., A. P. Martin, D. A. Lipson, and S. K. Schmidt.** 2003. Seasonal Dynamics of Previously Unknown Fungal Lineages in Tundra Soils. American Association for the Advancement of Science.
40. **Varner, R. K., M. L. White, C. H. Mosedale, and P. M. Crill.** 2003. Production of methyl bromide in a temperate forest soil. Geophysical Research Letters **30**.
41. **Stumm, W., and J. J. Morgan.** 1996. Aquatic Chemistry; Chemical Equilibria and Rates in Natural Waters, Wiley interscience ed. John Wiley & Sons Inc., New-York.

8. Annexe 1: Diel variations in photo-induced oxidation of Hg^0 in freshwater.

Edenise Garcia, Alexandre J. Poulain, Marc Amyot, and Parisa A. Ariya

Reprinted from Chemosphere, vol. 59: 977-981

Abstract.

Experiments have been conducted to determine diel variations in photo-induced Hg^0 oxidation in lake water under natural $Hg^0_{(aq)}$ concentrations. Pseudo–first order rates of photooxidation (*k'*) were calculated for water freshly collected in a Canadian Shield lake, Lake Croche (45°56' N, 74°00' W), at different periods of the day and subsequently incubated in the dark. Hg^0 oxidation rates ranged from 0.02 to 0.07 h^{-1}, increasing from sunrise to noon and then decreasing throughout the remainder of the day. These changes paralleled those in sunlight intensity integrated over one hour preceding water collection, and suggested that the water freshly collected in daylight was rich in photochemically produced Hg^0 oxidants. It was also estimated that under intense solar radiation, even if oxidation rates reached a peak, reduction of Hg(II) was the prevalent redox process. Inversely, Hg^0 oxidation overcame DGM production during the night or at periods of weaker light intensity. Overall, these findings explain the decreases in the DGM pool generally observed overnight. They also support previous reports that, during summer days, volatilization of Hg^0 from water represent an important step in the Hg cycle in freshwater systems.

Introduction.

The cycling of Hg between its reduced and oxidized forms in natural waters plays an important role in its fate in the environment. Reduction of Hg(II) to dissolved gaseous mercury (DGM), mostly as volatile Hg^0, has been pointed as an important mechanism of loss of Hg to the atmosphere (14, 19). Oxidation of Hg^0, in contrast, may increase the pool of Hg(II) in an aquatic system, ultimately affecting Hg accumulation by the aquatic biota.

In aquatic systems, solar radiation in the UV and visible ranges influences the production of DGM (3-5). As a consequence, DGM concentrations tend to follow a diel pattern, being the highest around noon and the lowest during the night. Dissolved organic carbon (DOC) and ferric iron have been pointed as mediators in the Hg(II) photoreduction (13, 16, 17, 23). The biotic production of DGM has also been observed (10, 15). Laboratory and field experiments have shown that Hg^0 photooxidation is stimulated in the simultaneous presence of chloride and semiquinones(8). This finding explains higher photooxidation rates observed in seawater and estuaries relatively to freshwaters (1, 9). In freshwater, oxidation in the dark has been observed (2, 23), but diel trends and mechanisms involved in the oxidation processes have been less extensively studied. The aim of this study is to investigate diel variations in the rates of sunlight-induced Hg^0 oxidation in lake water under natural DGM concentrations. Considering that reduction and oxidation of Hg can be both photochemically driven, this work also contributes to a better understanding of the balance between both processes in natural waters.

Methods.

The experiments were conducted in Lake Croche, a small (5.31 km2) slightly colored (DOC = 3.5 $mg.L^{-1}$) oligotrophic lake located at the Laurentian

Biological Station of the University of Montreal on the Canadian Shield (45°56' N, 74°00' W).

Subsurface water samples were taken in a 6-m deep portion of the lake during summer 2003. Samples were collected by hand, using quartz bottles (ø 8 cm x 40 cm). No headspace was present within the incubation bottles to avoid loss of Hg^0 by volatilization to the headspace. Clean procedures were adopted during sample collection and analysis: powder-free latex gloves were worn at all times; the glassware was soaked in 20% HNO_3 and rinsed three times with Milli-Q water, and the sampling bottles were rinsed three times with lake water prior to use.

To assess dark oxidation, samples were collected on July 22 around 23:00 in order to avoid the presence of photoreactive radicals during the experiment. DGM was then measured at 30-min intervals during 4 hours.

To observe diel variations in sunlight-induced Hg^0 oxidation, samples were collected on July 23 at different times of the day: 6:30, 9:30, 12:30, 15:30, 18:30 and 21:30. For each period, samples were kept in the dark, in a cooler, for up to five hours. Duplicate or triplicate samples were then analyzed for DGM at 30-min or 1-h intervals from 0 to 5 h. DOC fluorescence in lake water was used as a proxy for the photoreactants production. DOC fluorescence was measured at 1-h intervals at 355 nm excitation and 455 nm emission wavelengths. A 0.05 M H_2SO_4 solution was used as a blank. Values were calibrated against the fluorescence of quinine sulfate using standard solutions, with one quinine sulfate unit (QSU) = 1 ppb quinine sulfate in 0.05 M H_2SO_4.

To compare the rates of Hg(II) reduction and Hg^0 oxidation, water was sampled on July 25 at 6:20, 9:20, 12:50, 16:00 and 19:00. At each period, 15 samples were collected and incubated for up to two hour. Three samples were immediately analyzed for DGM, while three others were kept in a cooler for 2 hours as controls for dark oxidation or reduction. The remaining nine samples

were submerged in an 8-cm deep water bath and exposed to full surface solar radiation spectrum to induce the production of photoreductants and photooxidants. The water bath temperature was kept constant through water replacement. After one hour, three samples were analyzed for DGM, three others were placed in the dark, in a cooler, and three samples were kept under natural sunlight for another hour. DGM concentrations were measured at the end of the incubation period, and variations in DGM concentrations were calculated for the dark and light treatments at different periods of the day.

In all experiments, DGM analyses were performed within minutes of the incubation period. Approximately 500 mL of water was slowly decanted into 1-L glass bubblers and purged for 15 min with Hg-free air with a Tekran 1100 zero air generator. The volatile Hg compounds were trapped on a gold-coated sand column. The trap was dried for 3 minutes in an argon air stream and Hg was subsequently desorbed by pyrolysis at a flow rate of 60 $mL \cdot min^{-1}$, using the double amalgamation technique. Hg was quantified by gas-phase atomic fluorescence spectrometry with Tekran Hg analyzer model 2500. In this study, simultaneous analyses of replicates were possible due to the use of two analytical lines, each one consisting of two bubblers coupled to one Hg-free air generator and one Hg detector. Quality control was achieved through the intercalibration of the two lines, as well as by processing 3 or 4 system blanks before the beginning of the analysis. For the intercalibration, water from Lake Croche was collected ~ 4 hours after sunset in order to minimize the influence of photoreductants or photooxidants. Samples (n =30) were taken using either quartz or Teflon bottles, stored in a cooler, and DGM was immediately measured simultaneously in the two analytical lines. Results from this intercalibration exercise indicated a good correspondence between the two lines: 91.6 ± 6.3 $pg.L^{-1}$ and 88.9 ± 4.8 $pg.L^{-1}$.

Solar radiation in the visible range (400 – 700 nm) was measured during the incubations with a Li-Cor photometer. Light measurements in the UVB range were obtained from the weather station of the Laurentian Biological Station of the University of Montreal.

Results and Discussion.

Hg^0 photo-induced oxidation rates.

DGM concentrations in freshly-collected surface water sampled at different periods of the day and immediately placed in the dark tended to decrease over time (Fig. 1). The observed decreases in DGM concentration were primarily attributed to oxidation of Hg^0, and followed pseudo first-order kinetics, as described by equation 1, rather than zero- or second-order kinetics:

$$\ln \{[Hg^0]_t / [Hg^0]_0\} = -k't \qquad (1)$$

where $[Hg^0]_t$ and $[Hg^0]_0$ represent DGM concentrations at time t and at the beginning of the incubations, respectively. k' is the apparent rate of oxidation of Hg^0 and corresponds, in absolute value, to the slope of the regression of ln $\{[Hg^0]_t / [Hg^0]_0\}$ versus t. Clearly, assumption of linear behavior can not completely describe the observation, particularly in light of scattered data. However, this approximation seems to be valid in explaining the pattern observed during incubation experiments. We speculate that the scatter in the data can result from: (a) a gradual loss of photolytically-initiated oxidants and/or (b) the presence of different types of Hg^0 oxidants. Following light exposure, photooxidants would prevail over dark oxidants, increasing the oxidation rates of Hg^0. With the gradual degradation of photo-induced oxidants, only slower dark oxidation reaction could proceed.

We attempted more complex kinetic expressions to more appropriately describe the observed data than with simple pseudo-first order kinetics (e.g. consecutive reactions, intermediates via equilibriums, multiple equilibriums;

(21)). However, none could more adequately describe our observations. Hence, we continued employing equation (1). Note that using more complex kinetic expressions than a simple pseudo-first order equation (1) will not necessarily yield to more information for further interpreting our field data. Since the detailed chemical reactions are not known (e.g., intermediates, consecutive reactions, parallel reactions;(21)), various approximations will yield to an overall apparent exponential expression that can equally be described by equation (1).

The oxidation rates of Hg^0 varied from ~ 0.02 h^{-1} to 0.07 h^{-1} (Figure 1) and were significantly different from 0 ($p < 0.05$), except for k' estimated for samples collected in the beginning of the day (6:30). This range is around one-order of magnitude lower than oxidation rates observed in saline waters or in natural water exposed to UVB lamps and spiked either with $Hg^0_{(aq)}$ or KCl (k' between 0.2 and 0.9 h^{-1};(8)) or than the rate observed in a pond water spiked with Fe(III) (k' = 0.2 h^{-1};(23)). Note however that the present study was conducted using freshwater containing natural DGM concentrations (between 59 and 79 $pg \cdot L^{-1}$) and exposed to sunlight; it constitutes thus a clear evidence of the occurrence of Hg^0 oxidation in freshwater systems under natural conditions.

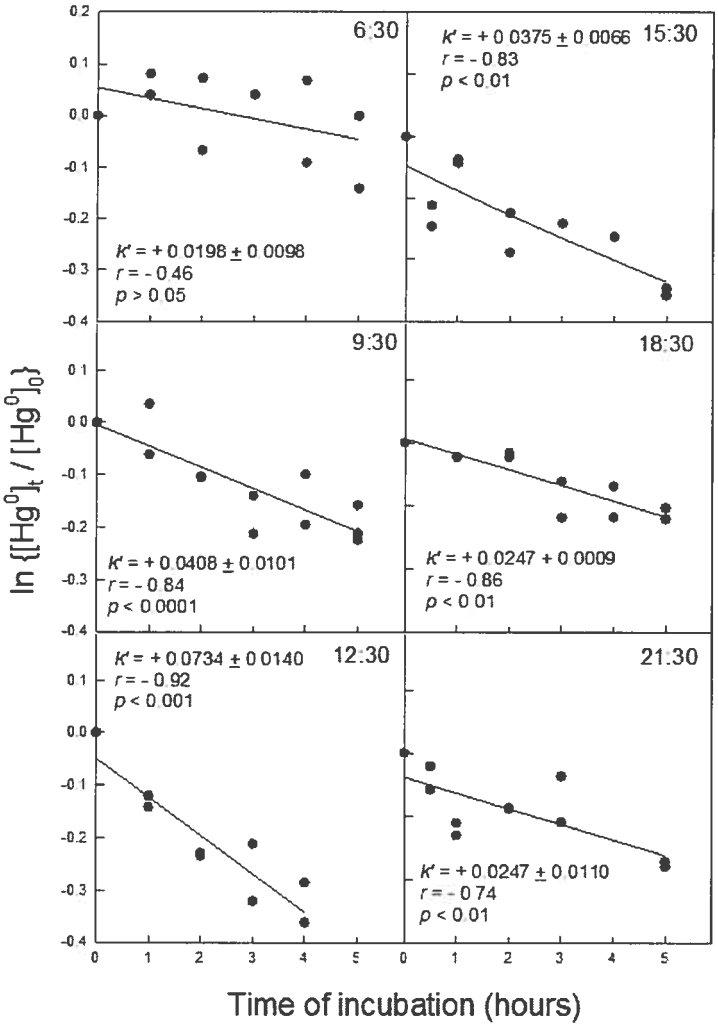

Figure 1. Hg0 photooxidation in subsurface water samples from Lake Croche collected at 6:30, 9:30, 12:30, 15:30, 18:30 and 21:30 on July 23, 2003, and incubated in the dark.

The oxidation rates of Hg^0 in surface water of Lake Croche varied over the course of the day and followed a sinusoidal pattern (Figure 3); *k'* values increased from sunrise to noon and decreased afterward. In fact, the slower rates (morning and evening) were similar to rates observed under dark oxidation (*k'* = 0.024, Figure 3). Overall, these results suggest that oxidation of Hg^0 is stimulated by solar radiation. Indeed, a cross correlation analysis indicated a high correlation between *k'* and the photosynthetically active radiation (PAR, λ = 400 – 700 nm) or UVB radiation at time lags of 15 to 75 minutes (*r* between 0.90 and 0.95). These findings are consistent with those of Zhang and Lindberg (2001), who observed a faster decrease in DGM concentrations in freshwater previously exposed to sunlight of higher intensity than in the same water exposed to sunlight of lower intensity.

DGM concentrations at the beginning of the incubations ranged from 59 to 79 $pg \cdot L^{-1}$ (average = 71.8 $pg \cdot L^{-1}$) and did not vary significantly among the different times of sampling, except for DGM concentrations in water collected at 6:30 AM, which was significantly lower. Thus, the observed diel variations in the rate of Hg^0 oxidation are probably more a function of the light intensity and availability of photooxidants than of the amount of substrate.

Decreases in DGM concentrations in the dark following water photo-exposure can be attributed to photo-induced generation of oxidants followed by continuous chemical reaction in dark. The similar diurnal dynamics of *k'* and DOC fluorescence (Fig. 2, $r = + 0.80$, $p = 0.0575$) suggests a participation of DOC in the Hg^0 oxidation process. Indeed, the absorption of light by chomophoric DOC can yield photoreactive intermediates and is often followed by losses of DOC fluorescence due to degradation of the chromophores (6). These intermediates include excited triplet states of DOC chromophores or DOC-derived radicals, such as hydroxyl ($OH^{\bullet}$), superoxide ($O_2^{-\bullet}$) and hydrogen

peroxidase (H_2O_2) (11, 22), which have been identified as potential Hg^0 oxidants (7, 9, 12).

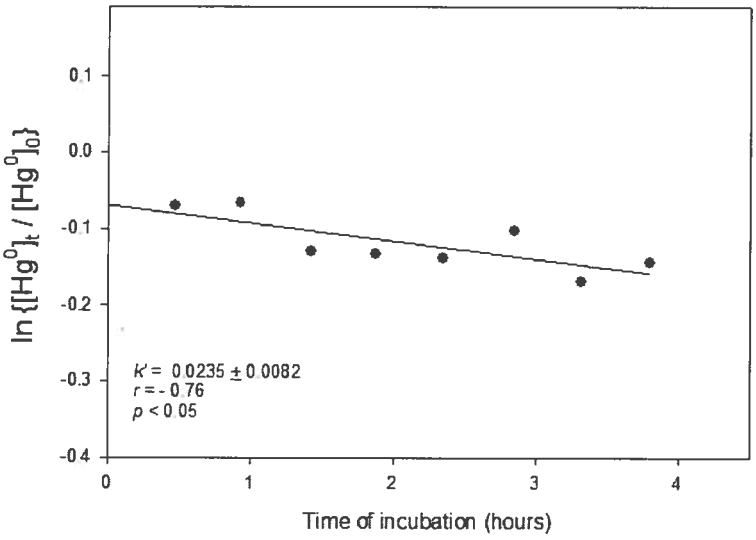

Figure 2. Hg0 oxidation in the dark in subsurface water samples from Lake Croche collected at 23:00 on July 22, 2003 and incubated in the dark.

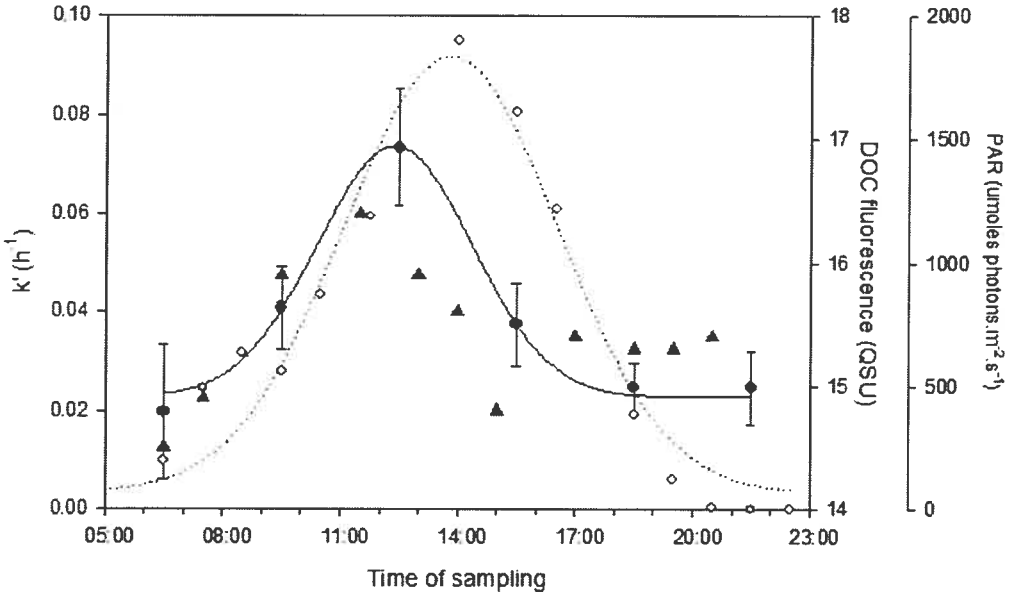

Figure 3. Diel variations in oxidation rates of Hg0 (k', dark circles), DOC fluorescence in lake Croche water (dark triangles), and photosynthetically active radiation (PAR, □ = 400 – 700 nm, open circles) observed on July 23, 2003. Error bars represent S.E.

Relative importance of photooxidation and photoreduction.

Experiments were conducted to assess the importance of Hg photo-induced oxidation relative to photoreduction at different periods of the day. Variations in DGM estimated for the dark and light treatments at different sampling periods are shown in Figure 4. Significant decreases in DGM concentrations (from 3 to 29 $pg \cdot L \cdot h^{-1}$) were observed in samples kept in the dark, in all sampling periods. The greatest decrease was observed in samples collected at 12:50. At this period, the oxidation in the dark was equivalent to 77% of the net production of DGM under sunlight exposure. A decrease in DGM

levels (6 $pg \cdot L \cdot h^{-1}$) was also noticed in samples from the light treatment collected at dusk (19:00). This decrease corresponded to approximately half of the DGM decrease observed in the dark during the same period. In all remaining light exposed samples, a DGM production occurred, varying from 28 to 43 $pg \cdot L \cdot h^{-1}$. On the whole, these results indicate that in the dark only Hg^0 oxidation is observed in freshwater. In sunlight, oxidation and reduction of Hg may occur simultaneously, but the leading process seems to depend on the light intensity: at higher solar irradiance DGM production overcomes oxidation, but as sunlight energy weakens at cloudy times or at sunset oxidation prevails over reduction.

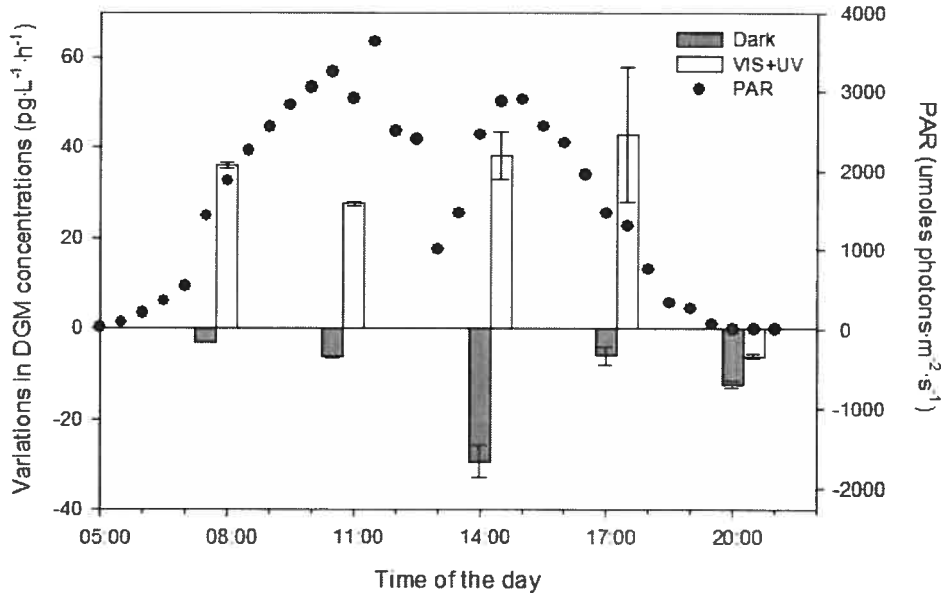

Figure 4. Variations in DGM concentrations in subsurface water samples from Lake Croche collected at 6:20, 9:20, 12:50, 16:00 and 19:00 on July 25, 2003, and incubated in the dark or under the full spectrum of solar radiation. Each value represents the mean ± S.D. based on three replicates.

This study demonstrates the occurrence of photo-induced oxidation of Hg^0 in surface freshwater kept in closed systems at natural DGM concentrations and light exposure. However, even at its maximum, the observed photo-induced oxidation seemingly proceeded slower than the concurrent DGM photoproduction. In open surface freshwater, Hg(II) reduction is especially important to Hg cycling due to the evasion of the produced DGM to the atmosphere, particularly on windy summer days. These findings contrast with those for saline waters (8, 9), where loss of DGM by photooxidation is often more important than volatilization of Hg^0 from the water column. However, at night, Hg^0 oxidation is the dominant process in freshwater and it may replenish the pool of Hg(II) available for methylation. Furthermore, deeper in the water column of a lake, where Hg^0 production is triggered by biological processes rather than solely by light (18, 20), dark oxidation can be a significant process.

Acknowledgements.

We thank Nicolas Milot and Justin Shead for help in the field and laboratory, and Hendrick Van Leeuwen for meteorological data. We also acknowledge funding from the Collaborative Mercury Reasearch Network (COMERN) to M.A.

References.

1. **Amyot, M., G. A. Gill, and F. M. M. Morel.** 1997. Production and loss of dissolved gaseous mercury in coastal seawater. Environmental Science & Technology **31:**3606-3611.
2. **Amyot, M., D. Lean, and G. Mierle.** 1997. Photochemical formation of volatile mercury in high Arctic lakes. Environmental Toxicology and Chemistry **16:**2054-2063.
3. **Amyot, M., G. Mierle, D. Lean, and D. J. McQueen.** 1997. Effect of solar radiation on the formation of dissolved gaseous mercury in temperate lakes. Geochimica Et Cosmochimica Acta **61:**975-987.
4. **Amyot, M., G. Mierle, D. R. S. Lean, and D. J. McQueen.** 1994. Sunlight-Induced Formation of Dissolved Gaseous Mercury in Lake Waters. Environmental Science & Technology **28:**2366-2371.

5. **Costa, M., and P. S. Liss.** 1999. Photoreduction of mercury in sea water and its possible implications for Hg-0 air-sea fluxes. Marine Chemistry **68:**87-95.
6. **Del Vecchio, R., and N. V. Blough.** 2002. Photobleaching of chromophoric dissolved organic matter in natural waters: kinetics and modeling. Marine Chemistry **78:**231-253.
7. **Demagalhaes, M. E. A., and M. Tubino.** 1995. A Possible Path for Mercury in Biological-Systems - the Oxidation of Metallic Mercury by Molecular-Oxygen in Aqueous-Solutions. Science of the Total Environment **170:**229-239.
8. **Lalonde, J. D., M. Amyot, A. M. L. Kraepiel, and F. M. M. Morel.** 2001. Photooxidation of Hg(0) in artificial and natural waters. Environmental Science & Technology **35:**1367-1372.
9. **Lalonde, J. D., M. Amyot, J. Orvoine, F. M. M. Morel, J. C. Auclair, and P. A. Ariya.** 2004. Photoinduced oxidation of Hg-0 (aq) in the waters from the St. Lawrence estuary. Environmental Science & Technology **38:**508-514.
10. **Lanzillotta, E., C. Ceccarini, R. Ferrara, E. Dini, E. Frontini, and R. Banchetti.** 2004. Importance of the biogenic organic matter in photo-formation of dissolved gaseous mercury in a culture of the marine diatom Chaetoceros sp. Science of the Total Environment **318:**211-221.
11. **Leifer, A.** 1988. The kinetics of environmental aquatic photochemistry - theory and practice. ACS professional reference book, New-York.
12. **Lin, C. J., and S. O. Pehkonen.** 1999. The chemistry of atmospheric mercury: a review. Atmospheric Environment **33:**2067-2079.
13. **Lindberg, S. E., A. F. Vette, C. Miles, and F. Schaedlich.** 2000. Mercury speciation in natural waters: Measurement of dissolved gaseous mercury with a field analyzer. Biogeochemistry **48:**237-259.
14. **Mason, R. P., and W. F. Fitzgerald.** 1993. The Distribution and Biogeochemical Cycling of Mercury in the Equatorial Pacific-Ocean. Deep-Sea Research Part I-Oceanographic Research Papers **40:**1897-1924.
15. **Mason, R. P., F. M. M. Morel, and H. F. Hemond.** 1995. The Role of Microorganisms in Elemental Mercury Formation in Natural-Waters. Water Air and Soil Pollution **80:**775-787.
16. **Matthiessen, A.** 1996. Kinetic aspects of the reduction of mercury ions by humic substances .1. Experimental design. Fresenius Journal of Analytical Chemistry **354:**747-749.
17. **O'Driscoll, N. J., S. Beauchamp, S. D. Siciliano, A. N. Rencz, and D. R. S. Lean.** 2003. Continuous analysis of dissolved gaseous mercury (DGM) and mercury flux in two freshwater lakes in Kejimkujik Park,

Nova Scotia: Evaluating mercury flux models with quantitative data. Environmental Science & Technology **37:**2226-2235.

18. **Poulain, A. J., M. Amyot, D. Findlay, S. Telor, T. Barkay, and H. Hintelmann.** 2004. Biological and photochemical production of dissolved gaseous mercury in a boreal lake. Limnology and Oceanography **49:**2265-2275.
19. **Rolfhus, K. R., and W. F. Fitzgerald.** 2001. The evasion and spatial/temporal distribution of mercury species in Long Island Sound, CT-NY. Geochimica Et Cosmochimica Acta **65:**407-418.
20. **Siciliano, S. D., N. J. O'Driscoll, and D. R. Lean.** 2002. Microbial reduction and oxidation of mercury in freshwater lakes. Environmental Science and Technology **36:**3064-3068.
21. **Steinfeld, J. I., J. S. Fransisco, and W. L. Hase.** 1998. Chemical kinetics and dynamics. Prentice-Hall, Upper Saddle River, New-Jersey.
22. **Zepp, R. G., G. L. Baughman, and P. F. Schlotzhauer.** 1981. Comparison of Photochemical Behavior of Various Humic Substances in Water .1. Sunlight Induced Reactions of Aquatic Pollutants Photosensitized by Humic Substances. Chemosphere **10:**109-117.
23. **Zhang, H., and S. E. Lindberg.** 2001. Sunlight and iron(III)-induced photochemical production of dissolved gaseous mercury in freshwater. Environmental Science & Technology **35:**928-935.

9. Annexe 2: Mercury (micro)biogeochemistry in polar environments.

Tamar Barkay and Alexandre J. Poulain

Reprinted from FEMS Microbiology and Ecology, vol. 59 (2): 232-241 Copyright (2007)

Abstract

The contamination of polar regions with mercury that is transported as inorganic mercury from lower latitudes has resulted in the accumulation of methylmercury in the food chain of polar environments risking the health of humans and wild life. This problem is likely to be particularly severe in coastal marine environments where active cycling occurs. Little is currently known about how mercury is methylated in polar environments. Relating observations on mercury deposition and transport through polar regions with knowledge of the microbiology of cold environments and considering the principles of mercury transformations as have been elucidated in temperate aquatic environments we propose that in polar regions (i) variable pathways for mercury methylation may exist, (ii) mercury bioavailability to microbial transformations may be enhanced, and (iii) microbial niches within sea ice are sites where active microbes are localized in proximity to high concentrations of mercury. Thus, microbial transformations, and consequently mercury biogeochemistry, in the Arctic and Antarctic are both unique and common to these processes in lower latitudes and understanding their dynamics is needed for the management of mercury contaminated polar environments.

Introduction.

Over the last few decades, concerns for the vulnerability of polar regions to organic and inorganic contaminants that originate from lower latitudes have increased. These contaminants may be subjected to direct long range atmospheric transport, repeated cycles of evaporation and condensation, or transport via migratory species such as seabirds (14, 61). Some contaminants are chemically transformed in the atmosphere before deposition. Mercury is among the most serious of these contaminants due to its accumulation in polar food chains resulting in health risks to both humans and wildlife (60). This problem is exacerbated by spring time mercury depletion events (MDE) in the high Arctic (57, 81), Subarctic (26) and the Antarctic (28), that result in rapid and massive deposition of ionic mercury, Hg(II), from the atmosphere. This springtime deposition is thought to be due to the oxidation of atmospheric elemental mercury, Hg(0), the form in which mercury is globally distributed, by reactive halogen radicals generated from sea-salt aerosols (5, 57). Furthermore, the highest concentration of Mercury ever reported in remote environments, up to 0.82 $\mu g.L^{-1}$ (ca. 4 $nmol \cdot L^{-1}$) was found during springtime only in direct proximity of Arctic sea leads and was associated with surface vapour crystals such as frost flowers and surface hoar (27). Such an increase represents a 1000 fold augmentation compared to Arctic inland locations (92) or to levels recorded during dark periods (93). Furthermore our own data suggest that oxidation processes are enhanced in Arctic coastal marine environments as compared to inland systems (Poulain et al. unpublished). Together, these results point to coastal and marine environments as being sites of intense mercury cycling and vulnerability to mercury toxicity.

Our concerns with mercury toxicity are focused on the production of the potent neurotoxic compound, methylmercury (MeHg), and its availability to aquatic food chains (104) since the consumption of contaminated fish and

shellfish is considered the major route of human exposure to MeHg (76). Methylmercury manifests its toxicity as a variety of symptoms ranging from mild numbness of the extremities, to blindness, and in severe cases, death (21, 22). Recent research showing that mercury in predators occupying the top levels of the Arctic food chain is almost exclusively methylated (18) and that blood and fatty tissue of native human populations have elevated levels of mercury (13, 96, 100) clearly show that the dynamics and impact of mercury contamination in the Arctic are similar to these phenomena in temperate zones of the world. As atmospherically deposited mercury is mostly in its inorganic forms (4, 56, 82), within-ecosystem transformations must play a critical role in the toxicity and distribution of mercury in polar regions.

In temperate zones, microbial activities critically impact MeHg accumulation. Recent reviews on mercury cycling in the environment (32, 71) and specifically on the role of microbes (8, 10) are available. In this review, we consider information on the role of microorganisms on the geochemical cycling of mercury in temperate regions together with information available from research on mercury and microbiology in polar environments. These sources of information have been summarized to propose junctures where microbes critically affect the geochemical cycle of mercury in polar regions (Figure 1) and to identify research questions that address gaps in our understanding of how microbes modulate the toxicity and mobility of mercury in Arctic and Antarctic environments (Table 1).

Table 1. Microbial transformations of Hg in polar regions, what is known about them, and the identification of research questions needing answers1.

Microbial transformation	What is unique about this transformation in the Arctic	Questions/research needs
Methylation	Presence of diMeHg in coastal water (73) MeHg present in snow and meltwaters SRB and *dsr* genes not detected in soil where MeHg is formed (59)	What are the pathways for methylation? Which organisms methylate mercury in polar regions?
Demethylation	Oxidation of C1 compounds is slow in high latitudes (43) *mer* gene expression in Arctic biomass (Poulain et al., unpublished) Photoreduction of MeHg in epilimnitic lake water (41)	What are the pathways for the degradation of MeHg in polar regions?
Hg(II) reduction	Hg resistant organisms are common in ancient permafrost (65) High bioavailability in snow (57) Possible concentration of Hg(II) in proximity to active microbes in sea ice *mer* gene expression in Arctic biomass (Poulain et al., unpublished)	Development of psychrophilic Hg biosensors. The interactions of microbes in sea ice with Hg. Measurement of mercury concentrations in the complex sea ice matrix Further assessment of the evolution of Hg resistance in polar areas.
Hg(0) oxidation	High chloride concentrations in coastal marine environments induce abiotic oxidation of Hg(0)	A better understanding of Hg(0) oxidation in Hg biogeochemistry

[1]See text for details.

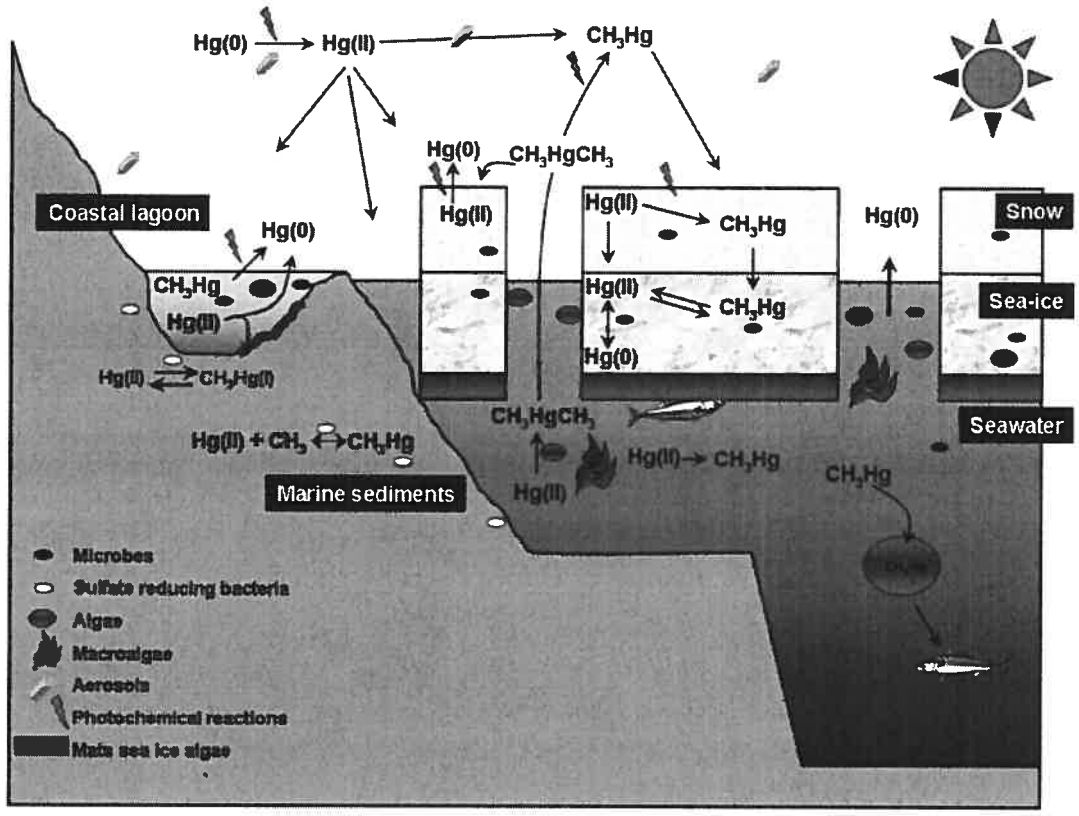

Figure 1. The biogeochemical cycle of mercury in coastal marine environments in polar regions. The various transfer pathways and transformation reactions are described in the text.

Microbial transformations in mercury biogeochemistry in polar environments.

Our current view of the role of microorganisms in the cycling of mercury in the environment is based on studies that were initiated by the discovery of the toxicity of MeHg to consumers of contaminated fish and shellfish in the 1960's (102). Results from environmental, geochemical, microbiological, biochemical, and molecular studies have converged to establish our current view of the mercury biogeochemical cycle (8, 10). Within that paradigm, microbes impact the production of MeHg directly by methylation and MeHg degradation, and indirectly by controlling the supply of Hg(II), the substrate for methylation, by carrying out redox transformations that affect the transitions between Hg(II) and Hg(0). These transformations and how they are likely to be impacted by the unique conditions of cold environments are discussed below.

Hg(II) methylation.

That anaerobic microbes methylate mercury has been known for almost 40 years (45). For the last 20 years this activity has been attributed to sulfate reducing bacteria (SRB) in anoxic sediments (23, 38, 49). The mechanism of methylation may (20) or may not (30, 31) be related to the production of acetyl CoA and methylcobalamine (B12). Very recently however, the possibility of methylation by iron reducing bacteria has been proposed (34), a hypothesis that awaits further confirmation. Methylation of Hg(II) by abiotic processes (89, 101) may be indirectly related to biological activities because of their dependence on biological products such as dissolved organic matter. Formation of MeHg in the Arctic has been documented in wetland soils (59) and streams (58), in freshwater ponds (92) and lakes and tundra watersheds (41). In the later study, a mass balance analysis showed that sediment production of MeHg accounted

for 80 – 91% of the whole lake MeHg production. The issue of which organisms methylate Hg(II) in the Arctic has been addressed by Loseto et al (59). Based on low abundance of SRB in soil samples and a failure to detect deltaproteobacteria - the major taxonomic group among the bacteria to include SRB – and genes encoding for the disulfite reductase enzyme (Dsr) in DNA that was extracted from the soil microbial biomass, the authors concluded that methylation was not mediated by SRB. We have made similar observations with samples collected from an Adirondack watershed. Further examination of water logged soils, however, using the additions of substrates (sulfate) and specific inhibitors (molybdate) as was described by Gilmour et al (38) and Compeau and Bartha (23), implicated SRB in Hg(II) methylation leading us to conclude that the sensitivity of molecular methods was not sufficient to detect SRB whose presence and activities resulted in MeHg production (Barkay and Hines, unbpublished). Indeed, SRB were readily detected when more sensitive molecular probes (24) were applied to the same samples (Yu and Barkay, unpublished). Thus, the involvement of SRB in methylation in the Arctic, especially in sediments of coastal environments where they are likely to carry out the bulk terminal oxidation under anaerobic conditions, remains to be examined. Their involvement is nevertheless supported by observations that SRB are abundant in Arctic coastal marine sediments (Svalbard, Norway) as detected by FISH and dot blot hybridization (77) and that psychrophilic SRB isolated from the same sediments actively reduced sulfate at *in situ* temperatures (16, 50).

Observations on the occurrence and distribution of MeHg suggest that several novel methylation pathways may occur in the Arctic in addition to methylation in sediments:

- An atmospheric source of MeHg – this hypothesis is supported by a large flux of MeHg at the initiation of snowmelt (58, 92) and a strong positive

correlation between MeHg and chloride in snow pack suggesting a marine source. This source could possibly be the evasion of dimethylmercury (diMeHg), from leads and polynyas where it may be formed by phytoplankton in the water column (see below and (73)), and its subsequent atmospheric photodegradation to monomethylmercury chloride (69) and deposition.

- Methylation in snow packs - An alternative explanation for the large flux of MeHg during snowmelt. Experiments using bioreporters (39, 85) indicated that Hg(II) that is deposited during MDE is highly bioavailable (57, 83). Moreover, organic compounds (e.g. dicarboxylic acids (47) are present in Arctic snow and may serve as a carbon source for microorganisms and as ligands for mercury complexation. Our direct bacterial counts by flow cytometry showed 2.10^5 cells per ml of melted snow from the High Canadian Arctic. Melted snow from Antarctica's dry valleys had 200 – 5,000 cells per ml (1, 19, 84). Some of these microbes were metabolically active as indicated by the reduction of INT, a respiratory indicator (1) and by low, but detectable, levels of protein and nucleic acid synthesis at *in situ* temperatures (19). Microbes in snow, therefore, may methylate Hg(II).
- Atmospheric methylation of Hg. It has been long suggested that aerosols could support life (37) and together with recent exciting reports of the transformation of organic compounds in aerosols by bacteria and fungi (3, 6), it is possible to hypothesize a possible atmospheric production of MeHg.
- Photomethylation as recently described in a northern temperate ecosystem (89), may be another pathway for methylation in snow where biological processes produce dissolved organic matter (17) which is the catalyst implicated in this process.

- Production of MeHg by phytoplankton in the marine water column – Pongratz and Heumann (73) observed overlapping chlorophyll and diMeHg optima in their depth profiles in the Antarctic coastal marine environment. They also reported activities for isolated pure cultures of phytoplankton.

Thus, several niches within the coastal marine environments of polar regions may support the production of MeHg, all requiring testing for a full understanding of the processes that result in MeHg production and availability to polar food chains.

Methylmercury degradation.

The degradation of MeHg is the other half, next to methylation, of the equation that determines the production of this neurotoxic substances. Three processes, photodegradation (86) and two microbially mediated ones (10, 80), are known for the degradation of MeHg. Photodegradation is the dominant mechanism for demethylation in surface water in many mercury impacted ecosystems. Very recent and elegant work showed it to be the sole process for the degradation of MeHg in the eplimnitic water of a highly oligotrophic freshwater Arctic lake (41). To the best of our knowledge, MeHg degradation has not been examined in sediments or samples from coastal marine environments in polar regions.

Microbial pathways for the degradation of MeHg are distinguished by the gaseous carbon products of the degradation process; in oxidative demethylation, carbon dioxide is produced and in the reductive process the product is methane. We (80) and others (40, 62) have shown that the choice between these processes is to a large extent controlled by environmental factors. Reductive demethylation, an activity that is mediated by the

organomercury lyase enzyme, which is a part of the mercury resistance (*mer*) system in bacteria (see below), is favored at high redox and at high concentrations of mercury, an effect that we have attributed to the dependence of the *mer* operon gene expression on inducing concentrations of Hg(II) (80). While the absolute concentrations required for induction depends on the complicated issue of mercury bioavailability, observations of *mer* gene expression from temperate regions suggested that in lakes and streams with less than nM concentrations of Hg, as observed in most polar waters, expression is repressed (74, 80). Thus, one would not expect reductive demethylation to be a dominant process in polar regions. However, this expectation is contradicted by a recent observation of *mer* transcripts in RNA extracts from microbial biomass collected in the Canadian high Arctic (see below).

Oxidative demethylation is favored for low redox potentials and is most likely related to C1 pathways in anaerobic prokaryotes (63). The occurrence and rates of C1 metabolism in microbes from cold environments has been getting a lot of attention due to anticipated effects of global warming on the release of carbon from large frozen reservoirs in the permafrost and polar tundra. While methanogenesis (12) using bicarbonate or acetate as substrates (78), and methanotrophy (12) have been noted, rates were drastically impacted by a drop in the incubation temperature, and degradation of C1 compounds such as methylbromide or acetate, common in temperate soils (42), are rarely observed at high latitudes proximal to polar areas (43). Based on these observations, the likelihood for oxidative MeHg degradation in polar regions is low. Nevertheless, demethylation plays an important role in determining MeHg production and availability to food chains and its occurrence and mechanisms in cold environments need to be addressed.

Redox Transformations of inorganic mercury.

Redox transformations between the ionic and elemental mercury forms affect MeHg production by controlling the amount of the substrate that is available for methylation (33). Among reduction processes, photoreduction dominates in surface waters (2, 35, 51, 70, 74, 105), has recently been discovered in snow (52, 55) and is thought to mediate the evasion of most of the Hg(II) that is deposited from the atmosphere onto snow during MDE's (26, 57). Reduction of Hg, non related to the activity of mercury-resistant microbes (see below), can be associated with the activity of microorganisms in fresh and salt waters via pathways that still are to be determined but are related to both heterotrophic and/or photosynthetic activity (11, 64, 74, 79). Hg reduction mediated by the activities of mercury resistant bacteria, impacts the partitioning of mercury into the gaseous phase in some environments (7, 10). This activity is mediated by the prokaryotic mercuric reductase enzyme (MerA), which is encoded by the *merA* gene, a part of the inducible mercury resistance (*mer*) operon (8). This operon is broadly distributed among Bacteria (8) and Archaea (90) from diverse environments (72, 98). The description of several *mer* operons in bacteria, one among them possibly the ancestor of the *mer* transposon, Tn*21* (48) from 10 - 40 thousand year old Siberian permafrost (65), as well as preliminary results showing the presence of *merA* in bacteria from a 120,000 years old glacial ice core (Lu-Irving and Barkay, unpublished), suggest together that mercury resistant prokaryotes may be endemic to cold environments. Their role in mercury biogeochemistry in polar regions remains to be examined.

In addition to *merA,* the *mer* operon contains several additional genes that actively transport Hg(II) into the cytoplasm as well as those that regulate *mer* gene expression. Some operons also encode for the organomercury lyase and microbes carrying such *mer* operons reductively degrade MeHg (see

above). The regulator of *mer* expression, MerR, plays a critical role in determining where and under what conditions Hg(II) reduction by MerA occurs. Expression is repressed in the absence of Hg(II) and is quantitatively induced in its presence (15, 94). Because of this requirement for induction, MerA mediated reduction has been considered of little relevance to transformations of mercury in natural environments (67). Indeed, a series of studies, performed in several environments that were impacted by various sources of mercury, showed mRNA transcripts of the *merA* gene in highly contaminated environments whereas microbial biomass from environments with low levels of contamination contained low to non-detectable levels of these transcripts (44, 68, 74, 80). Based on these observations one would not expect *merA* expression and microbial reduction of Hg(II) in polar microbial communities where mercury concentrations, during most times of the year, are in the pM range (92, 93).

Very recent observations of *merA* expression in biomass collected from coastal marine environments in the high Arctic during the summer of 2005 (Poulain et al. unpublished) challenge the paradigm that assigned MerA a minor role in mercury geochemistry (see above). This paradigm has been previously questioned by a report that suggested that MerA activities in protein extracts from lake microbial biomass were positively related to diel cycles of dissolved gaseous mercury increase in lake water that had pM total mercury concentrations (88). DGM is mostly comprised of Hg(0) in freshwaters, (97). It is most likely that the concentration of bioavailable mercury, rather than that of total mercury, is what determines *mer* induction in a given environment (9, 10). If so, the high levels of bioavailable mercury in snow during atmospheric MDE (57, 83) may explain the observed induction of *merA*. The development of mercury biosensors in psychrophilic bacteria, similar to the ones that have been employed for the detection and assessment of bioavailable mercury in

temperate environments (9) is needed as part of an approach for distinguishing bioavailable from total mercury in polar environments.

An alternative explanation for the induction of *merA* in high Arctic microbiota relates to the highly heterogeneous nature of microbial habitats in polar regions, most noticeably in sea ice (66, 95), leading to the formation of unique environments where mercury resistance might be essential for survival. The slow rates of transcript degradation previously reported in cold environments (99), might furthermore explain the detection of *merA* transcripts in sea ice associated biota. Sea ice, the habitat for most of the microbial biomass in coastal polar environments, may contain niches where both mercury and microorganisms are concentrated. It is likely that mercury, like other solutes in sea ice (29), is highly concentrated in brine channels where actively metabolizing microorganisms are located (25, 46). Furthermore and as stated above, some of the highest concentrations of mercury ever reported in natural samples were encountered in sea ice formations such as frost flowers and surface hoar (27). Our hypothesis on the localized proximity of microbes to mercury in brine channels is also supported by the observations that microbes in brine channels during winter are associated with particles (46), that a significant fraction of atmospherically derived mercury is bound to particles (81), and that mercury in snow - especially in marine environments - is almost exclusively associated with particles (Poulain et al., unpublished). Thus, the interaction of mercury with microbes in sea ice is likely a spatially fractured phenomenon and may be one of the most exciting aspects of future studies on mercury biogeochemistry in polar environments. Such studies will also bring new perspectives to mercury biogeochemistry at large since spatial constrains on mercury microbe interactions have not been considered to date although the chemical physical properties of mercury should clearly drive its heterogeneous distribution in any structured environment.

MerA-mediated reduction of Hg(II) may dramatically affect mercury cycling, thus MeHg production in polar regions. Our preliminary modeling effort suggest that the great majority of elemental Hg is of bacterial origin in Arctic marine surface waters and further studies should explore its role at the Arctic scale. The microbial oxidation of Hg(0) to Hg(II) is the part of the mercury biogeochemical cycle about which we know the least. Most research efforts have to date examined abiotic mechanisms of light and dark oxidation (4, 36, 53, 54, 75, 87, 103). Bacterial enzymes known for their role in preventing oxidative damage such as hydroperxidases oxidize Hg(0) in organisms that are common in natural waters and soils (91). Siciliano et al., (88) related levels of mercury oxidases in lake microbial biomass to variations in DGM concentrations. How these microbialy mediated oxidative processes affect mercury speciation in polar region and especially their impact on the fate of the volatile elemental mercury Hg(0) has not been examined.

Conclusion.

The study of mercury biogeochemistry in polar environments is at its early stages. In light of what we know about i) the distribution of mercury in polar regions ii) about microbiology in cold environments and iii) mercury biogeochemistry in temperate regions, it is clear that the understanding of Hg cycling in polar regions will require original knowledge and a unique synthesis of information already available. As in temperate environments, MeHg is accumulated by aquatic food chains but the sites where methylation occurs and the methylation pathways themselves, in polar areas, may differ from those in lower latitudes. A particularity of Arctic ecosystems reside in the enhanced vulnerability of marine/coastal environments to mercury toxicity as evidence suggests that mercury cycling is highly dynamic at these sites.

Most intriguingly, polar coastal marine environments are characterized by spatially and temporally fractured environments in term of their physical, chemical and biological features, and therefore are composed of a multitude of microbial niches. These unique niches may alter, or modulate, the pathways of microbial transformations of mercury relative to their characteristics in temperate environments. Specifically, high bioavailability of Hg(II) and the presence of niches where mercury and microbes are concentrated may alter the production of MeHg by enhancing bacterial reduction of Hg(II). Thus, our current state of knowledge provides us with a starting point for studies on mercury transformations at the poles, and such studies promise to add new dimensions to our perception of the mechanisms and pathways that determine mercury toxicity and facilitate life in its presence.

Acknowledgements.

The authors' research on mercury biogeochemistry is supported by the Environmental Remediation Science program (ERSP) and the Biological and Environmental Research (BER) of the U.S. Department of Energy, the National Science Foundation, and the Fond Québecois de la Recherche sur la Nature et les Technologies.

References.

1. **Alfreider, A., J. Pernthaler, R. Amann, B. Sattler, F. O. Glockner, A. Wille, and R. Psenner.** 1996. Community analysis of the bacterial assemblages in the winter cover and pelagic layers of a high mountain lake by in situ hybridization. Applied and Environmental Microbiology **62:**2138-2144.
2. **Amyot, M., G. Southworth, S. E. Lindberg, H. Hintelmann, J. D. Lalonde, N. Ogrinc, A. J. Poulain, and K. A. Sandilands.** 2004. Formation and evasion of dissolved gaseous mercury in large enclosures amended with (HgCl2)-Hg-200. Atmospheric Environment **38:**4279-4289.

3. **Ariya, P. A., and M. Amyot.** 2004. New Directions: The role of bioaerosols in atmospheric chemistry and physics. Atmospheric Environment **38:**1231-1232.
4. Ariya, P. A., A. P. Dastoor, M. Amyot, W. H. Schroeder, L. Barrie, K. Anlauf, F. Raofie, A. Ryzhkov, D. Davignon, J. Lalonde, and A. Steffen. 2004. The Arctic: a sink for mercury. Tellus Series B-Chemical and Physical Meteorology 56:397-403.
5. **Ariya, P. A., A. Khalizov, and A. Gidas.** 2002. Reactions of gaseous mercury with atomic and molecular halogens: Kinetics, product studies, and atmospheric implications. Journal of Physical Chemistry A **106:**7310-7320.
6. **Ariya, P. A., O. Nepotchatykh, O. Ignatova, and M. Amyot.** 2002. Microbiological degradation of atmospheric organic compounds. Geophysical Research Letters **29**.
7. **Barkay, T.** 1987. Adaptation of Aquatic Microbial Communities to Hg-2+ Stress. Applied and Environmental Microbiology **53:**2725-2732.
8. **Barkay, T., S. M. Miller, and A. O. Summers.** 2003. Bacterial mercury resistance from atoms to ecosystems. Fems Microbiology Reviews **27:**355-384.
9. **Barkay, T., R. R. Turner, L. D. Rasmussen, C. A. Kelly, and J. W. Rudd.** 1998. Luminescence facilitated detection of bioavailable mercury in natural waters. Methods Mol Biol **102:**231-46.
10. **Barkay, T., and I. Wagner-Dobler.** 2005. Microbial transformations of mercury: Potentials, challenges, and achievements in controlling mercury toxicity in the environment, p. 1-52, Advances in Applied Microbiology, Vol 57, vol. 57.
11. **Ben-Bassat, D., and A. M. Mayer.** 1978. Light induced Hg volatilization and O2 evolution in Chlorella and the effect of DCMU and methylamine. Physiol. Plant **42:**33-38.
12. **Berestovskaya, Y. Y., Rusanov, Ii, L. V. Vasil'eva, and N. V. Pimenov.** 2005. The processes of methane production and oxidation in the soils of the Russian Arctic tundra. Microbiology **74:**221-229.
13. **Bjerregaard, P., and J. C. Hansen.** 2000. Organochlorines and heavy metals in pregnant women from the Disko Bay area in Greenland. Science of the Total Environment **245:**195-202.
14. Blais, J. M., L. E. Kimpe, D. McMahon, B. E. Keatley, M. L. Mattory, M. S. V. Douglas, and J. P. Smol. 2005. Arctic seabirds transport marine-derived contaminants. Science 309:445-445.
15. **Brown, N. L., J. V. Stoyanov, S. P. Kidd, and J. L. Hobman.** 2003. The MerR family of transcriptional regulators. Fems Microbiology Reviews **27:**145-163.

16. **Bruchert, V., C. Knoblauch, and B. B. JÃ¸rgensen.** 2001. Controls on stable sulfur isotope fractionation during bacterial sulfate reduction in Arctic sediments. Geochimica et Cosmochemica Acta **65:**763-776.
17. **Calace, N., E. Cantafora, S. Mirante, B. M. Petronio, and M. Pietroletti.** 2005. Transport and modification of humic substances present in Antarctic snow and ancient ice. Journal of Environmental Monitoring **7:**1320-1325.
18. **Campbell, L. M., R. J. Norstrom, K. A. Hobson, D. C. G. Muir, S. Backus, and A. T. Fisk.** 2005. Mercury and other trace elements in a pelagic Arctic marine food web (Northwater Polynya, Baffin Bay). Science of the Total Environment **351:**247-263.
19. **Carpenter, E. J., S. J. Lin, and D. G. Capone.** 2000. Bacterial activity in South Pole snow. Applied and Environmental Microbiology **66:**4514-4517.
20. **Choi, S. C., J. Chase, T., and R. Bartha.** 1994. Metabolic pathways leading to mercury methylation in Desulfovibrio desulfuricans LS. 1994 **60:**4072-4077.
21. **Clarkson, T. W.** 2002. The three modern faces of mercury. Environmental Health Perspectives **110:**11-23.
22. **Clarkson, T. W.** 1997. The toxicology of mercury. Critical Reviews in Clinical Laboratory Sciences **34:**369-403.
23. **Compeau, G. C., and R. Bartha.** 1985. Sulfate-reducing bacteria: principle methylators of mercury in anoxic estuarine sediment. Applied and Environmental Microbiology **50:**498-502.
24. **Daly, K., R. J. Sharp, and A. J. McCarthy.** 2000. Development of oligonucleotide probes and PCR primers for detecting phylogenetic subgroups of sulfate-reducing bacteria. Microbiology-Uk **146:**1693-1705.
25. **Deming, J. W.** 2002. Psychrophiles and polar regions. Curr Opin Microbiol **5:**301-9.
26. **Dommergue, A., C. P. Ferrari, L. Poissant, P. A. Gauchard, and C. F. Boutron.** 2003. Diurnal cycles of gaseous mercury within the snowpack at Kuujjuarapik/Whapmagoostui, Quebec, Canada. Environmental Science & Technology **37:**3289-3297.
27. **Douglas, T. A., M. Sturm, W. R. Simpson, S. Brooks, S. E. Lindberg, and D. K. Perovich.** 2005. Elevated mercury measured in snow and frost flowers near Arctic sea ice leads. Geophysical Research Letters **32**.
28. Ebinghaus, R., H. H. Kock, C. Temme, J. W. Einax, A. G. Lowe, A. Richter, J. P. Burrows, and W. H. Schroeder. 2002. Antarctic springtime depletion of atmospheric mercury. Environmental Science & Technology 36:1238-1244.

29. **Eicken, H.** 2003. From the microscopic, to the macroscopic, to the regional scale: Growth, microstructure and properties of sea ice., p. 416. *In* D. N. Thomas and G. S. Dieckmann (ed.), Sea ice. An introduction to its physics, chemistry, biology and geology, Blackwell ed. Blackwell Science Ltd., Oxford.

30. **Ekstrom, E. B., and F. M. Morel.** 2004. Mercury methylation by sulfate-reducing bacteria independent of vitamin B12. Materials and Geoenvironment **51:**968-970.

31. **Ekstrom, E. B., F. M. M. Morel, and J. M. Benoit.** 2003. Mercury methylation independent of the acetyl-coenzyme a pathway in sulfate-reducing bacteria. Applied and Environmental Microbiology **69:**5414-5422.

32. **Fitzgerald, W. F., and C. Lamborg.** 2004. Geochemistry of mercury in the environment, p. 107-148. *In* B. Sherwood Lollar (ed.), Environmental Geochemistry, vol. 9. Elsevier.

33. **Fitzgerald, W. F., R. P. Mason, and G. M. Vandal.** 1991. Atmospheric Cycling and Air-Water Exchange of Mercury over Midcontinental Lacustrine Regions. Water Air and Soil Pollution **56:**745-767.

34. **Fleming, E. J., E. E. Mack, P. G. Green, and D. C. Nelson.** 2006. Mercury methylation from unexpected sources: Molybdate-inhibited freshwater sediments and an iron-reducing bacterium. Applied and Environmental Microbiology **72:**457-464.

35. **Garcia, E., M. Amyot, and P. A. Ariya.** 2005. Relationship between DOC photochemistry and mercury redox transformations in temperate lakes and wetlands. Geochimica et Cosmochimica Acta **69:**1917-1924.

36. **Garcia, E., A. J. Poulain, M. Amyot, and P. A. Ariya.** 2005. Diel variations in photoinduced oxidation of Hg-0 in freshwater. Chemosphere **59:**977-981.

37. **Gidlen, T.** 1948. Aerial plankton and its conditions of life. Biological review **23:**109-126.

38. **Gilmour, C. C., E. A. Henry, and R. Mitchell.** 1992. Sulfate stimulation of mercury methylation in freshwater sediments. Environmental Science and Technology **26:**2281-2287.

39. **Golding, G. R., C. A. Kelly, R. Sparling, P. C. Loewen, J. W. M. Rudd, and T. Barkay.** 2002. Evidence for facilitated uptake of Hg(II) by Vibrio anguillarum and Escherichia coli under anaerobic and aerobic conditions. Limnology and Oceanography **47:**967-975.

40. **Gray, J. E., M. E. Hines, P. L. Higueras, I. Adatto, and B. K. Lasorsa.** 2004. Mercury speciation and microbial transformations in mine wastes, stream sediments, and surface waters at the Almaden Mining District, Spain. Environmental Science & Technology **38:**4285-4292.

41. **Hammerschmidt, C. R., W. F. Fitzgerald, C. Lamborg, P. H. Balcom, and C. M. Tseng.** 2006. Biogeochemical Cycling of Methylmercury in Lakes and Tundra Watersheds of Arctic Alaska. Environmental Science & Technology.
42. **Hines, M. E., P. M. Crill, R. K. Varner, R. W. Talbot, J. H. Shorter, C. E. Kolb, and R. C. Harriss.** 1998. Rapid consumption of low concentrations of methyl bromide by soil bacteria. Applied and Environmental Microbiology **64:**1864-1870.
43. **Hines, M. E., K. N. Duddleston, and R. P. Kiene.** 2001. Carbon flow to acetate and C-1 compounds in northern wetlands. Geophysical Research Letters **28:**4251-4254.
44. Hines, M. E., M. Horvat, J. Faganeli, J. C. J. Bonzongo, T. Barkay, E. B. Major, K. J. Scott, E. A. Bailey, J. J. Warwick, and W. B. Lyons. 2000. Mercury biogeochemistry in the Idrija River, Slovenia, from above the mine into the Gulf of Trieste. Environmental Research 83:129-139.
45. **Jensen, S., and A. Jernelov.** 1969. Biological methylation of mercury in aquatic organisms. Nature **223:**753-754.
46. **Junge, K., H. Eicken, and J. W. Deming.** 2004. Bacterial activity at-2 to-20 degrees C in Arctic wintertime sea ice. Applied and Environmental Microbiology **70:**550-557.
47. **Kawamura, K., A. Yanase, T. Eguchi, T. Mikami, and L. A. Barrie.** 1996. Enhanced atmospheric transport of soil derived organic matter in spring over the high Arctic. Geophysical Research Letters:3735-3738.
48. **Kholodii, G., S. Mindlin, M. Petrova, and S. Minakhina.** 2003. Tn5060 from the Siberian permafrost is most closely related to the ancestor of Tn21 prior to integron acquisition. Fems Microbiology Letters **226:**251-255.
49. **King, J. K., J. E. Kostka, M. E. Frischer, and F. M. Saunders.** 2000. Sulfate-reducing bacteria methylate mercury at variable rates in pure culture and in marine sediments. Appl Environ Microbiol **66:**2430-7.
50. **Knoblauch, C., B. B. Jorgensen, and J. Harder.** 1999. Community size and metabolic rates of psychrophilic sulfate-reducing bacteria in Arctic marine sediments. Applied and Environmental Microbiology **65:**4230-4233.
51. **Krabbenhoft, D. P., J. P. Hurley, M. L. Olson, and L. B. Cleckner.** 1998. Diel variability of mercury phase and species distributions in the Florida Everglades. Biogeochemistry **40:**311-325.
52. **Lalonde, J. D., M. Amyot, M. R. Doyon, and J. C. Auclair.** 2003. Photo-induced Hg(II) reduction in snow from the remote and temperate Experimental Lakes Area (Ontario, Canada). Journal of Geophysical Research-Atmospheres **108**.

53. **Lalonde, J. D., M. Amyot, A. M. L. Kraepiel, and F. M. M. Morel.** 2001. Photooxidation of Hg(0) in artificial and natural waters. Environmental Science & Technology **35:**1367-1372.
54. **Lalonde, J. D., M. Amyot, J. Orvoine, F. M. M. Morel, J. C. Auclair, and P. A. Ariya.** 2004. Photoinduced oxidation of Hg-0 (aq) in the waters from the St. Lawrence estuary. Environmental Science & Technology **38:**508-514.
55. **Lalonde, J. D., A. J. Poulain, and M. Amyot.** 2002. The role of mercury redox reactions in snow on snow-to-air mercury transfer. Environmental Science & Technology **36:**174-178.
56. **Lin, C. J., P. Pongprueksa, S. E. Lindberg, S. O. Pehkonen, D. Byun, and C. Jang.** 2006. Scientific uncertainties in atmospheric mercury models I: Model science evaluation. Atmospheric Environment **40:**2911-2928.
57. **Lindberg, S. E., S. Brooks, C. J. Lin, K. J. Scott, M. S. Landis, R. K. Stevens, M. Goodsite, and A. Richter.** 2002. Dynamic oxidation of gaseous mercury in the Arctic troposphere at polar sunrise. Environmental Science & Technology **36:**1245-1256.
58. **Loseto, L. L., D. R. Lean, and S. D. Siciliano.** 2004. Snowmelt sources of methylmercury to high arctic ecosystems. Enivronmental Science and technology **38:**3004-3010.
59. **Loseto, L. L., S. D. Siciliano, and D. R. Lean.** 2004. Methylmercury production in High Arctic wetlands. Environmental Toxicology and Chemistry **23:**17-23.
60. **Macdonald, R. W.** 2005. Climate change, risks and contaminants: A perspective from studying the Arctic. Human and Ecological Risk Assessment **11:**1099-1104.
61. **Macdonald, R. W., T. Harner, and J. Fyfe.** 2005. Recent climate change in the Arctic and its impact on contaminant pathways and interpretation of temporal trend data. Science of the Total Environment **342:**5-86.
62. **Marvin-DiPasquale, M., J. Agee, C. McGowan, R. S. Oremland, M. Thomas, D. Krabbenhoft, and C. C. Gilmour.** 2000. Methyl-mercury degradation pathways: A comparison among three mercury-impacted ecosystems. Environmental Science & Technology **34:**4908-4916.
63. **Marvin-Dipasquale, M. C., and R. S. Oremland.** 1998. Bacterial methylmercury degradation in Florida Everglades peat sediment. Environmental Science & Technology **32:**2556-2563.
64. **Mason, R. P., F. M. M. Morel, and H. F. Hemond.** 1995. The Role of Microorganisms in Elemental Mercury Formation in Natural-Waters. Water Air and Soil Pollution **80:**775-787.

65. **Mindlin, S., L. Minakhin, M. Petrova, G. Kholodii, S. Minakhina, Z. Gorlenko, and V. Nikiforov.** 2005. Present-day mercury resistance transposons are common in bacteria preserved in permafrost grounds since the Upper Pleistocene. Research in Microbiology **156:**994-1004.
66. **Mock, T., and D. N. Thomas.** 2005. Recent advances in sea-ice microbiology. Environ Microbiol **7:**605-19.
67. **Morel, F. M. M., A. M. L. Kraepiel, and M. Amyot.** 1998. The chemical cycle and bioaccumulation of mercury. Annual Review of Ecology and Systematics **29:**543-566.
68. **Nazaret, S., W. H. Jeffrey, E. Saouter, R. Vonhaven, and T. Barkay.** 1994. Mera Gene-Expression in Aquatic Environments Measured by Messenger-Rna Production and Hg(Ii) Volatilization. Applied and Environmental Microbiology **60:**4059-4065.
69. **Niki, H., P. S. Maker, C. M. savage, and L. P. Breitenbach.** 1983. A Fourier transform infrared study of the kinetics and mechanism for the reaction Cl+CH3HgCH3. Journal of Physical Chemistry **87:**3722-3724.
70. **O'Driscoll, N. J., D. R. S. Lean, L. L. Loseto, R. Carignan, and S. D. Siciliano.** 2004. Effect of dissolved organic carbon on the photoproduction of dissolved gaseous mercury in lakes: Potential impacts of forestry. Environmental Science & Technology **38:**2664-2672.
71. **O'Driscoll, N. J., A. Rencz, and D. R. S. Lean.** 2005. The biogeochemistry and fate of mercury in the environment, p. 221-238. *In* A. Sigel, H. Sigel, and R. Sigel (ed.), Biogeochemical cycles of elements, vol. 43. Marcell Dekker, New-York.
72. **Osborn, A. M., K. D. Bruce, P. Strike, and D. A. Ritchie.** 1997. Distribution, diversity and evolution of the bacterial mercury resistance (mer) operon. Fems Microbiology Reviews **19:**239-262.
73. **Pongratz, R., and K. G. Heumann.** 1999. Production of methylated mercury, lead and cadmium by marine bacteria as a significant natural source for atmospheric heavy metals in polar regions. Chemosphere **39:**89-102.
74. **Poulain, A. J., M. Amyot, D. Findlay, S. Telor, T. Barkay, and H. Hintelmann.** 2004. Biological and photochemical production of dissolved gaseous mercury in a boreal lake. Limnology and Oceanography **49:**2265-2275.
75. **Poulain, A. J., J. D. Lalonde, M. Amyot, J. A. Shead, F. Raofie, and P. A. Ariya.** 2004. Redox transformations of mercury in an Arctic snowpack at springtime. Atmospheric Environment **38:**6763-6774.
76. **Ratcliffe, H. E., G. M. Swanson, and L. J. Fischer.** 1996. Human exposure to mercury: A critical assessment of the evidence of adverse

health effects. Journal of Toxicology and Environmental Health **49:**221-270.

77. **Ravenschlag, K., K. Sahm, and R. Amann.** 2001. Quantitative molecular analysis of the microbial community in marine arctic sediments (Svalbard). Appl Environ Microbiol **67:**387-95.
78. **Rivkina, E., K. Laurinavichius, J. McGrath, J. Tiedje, V. Shcherbakova, and D. Gilichinsky.** 2004. Microbial life in permafrost, p. 1215-1221, Space Life Sciences: Search for Signatures of Life, and Space Flight Environmental Effects on the Nervous System. PERGAMON-ELSEVIER SCIENCE LTD, KIDLINGTON.
79. **Rolfhus, K. R., and W. F. Fitzgerald.** 2004. Mechanisms and temporal variability of dissolved gaseous mercury production in coastal seawater. Marine Chemistry **90:**125-136.
80. **Schaefer, J. K., J. Yagi, J. R. Reinfelder, T. Cardona, K. M. Ellickson, S. Tel-Or, and T. Barkay.** 2004. Role of the bacterial organomercury lyase (MerB) in controlling methylmercury accumulation in mercury-contaminated natural waters. Environmental Science & Technology **38:**4304-4311.
81. **Schroeder, W. H., K. G. Anlauf, L. A. Barrie, J. Y. Lu, A. Steffen, D. R. Schneeberger, and T. Berg**. 1998. Arctic springtime depletion of mercury. Nature 394:331-332.
82. **Schroeder, W. H., and J. Munthe.** 1998. Atmospheric mercury - An overview. Atmospheric Environment **32:**809-822.
83. **Scott, K. J.** 2001. Bioavailable mercury in arctic snow determined by a light-emitting mer-lux bioreporter. Arctic **54:**92-95.
84. **Segawa, T., K. Miyamoto, K. Ushida, K. Agata, N. Okada, and S. Kohshima.** 2005. Seasonal change in bacterial flora and biomass in mountain snow from the Tateyama Mountains, Japan, analyzed by 16S rRNA gene sequencing and real-time PCR. Applied and Environmental Microbiology **71:**123-130.
85. **Selifonova, O., R. Burlage, and T. Barkay.** 1993. Bioluminescent sensors for detection of bioavailable Hg(II) in the environment. Appl Environ Microbiol **59:**3083-90.
86. **Sellers, P., C. A. Kelly, J. W. M. Rudd, and A. R. MacHutchon.** 1996. Photodegradation of methylmercury in lakes. Nature **380:**694-697.
87. **Sheu, G. R., and R. P. Mason.** 2004. An examination of the oxidation of elemental mercury in the presence of halide surfaces. Journal of Atmospheric Chemistry **48:**107-130.
88. **Siciliano, S. D., N. J. O'Driscoll, and D. R. Lean.** 2002. Microbial reduction and oxidation of mercury in freshwater lakes. Environmental Science and Technology **36:**3064-3068.

89. **Siciliano, S. D., N. J. O'Driscoll, R. Tordon, J. Hill, S. Beauchamp, and D. R. Lean.** 2005. Abiotic production of methylmercury by solar radiation. Environ Sci Technol **39:**1071-7.
90. **Simbahan, J., E. Kurth, J. Schelert, A. Dillman, E. Moriyama, S. Jovanovich, and P. Blum.** 2005. Community analysis of a mercury hot spring supports occurrence of domain-specific forms of mercuric reductase. Applied and Environmental Microbiology **71:**8836-8845.
91. **Smith, T., K. Pitts, J. A. McGarvey, and A. O. Summers.** 1998. Bacterial oxidation of mercury metal vapor, Hg(0). Applied and Environmental Microbiology **64:**1328-1332.
92. **St Louis, V. L., M. J. Sharp, A. Steffen, A. May, J. Barker, J. L. Kirk, D. J. Kelly, S. E. Arnott, B. Keatley, and J. P. Smol.** 2005. Some sources and sinks of monomethyl and inorganic mercury on Ellesmere Island in the Canadian High Arctic. Environmental Science and Technology **39:**2686-2701.
93. **Steffen, A., W. Schroeder, J. Bottenheim, J. Narayan, and J. D. Fuentes.** 2002. Atmospheric mercury concentrations: measurements and profiles near snow and ice surfaces in the Canadian Arctic during Alert 2000. Atmospheric Environment **36:**2653-2661.
94. **Summers, A. O.** 1992. Untwist and Shout - a Heavy Metal-Responsive Transcriptional Regulator. Journal of Bacteriology **174:**3097-3101.
95. **Thomas, D. N., and G. S. Dieckmann.** 2002. Ocean science - Antarctic Sea ice - a habitat for extremophites. Science **295:**641-644.
96. V**an Oostdam, J., S. G. Donaldson, M. Feeley, D. Arnold, P. Ayotte, G. Bondy, L. Chan, E. Dewaily, C. M. Furgal, H. Kuhnlein, E. Loring, G. Muckle, E. Myles, O. Receveur, B. Tracy, U. Gill, and S. Kalhok**. 2005. Human health implications of environmental contaminants in Arctic Canada: A review. Science of the Total Environment:165-246.
97. **Vandal, G. M., R. P. Mason, and W. F. Fitzgerald.** 1991. Cycling of Volatile Mercury in Temperate Lakes. Water Air and Soil Pollution **56:**791-803.
98. **Vetriani, C., Y. S. Chew, S. M. Miller, J. Yagi, J. Coombs, R. A. Lutz, and T. Barkay.** 2005. Mercury adaptation among bacteria from a deep-sea hydrothermal vent. Applied and Environmental Microbiology **71:**220-226.
99. **Vlassov, A. V., S. A. Kazakov, B. H. Johnston, and L. F. Landweber.** 2005. The RNA world on Ice: A new scenario for the emergence of RNA information. Journal of Molecular Evolution **61:**264-273.
100. **Walker, J. B., J. Houseman, L. Seddon, E. McMullen, K. Tofflemire, C. Mills, A. Corriveau, J. P. Weber, A. LeBlanc, M. Walker, S. G. Donaldson, and J. Van Oostdam**. 2006. Maternal and umbilical cord

blood levels of mercury, lead, cadmium, and essential trace elements in Arctic Canada. Environmental Research 100:295-318.

101. **Weber, J. H.** 1993. Review of possible paths for abiotic methylation of mercury(II) in the aquatic environment. Chemosphere **26:**2063-2077.
102. **Westöö, G.** 1966. Determination of methylmercury compounds in foodstuffs. I. methylmercury compounds in fish, identification and determination. Acta Chemica Scandinavica **20:**2131-2137.
103. **Whalin, L. M., and R. P. Mason.** 2006. A new method for the investigation of mercury redox chemistry in natural waters utilizing deflatable Teflon (R) bags and additions of isotopically labeled mercury. Analytica Chimica Acta **558:**211-221.
104. **Wren, C. D.** 1986. A Review of Metal Accumulation and Toxicity in Wild Mammals .1. Mercury. Environmental Research **40:**210-244.
105. **Zhang, H., C. Dill, T. Kuiken, M. Ensor, and W. C. Crocker.** 2006. Change of dissolved gaseous mercury concentrations in a southern reservoir lake (Tennessee) following seasonal variation of solar radiation. Environmental Science & Technology **40:**2114-2119.

10. Annexe 3: Utilisation d'un bioreporter afin de mieux appréhender la prise en charge du Hg.

10.1. Fonctionnement d'un biorapporteur

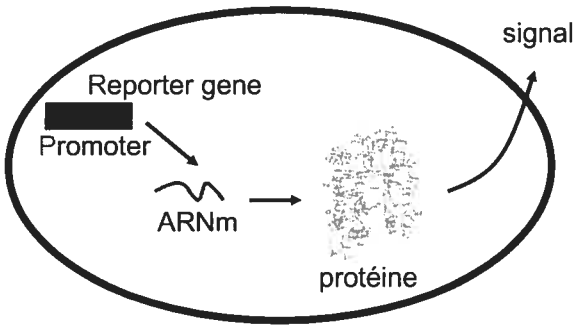

Le promoteur est sensible à l'élément cible (e.g. Hg) que l'on cherche a mettre en évidence. Le promoteur, si l'élément cible est présent, déclenche,
la transcription de la séquence du gène rapporteur (production de lumière)

10.2. Effets de certains inhibiteurs du métabolisme communément utilisés lors d'étude sur les transformations du Hg en milieu naturel

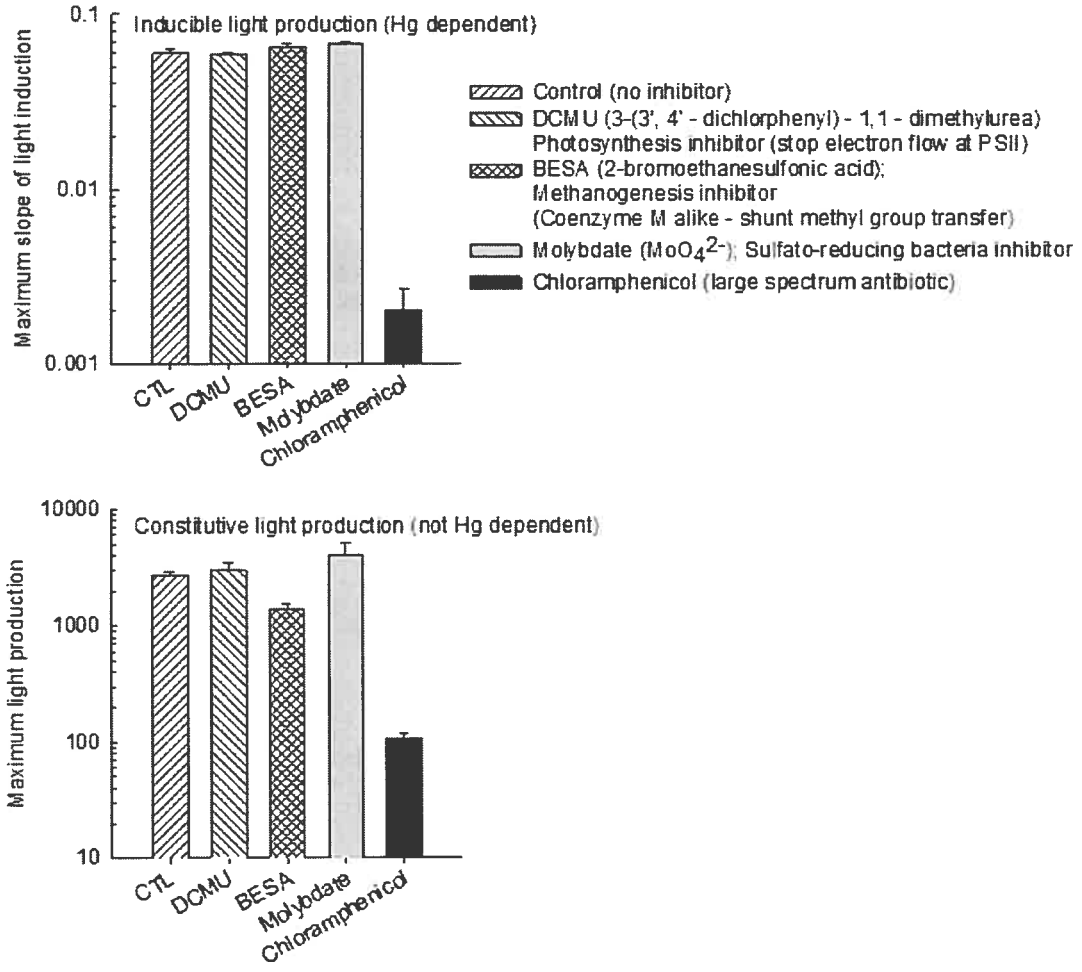

10.3. Étude de la prise en charge du Hg dans la neige fraîche et dans l'eau de la baie Saint-François (Lac St. Pierre)

Biodisponibilité du Hg dans la neige (panneau du haut) : aucun ajout de Hg n'a été effectué à l'échantillon naturel. Les symboles noirs et blancs représente des ajouts de Hg dans le milieu minimal et servent à déterminer la concentration de Hg biodisponible dans la neige (ici, entre 1 et 3 $ng \cdot L^{-1}$).

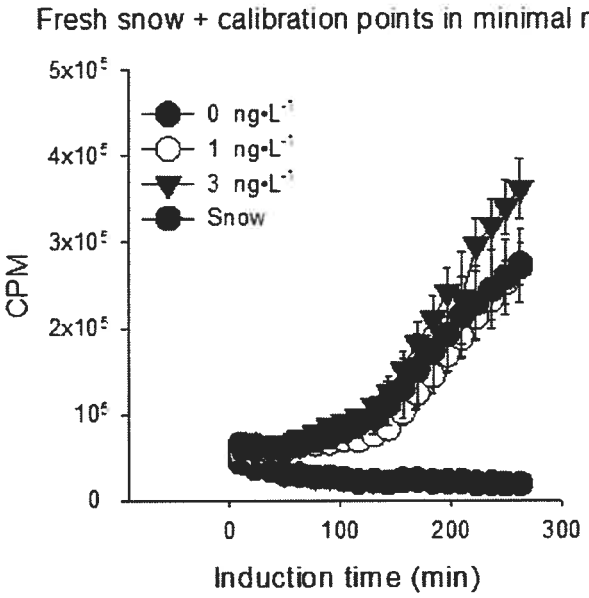

Biodisponibilité du Hg dans l'eau de la baie Saint-François (panneau du bas) : Hg biodisponible non détectable (correspond à 0 $ng \cdot L^{-1}$). L'ajout de 8 $ng \cdot L^{-1}$ de Hg(II) a été nécessaire afin d'observer la production de lumière.

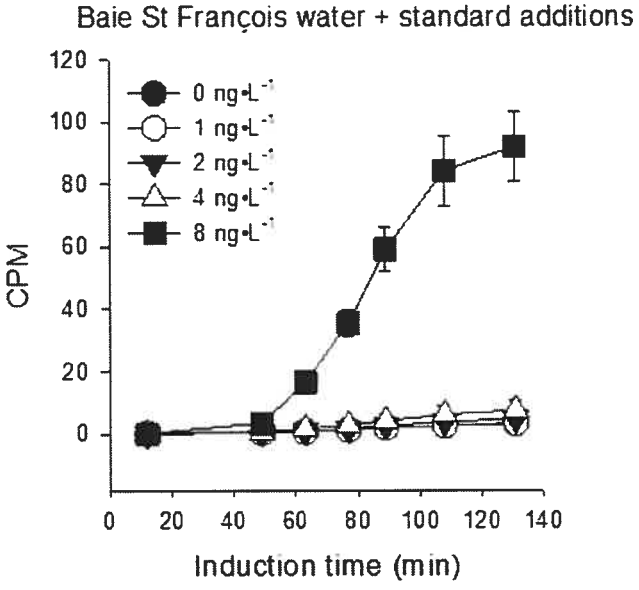

10.4. Rôle des substances humiques commerciales (sigma Aldrich) sur la prise en charge du Hg

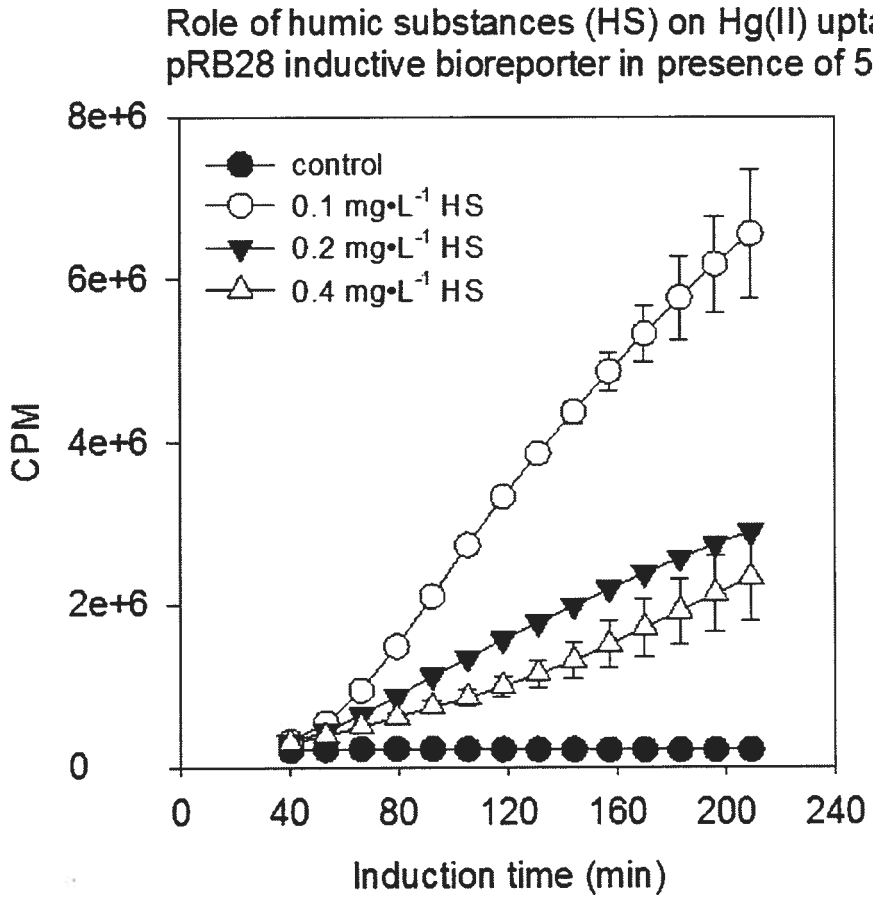

10.5. Effet du pH sur la prise en charge du Hg(II) en présence ou en absence de substances humiques commerciales

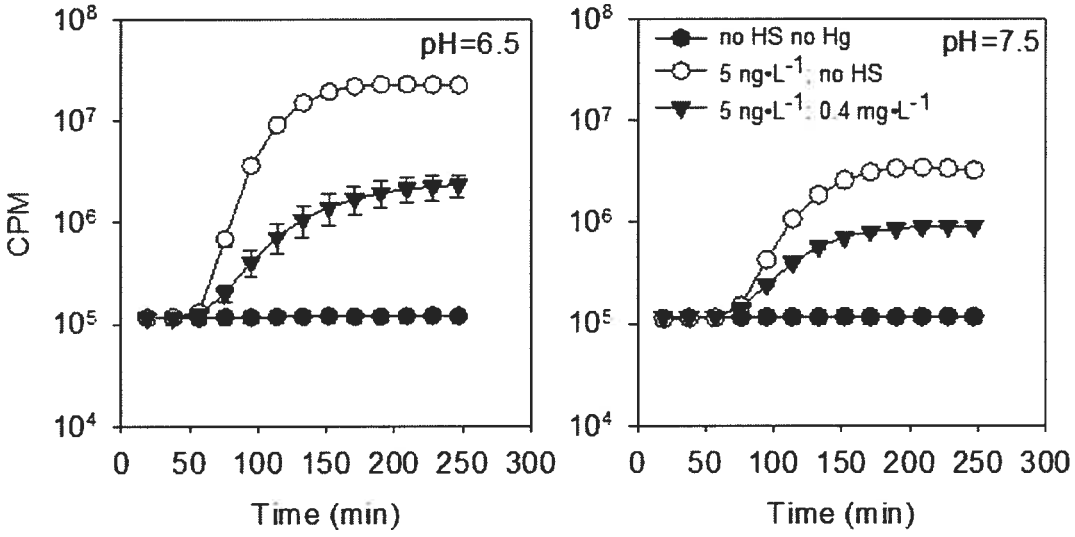

10.6. Influence de concentrations croissantes en Glutathion (forme réduite) sur la prise en charge du Hg(II)

Influence of GSH (reduced) on the uptake of Hg(II) (5 ng•L^{-1}) by *E. Coli* HMS174 pRB28

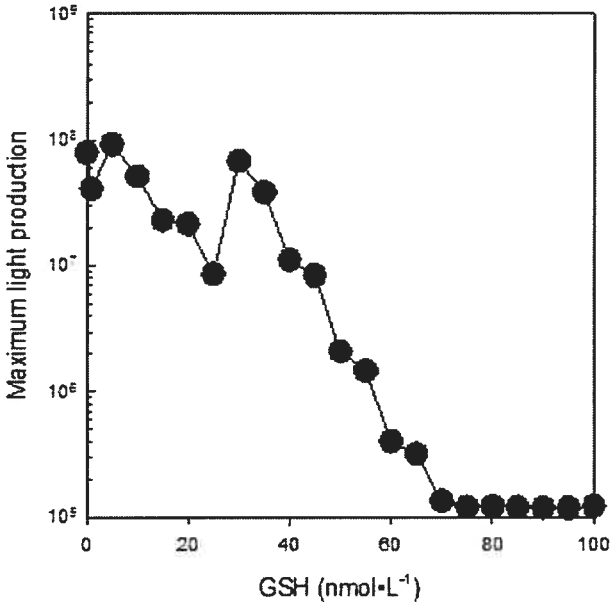

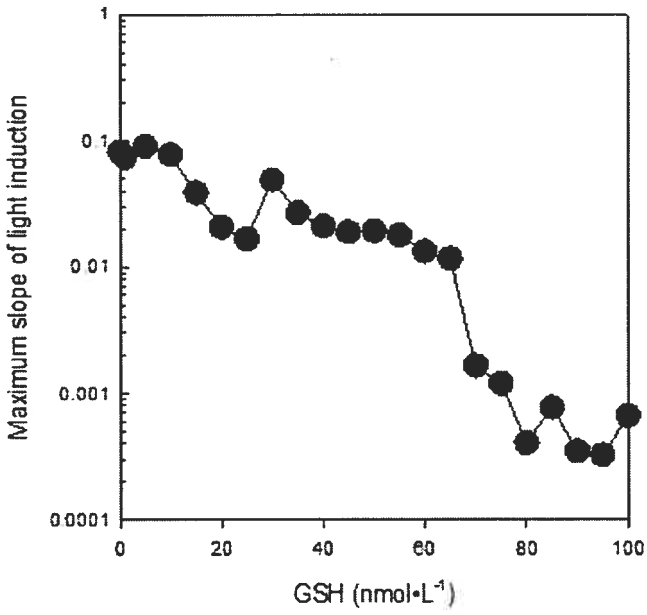

10.7. Comparaison de la prise en charge du Hg(II) et du Hg(0)